# Assessing Marine Renewable Energy Contribution to Indonesia's Net-Zero Transition

Through Energy System Optimization Modelling Approach

MSc Graduation Project

Daoni Gabrielle

Delft University of Technology

TU Delft

# Assessing Marine Renewable Energy Contribution to Indonesia's Net-Zero Transition

## Through Energy System Optimization Modelling Approach

by

Daoni Gabrielle

Student Number : 5944090

Faculty of Mechanical Engineering

| | |
|---|---|
| Chairman & Daily Supervisor: | Dr. George Lavidas<br>[Faculty of Civil Engineering & Geosciences, Section Offshore Engineering] |
| Supervisor: | Dr. S.J. (Stefan) Pfenninger-Lee<br>[Faculty of Technology, Policy, and Management, Section Energy & Industry] |
| External Advisor: | Dr. J.K.A. (Jannis) Langer |

Cover: Foamy Waves on the Sea; retrieved from https://www.pexels.com/photo/foamy-waves-on-the-sea-15828946/

Style: TU Delft Report Style, with modifications by Daan Zwaneveld

TU Delft

# Acknowledgements

*Undertaking this thesis has been both an intellectual challenge and a deeply personal journey. The research on integrating wave and tidal energy into Indonesia's future energy system was driven not only by academic curiosity, but also by the belief that it is always worth exploring new paths for renewables in Indonesia. Especially in the offshore domain, which has always been my happy place.*

*First and foremost, I give thanks to my Father. Without Him, I am nothing. I wish to express my heartfelt gratitude to my family, whose unwavering love and encouragement from thousands of miles away has sustained me throughout this process. To my friends whom I met along the way, thank you for the beautiful moments that I will always treasure.*

*I am deeply grateful to my daily supervisor, Dr. George Lavidas. His willingness to accept my thesis idea, and his critical insights, were invaluable in shaping this work. I also wish to thank Dr. Stefan Pfenninger, whose expertise in energy system modelling sharpened my approach; I am grateful for his development of the Calliope model and wish him the best in continuing this line of research. To Dr. Jannis Langer, thank you for your encouragement in every meeting and for laying the foundation with Calliope-Indonesia, without which this thesis would not exist.*

*I gratefully acknowledge the support of the Lembaga Pengelola Dana Pendidikan (LPDP) Indonesia, whose scholarship enabled me to pursue this master study.*

*Finally, to my husband; my best friend, my mentor, my strength, my everything. Thank you for your endless support. This work would not have been possible without you. Let us continue the next chapter side by side.*

*Daoni Gabrielle*
*Delft, August 2025*

# Abstract

Indonesia's decarbonisation strategy hinges on how quickly the power system can absorb new renewable classes beyond wind and solar, yet the role of marine renewables has rarely been tested at system scale across the country's grid, notably due to cost constraints. This thesis extends the energy system optimization framework by Langer et al. (2024) [1], Calliope-Indonesia, to analyze wave point-absorber and tidal stream resources' optimal contribution to the national energy system by 2050 under two grid configurations: a Supergrid with inter-island transmission versus today's fragmented provincial networks.

The methodology integrates new technology definitions, provincial-level resource assessments from ERA5 reanalysis and TPXO tidal data, and hourly generation profiles into the established Calliope model structure. Four research questions examine MRE impacts on storage requirements, transmission expansion priorities, cost competitiveness against established renewables, and optimal system configurations for least-cost decarbonisation. Wave energy uses point-absorber performance matrices calibrated to Indonesian coastal conditions, while tidal analysis applies velocity-power curves for horizontal-axis turbines deployed in high-flow straits.

Results show that transmission architecture controls MRE integration value. Under Supergrid operation, total storage capacity decreases from 135.7 to 125.1 GW with reference MRE costs ($-7.8\%$) and to 120.2 GW under optimistic learning trajectories ($-11.4\%$). Fragmented networks show minimal storage reduction (+0.6 GW), indicating that MRE benefits require coordinated inter-island power flows. Tidal energy displaces storage more efficiently than wave (0.94 versus 0.09 GW per GW installed) due to predictable semidiurnal generation patterns. Grid expansion concentrates in specific high-value corridors rather than uniform network reinforcement: HVDC capacity increases from 97.1 to 137.6 GW, with the Lampung–Banten connection handling disproportionate additional flows.

Cost competitiveness emerges when interconnection enables optimistic learning curves. Under the Supergrid configuration with accelerated cost reduction, tidal energy reaches 66.1 US$/MWh and wave energy 69.5 US$/MWh.This positions both technologies within the competitive renewable band alongside small hydro (67.5 US$/MWh) and geothermal (61.7 US$/MWh). Marine generation reaches 261.4 TWh annually (17.3% of total demand), compared to 122.8 TWh under fragmented operation, showcasing transmission's role as a primary value driver rather than background infrastructure.

The analysis identifies targeted deployment strategies: wave clusters positioned behind reinforced transmission gateways on high-resource coasts, and tidal installations near demand centres where network access maximizes predictability benefits. However, single-year operational modeling, coarse nearshore resource resolution, and incomplete spatial exclusions limit precision in site-specific assessments. Despite these constraints, the evidence indicates that MRE technologies can contribute meaningfully to Indonesia's 2050 power system under cost-optimistic assumptions (CAPEX: 986,000 US$(2023)/MW, OPEX: 50,000 US$(2023)/MW) and remain viable even under reference cost scenarios (CAPEX: 1.76 million US$(2023)/MW, OPEX: 88,000 US$(2023)/MW) when supported by strategic interconnection investments and disciplined resource targeting.

# Contents

# 1. Introduction

## 1.1. Background

Indonesia's energy landscape is characterized by a significant reliance on fossil fuels, with coal comprising for 63.3% of the nation's total electricity generation in 2023, followed by dispatchable renewables (18.6%), natural gas (15.8%), oil (1.9%), and variable renewables (0.4%) [2]. This heavy dependence on coal highlights the urgent need for a transition to cleaner sources to meet the country's ambitious net zero emissions target by 2060, as pledged under the Paris Agreement. The National Energy General Plan ('Rencana Umum Energi Nasional' or 'RUEN'), the nation's strategic energy planning framework, outlines a goal of achieving 23% renewable energy in the primary energy mix by 2025 and 31% by 2050, targeting an installed renewable capacity of 45.2 GW by 2025 and 167.7 GW by 2050 [2, 3]. However, recent assessments indicate that the 2025 target may only reach 17 to 20%, pointing to the urgency of expanding renewable adoption [4].

As the world's largest archipelagic nation, Indonesia spans a vast maritime territory of 7.9 million $km^2$, including territorial seas, archipelagic waters, and an exclusive economic zone (EEZ) [5, 6]. This geography presents significant opportunities for marine renewable energy (MRE), particularly in this thesis context: wave and tidal energy, which are recognized globally as clean, reliable, and predictable resources [7, 8]. Studies estimate Indonesia's marine renewable potential at 288 GW theoretically, with a technical potential of 18–72 GW, and hotspots in Bali (9 GW) and West Nusa Tenggara (8.1 GW), which officially published by Indonesia's Directorate General of New Renewable Energy and Energy Conservation [9, 10]. For wave energy specifically, recent research indicate significant potential, with wave power exceeding 30 kW/m year-round along the southern coasts of Java, Bali, and West Nusa Tenggara [11], and 67.29 kW/m on Sumatra's west coast although only available during peak seasons [12]. Tidal energy also shows promise, particularly in straits like Larantuka and Alas, where currents exceed 3.0 m/s, leveraging the predictability of tidal streams for consistent power generation [13, 9].

Despite this potential, offshore renewables remain largely untapped in Indonesia, hindered by high capital costs, the absence of specific policies and regulations, and grid infrastructure limitations [9]. The National Electricity General Plan ('Rencana Umum Ketenagalistrikan Nasional' or 'RUKN') published in 2024 [14], serves as tangible manifestation of RUEN's strategic framework that translates these goals into electricity sector actions [15]. A key component of this roadmap is the 'Supergrid' concept, a high-voltage inter-island transmission master plan designed to support nationwide renewable energy integration. This infrastructure expansion is planned in stages (e.g. Sumatra-Java interconnection by 2031). By 2060, Indonesia's electricity demand projection reaching 1,813 TWh or 5,038 kWh per capita and renewable energy is planned to dominate the national power mix at 49.5% [14], including the target to install 3.0 GW of marine renewables by 2050 [15].

Energy system optimization models (ESOMs) provide a framework to guide this transition, optimizing generation, storage, and transmission capacities to identify least-cost scenarios [16, 1]. Recent global study, Lavidas et al. (2023) [17], demonstrated wave energy's integration into PyPSA-MREL-TUD model, showcasing grid reliability enhancement during low-solar periods, particularly in Europe. A recently published research by Langer et al. (2024) [1] utilized energy system optimization modelling approach, producing open-source model called *'calliope-indonesia'* based on Calliope framework [18] to model renewables, storage, as well as inter-island transmission, including subsea power cables, without assuming a copperplate approach like previous studies. Instead, the study uses multi-node setup with one node per province to reflect Indonesia's complex grid topology [1]. The outputs of the Calliope-Indonesia model can be used to assess the effectiveness of offshore renewable energy technologies, offering a system-wide perspective on their role in energy transitions.

To assess the economic effectiveness of power generation technologies, Levelized Cost of Electricity (LCOE) is often used as a key metric of competitiveness among generation technologies, comparing costs per unit of energy produced.

## 1.2. Problem Statement

Indonesia's pathway to achieving its Net Zero Emissions target faces significant challenges in diversifying its renewable energy portfolio [15, 2] with offshore renewables, like wave and tidal energy, which remain largely overlooked in national energy strategies. Despite its vast potential, offshore renewable energy technologies has not been integrated into system-wide energy optimization models, leaving critical uncertainties about its role in decarbonizing Indonesia's complex, multi-island power grid. While onshore renewables such as solar PV, wind, and hydro are well-represented in recent energy planning frameworks, marine renewables are notably absent, limiting insights into their technical feasibility, grid reliability contributions, and economic viability [1].

A critical knowledge gap exists in the *'calliope-indonesia'* model published by Langer et al. (2024), which uses a multi-node setup (one per province) to account for renewable energy technologies, such as solar PV, wind, and hydro, and emphasizes inter-island transmission in Indonesia's power system [1]. The model includes ocean thermal energy conversion (OTEC) but excludes other marine renewables, such as wave and tidal energy, overlooking their potential to enhance system-wide decarbonization, particularly given Indonesia's plan to install 3.0 GW of marine renewables by 2050 [3, 15].

## 1.3. Research Objectives

Building on the challenges outlined in the problem statement, this study aims to assess the system-wide role of marine renewable energy (MRE) in achieving net-zero emissions in Indonesia by 2050; supporting a decarbonization pathway that is ten years ahead of the national target of 2060. using energy system optimization modeling with *'calliope-indonesia'* and techno-economic evaluations. By integrating MRE into 'calliope-indonesia', we will explore its contribution to decarbonization under Supergrid and fragmented grid scenarios, focusing on how it can support the multi-island grid's reliability with least-cost planning and inter-island subsea power cables. Focusing at the local level, the impact of integrating MRE in very high-demand regions like Java can be investigated by refining the resolution through more reliable multi-node representations.

Using the modelling outputs, the study will determine the economic competitiveness of marine renewables in Indonesia, comparing it with other renewables, such as offshore floating solar PV, to evaluate its cost-effectiveness. These objectives address the gaps identified in current literature, drawing on recent ESOM insights [1, 17].

### 1.3.1. Research Questions

As a trajectory for this study, the following research questions have been formulated to address the challenges identified in the problem statement and to explore the contribution of MRE in Indonesia's energy transition:

*How can marine renewable energy be optimally integrated into Indonesia's power system to support the net-zero strategy by 2050, and what role does it play in achieving this goal?*

1. What is the impact of marine renewable energy integration on energy storage requirements within Indonesia's power system?
2. What is the optimal grid expansion strategy to accommodate marine renewable energy in Indonesia's power system?
3. What are the Levelized Cost of Electricity (LCOE) for marine renewable energy technologies in Indonesia, and how do they compare with other renewable energy sources?
4. What is the optimal configuration for integrating marine renewable energy into Indonesia's power system under different grid configurations (Supergrid vs. fragmented grid) to support the net-zero strategy?

## 1.4. Research Approach

This research extends the Calliope-Indonesia model [1] to assess the contribution of MRE, specifically wave and tidal energy, to Indonesia's net-zero emission pathway by 2050. Drawing on the Chapter 2, the proposed methodology integrates selected MRE technologies into the energy system framework, adapts the model to reflect their distinct characteristics, and performs a techno-economic analysis. The approach is designed to address research questions 1.3.1. The following subsections outline the three

primary components of the research approach.

### 1.4.1. MRE Integration

To incorporate MRE into the Calliope-Indonesia model, two specific technologies are selected based on their technological maturity and relevance to Indonesia's coastal and marine conditions: (1) wave energy using nearshore point absorbers (1000 kW capacity, 20–60 m depth), and (2) tidal energy using tidal stream systems (typically 500-1500 kW, deployed in high-velocity tidal channels). Point absorbers are chosen for wave energy due to their high Technology Readiness Level (TRL 8) and adaptability to Indonesia's moderate wave climate, while tidal stream systems exploit energetic flows in straits.

Wave data is sourced from the ERA5 reanalysis dataset [19] that will provides hourly significant wave height ($H_s$) and energy period ($T_e$). These are overlaid with bathymetry data from the General Bathymetric Chart of the Oceans (GEBCO) [20] to identify nearshore sites (40–150 m) along Indonesia's southern coasts, such as Java. WaveStar power matrix, adapted from Lavidas et al. [17], convert wave conditions into hourly electricity output.

For tidal energy, tidal current velocities could be derived from the TPX10 model [21] using provincial analysis approach then overlaid with GEBCO bathymetry to refine site selection (20–60 m depth). The open-source tool PyTMD [22] extracts tidal constituents (e.g., M2, S2) to compute hourly velocity profiles, which are converted to tidal stream power output using a velocity-power curve (cut-in 1 m/s, rated 2.5 m/s) based on SeaGen 2MW device specifications [23]. Hourly tidal and wave power profiles are then input into the 'calliope-indonesia' model.

### 1.4.2. Energy System Modelling

The 'calliope-indonesia framework' by Langer et al. [1] is modified to include wave and tidal energy as supply generations and the use of realistic demand profile from PLN, electricity company in Indonesia.

The modified 'calliope-indonesia' model optimizes total system costs under two grid scenarios:

1. Scenario #1: Supergrid with inter-island transmission links, according to RUKN 2024 plan [14]
2. Scenario #2: Fragmented grid mirroring current limited interconnections between islands

Interactions between wave & tidal energy, and previously modelled technologies are assessed at hourly resolution for a target year (e.g. 2050), particularly for newly wave and tidal technology inputs are based on 1.4.1. Scenario analyses test high-cost (conservative) and low-cost (optimistic) deployment trajectories for both MRE technologies, using learning curve projection approach from [17]. This energy system optimization modelling approach addresses research questions RQ1 (optimal configuration for MRE integration under grid scenarios), RQ2 (impact on storage requirements), and RQ3 (optimal grid expansion strategy to accommodate MRE).

### 1.4.3. Techno-economic Metrics

Economic evaluation employ conventional technology comparison metric which is the Levelized Cost of Electricity (LCOE), aiming to assess the economic value of wave and tidal energy to the future Indonesia's power system. LCOE is derived from Calliope outputs (annualized costs and generation) for wave (point absorbers) and tidal (tidal stream) technologies, addressing RQ4. Besides, sensitivity analyses explore cost trajectories (2030, 2040, 2050) for both technologies and will reflect potential cost reductions.

## 1.5. Thesis Outline

The thesis document is structured as follows: ***Chapter 2*** provides a literature review, covering MRE potential, previous efforts to integrate wave and tidal power into energy models, the capabilities of the Calliope-Indonesia model for economic and grid analyses and techno-economic metrics like LCOE. ***Chapter 3*** describes the methodology, including enhancements to the Calliope-Indonesia model for wave and tidal energy, Supergrid and fragmented grid scenario definitions, and the approach for calculating LCOE. ***Chapter 4*** presents simulation results for various scenarios, detailing capacity expansion, energy storage impacts, grid expansion strategies, and economic comparisons when MRE is available. ***Chapter 5*** discusses the findings, integration challenges within Indonesia's generation mix, and thesis limitations. Finally, ***Chapter 6*** concludes the thesis, summarizing insights on MRE integration by 2050

and future research recommendations.

# 2. Literature Review

This chapter reviews existing literature on marine renewable energy (MRE) and its role in Indonesia's pathway to net zero emissions by 2050, addressing challenges from Chapter 1. The literature review aims to synthesize existing research on MRE integration to identify gaps and guide energy system modeling for Indonesia's net-zero transition, focusing on energy system optimization modeling, techno-economic metrics, and inter-island transmission infrastructure. It evaluates MRE technologies (wave and tidal energy), their integration, and economic and grid-related implications for Indonesia's multi-island power system, identifying research gaps to generate new insights in this field of study.

## 2.1. Literature Search

This section describes the systematic approach to identify relevant literature for this study. The literature search is conducted through Google Scholar for scientific articles and relevant chapters from books. The main keywords are selected to suit the research topic. Official reports from formal institutions were found as references of the relevant paper, as well as other scientific articles.

### 2.1.1. Search Methodology

To ensure a comprehensive literature review, the search was conducted across multiple academic and institutional sources:

- Academic databases: Google Scholar (main search engines) that leads to Scopus, ScienceDirect, etc.
- Government and institutional reports: International Energy Agency (IEA), Indonesian Ministry of Energy and Mineral Resources (ESDM), PLN (Indonesia's state-owned power company), IESR (Institute for Essential Services Reform)
- Books and conference proceedings: IEEE Conferences and Springer publications related to offshore renewable energy and energy system modelling

The search employed a combination of keyword searches and Boolean operators (e.g. AND, OR) to refine the results. The primary keywords used in the search are listed as follows:

*Keywords: Offshore Renewable Energy, Marine Renewable Energy, Wave Energy, Tidal Energy, Energy System Model, Indonesia, Beyond LCOE, VALCOE*

### 2.1.2. Key Literature & Relevant Insights

Based on the literature search, key findings and relevant works were identified, focusing on MRE integration, energy system modeling, techno-economic analysis, and Indonesia's energy transition policies. A summary of these relevant works, including their contributions and identified gaps, is provided in Appendix A.1.

## 2.2. Overview of Indonesia's Energy Transition Plan

Indonesia is the largest archipelagic country in the world with total land area reaching 1.9 million $km^2$, almost half the size of European Union. Geographically, Indonesia is located between the Indian and Pacific Oceans. The country spans from the westernmost province of Aceh to the eastern province of South Papua, forming a vast and diverse maritime nation [24]. Indonesia consists of 38 provinces, each with unique cultural and economic significance. The visual representation of the country's current administrative divisions can be seen in Figure 2.1.

Recognized as the fourth most populous country in the world [26], Indonesia faces the critical challenge of meeting its growing energy demands while ensuring environmental responsibility. The country's energy consumption continues to rise alongside its economic development, with coal dominating the energy mix. In the industrial sector alone, coal accounted for 42% of total final energy consumption in 2022 [27]. This heavy reliance on fossil fuels stresses the urgent need to transition toward cleaner energy sources. As part of its commitment to the Paris Agreement, Indonesia has pledged to reach net-


**Figure 2.1:** Map: Current Provinces of Indonesia [25]

zero emissions by 2060, reduce greenhouse gas emissions and implement strategies for sustainable energy development.

Aligning its long-term energy transition strategy with the global climate commitment, Indonesia established the National Energy General Plan ('Rencana Umum Energi Nasional' or 'RUEN') [28], which was issued in 2015 based on data collected until that year and projected up to 2050. The document serves as the country's official national energy planning framework and is only available in Bahasa Indonesia. Providing broader accessibility, the Institute for Essential Services Reform (IESR) publishes independent reports in English, including assessments of RUEN's progress [15] and the Indonesia Renewable Energy Outlook [2].

According to RUEN, Indonesia aims for 23% of the primary energy mix to be sourced from renewables by 2025 and 31% by 2050. This includes increasing renewable energy capacity to 45.2 GW by 2025 and 167.7 GW by 2050 [15]. Unfortunately, recent evaluations suggest that the 2025 target may not be met [2, 4] and is now projected to reach only 17 up to 20%. To avoid a domino effect impacting future goals, particularly the net-zero emission target, active participation from various sectors is crucial, including marine energy.

MRE is included in RUEN's renewable energy roadmap with a target of 3.0 GW of installed capacity by 2050 [15]. However, its implementation remains absent to date. The potential and challenges surrounding MRE will be further elaborated in Section 2.2.2.

While energy planning in Indonesia is guided by the RUEN, electricity or power sector, also has its own dedicated framework in the National Energy General Plan ('Rencana Umum Ketenagalistrikan Nasional' or 'RUKN') [14]. The following section explores Indonesia's electricity sector and the recently published RUKN strategies.

### 2.2.1. Indonesia's Current Electricity Sector and Future Outlook

Despite Indonesia's commitment to a cleaner energy future, its electricity generation remains predominantly fossil-fuel based. As for the current state, Institute for Essential Services Reform (IESR) reported 63.3% of total 107 GW power generated in Indonesia by coal burning, followed by dispatchable renewable energy (18.6%), extraction of natural gas (15.8%), oil (1.9%), and variable renewables (0.4%) [2]. This coal reliance, emitting over 650 $MtCO_2$/year [29], contrasts with rising demand-projected at 1,813 TWh by 2060 (5,038 kWh/capita) [14], highlighting the need for scalable renewable energy, such as marine renewables.

As previously mentioned, Indonesia's electricity development strategy is outlined in the National Electricity General Plan (RUKN) 2024 [14] and PLN's Electricity Supply Business Plan (RUPTL) 2021-2030 [30], which focus on current power sector status while supporting the country's commitment to achieving Net Zero Emissions (NZE) by 2060 with 49.5% renewable generation. Available only in Bahasa

Indonesia, these documents limit global critique and notably omit wave energy as an option [9], while including tidal energy (e.g. 0.1 GW pilot projects). Electrical demand data, which is critical for grid modelling, shows regional disparities within Indonesia (e.g. Java's 70% share vs the eastern islands' deficits), yet RUKN lacks granularity for wave-rich coastal zones.

One of the key initiatives to support these efforts is the **Supergrid** concept, a large-scale transmission network designed to interconnect major electricity systems within and between islands in Indonesia while accommodating the future integration plan of variable renewable energy sources. Priority interconnections include internal networks within Sumatra, Kalimantan, Sulawesi, and Papua, as well as cross-island connections, which are planned in stages as mentioned in 2.7.3 [14]. This infrastructure, costing 171–1,261 US$ 2021/MW/km for HVDC links [1], aims to improve electricity access and reduce fossil fuel dependency, but its high capital cost challenge MRE deployment. Additionally, RUKN's focus on tidal over wave energy overlooks the latter's potential for demand-heavy Java, while cost implications remain underexplored in these plans, gaps this study addresses via energy optimization modelling approach.

### 2.2.2. Marine Renewable Energy

The ocean holds vast energy potential in various forms; kinetic, potential, chemical, and thermal, that can be harnessed and converted into different types of energy (referred as energy carriers), such as electricity, heat, gas, or hydrogen.

In this study, a distinction is made between two key terms: *'marine renewable energy'* and *'offshore renewable energy'*. By definition, marine renewable energies ('MRE', also known as marine renewables, blue or ocean energy) are energy sources that can be generated from wind, waves, tides, salinity gradient, and marine biofuel according to European Commission [7], as well as ocean thermal gradients. Within the scope of this study, the term marine renewable energy refers specifically to ocean thermal energy, tidal energy, and the primary focus of this study, ***wave and tidal energy***. In a broader sense, some definitions also include offshore wind energy and solar energy, which utilize the sea surface [8], and will be classified as offshore renewable energy, 'ORE'.

For many years, the world has studied MRE and recognized its massive power to support the energy system in the future, highlighting its clean, reliable, and predictable nature [31]. Given the massive potential of MRE worldwide, Indonesia, as the largest archipelagic country, holds significant prospects for its development.

Stretching beyond the archipelago, Indonesia has a total sea area of 7.9 million $km^2$ [5] [32] consisting of territorial sea, archipelagic waters, and claimed exclusive economic zone (EEZ) [6]. With its vast ocean territory, Indonesia possesses great opportunities to harness the renewable energy beyond land-based sources.

To estimate the technical potential of marine energies in Indonesia, we examined official documents published by the government agencies. In 2016, The Directorate General of New Renewable Energy and Energy Conservation (NREEC) estimated a theoretical potential of 288 GW in 2016, with a technical range of 18–72 GW [9] without explicitly defining the types of marine energy included in these estimates. More recently, the National Energy Council published the 'Indonesia Energy Outlook' in 2023, which cited updated data from NREEC stating the specific number of marine energy potential as 63 GW, peaking in Bali and Maluku (9 GW) and West Nusa Tenggara (8.1 GW) [10]. However, we were unable to find any technical studies that provide detailed methodologies and assumptions supporting these estimates, limiting their reliability for system planning. Globally, MRE's predictability and high capacity factors (CF) suggest system-wide value, yet Indonesia's RUEN targets only 3.0 GW of MRE by 2050, with tidal prioritized over wave energy [3].

A major barrier to the development of marine energy in Indonesia, as one of the most under-utilized renewable energy sources is the absence of policies and regulations governing its utilization [9]. Despite the so-called immense potential of marine energy, its development has yet to progress, largely due to intertwined challenges in Indonesia. High capital costs (e.g. WECs at 100-300 €/MWh vs. solar PV's 30-60 €/MWh [33, 34]) hinder investment, while the absence of specific regulations and rigid framework further delays progress. Conversely, without established policies and incentives, it is difficult to attract related investments to drive down costs. This cyclical challenge continues to stall progress, leaving the

blue energy largely untapped.

Recent global advancements in ORE technology have led to the development of various renewable solutions. Offshore wind turbines and floating solar PV systems have seen significant progress, while WECs and tidal stream devices are increasingly recognized for their promising potential. WECs can operate in a wider range of locations, unlike tidal energy which is dependent on specific geographical features [33]. Compared to salinity gradient and ocean thermal energy conversion, WECs prevail higher technological readiness level (TRL) to date. Nonetheless, only a limited number of scientific studies have explored topic around MRE integration to an energy system through modelling approach. Before delving further in the integration of the selected MRE into energy system, the section 2.3 will explain the relevant study regarding wave energy.

Environmentally, MRE poses trade-offs; wave energy may disrupt marine ecosystems, while offering cleaner alternatives to fossil fuel-based [35]. WECs may disrupt fisheries, as seen in European trials [31], though mitigation via site selection is possible. In the social context, coastal communities could gain benefits from localized power, but deployment may also lead to displacement, a risk often missing from policy discussions [8]. Counterarguments suggest MRE's high costs and grid challenges outweigh benefits, yet global cases (e.g. Europe's 100 MW wave target [31]) counter this with strategic investment. Indonesia's MRE lag thus reflects a gap in system-level analysis, driving this study's MRE exploration.

## 2.3. Wave Energy

Wave energy is derived from wind-driven ocean surface motion. Looking solely at the energy aspect, wave energy offers several advantages, including continuous input, high power density compared to mature technologies like wind power, and a more stable generation profile compared to VRE sources like solar PV and wind [33]. Relatively, it demonstrates competitive CF (e.g. wave energy's mean CF of 22.3-25% with maximum potential up to 53.6% vs solar PV's 15-20% [36]). With the increasing share of various VRE in the energy system to achieve net-zero or even 100% renewable energy goals worldwide, system reliability and flexibility have become prominent topics nowadays. In this thesis context, wave energy presents an attractive solution on reducing the need for costly large-scale energy storage systems. In Indonesia, with demand concentrated (e.g. Java's 70% share [14]), wave energy's proximity could optimize grid efficiency under Supergrid or fragmented scenarios.

To understand the process of wave power utilization, the study can be divided into two main aspects: *the wave resources*, study towards assessment of the available energy from ocean waves, and technology to produce, *wave energy converters (WECs)*, which are devices designed to harness and convert wave energy into usable power. The section also covers wave energy's development in Indonesia, as the base for assessing its system-wide role and economic viability.

### 2.3.1. Wave Energy Resources

Wave energy's global technical potential reaches 500 GW at 40% efficiency, concentrated in wave-active regions [37]. The potential is unevenly distributed, mostly concentrated in specific regions exposed to consistent wave activity. An advantage is that wave energy resources are often located near coastal areas, where population densities are high and energy demand are concentrated, thus energy delivery is more efficient with minimal transmission losses.

To harness wave energy, the first step that needs to be taken is to conduct wave energy resource assessments. It typically involves analyzing historical wave conditions through metocean data to estimate its potential in a specific area of interest. According to Indonesia's ESDM, theoretical potential accounts for total energy available based on field data via a modelling system. Technical potential refers to identified potential that can be implemented at a certain location, and economic potential only covers the energy that can be actually utilized [3].

A widely adopted approach for such assessments involves the use of reanalysis datasets, such as ERA5 [19], which provide comprehensive historical wave and wind data. Produced by the European Centre for Medium-Range Weather Forecasts (ECMWF), ERA5 offers global coverage with a spatial resolution of approximately $0.3^o$ ($\sim$27 km) and hourly temporal resolution, enabling the characterization of wave parameters like significant wave height ($H_{m0}$), energy period ($T_{m10}$), mean zero-crossing period ($T_{m0}$), peak wave period ($T_{peak}$), and peak wave direction ($P_{kdir}$) [17]. While its coarse resolution

may limit nearshore accuracy due to bathymetric influences, ERA5 is considerably valuable for initial exploration of wave energy potential across broader regions, including Indonesia's expansive maritime domain.

Indonesia's geography, bordered by the Indian and Pacific Oceans with Southern Ocean swells, offers some promising wave energy sites. A site is considered feasible for wave energy generation if the annual mean wave energy exceeds 15 kW/m [38]. Ribal et al. (2020) [11] assessed national potential at $0.05^{o}$ (≈5.5 km) resolution using the spectral wave model WAVEWATCH III, then downscaled wave hindcast on a high-resolution grid (Nest-2). Their findings indicate >30 kW/m energy flux year-round along southern Java, Bali, and West Nusa Tenggara, with seasonal peaks (March–November) up to 60 kW/m on Sumatra's west coast (99th percentile). Validation with buoy data, including those from the Indonesian Agency for Meteorology, Climatology, and Geophysics (BMKG) and global wave buoy networks, confirmed the model's accuracy. Rizal et al. (2020) [12] further validated that Sumatra's west coast peaks at 67.29 kW/m over 25 years, though it drops to 10 kW/m during monsoon months.

These findings confirm the regions' wave energy potential, forming a strong basis for further technical assessments that this study intended to do. Though both studies can be considerably robust, they lack integration approach into energy system models, a gap limiting system-value insights.

### 2.3.2. Wave Energy Converter (WEC)

Wave energy converters (WECs) is devices designed to harness the power of ocean waves and transform it into other form of usable energy. The wave energy extraction has been explored since the 1790s (one of the first known patents was filed by Pierre-Simon Girard, proposing method of harnessing wave power for water pumping in irrigation [39]), leading to the development of various technologies to date. Each system employs different method to capture wave energy, with deployment based on water depth and location; whether onshore, nearshore, or farshore. This diversity reflects the sector's ongoing development and availability of multiple alternatives to make use of wave power under different conditions [37].

The influential research of this thesis, Lavidas (2023) [17] explored the integration of wave energy into the PyPSA-EUR energy model to assess its impact on system dynamics. In their study, they considered three WEC types based on deployment depth and power extraction motion:

- *Shallow:* A 600 kW terminator surge-oriented device, designed for waters with a maximum depth of 20 m
- *Nearshore:* A point absorber WEC with 1000 kW capacity, operating at depths of 20-80 m
- *Farshore:* A flexible attenuator WEC with 750 kW capacity, suitable for depths of 50-150 m

***Point absorbers*** exhibit mature Technology Readiness Levels (TRL 8, according to [40]), reflecting reliable technologies that have passed concept validation and full-scale prototype testing at sea with ongoing efforts toward full commercial deployment. Their adaptability across Indonesia's varied coastal depths (20-150 m) aligns with the archipelago's bathymetry; unlike oscillating water columns or overtopping devices, which require specific site conditions [17, 33]. According to Lavidas et al. (2021), the optimal mean CF of point absorber (e.g. WaveStar, 600 kW, peak production at $\tilde{1}6$ kW/m, deployed in nearshore) prevails 22.3%, with peak reaches 30.9% [36], enhancing reliability. These indicates suitability of point absorber as a representative WEC device for this energy modelling approach.

#### Techno-economic Aspects of WECs

The economic viability of WECs remains as the primary obstacle to their commercial advancement up until when the thesis is conducted. This is largely driven by the complexity and expense of critical component, the power take-off (PTO) system, which influences the CF of WECs. According to IRENA (2014), PTO costs account for roughly 22% of lifetime expenses, driving up the levelized cost of energy (LCOE) and putting WECs at a competitive disadvantage [37].

The assessment of WEC performance and economic feasibility typically employs metrics such as the *power matrix, capacity factor (CF)*, and *LCOE*. The power matrix correlates device characteristics with energy production across varying sea conditions, equivalent to wind power curves, as noted in global studies [41]. The CF, an indicator of operational efficiency, varies according to local wave climates [17] and contributes to system-level benefits, including reduced storage requirements. LCOE, which taking

into account the capital and operational costs, currently ranges from 100–300 €/MWh for modern WECs [33], far exceeding solar PV's 30–60 €/MWh [34]). While these metrics could inform wave energy's potential, their application to Indonesia's multi-island grid via energy system modelling approaches remains underexplored in existing literature.

To estimate future cost trajectories, learning curves or multi-year scenarios for modeling the economic feasibility of wave energy are required for energy system modelling approach. Unlike mature renewables like solar PV and wind, wave energy remains at an early deployment stage, meaning cost projections in Indonesia must rely on international benchmarks and learning curve modeling.

Future cost reductions on WECs are considered achievable. Lavidas et al. (2023) showed that wave deployment is highly sensitive to cost assumptions [17], therefore one should not rely on a single cost input for wave. They argue that learning curves, whereby costs decline as installed capacity increases, could substantially reduce wave energy's LCOE by 2050, potentially by 30–50% depending on deployment and technological advancements [17]. Such projections rely on the pace of implementation and innovation, yet Indonesia-specific estimates remain unavailable, with the 2024 Indonesia Technology Catalogue providing no wave energy cost data [42], while tidal energy data is included.

The ***learning curve approach*** assumes cost reductions occur as cumulative installed capacity grows. Lavidas et al. employ a staged learning curve model, estimating cost reductions of 12% from 2020–2030, 8% from 2030–2040, and 4% from 2040–2050 [17]. In the absence of localized data, these international benchmarks delineate wave energy's economic potential, yet their relevance to Indonesia's grid necessitates further investigation; showing a gap this study seeks to address.

In this research, an approach will be to study realistic cost evolution scenarios (e.g. conservative case with high WEC CAPEX and an optimistic case with steep cost reductions by 2050) by introducing different cost assumptions or time points (periodically, e.g. 2030, 2040, and 2050). The results will highlight how different cost trajectories influence the competitiveness of wave energy in Indonesia's future energy mix.

### 2.3.3. Wave Energy Development in Indonesia

With its promising potential and consistent energy output, Indonesia has started exploring wave energy through research and pilot projects. According to the National Research and Innovation Agency of Indonesia (BRIN) [9], several initiatives have been undertaken related to wave energy converters.

In the early 2000s, the Agency for the Assessment and Application of Technology (BPPT) developed a medium-scale wave energy prototype at Baron Beach, Yogyakarta, known as *(Pembangkit Listrik Tenaga Gelombang Laut, 'PLTGL')*. This educational project operated between 2004 and 2006 but was discontinued due to changes in policy and research priorities, and recently revived with optimization efforts by Kurniawan et al. (2024) [43], to improve the previous prototypes' efficiency. BRIN also noted the recent effort of PLN, the state-owned electricity company, signed MoU with Waves4Power in 2022 to study feasibility of point absorber parks in Bali and Nusa Tenggara. Other studies was done by PT Pembangkitan Jawa Bali (PJB) in collaboration with Energy Study Center of Universitas Gadjah Mada (UGM). They highlighted Southeast Maluku's Yamdena Island in the eastern part of Indonesia, as a promising site for wave energy deployment. The study estimated a levelized cost of electricity (LCOE) of $38.10/kWh for a 1 MW installation, with costs expected to drop to $16.25/kWh for projects exceeding 11 MW; compelling findings with high local electricity tariffs in the eastern part of Indonesia [9].

These ongoing initiatives and research efforts reflect Indonesia's increasing openness to wave energy as a viable renewable energy sources, which motivates this study to assess MRE, particularly wave energy's contribution to Indonesia's energy system planning.

## 2.4. Tidal Energy

Tidal energy is a form of renewable energy that harnesses the power of ocean tides to generate electricity. It is derived from the gravitational interactions between the Earth, the moon, and the sun, creating predictable and regular tidal cycles. Tidal energy can be captured through the potential energy from the difference in water levels (tidal range; using barrages or lagoons) or the kinetic energy of moving water in tidal currents (tidal stream; deploying turbines in fast-moving water currents) [44, 45].

***Tidal stream*** technology is selected for this thesis scope due to its cost competitiveness. According to the Technology Catalogue for Indonesia [42], the costs of tidal stream energy are expected to decrease as technology improves and more projects are developed. Global trends suggest that costs could reach levels competitive with other renewables, such as offshore wind, by 2030 with broader deployment. Indonesia's geography, with numerous straits and channels like the Larantuka and Alas Straits, offers sites with tidal currents exceeding 3.0 m/s, making it ideal for tidal stream technology [42].

Tidal stream energy harnesses the kinetic energy from fast-moving tidal currents using underwater turbines to generate electricity. This method is preferred over other tidal technologies, such as tidal range, due to its potential for greater cost competitiveness, advancements in technology, and reduced environmental impact by avoiding large structures like barrages or dams [45]. A significant advantage of tidal stream energy is its predictability. Tides follow a regular pattern driven by the gravitational forces of the moon and sun, allowing for accurate forecasting of energy production. This predictability facilitates easier integration into the power grid compared to less predictable renewable sources like wind or solar [45].

To determine the energy production potential at a specific site, researchers rely on hourly production profiles. These profiles illustrate how power output varies over time based on tidal current speeds. Lewis et al. (2019) conducted a study using ocean models to simulate tidal currents, often incorporating data from global tidal models such as TPXO, at resolutions suitable for hourly profiles [45]. Tools like PyTMD [22], a powerful, open-source Python library, can process this data to generate accurate hourly current speed profiles. With these hourly speeds, the power output of a turbine can be estimated using its performance specifications.

### 2.4.1. Tidal Energy Resources and Global Deployment

Tidal energy resources are highly site-specific, shaped by local bathymetry, hydrodynamic conditions, and astronomical tidal forcing. Assessing tidal energy potential requires detailed analysis of tidal current velocities, which drive electricity generation in tidal stream turbines. A widely used approach involves extracting tidal constituents (e.g. M2, S2, K1) from global tidal models like TPXO [21], a dataset providing harmonic constants for predicting tidal heights and currents worldwide. These constituents (each defined by a specific frequency, amplitude, and phase) enable the computation of hourly tidal velocity profiles at any location. Such profiles are critical for estimating the power output of tidal turbines, calculating metrics like average power density, and identifying periods of peak generation potential [46].

Globally, regions with tidal current velocities exceeding 2.5 m/s are considered viable for tidal energy generation. Examples include the Pentland Firth in Scotland, where the MeyGen project has produced over 50 GWh since 2018 [40], and the Bay of Fundy in Canada, known for its extreme tidal ranges. In Indonesia, straits such as Larantuka and Alas have been identified as promising sites, with tidal currents surpassing 3.0 m/s [13, 9]. However, accurately quantifying Indonesia's exploitable tidal potential requires integrating TPXO data with high-resolution hydrodynamic models (e.g. Delft3D, FVCOM) and in-situ measurements to refine velocity profiles and optimize turbine placement [46, 47].

### 2.4.2. Technological Developments and Cost Trends

The tidal energy sector has advanced significantly, particularly in turbine efficiency and cost reduction, though high costs and logistical challenges continue to hinder commercial-scale deployment. The UK leads in tidal stream technology, with projects like Nova Innovation and MeyGen demonstrating sustained performance, having produced over 50 GWh since 2018 [48, 40]. Floating and bottom-mounted tidal turbines, typically rated at 1-2 MW, are emerging as dominant technologies [48].

Early-stage tidal stream projects exhibit a levelized cost of energy (LCOE) of €150-200/MWh, but projections indicate this could decrease to €80-100/MWh by 2030 through economies of scale, technological advancements, and increased deployment [48, 40]. The European Commission's Joint Research Centre (JRC) suggests an LCOE of €90/MWh is achievable at 1 GW of installed capacity, nearing competitiveness with offshore wind [40]. Cost reduction strategies include scaling turbine production, streamlining installation processes, and enhancing turbine efficiency to maximize energy capture from tidal flows [48, 47]. Orhan et al. (2016) highlight that optimizing turbine placement based on detailed velocity profiles can further improve efficiency and reduce costs [46].

### 2.4.3. Tidal Energy Development in Indonesia

Indonesia holds significant tidal energy potential, notably in the Larantuka and Alas Straits, where tidal currents exceed $3.0\,\text{m/s}$ [13, 9]. The National Energy Plan targets 3.0 GW of ocean energy by 2050, reflecting government recognition of marine renewables as a key development area [9]. However, no grid-connected tidal projects exist yet, with progress hindered by regulatory uncertainty, inadequate infrastructure, and high costs [13].

Feasibility studies and planned pilot projects, such as the 10 MW initiative in East Nusa Tenggara, signal growing interest in commercial deployment [13]. Key challenges include an unclear regulatory framework deterring investors, low technology readiness requiring further R&D, and infrastructure gaps in remote, high-potential sites needing grid expansion [13].

Further research is needed to enhance tidal resource assessments, refine cost models, and validate techno-economic viability within multi-renewable grids. Advanced modeling frameworks like Calliope could improve evaluations of tidal energy's role in Indonesia's energy transition.

## 2.5. Energy Storage

Energy storage stands as a critical component of Indonesia's island-based power system, particularly as the nation aims to source nearly half of its energy from renewables [14]. Given the country's fragmented geography and ambitious renewable targets, balancing supply and demand depends heavily on effective storage solutions. MRE, particularly wave and tidal power, offers distinct generation patterns that could ease this pressure. Wave energy, with its seasonal peaks and consistent output along Indonesia's coastlines [12, 11], complements the daily fluctuations of solar power. Tidal energy, driven by the predictable gravitational forces in straits such as Larantuka [13], provides a steadier output, unlike the shorter-term variability of waves. Together, these sources present an opportunity to reduce the storage demands of Indonesia's dispersed grid.

Insights from global research highlight MRE's potential to ease storage requirements. Lavidas et al. (2023) observed that wave energy's strong performance during Europe's winter months reduced battery dependence by 15%, a finding that resonates with Indonesia's monsoon-driven demand peaks [17]. Lavidas et al. (2023) show that in Romania and Hungary, wave energy smooths out wind and solar intermittency, hence stabilized the grid [17]. Romania's mix of offshore wind, wave energy, and hydropower yields a steady generation profile year-round, while Hungary's solar-heavy system produces sharp daily dips, leaning on imports and storage.

Similarly, the MeyGen tidal project in Scotland demonstrates how steady generation can lower the need for reserves, though its reliance on specific locations limits broader application [40]. In Indonesia's context, wave energy's alignment with wet-season needs could offset solar's variability, while tidal power's consistency might stabilize supply in select regions. Yet, challenges persist: the nation's isolated grids depend on costly storage options like batteries or scarce pumped hydro sites [1]. Still, MRE's relatively predictable nature suggests it could reduce the volume of backup reserves required, enhancing overall system efficiency [34].

Existing studies, such as the 'calliope-indonesia' model, attempt to address these dynamics but fall short due to their simplified design, treating each province as a single unit [1]. The approach overlooks the local variations, such as wave-rich regions or tidal-rich straits, that shape storage needs, especially in high-demand zones like Java. This leaves open the question of how wave and tidal energy might reshape storage strategies, whether in a unified Supergrid or the fragmented island systems, as Indonesia pursues its net-zero goal by 2050; ten years ahead of the national target of 2060.

## 2.6. MRE Integration into Energy System Models

Recent literature shows MRE integration into energy system models aids decarbonization, with global insights relevant to Indonesia's grid [17]. Here, MRE integration means adding wave and tidal energy to calliope-indonesia to evaluate their role in Indonesia's net zero goal [1].

### 2.6.1. Wave Energy Integration

Integrating wave energy into large-scale energy system models is a relatively recent development, driven by the increasing recognition of its potential to complement wind and solar power. Early studies

on wave integration primarily relied on simplified capacity factor assumptions or considered isolated, non-interconnected systems, limiting their applicability in real-world energy planning [17, 40]. Recent advancements have improved the modeling of wave power by incorporating high-resolution climate datasets, technology-specific power matrices, and multi-resource optimization frameworks, enabling a more comprehensive assessment of wave energy's role in future energy systems.

A notable example is the work by Lavidas et al. (2023), who extended the PyPSA-Eur framework to develop the PyPSA-MREL-TUD model, which explicitly integrates wave energy as a generation source alongside wind, solar, and storage [17]. The methodology employs a power matrix approach, where wave energy converters (WECs) are characterized based on their performance across different sea states, enabling a more realistic representation of wave power's temporal variability. ERA5 reanalysis climate data is used to derive site-specific wave energy availability, ensuring that modeled wave generation profiles reflect real-world seasonal and interannual variability.

Beyond PyPSA, other modeling frameworks have explored wave energy integration, albeit with varying levels of sophistication. The Joint Research Centre's (JRC) TIMES-EU energy model included wave energy in long-term European decarbonization scenarios but relied on fixed cost assumptions rather than dynamic learning curves, potentially underestimating wave power's future competitiveness [40].

Wave energy's system benefits include winter peak generation, aligning with low solar periods, and lower short-term variability than wind, reducing balancing needs [17]. PyPSA-MREL-TUD simulations for a 100% renewable Europe scenario showed wave power enhancing resilience in Atlantic regions, where high wave energy potential aligns with demand centers, suggesting potential parallels for Indonesia [17]. However, modeling challenges persist, such as capturing curtailment and storage interactions in high-renewable scenarios.

Wave energy integration into calliope-based models is underexplored, offering research potential [1]. Calliope's modular, high-resolution framework could improve energy system studies by including wave energy as a distinct asset, especially for multi-resource optimization. Research could prioritize developing cost and learning rate projections and extending open-source models with spatially and technologically disaggregated wave energy datasets. Despite progress in large-scale modeling [17, 40], methodological enhancements are important, to fully assess wave energy's system-wide benefits and constraints.

### 2.6.2. Tidal Energy Integration

Tidal energy, distinguished by its predictable cycles, presents a promising renewable resource for archipelagic nations like Indonesia, yet its integration into energy system optimization models (ESOMs) remains less developed compared to wind or solar, largely due to cost and technological challenges. Studies have begun to address this by exploring how tidal energy's reliable output can be modeled to support decarbonization goals. Recently, Dixon et al. (2025) [49] integrated in-stream tidal energy into the OSeMOSYS model for the Philippines, using site-specific current velocities and turbine power curves to generate time-series power outputs, which were then incorporated as a dispatchable supply technology. Their approach involves collecting velocity data (often from numerical models) selecting suitable tidal stream turbines, and embedding these profiles into the ESOM while respecting grid stability and capacity constraints.

This method offers a blueprint for the 'calliope-indonesia' model, which has yet to include tidal energy [1]. Calliope's adaptable structure supports the addition of tidal energy as a supply technology, requiring inputs like site-specific capacity factors and cost trajectories. Orhan et al. (2016) [46] provide a relevant example, assessing tidal currents in straits like Alas Strait using high-resolution Delft3D models, calibrated with TPXO tidal data and local bathymetry, revealing peak velocities of 3–4 m/s. By adapting such data (potentially sourced from TPXO and GEBCO for broader coverage) one could construct power output profiles for Indonesian sites, enabling the 'calliope-indonesia' model to evaluate tidal energy's contribution to system reliability and cost reduction. While wave energy integration, as explored by Lavidas et al. (2023) [17], shares similarities, tidal energy demands distinct handling of current-driven turbine outputs.

For projected cost estimations, 2024 Indonesia technology catalogue [42] can be a valuable reference for both CAPEX and OPEX assumptions of tidal stream's technology for this thesis, similar approach

taken by Langer et al. (2024) in their study [1].

## 2.7. Energy System Models

The pathway to achieve target of 3.0 GW offshore energy technologies installed capacity by 2050 from zero is undoubtedly challenging. Although the resource potentials are immense in Indonesia, the realization process requires careful planning and strategic integration, including a modelling approach for energy system.

### 2.7.1. Models Overview and Comparison

As comprehensive planning tools, Energy System Models (ESMs) are designed to explore diverse configurations of energy systems by integrating a mix of energy generation & storage technologies and network infrastructure. According to Pfenninger et al. (2014), ESMs are categorized into four types: optimization, simulation, power system, and qualitative models, each serving distinct analytical roles in energy planning [16].

Many scientific reviews exist on ESMs, with most of them focusing on the comparison of optimization vs. simulation approaches, spatiotemporal resolution, sectoral coverage, and their ability to integrate renewable energy sources. For example, Ringkjøb et al. (2018) reviewed 75 modelling tools, classifying them based on their capability to assess energy systems with high shares of variable renewables [50]. Groissböck (2019) assessed 31 mostly open-source optimization tools, comparing them based on technical maturity and functional capabilities against available commercial models [51]. Laveneziana et al. (2023) critically emphasized the trade-off between long-term planning and operational modelling for sustainable development while comparing alternative energy system models to support investment strategy at company-level [52]. Through this literature study, a comparison of relevant ESMs for the thesis context is presented in Appendix A.2.

For this thesis, which investigates the optimal integration of wave and tidal energy into Indonesia's multi-island grid by 2050, an *Energy System Optimization Models (ESOMs)*. ESOMs excel at determining the least-cost configuration of generation, storage, and transmission assets over time, making them ideal for long-term decarbonization planning [1]. Unlike simulation models, which forecast predefined scenarios, or power system models, which focus narrowly on electricity markets, ESOMs provide the system-wide optimization needed to assess the economic and technical feasibility of emerging technologies like wave and tidal energy.

Past studies indicated that Indonesia has implemented energy system modelling approach to assess and plan the national power sector, reflected in official planning documents like RUEN (by National Energy Council, utilizing *Long-range Energy Alternatives Planning 'LEAP'* tools, RUPTL (by PLN) and Indonesia Energy Outlook (by Ministry of Energy and Mineral Resources). Unfortunately, most rely on proprietary software (e.g. IESR used commercial software *PLEXOS* [53]), hence tracing the steps, reproducing, or conducting future works are difficult.

**Open-source Modelling Tools**

Over the last decade, ESMs have evolved from proprietary, closed tools toward open-source framework to meet modern research and policy needs. Transparency is now seen essential for credibility in energy modelling. According to Pfenninger et al. [16], the lack of openness in national energy planning may hinder scrutiny and adaptation. They emphasize the need for open-source code, data, and clear assumptions, so that other experts may understand and trust the model. In line with this, recent surveys show a surge in open-source development, with Python dominating due to its flexibility [51]. Chang et al. (2021) also note a push for open access and high-resolution temporal modelling to handle variable renewables [54]. Python-based models allow customization by the script, which is a major advantage for tailoring the models to include active innovations like wave energy in this study.

Research focus has also turned to modelling renewable-based power systems in Indonesia recently, although often using a copperplate assumption, where electricity generation and consumption occur in a single national node and most studies focus on local scales [1]. This overlooks disconnected nature of Indonesia's island-based grid and the mismatch between renewable energy generation and demand, such as Java's high demand but limited space for onshore renewables). Langer noted a common drawback found in most of existing energy models for Indonesia, which is overlooking the spatial and temporal variations in renewable energy production and electricity demand. Further investigation on

the current knowledge gap in energy system modelling is recommended, such as to consider alternative power from ocean [1], including wave and tidal energy as the focus of the study.

**Spatial and Temporal Resolution Requirements**
Integrating MRE into an energy system model also introduces specific spatial and temporal requirements. Wave and tidal energy are variable renewable resources, characterized by location-specific availability (although not as limited as tidal energy) and fluctuations over hours to days. Models must therefore support *multi-regional resolution* (to represent distinct wave resource sites and grid connection points) and *high-frequency time-steps* (to capture the variability).

Ringkjøb et al. [50] highlighted that many newer models can cover multiple geographic scales and finer time resolution, which is crucial for high renewables. In their comparison, *Calliope* stands out with completely user-defined spatial and temporal resolution, able to model anything from a single community microgrid to continental systems with hourly (or finer) time-steps. Likewise, *PyPSA* is designed for nodal network modelling and typically runs at hourly resolution for a specific year. In contrast, some long-term planning models aggregate time into a few representative periods, which may miss short-term variability. For instance, *OSeMOSYS*, a combined TIMES-PLEXOS model, uses an intra-annual time-slice approach (e.g. 12 representative day types), reduces computational complexity but comes at the cost of acuracy for variability, e.g. prone to over- or underestimate the contribution of wind energy (impact on backup generation or storage requirements) that may misguide policy and investment decisions. Recent research confirms this, Chang et al. [54] found that improving temporal detail has been a key focus to enable modelling future scenarios with high shares of variable renewables. Thus, model for MRE integration should allow at least hourly resolution and flexible time-step definitions as well as multiple regions or nodes representation so that wave resource locations can be distinguished on the grid.

Another important criterion is scalability, to use the same modelling framework at different spatial scales, ranging from a broad national level down to regional or local subsystems. It is particularly relevant for this study to examine MRE integration at a national level, then zoom into specific regions to examine local grid impacts. Laveneziana et al. (2023) stress that the ”best compromise” for energy planning comes from multi-scale tools that combine long-term planning with detailed operational modeling [52]. Table 2.1 compares the scalability characteristics of major energy system models.

**Table 2.1:** Energy System Models: Scalability and Multi-Scale Capabilities for MRE Integration

| Model | Spatial Scale | Multi-node | Temporal Resolution | MRE Suitability | Key Limitations |
|---|---|---|---|---|---|
| Calliope | Local to Continental | Yes | Hourly to Annual | High | High computational requirements for large-scale models |
| Backbone | Local to Continental | Yes | Hourly to Annual | High | Limited documentation compared to Calliope |
| oemof | Local to National | Yes | Hourly to Annual | High | Steeper learning curve for beginners |
| FINE | Local to Continental | Yes | Hourly to Annual | High | Relatively new framework, smaller user community |
| SpineOpt | Local to Continental | Yes | Sub-hourly to Annual | High | Complex setup for simple applications |
| EnergyPLAN | National | No | Hourly | Medium | Single aggregated unit, loses spatial distinctions for coastal MRE |
| MARKAL/TIMES | National/Regional | Limited | Annual/Seasonal | Low | Typically one node per country, not suitable for location-specific MRE |

For harnessing location-specific wave and tidal energy resources that are abundant in some regions but absent elsewhere, multi-node models are preferred to capture geographic disparities [17]. Calliope's flexible architecture allows users to define spatial scope (number of regions/nodes) and temporal scope without changing the core code, treating data and mathematical structure separately [55].

Based on the above comparison, Calliope is one of the model that satisfies key criteria for this intended research. The following section 2.7.2 will elaborate Calliope in more detail as the chosen framework, including the 'calliope-indonesia' model limitations [1] that can be further addressed.

### 2.7.2. Calliope Framework

Calliope is one of state-of-the-art energy system optimization modelling framework which was developed and later published in 2018 by Pfenninger et al. [18]. Its implementation in Python with a Pyomo back-end makes it highly customizable while still leveraging powerful solvers for optimization. It is free (distributed under Apache 2.0 license) and has open-source code which can be analyzed and modified by users for further research. While it is designed for the Python environment, Calliope also provides a command-line interface option for users who prefer a simpler setup over scripting. The framework employs *linear programming* to model energy production, storage, and consumption through mathematical formulations. Its modular design makes it easy to adjust generation profiles, cost assumptions, and technology parameters without changing the core optimization algorithms, supporting scenario testing and sensitivity analysis [55].

Although Calliope can operate on standard computers, high-performance computing systems (e.g. virtual machines) are recommended for large-scale models (including Indonesia's archipelago) due to the framework's high number of constraints compared to other ESOMs [56]. These constraints, defined through equality or inequality expressions, limit one or more variables. For example, technological constraints include allowed capacities, conversion capacities, lifetime (for levelized cost calculations), and resource consumption. A complete list of available technology constraints can be found under Technology Constraints in the calliope website.

Calliope has been applied across diverse scales, proving its adaptability. National studies in the UK [57], Switzerland [58], Italy [59], India [60], Africa [61], and Indonesia [1] have used it to plan energy transitions, while smaller-scale efforts model a Swiss residential building [62], an Indian city [63], and European networks [64, 65]. This range of applications highlights its ability to handle both broad and localized energy systems, a key reason for its selection in this study, building on the 'calliope-indonesia' model [1], which has yet to include wave and tidal energy despite its relevance to Indonesia's decarbonization pathway.

What sets Calliope apart for this thesis project is the foundation laid by earlier modeling efforts, particularly the national-scale framework developed by Langer et al. (2024) [1], which this thesis builds upon to sustain momentum in Indonesia's energy transition, extending the model to incorporate marine renewable energy (wave and tidal power) into the scenarios and assessing their contribution to the system. Moreover, the framework's ability to represent Indonesia's islanded grid as distinct nodes, such as Java's provinces (Banten, Jakarta, West Java, Central Java, Yogyakarta, East Java), where high demand aligns with wave energy potential [66]. This allows for detailed analysis of MRE's role, both nationally and within specific regions, by integrating it as a supply technology alongside co-optimized generation and storage. The model can operate at hourly resolution over a year—or even multiple years—to capture wave power's daily and seasonal patterns accurately. Compared to other open models like PyPSA, which needs extra setup for multi-year planning, or Oemof, which requires more initial configuration, Calliope offers a strong mix of flexibility, high-resolution data handling, and multi-scale scope. Specifically, Calliope's flexibility makes it superior for MRE integration in Indonesia's fragmented grid compared to PyPSA's static focus. For Indonesia's energy transition, covering generation, grid dynamics, and long-term climate goals—Calliope proves a fitting choice, though Calliope computational demands require careful management with large datasets.

ESOMs, such as Calliope, depend on efficient solvers to tackle the computational challenges of large-scale linear and mixed-integer linear programming problems. Among these, the Gurobi solver [67], a commercial optimization tool, is widely recognized for its ability to deliver rapid and reliable solutions. Within the Calliope framework, Gurobi optimizes system configurations by minimizing total costs—balancing supply and demand, transmission constraints, and the variable output of renewable sources like wave and tidal energy. Its key strengths include swift computation of complex scenarios, adept handling of integer constraints (e.g. discrete technology investments), and support for high spatial and temporal resolutions. Unlike open-source alternatives such as CBC or GLPK, which are also supported by Calliope, Gurobi offers superior performance for large-scale models, reducing solution times significantly [55]. Though its commercial licensing may limit post-academic use, free academic licenses and superior performance make it a robust choice, provided input data is well-prepared to maintain numerical stability.

### 2.7.3. Existing Framework: Calliope-Indonesia

In the context of Indonesia, prior extensive research by Langer et al. (2024) [1] developed a comprehensive model of the country's electricity system to assess pathways for achieving full decarbonization as pleged before. The model is developed using Calliope version v0.6.10 and openly accessible via Github link 'calliope-indonesia' [1]. This research intends to build upon the foundation by incorporating wave and tidal energy into the model, aiming to portray the contribution of MRE in the future net-zero emission power system of Indonesia.

To integrate both energies into the existing model, understanding the existing framework developed in [1] is mandatory. The analysis taken during the literature review include studying the technologies which already considered (energy generator and storage), the simplification of power transmission grid, and scenario analyses that already done.

Key parameters taken in Langer's model is presented in 2.2.

| Parameters | Description |
|---|---|
| Generation Technology | Coal (supercritical), Diesel (reciprocrating engine), CCGT, OCGT, Large hydro (reservoir), biomass (direct combustion steam turbine), Geothermal, Small hydro (run-of-river), Solar PV (ground-mounted, utility-scale), Offshore Floating Solar PV, Onshore Wind, Offshore Wind, Nuclear, OTEC |
| Storage Technology | Battery (lithium-iron), Pumped hydro (closed-loop) |
| Transmission | Onshore power transmission (AC), Subsea Power Transmission (HVDC) |
| Energy carrier | Electricity (Power); heat and gas are not considered |
| Spatial Resolution | National scale (34 provinces; each represented by single node) |
| Temporal Resolution | 3-hour time steps |
| Network Topologies | With island links and without island links |
| Decarbonization Pathways | Models pathways from 2020 to 2050, with full power system decarbonization by 2040 and 2050 |

**Table 2.2:** Key parameters in Langer study (2024) [1]

In [1], node and interconnection features of Calliope framework is used to establish model regions, including production, consumption, storage, and exchange of energy carriers (electricity; heat and gas are beyond the scope of the study). Langer modelled each province as a single-node (considering 34 provinces of Indonesia), as seen in Figure 2.2.

Offering a diverse solutions using high spatial and temporal resolution ESOM to minimize costs, the current 'calliope-indonesia' model can be further improved for Indonesia's power system decarbonization plan.

#### Modelling Constraints in Calliope-Indonesia

ESOMs like Calliope optimize least-cost energy configurations based on detailed inputs ('constraints' to the model) [18, 55]. This model minimizes annualized system costs; capital, fixed, and variable operational expenses, across user-defined nodes and hourly timesteps, to ensure supply-demand balance for a target year (e.g. 2050).

#### Grid Scenarios

Indonesia's net-zero emissions target may relies on *grid strategies* to account MRE power like wave and tidal energy. Two scenarios dominate the literature: a centralized 'Supergrid' and the current fragmented grid. Langer et al. (2024) [1] modelled these extremes, with the fragmented setup isolating islands (except Java-Bali connection), while the Supergrid, endorsed by RUKN (2024) [14], envisions inter-island links by 2040 [1].

1. *'Supergrid' scenario (a):* Concept that connects islands via a robust network; enabling MRE from southern coast wave resources to supply demand centers (e.g. Java island). This may reduce

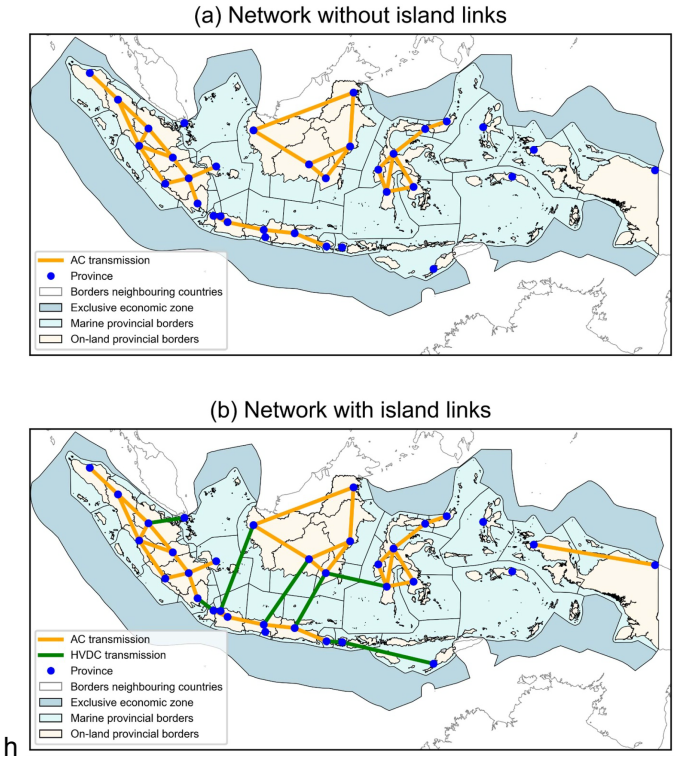


h

**Figure 2.2:** Indonesia's electricity transmission network modelled in Langer et al. (2024) [1]: (a) current state without island links, and (b) proposed 'supergrid' with interconnections

curtailment, but high HVDC costs and environmental risks (e.g. seabed disruption) challenge its feasibility

2. *Fragmented grid scenario (b):* Each island relies on its own grid; emphasizing local energy solutions, particularly in wave-rich regions. Yet, their system-wide impact is constrained without inter-island links, often relies on local storage solutions or fossil backups to manage variability (risks are higher costs and emissions, clashing with net-zero goals, as isolated grids struggle to optimize renewable resources efficiently)

Extending the 'calliope-indonesia' framework to include MRE could reveal how wave and tidal energy perform under a Supergrid, potentially reducing reliance on fossil peaking plants, or in fragmented grids, where localized solutions dominate. Global studies, such as Lavidas et al. (2023), suggest MRE's complementary temporal profile (e.g. winter peaks) enhances grid stability in interconnected systems, an insight yet to be tested in Indonesia's context [17].

The Supergrid aligns with RUKN's plan to link coastal MRE to demand centers, cutting fossil fuel use, though grid capacity constraints may limit its effectiveness in supporting large-scale renewable integration [14]. Conversely, the fragmented scenario limits MRE's scalability, trading local gains for national scale. Thus, MRE's contribution to Indonesia's net-zero strategy depends heavily on the chosen grid pathway, with ESOMs providing a critical lens to evaluate these dynamics.

### Grid Expansion Requirements

The integration of MRE into Indonesia's power system is contingent on the development of a robust transmission network. Given Indonesia's fragmented geography, efficient energy transmission from offshore and coastal generation sites to high-demand areas, particularly Java, necessitates strategic grid expansion. The optimal grid development strategy will be explored to accomodate MRE by 2050 through this study, addressing existing limitations in the 'calliope-indonesia' model.

As of 2024, Indonesia's power system operates with a total transmission network spanning 71,834 km and a substation capacity of 175,139 MVA [14]. Java, the nation's economic hub, is supported by a 500 kV backbone and 150 kV regional networks. However, these networks experience congestion,

particularly in urban demand centers, limiting future variable renewable energy penetration, including MRE.

The 'calliope-indonesia' model [1], represents each province as a single-node, simplifies the grid structure but does not capture intra-provincial transmission bottlenecks. Furthermore, inter-island links are modeled as optimizable HVDC connections with a maximum capacity of 50 GW per link, a constraint that may not reflect realistic technical or economic limitations. While the model effectively optimizes system-wide costs, it does not explicitly consider marine renewables, which are location-dependent and require extensive grid integration strategies.

*Implications to MRE*
Indonesia's long-term transmission strategy, as outlined in the updated RUKN 2024 [14], includes significant capacity upgrades, reaching a projected 353 GW (by 2060) from 91 GW (in 2023) [14]. This government's roadmap prioritizes Supergrid interconnections, which will facilitate the large-scale integration of renewables. Key inter-island transmission links include:

1. *Sumatra-Java (2031)* facilitating transmission of offshore and wave energy from Sumatra's western coast
2. *Bali-Lombok-Sumbawa (2035)* may unlocks potential tidal stream energy corridors in eastern Indonesia
3. *Jawa-Kalimantan (2040)* to enable export of 'affordable' renewables from Kalimantan, such as future offshore wind
4. *Kalimantan-Sulawesi (2041)* could strengthen long-distance electricity transport from Sulawesi's marine energy hotspots

Economically, the total estimated investment for transmission infrastructure over the period 2024-2060 is US$ 1.1 trillion, or approximately US$ 30 billion per year [14]. Given the capital intensity of HVDC subsea cable deployment (US$ 1-3 million per km), a strategic expansion plan is critical to optimize MRE contribution while maintaining cost-effectiveness aspect.

The Supergrid projects could enhance MRE integration potential, however, delays in execution would entail alternative strategies, localized storage solutions, and well-distributed generation should be considered to ensure system resilience and efficient MRE utilization.

## 2.8. Techno-economic Metrics

Economic assessments of power generation technologies have historically relied on the Levelized Cost of Electricity (LCOE), which measures the average cost of electricity production over a plant's lifetime.

The levelized cost of electricity (LCOE), expressed in €/MWh, represents the average net present cost of electricity generation over the entire operational lifespan of a power plant [68]. It is used as a comparison metric of feasibility and competitiveness of different electricity generation technologies [69].

According to [34], LCOE was originally developed as a comparison among different dispatchable based load technologies in regulated systems; therefore, it serves as an important measure for policy-making and modelling. LCOE is calculated based on a levelised average lifetime cost approach, using the discounted cash flow method.

Calculated via discounted cash flow, LCOE incorporates capital costs, fixed and variable operation and maintenance (O&M), energy output (capacity factor, CF), project lifetime, discount rates, and degradation rates for VRE like MRE [69]. Additional inputs are also considered, such as financial data (e.g. debt terms), fuel costs (if applicable), and plant characteristics (e.g. outages) [68]. The formula of LCOE calculation which suggested by IRENA [70], is:

$$LCOE = \frac{\sum_{t=1}^{n} \frac{I_t + M_t + D_t}{(1+r)^t}}{\sum_{t=1}^{n} \frac{E_t}{(1+r)^t}} \tag{2.1}$$

where $I_t$ is investment costs, $M_t$ is maintenance, $D_t$ is decommissioning, $E_t$ is the sum of all electricity generated over the years of operation, $r$ is the discount rate of the project, and $n$ is the life of the project.

In conclusion, this chapter has examined the literature concerning MRE integration, with 'calliope-indonesia' framework published by Langer (2024) [1] as the groundwork for this thesis research, focusing on grid expansion, energy storage demands, and techno-economic evaluation aspects. Existing research provides valuable perspectives on MRE's potential, highlighting its capacity to enhance grid reliability [17] and economic viability. However, the specific implications for Indonesia's unique archipelagic grid structure and inter-island transmission requirements remain underexplored. The following chapters aim to address these shortcomings through modelling efforts and system-level analysis, thereby generating insight into MRE's contribution to Indonesia's net-zero objectives.

# 3. Methodology

## 3.1. Wave Energy Modeling

Waves are the energy generated when the wind imparts its kinetic energy to the ocean's surface. They carry both kinetic and potential energy that can be computed based on two main parameters: *wave height* and *wave period*. Real ocean waves are complex and most of them are irregular waves. To simplify, regular waves has a single frequency and amplitude, while random / irregular waves have variable frequencies and amplitudes. One important characteristic of waves is that they are location-dependent, thus one should assess wave conditions in a specific area to be able to harness the energy they contained.

### 3.1.1. Wave Power Theory

Wave power represents the rate at which energy is transported by ocean waves across a given wave crest length. It can be computed by analyzing wave characteristics, such as significant wave height ($H_s$) and energy period ($T_e$). The wave power level is expressed as power per unit length (e.g. $kW/m$) [41].

Under deep-water conditions, the wave power equation is expressed as a function of significant wave height ($H_s$) and energy period ($T_e$):

$$P = \frac{\rho g^2}{64\pi} H_s^2 T_e$$

where $\rho$ represents seawater density and $g$ is gravitational acceleration. Here, $H_s = 4\sqrt{m_0}$ and $T_e = \frac{m_{-1}}{m_0}$, where $m_n$ represents the $n$-th order spectral moment.

For practical applications, $T_e$ is commonly approximated using the peak wave period $T_p$ and a calibration coefficient $\alpha$, where $T_e = \alpha T_p$. The value of $\alpha$ typically ranges between 0.8 and 1.0, depending on the sea state and spectral shape [41].

The theoretical foundation bridges the gap between raw wave energy availability and the technical energy output achievable by wave energy converters (WECs).

### 3.1.2. Wave Energy Converter

In general, wave energy devices consist of four main components, which are the *structure and primary mover* as the energy catcher, *foundation or mooring* that keeps the structure and primary mover in position, the *power take-off (PTO) system* that convert mechanical energy into energy carrier (e.g. electricity), and the *control systems* for performance optimization and protection during operation.

Beyond the components, understanding the process of harnessing wave energy is important. Wave energy is excited through movement of the ocean's free surface. WECs typically generate electricity by converting the relative motion between two bodies; one moving with the waves and the other remaining completely static or semi-static. These bodies can both float on the surface, be fixed to the seabed, or remain fully submerged, as long as relative movement occurs between them. The forces generated by this motion are captured and converted into electricity through the PTO system.

The Power Matrix ($PM$) is used to estimate the energy generation of WECs, considering device characteristics such as size, weight, response amplitudes, and excitation forces, which directly affect power production under specific metocean conditions. Consequently, estimating energy output requires integrating the wave scatter diagram with the device's power matrix. To conduct the wave energy modelling in this study, we will utilize the power matrices of the selected WEC technologies to assess their potential energy generation. Power matrices work like power curves in wind energy, showing how much power a device can produce under different sea conditions based on wave height (Hs) and wave period (Tp). Each combination of wave height and wave period corresponds to a specific power output.

The wave energy output ($E_o$) is calculated using the following equation:

$$E_o = \sum_{i=1}^{n_{T_p}} \sum_{j=1}^{n_{H_s}} F(H_{s_{ij}} \cap T_{p_{ij}}) \times PM_{ij} \times \Delta T \tag{3.1}$$

where $n_{T_p}$ and $n_{H_s}$ represent the number of peak wave periods and significant wave height classes, respectively. Here, $F(H_s, T_p)$ denotes the joint probability of sea states, $PM_{ij}$ corresponds to the power matrix output for each sea state, and $\Delta T$ represents the time interval considered.

The energy production further depends on the rated power of the WEC ($P_o$), indicating that devices with higher installed capacities are capable of generating more electricity. However, to evaluate the overall efficiency and performance of a WEC, the capacity factor ($CF$) is often utilized. This metric reflects the proportion of time a technology operates at full capacity and can be expressed as:

$$CF = \frac{E_o}{P_o \times \Delta T} \tag{3.2}$$

Higher CF indicate better energy production efficiency, while lower values suggest suboptimal device performance relative to site-specific wave conditions. The CF is influenced by intra-annual, seasonal, and monthly variability of the wave climate, emphasizing the need for careful WEC selection suited to the deployment location.

In addition to performance metrics, the economic viability of WEC deployment is often assessed using the Levelized Cost of Energy (LCoE). LCoE estimates the cost per unit of electricity generated over the project's lifespan, considering capital expenditure (CapEx), operational and maintenance (O&M) costs, and energy production. It is defined as:

$$LCoE = \frac{PV(CapEx + OM) - PV(S)}{AEP} \tag{3.3}$$

where $AEP$ represents the annual energy production, and $PV(S)$ refers to the present value of salvage costs. While LCoE is a crucial metric for project evaluation, it does not solely determine economic feasibility, as other financial indicators such as Net Present Value (NPV) and Internal Rate of Return (IRR) are also considered [41].

### 3.1.3. Site Selection

To identify suitable locations for WEC deployment, a geospatial site selection process was implemented using physical and regulatory constraints. The spatial resolution and filtering logic are setup to create realistic deployment feasibility in Indonesia's maritime zones for energy system modeling.

#### Input Datasets

**Table 3.1:** Datasets used for wave site selection

| Dataset | Description |
|---|---|
| GEBCO 2024 | 15 arc-second global bathymetry, interpolated to ERA5 grid resolution |
| ERA5 Ocean Wave Data (2018) | Hourly significant wave height ($H_s$) and energy period ($T_p$) at $0.5° \times 0.5°$ spatial resolution |
| GADM v4.1 | Administrative boundaries for Indonesia (Level 0 and 1) |
| WDPA | World Database on Protected Areas, used for exclusion masking |
| Indonesia EEZ boundary | Shapefile defining Indonesia's Exclusive Economic Zone |

#### Filtering Criteria

**Table 3.2:** Geophysical and regulatory constraints for WEC site selection

| Filter | Description |
|---|---|
| Bathymetry | Depth between 40–150 m based on interpolated GEBCO values |
| Shoreline Distance | Maximum 100 km from coast, computed using BallTree and haversine distances (with projected CRS) |
| Marine Protected Areas | Exclude grid points within buffered MPA boundaries |
| Exclusive Economic Zone | Include only sites within Indonesia's EEZ |

### 3.1.4. Wave Power Conversion

Each valid WEC site was modeled to estimate hourly power output using device-specific conversion from sea state parameters to electrical energy. The chosen device for this study is the **WaveStar**, a point absorber wave energy converter with a rated capacity of 600 kW 3.3. Power output was determined based on local wave conditions at each grid cell, using a bilinear interpolation method applied to the device's power matrix.

#### Device Specification

**Table 3.3:** Technical Specification of WaveStar Device

| Metric | WaveStar |
|---|---|
| Device Technology | Multi-Point Absorber |
| Rated Capacity (kW) | 600 |
| Technology Readiness Level | TRL 8 |
| Deployment Depth Range | 40–150 m |
| Spatial Packing Density | 20 MW/km$^2$ |

The WaveStar conversion matrix defines the device's output power as a function of two wave parameters:

- **Significant wave height** ($H_s$), in meters
- **Peak wave period** ($T_p$), in seconds

The matrix contains 11 bins for $H_s$ ranging from 0.5 m to 6.0 m, and 11 bins for $T_p$ ranging from 1.0 s to 16.0 s, resulting in an 11 x 11 grid of rated power outputs (in kW). Each matrix cell represents the expected electrical output under a given combination of $H_s$ and $T_p$, derived from the manufacturer's performance data and literature-based assumptions.

Figure 3.1 presents the power conversion matrix of the WaveStar device, which maps sea state conditions—defined by significant wave height ($H_s$) and peak wave period ($T_p$)—to electrical output in kilowatts. This matrix forms the foundation of the interpolation-based conversion process.

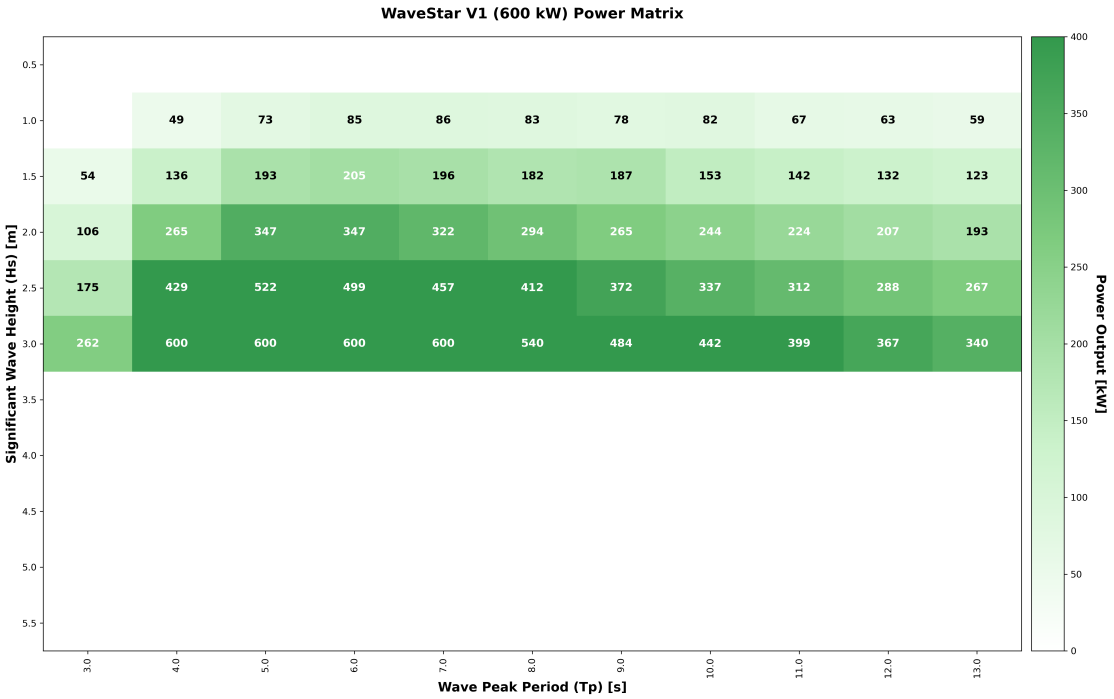


**Figure 3.1:** Power Matrix of the WaveStar Device (Output in kW as a Function of $H_s$ and $T_p$)

To estimate the total deployable capacity per WEC site, a spatial packing density of 20 MW/km$^2$ was applied, consistent with WEC farm studies [71]. The effective ocean area associated with each ERA5 wave grid point was calculated using latitude-dependent geodesic approximation:

$$A(\phi) = \Delta x \cdot \Delta y \cdot \cos(\phi) \cdot R^2 \tag{3.4}$$

where $\phi$ is the latitude, $\Delta x = \Delta y = 0.5°$ are the grid spacing intervals, and $R \approx 111.32$ km is the mean Earth radius per degree. This results in site-specific area estimates ranging between 570–650 km$^2$ depending on location.

Each site's installed capacity (MW) was computed by multiplying its estimated area by the packing density. The number of individual WaveStar devices was then inferred by dividing the site capacity by the unit rating (600 kW) and rounding up to the nearest integer.

This deployment logic allows for heterogeneous site sizing and avoids artificial grid caps, in contrast to fixed per-cell limits. It is consistent with spatial planning practices for wave energy zones (e.g., [72]).

For each of the 202 valid sites, hourly sea state parameters ($H_s$, $T_p$) were extracted from the ERA5 reanalysis dataset for the year 2018 [19] at a spatial resolution of $0.5° \times 0.5°$. These hourly values were then passed through the power matrix interpolation routine.

### Power Output Calculation

Hourly power production was calculated using bilinear interpolation over the two-dimensional power matrix. This method estimates output based on the weighted contribution of the four nearest matrix points surrounding each $(H_s, T_p)$ pair. All calculations were conducted in kilowatts and converted to megawatts for compatibility with the Calliope framework.

### 3.1.5. Aggregation and Normalization

Following the hourly power output calculation at each valid site, the data was post-processed to produce Calliope-ready inputs at the provincial level. This included filtering out inactive sites, assigning sites to provinces, aggregating hourly outputs, and normalizing the results.

To avoid distortion in the final dataset, any WEC sites with zero energy output across all 8,760 hours were excluded. These typically correspond to locations where local sea states remained consistently outside the WEC's operating envelope despite meeting geophysical criteria.

After filtering, the remaining productive sites were spatially joined to Indonesian provinces using buffered GADM Level 1 shapefiles. Each site was mapped to a single province based on its centroid location, ensuring compatibility with the 'calliope-indonesia' node structure. This province-level mapping was performed *after* the power conversion step to avoid including technically valid but unproductive sites.

For each province, the hourly power output of all assigned sites was summed, weighted by their individual installed capacities. This produced one 8,760-hour time series per province, representing the total modeled wave energy generation assuming full deployment of the WaveStar devices across the available sea area.

In parallel, the total installed capacity in megawatts for each province was also computed by summing the assigned site-level capacities. This was saved as a separate input variable for Calliope to define the `energy_cap_max` constraint.

To make the generation profile compatible with Calliope's `energy_per_cap` convention, each provincial time series was divided by its respective total installed capacity. The result is a normalized hourly capacity factor (0–1) per province, assuming ideal dispatch from the modeled wave resource.

## 3.2. Tidal Energy Modeling

This section describes the methodology used to model tidal stream energy resources for integration into the 'calliope-indonesia' framework. A two-stage filtering process was implemented to identify technically and geographically viable locations based on depth, proximity to shore, exclusion zones, and predicted current velocities. The process relies on harmonic tidal constituent data from TPXO10-atlas-v2 and was fully implemented in Python using geospatial and scientific computing libraries.

### 3.2.1. Data Sources

The tidal resource assessment utilized the TPXO10-atlas-v2 global tidal model developed by Egbert & Erofeeva (2002). This model provides gridded harmonic constituents for both the east–west ($u$) and north–south ($v$) tidal transport components at a spatial resolution of $1/30^\circ$ (approximately $3.7\,\mathrm{km}$ at the equator). Additional spatial datasets were used for geophysical filtering and jurisdictional boundaries, as summarized in Table 3.4.

**Table 3.4:** Datasets used in tidal energy site screening

| Dataset | Description and Purpose |
|---|---|
| TPXO10-atlas-v2 | Harmonic constituents of 15 tidal components; used for predicting depth-averaged current velocities (Egbert & Erofeeva, 2002). |
| GEBCO 2024 (via TPXO `hz`) | Global bathymetry used for site depth filtering. |
| GADM Level 0 | Used to extract Indonesian shoreline for proximity analysis [73]. |
| WDPA (2025) | Marine Protected Areas; used to exclude environmentally restricted zones [74]. |
| World EEZ v12 | Exclusive Economic Zones; used to retain only Indonesian territorial waters [75]. |

Python libraries used in the filtering pipeline include `xarray` for multidimensional NetCDF processing, `geopandas` for spatial filtering and joins, and `BallTree` from `sklearn.neighbors` for shoreline distance calculations.

### 3.2.2. Site Selection Methodology

Tidal stream site selection was implemented as a two-stage filtering process, adapted from published practices by Orhan et al. (2016), Segura (2017), and Firdaus (2021). The objective was to identify valid sites that meet geophysical, environmental, and turbine-operational constraints.

1. Filter I: Geophysical constraints — selects grid points with acceptable depth, proximity to shore ($\leq 20\,\mathrm{km}$), and no intersection with marine protected areas or non-Indonesian waters.
2. Filter II: Technical constraints — retains only those sites with predicted peak tidal velocity exceeding the turbine cut-in threshold ($1.0\,\mathrm{m/s}$).

The complete pipeline is reproducible and scalable, and is built on scientific tidal modeling libraries including pyTMD [22].

### 3.2.3. Filter I – Geophysical Constraints

The first filter screened for physically deployable locations by enforcing four main conditions:

1. Depth Filtering: Grid cells from TPXO10 with water depths between $20$ and $60\,\mathrm{m}$ were selected. This range is consistent with bottom-mounted turbine deployment guidelines for minimizing installation costs and avoiding navigation conflicts [45, 76],
2. Shoreline Distance: The Indonesian coastline was extracted from GADM Level 0 by sampling boundary points. Coordinates were projected to UTM Zone 50S (EPSG:32750), and the distance from each site to the nearest shoreline point was computed using BallTree. A threshold of $20\,\mathrm{km}$ was applied to filter sites for feasible grid connection,
3. Marine Protected Areas: Sites intersecting with any WDPA-defined MPA were removed via spatial join operations in GeoPandas [74]
4. Indonesian Waters (EEZ): Final spatial filtering retained only sites located within Indonesia's Exclusive Economic Zone, based on World EEZ v12 [75]

After Filter I, each retained site included geographic coordinates, depth, and distance to shore. This dataset formed the input to the technical screening stage.

### 3.2.4. Filter II – Technical Constraints

For each location that passed Filter I, tidal harmonic constituents were extracted using pyTMD [22], including amplitude and phase for both $u$ and $v$ transport components across 15 tidal constituents. Using these harmonics, a synthetic hourly tidal time series over a $15$-day period was generated for each site. This period covers a full spring–neap cycle to capture both peak and sustained velocity events.

To assess whether a site meets the turbine's minimum operational velocity, the time series was converted from depth-integrated transport (in $\mathrm{m^2/s}$) to depth-averaged velocity ($\mathrm{m/s}$) using local bathymetry. Only sites with:

$$V_{\text{peak}} \geq 1.0\,\mathrm{m/s}$$

were retained, where $V_{\text{peak}}$ is the maximum hourly velocity over the 15-day period. Additionally, the 90th percentile velocity, $V_{90\%}$, was recorded for each site for use in energy yield estimation.

### 3.2.5. Velocity Prediction

The tidal current prediction method used pyTMD's harmonic synthesis routines to compute velocity components $u(t)$ and $v(t)$ from harmonic amplitudes and phases:

$$u(t) = \sum_{i=1}^{N} A_i^u \cos(\omega_i t + \phi_i^u) \tag{3.5}$$

$$v(t) = \sum_{i=1}^{N} A_i^v \cos(\omega_i t + \phi_i^v) \tag{3.6}$$

The harmonic constants were transformed to complex exponential form for efficient synthesis:

$$h_u = A_i^u e^{-j\phi_i^u}, \quad h_v = A_i^v e^{-j\phi_i^v} \tag{3.7}$$

The transport values were converted to depth-averaged velocities using local water depth $d$:

$$u_{\text{vel}}(t) = \frac{u(t)}{d}, \quad v_{\text{vel}}(t) = \frac{v(t)}{d} \tag{3.8}$$

The scalar velocity magnitude was then computed as:

$$V(t) = \sqrt{u_{\text{vel}}(t)^2 + v_{\text{vel}}(t)^2} \tag{3.9}$$

From this time series, the following two statistics were derived for each site:

$$V_{\text{peak}} = \max V(t) \tag{3.10}$$
$$V_{90\%} = \text{Percentile}_{90}(V(t)) \tag{3.11}$$

Sites with $V_{\text{peak}} < 1.0\,\text{m/s}$ were excluded.

This structured output is used in the next stage of the modeling process (Section 3.2.8) to generate hourly power production profiles per province. All filtering logic is fully reproducible using open-source scientific libraries and geospatial datasets [22, 75, 74, 73].

### 3.2.6. Spatial Deployment Parameters

Each valid tidal stream site was assumed to host a small-scale commercial tidal farm using SeaGen S-2MW turbines [23]. To estimate realistic installed capacity per TPXO grid cell, spatial deployment constraints were applied based on rotor spacing and grid resolution.

The TPXO10-atlas-v2 grid has a spatial resolution of approximately $3.7\,\text{km} \times 3.7\,\text{km}$ at the equator, yielding a total area of:

$$A_{\text{grid}} = (3.7)^2 = 13.69\,\text{km}^2 \tag{3.12}$$

Following standard spacing recommendations for horizontal-axis tidal stream turbines, each turbine requires:

- Lateral spacing: $3 \times D = 60\,\text{m}$
- Longitudinal spacing: $10 \times D = 200\,\text{m}$

where $D = 20\,\text{m}$ is the rotor diameter of SeaGen S. This results in a required spacing area per turbine of:

$$A_{\text{spacing}} = 60\,\text{m} \times 200\,\text{m} = 12{,}000\,\text{m}^2 = 0.012\,\text{km}^2 \tag{3.13}$$

The maximum number of turbines deployable per grid cell is thus:

$$N_{\text{turbines}} = \left\lfloor \frac{A_{\text{grid}}}{A_{\text{spacing}}} \right\rfloor = \left\lfloor \frac{13.69}{0.012} \right\rfloor = 1140 \tag{3.14}$$

Each turbine has a rated capacity of $2.0\,\text{MW}$, resulting in a total site-level installed capacity of:

$$P_{\text{site}} = N_{\text{turbines}} \times 2.0 = 1140 \times 2.0 = 2280\,\text{MW} \tag{3.15}$$

This installed capacity was applied during power profile generation to reflect realistic farm-scale output. All subsequent steps in the modeling pipeline—including power calculation, capacity factor estimation, and provincial aggregation—incorporate this spatial deployment constraint to avoid overestimation of tidal energy potential.

### 3.2.7. Power Curve Implementation

To convert predicted tidal current velocities into electrical power output, a device-specific power curve was implemented for the SeaGen S-2MW tidal turbine. The power function was defined based on the manufacturer brochure and adjusted according to curve shapes shown in Giorgi (2025, Fig. 4.2-4). The function accounts for the four operating regimes of a horizontal-axis tidal turbine:

1. Sub-cut-in region: For $v < 1.0\,\mathrm{m/s}$, the turbine produces no power.
2. Partial load region: For $1.0 \leq v < 2.5\,\mathrm{m/s}$, the power increases smoothly from a non-zero starting point to rated output.
3. Rated region: For $2.5 \leq v < 4.0\,\mathrm{m/s}$, the turbine delivers its full rated power.
4. Cut-out region: For $v \geq 4.0\,\mathrm{m/s}$, the turbine shuts down for safety and power drops to zero.

The turbine rating was set to $2.0\,\mathrm{MW}$ (two $1.0\,\mathrm{MW}$ rotors). The modeled power function $P(v)$ followed a nonlinear ramp during the partial load region, starting at approximately $5\%$ of the rated output ($100\,\mathrm{kW}$) at the cut-in velocity. The curve was implemented as a vectorized Python function and validated at key control points from the Giorgi (2025) curve:

- $P(1.0\,\mathrm{m/s}) \approx 100\,\mathrm{kW}$
- $P(2.5\,\mathrm{m/s}) = 2000\,\mathrm{kW}$ (rated)
- $P(v) = 0$ for $v < 1.0\,\mathrm{m/s}$ and $v \geq 4.0\,\mathrm{m/s}$

The full function is shown in Fig. 3.2, which confirms the expected behavior in all four regions. The use of a continuous and realistic partial-load curve avoids common oversimplifications found in stepwise models.

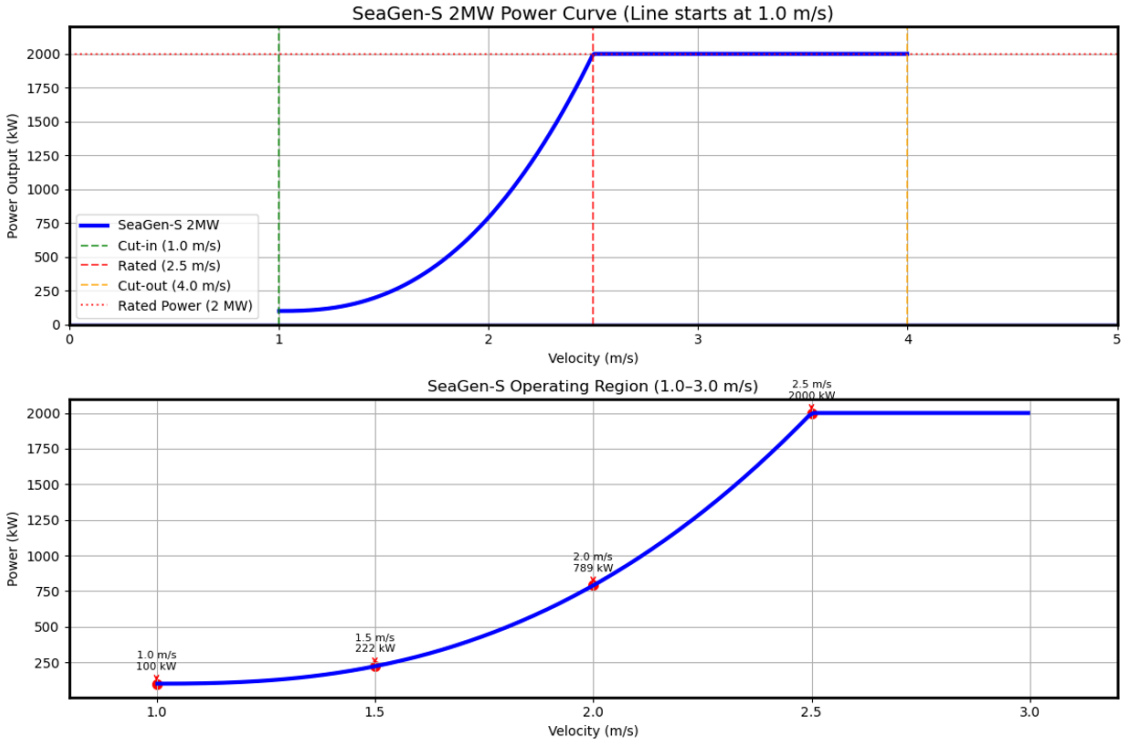


**Figure 3.2:** SeaGen S-2MW tidal turbine power curve, adapted from Giorgi (2025). Line begins at cut-in velocity $v = 1.0\,\mathrm{m/s}$.

This power function was applied to hourly depth-averaged velocities $V(t)$ predicted from TPXO harmonic synthesis, as described in Section 3.2. The resulting turbine-scale output was then scaled up using the spatial deployment factor of $1140$ devices per grid cell (Eq. 3.2.6), yielding a farm-scale power profile per valid site.

### 3.2.8. Power Profile Generation

Hourly tidal current velocities were predicted using harmonic synthesis of the TPXO10-atlas-v2 global tidal model. The model provides 15 tidal constituents in the $u$ and $v$ transport components, from which depth-averaged horizontal velocities were reconstructed.

For each valid site $(\phi, \lambda)$, the following steps were implemented:

1. Extract $u$ and $v$ harmonic amplitudes and phases using `pyTMD` [22], scaled by local depth to convert from transport units ($\mathrm{cm}^2/\mathrm{s}$) to velocity ($\mathrm{m}/\mathrm{s}$).
2. Predict the hourly tidal velocity components $u(t)$ and $v(t)$ over 8760 hours for the year 2050 using TPXO harmonic synthesis.
3. Compute the magnitude of the depth-averaged velocity:
$$V(t) = \sqrt{u(t)^2 + v(t)^2} \tag{3.16}$$
4. Apply the SeaGen S-2MW power curve (Section 3.2.7) to obtain hourly power output $P(t)$ at the turbine level.
5. Multiply by the spatial deployment factor ($1140$ devices per grid cell) to produce a farm-scale profile per site:
$$P_{\text{farm}}(t) = 1140 \times P(v(t)) \tag{3.17}$$

Sites that failed the harmonic validity check (e.g., missing constituent amplitudes or zero depth) were excluded. After velocity and power calculation, additional site-level statistics were computed:

- Peak velocity $V_{\text{peak}} = \max V(t)$
- Mean power $\overline{P} = \frac{1}{8760} \sum P(t)$
- Capacity factor:
$$\text{CF} = \frac{\overline{P}}{1140 \times 2000\,\text{kW}} = \frac{\overline{P}}{2.28\,\text{GW}} \tag{3.18}$$

A final velocity threshold of $V_{\text{peak}} \geq 1.0\,\mathrm{m}/\mathrm{s}$ was applied to match the cut-in constraint and ensure practical deployment. After this filter, a total of $5143$ sites remained. These profiles were used for the provincial aggregation described next. The next step aggregated the hourly farm-scale power profiles into Calliope-compatible provincial inputs. This required assigning each tidal site to an Indonesian province, normalizing by total installed capacity, and exporting profiles and capacity limits in the required format.

### 3.2.9. Province Assignment

Each site was spatially joined with the GADM Level-1 shapefile [73] using a $55\,\mathrm{km}$ buffer to ensure nearshore locations were assigned correctly. Sites falling outside all province polygons were assigned to the nearest province centroid based on minimum distance. Province names were standardized to match the Calliope node naming convention (e.g., `Daerah_Khusus_Ibukota_Jakarta`).

### 3.2.10. Farm-Scale Aggregation

Within each province $p$, the hourly power outputs from all sites were summed:

$$P_p(t) = \sum_{i=1}^{N_p} P_i(t) \tag{3.19}$$

where $P_i(t)$ is the farm-scale power profile of site $i$, and $N_p$ is the number of valid sites in province $p$.

### 3.2.11. Profile Normalization

Furthermore, hourly power production profile from each province was normalized by the total farm-scale rated capacity in that province:

$$\texttt{energy\_per\_cap}_p(t) = \frac{P_p(t)}{N_p \times 1140 \times 2.0\,\mathrm{MW}} = \frac{P_p(t)}{2280 \times N_p} \tag{3.20}$$

This normalization ensures the resulting profile is a unitless time series with a maximum value less than or equal to 1.

### 3.2.12. Energy Capacity Limits

Each province's maximum deployable tidal capacity was computed by multiplying the number of eligible grid cells by the site-level capacity:

$$\texttt{energy\_cap\_max}_p = N_p \times 2280\,\mathrm{MW} \tag{3.21}$$

The total national capacity potential across all provinces was calculated to be:

$$\sum_p \texttt{energy\_cap\_max}_p = 11.7\,\mathrm{GW} \tag{3.22}$$

Two outputs were generated for integration with Calliope:

This process yielded two CSV files for Calliope input:

- `TIDAL_Profiles_2050_SeaGen.csv` → Normalized hourly power profiles per province (`energy_per_cap`)
- `energy_cap_max_per_province.csv` → Maximum deployable capacity (MW) per-province (`energy_cap_max`)

These inputs were used in all scenario simulations involving tidal energy within the 'calliope-indonesia' framework.

The use of total 8760 hourly timesteps for the year 2050 assumes the same the power profile pattern from historical weather data in 2018. The resulting data provides the necessary input for techno-economic analysis and optimization of tidal stream integration scenarios, with spatial and temporal characteristics preserved.

## 3.3. Cost Projection Modeling for Marine Renewable Energy

The competitiveness of wave and tidal energy in Indonesia's future electricity mix depends not only on resource availability, but also on how their costs evolve relative to other technologies. As both technologies remain at an early stage of deployment, their current capital and operational costs are high, yet substantial reductions are expected with broader adoption. Previous studies—such as [77] for OTEC and [17] for wave energy—use learning effect approaches to model future cost trajectories. Cost declines of around 30% for OTEC [77], or even higher for less mature but scalable technologies like marine renewables, appear plausible under learning-based assumptions, showing the importance of including dynamic cost parameters in energy system modeling.

Because optimization outcomes in Calliope are highly sensitive to techno-economic inputs, this thesis incorporates time-varying cost projections for wave and tidal energy. Costs are modeled using Wright's Law, which links cost reductions to cumulative installed capacity similar to previous studies [78, 77]. To produce realistic deployment trajectories, a logistic (S-shaped) growth model is used to simulate uptake from 2023 to 2050 3.3.1. Together, these methods support the development of scenario-based inputs that address Research Question 3 (RQ3): how cost trajectories influence the role of marine renewables in Indonesia's decarbonization pathways. This framework is applied as separate cost modeling effort to wave 3.1 and tidal 3.2 technologies to derive cost trajectories used in the system model.

### 3.3.1. Learning Curve Approach

To simulate how capital and operational costs for marine renewable energy technologies might decrease over time, this study adopts a learning curve approach based on Wright's Law. It was first formulated in 1936 and later applied to energy technologies, including by Junginger et al. [78] in their global experience curve for wind power, aiming to improve the reliability of technology cost decline projections approach. Wright's Law posits that the unit cost of a technology decreases by a constant fraction with every doubling of cumulative production or installed capacity.

In this formulation, the cost in year $t+1$ is derived from the cost in year $t$ and the change in cumulative installed capacity, using the equation:

$$C_{t+1} = C_t \left( \frac{X_{t+1}}{X_t} \right)^b \quad \text{with} \quad b = \frac{\log(1 - LR)}{\log 2}$$

- $C_t$: cost (CAPEX or OPEX) in year $t$
- $X_t$: cumulative installed capacity in year $t$
- $LR$: learning rate (fractional cost reduction per capacity doubling)
- $b$: learning exponent, derived from the learning rate

This approach allows technology costs to evolve over time based on deployment progress rather than relying on static projections. Lavidas [17] applies a similar framework to wave energy, emphasizing the importance of learning-by-doing, upscaling, and manufacturing effects in early-stage technologies. Langer [77] uses Wright's Law to estimate cost reductions for OTEC, assuming a 30% reduction after four to five doublings of cumulative capacity.

Because real-world learning rates for wave and tidal technologies remain highly uncertain, this thesis applies a staged learning curve: learning rates vary across three decades (2020–2030, 2030–2040, 2040–2050) to reflect expected changes in technology maturity and learning saturation. These learning rates differ by scenario to represent conservative, moderate, and optimistic assumptions about future cost evolution.

### 3.3.2. Cumulative Capacity Projection

An essential input to the learning curve model is the evolution of cumulative installed capacity over time. Rather than assuming constant or exponential growth, this study applies a logistic (S-shaped) diffusion model following the formulation of Grübler (1998) [79]. Originally developed to describe the historical adoption of industrial technologies, the logistic curve captures three characteristic phases: slow emergence in early years (due to R&D and demonstration), rapid growth during commercialization and policy support, and eventual saturation as market size limits further expansion. 3.3

The logistic function is defined as:

$$X(t) = \frac{K}{1 + \exp\left(-r(t - t_0)\right)}$$

Where:

- $X(t)$: cumulative installed capacity at time $t$
- $K$: saturation level (2050 capacity target in MW)
- $r$: growth rate (steepness of adoption)
- $t_0$: inflection point (midpoint year when 50% of $K$ is reached)

In this thesis, $K$ is set based on Indonesian policy and scenario assumptions:

- 1050 MW for a conservative (pessimistic) scenario
- 3000 MW based on the ocean energy target in RUEN
- 5000 MW for an optimistic scenario with increased policy support

To ensure that the modeled curve reaches the target capacity $P_{\text{target}}$ by 2050, the growth rate $r$ is solved analytically using:

$$r = -\frac{\ln\left(\frac{L}{P_{\text{target}}} - 1\right)}{t_{\text{target}} - t_0}$$

where $L$ is a slightly inflated version of the target (e.g., $L = 1.01 \times P_{\text{target}}$). This prevents mathematical errors when computing the logarithm and ensures the curve converges to the desired value. For example, setting $P_{\text{target}} = 3000$ MW, $L = 3030$ MW, $t_{\text{target}} = 2050$, and $t_0 = 2038$, gives:

$$r = -\frac{\ln(0.01)}{12} = \frac{4.6052}{12} \approx 0.384$$

This value lies within the range of $r = 0.2$–$0.4$ recommended by Grübler [79] for typical technology diffusion curves, providing a realistic growth profile.

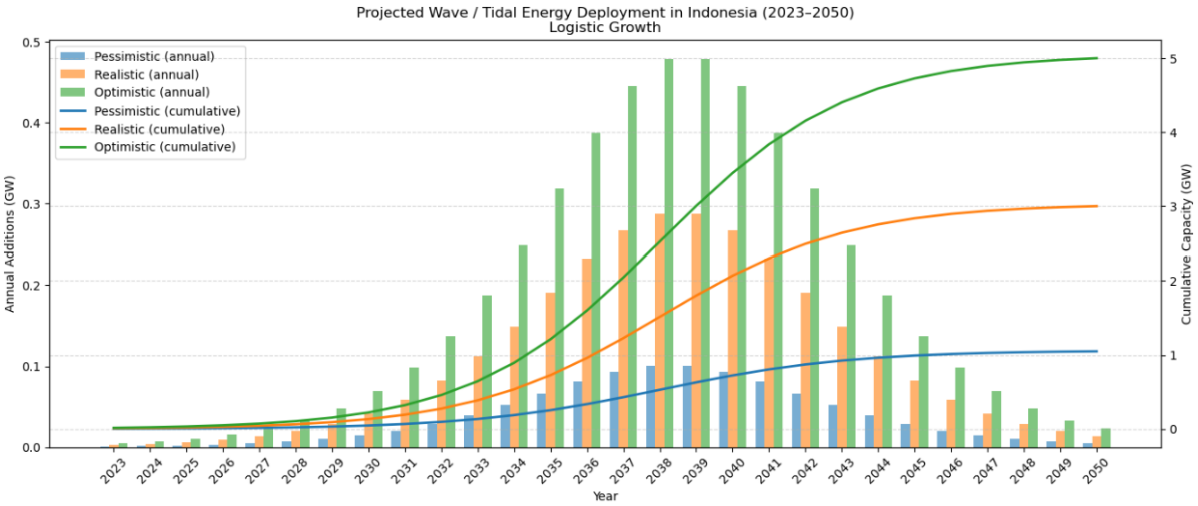


**Figure 3.3:** Projected wave and tidal energy deployment in Indonesia (2023–2050) under three scenarios using logistic growth. Annual capacity additions are shown as bars (left axis), while cumulative capacity is plotted as lines (right axis).

This logistic formulation ensures smooth and plausible deployment of wave and tidal energy in Indonesia, reflecting constraints such as policy lag, supply chain ramp-up, and financing cycles. By linking these trajectories to the learning curve, the model supports more grounded estimates of future cost evolution for marine technologies.

### 3.3.3. MRE Cost Assumptions

To enable comparative assessment of wave and tidal stream energy in Indonesia's future power system, this study applies the same cost projection framework to both technologies. This methodological choice allows differences in system contribution to be attributed to temporal and spatial generation characteristics, rather than differences in techno-economic input assumptions.

The IEA-OES (2015) report [80] provides cost ranges for wave and tidal energy technologies across different deployment stages, showing comparable magnitudes for both. For example, CAPEX for first commercial-scale projects was reported in the range of 4000–18100 US$/kW for wave and 5100–14600 US$/kW for tidal energy—indicating overlapping cost dynamics at similar maturity levels.

More recent techno-economic assessments further support this convergence. De Castro et al. (2024) [33] evaluated WEC cost with cost ranges representing a sensitivity approach, 1.5–5.0 million EUR/MW (conversion rate to US$ in 2024: 1.08 3.9). Satymov et al. (2024) [81] reported a projected 2050 CAPEX range of 1.5–2.3 million EUR/MW for Indonesian sites (within 300 km offshore and 1000 m depth). To

maintain consistency and realism, the pessimistic scenario in this thesis adopts a 2023 CAPEX value of 6.2 million US$/MW, reflecting the WaveStar converter benchmark described by Jahangir (2024) [82].

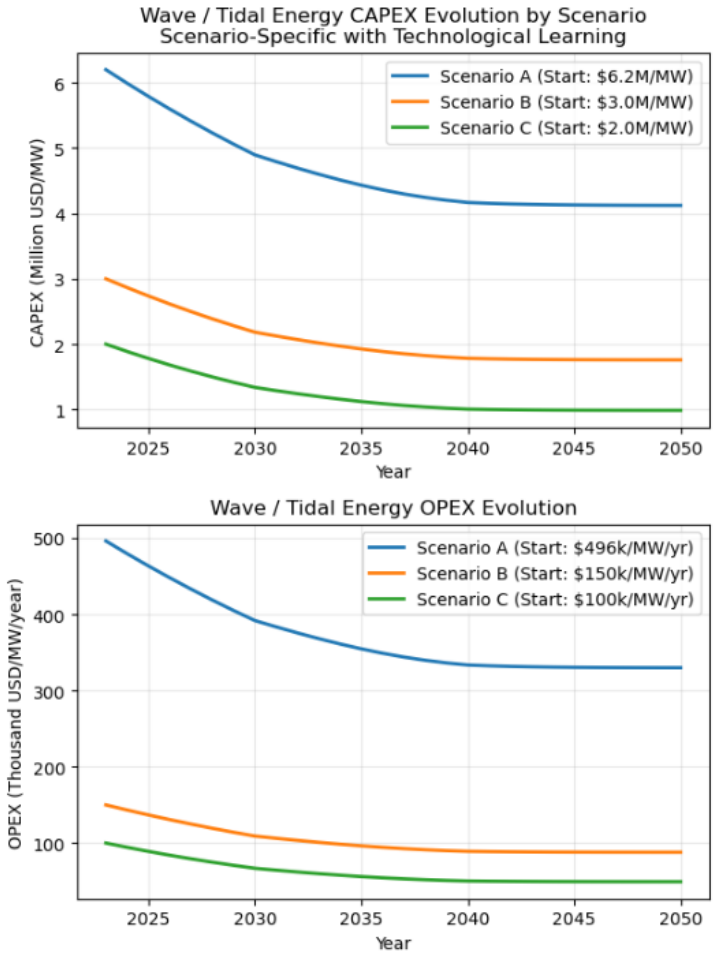


**Figure 3.4:** Scenario-based capital (CAPEX) and operational (OPEX) expenditure evolution for wave and tidal energy in Indonesia, assuming technology-specific learning over time. CAPEX values are shown in million US$/MW and OPEX in thousand US$/MW/year.

Table 3.5 summarizes the three cost trajectories used in this thesis. These cost inputs evolve dynamically over time using the learning-based model described in 3.3.1, and are applied identically to both wave and tidal stream technologies in all optimization scenarios.

**Table 3.5:** Cost scenario assumptions for marine renewable energy derived as Figure 3.4

| Scenario | Target Capacity [MW] | Learning Rates [%] | Starting CAPEX [MUS$/MW] | Starting OPEX [kUS$/MW/yr] |
|---|---|---|---|---|
| Pessimistic | 1,050 | 6, 4, 2 | 6.2 | 496[a] |
| Realistic | 3,000 | 8, 5, 2.5 | 3.0 | 150[b] |
| Optimistic | 5,000 | 10, 7, 3.5 | 2.0 | 100[b] |

[a] 8% of CAPEX (harsh environment) [b] 5% of CAPEX

**Table 3.6:** MRE Projected Costs in 2050 (3.11): optimistic (min cost), realistic (baseline cost), and pessimistic (max cost) used in Calliope modeling

| Technology | Cost Type | Cost Min | Cost Baseline | Cost Max | Unit |
|---|---|---|---|---|---|
| Wave | CAPEX | 986,000 | 1,760,000 | 4,123,000 | US$(2023)/MW |
| | Fixed OPEX | 50,000 | 88,000 | 330,000 | US$(2023)/MW/year |
| Tidal | CAPEX | 986,000 | 1,760,000 | 4,123,000 | US$(2023)/MW |
| | Fixed OPEX | 50,000 | 88,000 | 330,000 | US$(2023)/MW/year |

## 3.4. Demand Projection Framework

This study develops a dual-scenario demand projection framework to assess marine renewable energy (MRE) integration under methodological and growth trajectory uncertainty in Indonesia's 2050 energy transition. The framework builds upon the calliope-indonesia energy system model [1] by incorporating higher-resolution Indonesian operational data while maintaining compatibility with the established modeling architecture.

Previous energy system modeling for Indonesia has relied on proxy demand profiles due to limited availability of Indonesian operational data. Langer et al. [1] utilized Malaysian demand profiles scaled to Indonesian provincial electricity sales, achieving national-scale coverage but with inherent limitations in capturing Indonesian-specific demand patterns. The present methodology advances this approach by integrating actual Indonesian utility operational data where available, while acknowledging that significant reliance on proxy methods remains necessary for comprehensive national coverage.

The dual-scenario approach addresses two primary sources of uncertainty in long-term Indonesian energy planning: (1) methodological uncertainty in demand baseline establishment, and (2) growth trajectory uncertainty over the 2024-2050 projection period. This framework enables systematic assessment of how demand projection methodology affects optimal MRE deployment patterns, storage requirements, and transmission expansion strategies.

### 3.4.1. Two-Scenario Uncertainty Framework

Energy demand projections carry substantial uncertainty over 26-year horizons, particularly in developing economies undergoing rapid structural transformation [1]. The methodology recognizes that both the baseline establishment method and growth trajectory assumptions significantly influence energy system optimization outcomes. Rather than pursuing false precision through multiple intermediate scenarios, the dual-scenario approach brackets the uncertainty space through technically grounded and policy-aligned projections with distinct methodological foundations.

The methodology generates two complete demand scenarios covering all 34 Indonesian provinces:

$$\text{Bottom-Up Scenario:} \quad D^{\text{BU}}_{p,2050}(t) \in \mathbb{R}^{8760} \quad \forall p \in \{1, 2, \ldots, 34\} \tag{3.23}$$

$$\text{Top-Down Scenario:} \quad D^{\text{TD}}_{p,2050}(t) \in \mathbb{R}^{8760} \quad \forall p \in \{1, 2, \ldots, 34\} \tag{3.24}$$

where $D^{\text{BU}}_{p,2050}(t)$ and $D^{\text{TD}}_{p,2050}(t)$ represent distinct hourly demand profiles for province $p$ in target year 2050, derived from bottom-up technical projections and top-down policy alignment methodologies respectively.

The *Bottom-Up Scenario* employs provincial demand development using Indonesian utility operational data (UP2B system) where available, supplemented by regionally appropriate proxy scaling, with growth projections based on official PLN utility planning documents (RUPTL 2025-2034) [30]. This approach reflects technical projections grounded in utility operational experience and planning practices.

The *Top-Down (Policy-Aligned) Scenario* distributes national policy targets from RUKN 2024 spatially to provinces using economic activity indicators, representing demand levels required to achieve Indonesia's stated energy transition objectives [14]. This approach ensures alignment with national policy frameworks while maintaining provincial-level spatial resolution.

The scenarios employ fundamentally different baseline establishment approaches, creating distinct 2024 provincial demand profiles that propagate through all subsequent projections. This methodologi-

cal divergence enables assessment of how baseline development uncertainty affects MRE integration outcomes, complementing the growth trajectory uncertainty captured through different projection methods.

The methodology employs a structured data hierarchy reflecting availability and quality constraints across Indonesia's diverse electricity sectors. The mathematical framework encompasses both baseline profiles and growth projections:

$$\text{Bottom-Up Profiles:} \quad D^{\text{BU}}_{p,2024}(t) \in \mathbb{R}^{8760} \quad \forall p \in \{1, 2, \ldots, 34\} \tag{3.25}$$

$$\text{Top-Down Profiles:} \quad D^{\text{TD}}_{p,2024}(t) \in \mathbb{R}^{8760} \quad \forall p \in \{1, 2, \ldots, 34\} \tag{3.26}$$

$$\text{Growth Rate Arrays:} \quad r_{p,y} \in \mathbb{R}^{34\times 26} \quad y \in \{2025, \ldots, 2050\} \tag{3.27}$$

where $D^{\text{BU}}_{p,2024}(t)$ and $D^{\text{TD}}_{p,2024}(t)$ represent distinct hourly demand profiles for province $p$ in base year 2024 derived from bottom-up and top-down methodologies respectively, and $r_{p,y}$ denotes provincial growth rates for year $y$.

### Primary Data Sources

High-quality data covers the *Java-Madura-Bali (JAMALI)* interconnected system through PLN's UP2B operational dispatch system, providing 30-minute resolution measurements across five separate dispatch files (UP2B1 through UP2B5) covering seven provinces. This operational data represents approximately 60% of Indonesian electricity demand and serves as the foundation for both scenarios. The UP2B files contain dispatch data in Excel matrix format, with dates in column A and time intervals across 48 columns representing half-hourly timesteps.

Medium-quality data addresses the remaining 27 non-JAMALI provinces through proxy scaling methodologies, where Jawa Barat operational patterns provide temporal reference profiles scaled by provincial electricity sales data from PLN Statistics 2024. This approach represents 40% of national demand through systematic proxy scaling rather than direct operational measurement.

Growth projections employ RUPTL 2025-2034 official utility growth rates for the bottom-up scenario and RUKN 2024 policy targets for the top-down scenario. The detailed provincial growth rates are presented in Appendix C.7.

### UP2B Data Processing and Temporal Aggregation

The temporal aggregation methodology converts 30-minute measurements to hourly profiles through mean aggregation within each hour:

$$D_{\text{hourly}}(p, h) = \frac{1}{n_h} \sum_{i \in H_h} D_{\text{30min}}(p, i) \tag{3.28}$$

where $H_h$ represents the set of 30-minute timesteps within hour $h$, $n_h$ is the number of valid measurements within that hour, and $D_{\text{30min}}(p, i)$ denotes the 30-minute dispatch measurement for province $p$ at timestep $i$. This approach provides robust handling of irregular timesteps and missing data while preserving energy conservation.

The processing pipeline includes automatic unit detection and conversion, handling mixed format UP2B data where values may be recorded in either MW or GW units. A threshold-based detection system identifies the appropriate scaling factor and standardizes all values to MW format for consistency across the modeling framework.

### Uncertainty Quantification and Methodological Limitations

Provincial demand projections carry estimated uncertainty ranges of ±15% for UP2B-derived profiles (reflecting operational data quality and disaggregation methods) and ±25% for proxy-scaled profiles (reflecting inherent limitations of Jawa Barat representativeness across diverse Indonesian provinces).

Growth trajectory uncertainty adds an additional ±20% range over the 26-year projection period, resulting in compound uncertainty bounds that justify the dual-scenario approach for energy system sensitivity analysis.

The study explicitly adopts a two-scenario framework based on: (1) computational tractability for comprehensive MRE integration analysis across multiple grid configurations, (2) clear methodological distinction enabling uncertainty attribution, and (3) consistency with Indonesian energy planning practice which typically employs reference and alternative demand scenarios [14, 30].

Methodological limitations include spatial representativeness constraints where 27 of 34 provinces rely on Jawa Barat proxy scaling, introducing systematic bias toward Java demand patterns. Temporal pattern persistence assumptions maintain 2024 diurnal and seasonal patterns through 2050, excluding structural demand evolution from economic transformation or sectoral transitions. Despite different baseline approaches, scenarios may exhibit convergence due to common proxy dependencies for the majority of provinces.

Scenario outputs are validated for internal consistency (energy conservation, temporal integrity, statistical realism) and external plausibility (comparison with regional energy studies, consistency with Indonesian development trajectories). Cross-validation is limited by data availability but includes comparison with Langer et al. [1] projections where methodological overlap permits direct comparison.

### 3.4.2. Bottom-Up Technical Scenario Development

#### JAMALI Province Processing

The Java-Madura-Bali (JAMALI) interconnected system represents Indonesia's most advanced electricity grid, operating under centralized dispatch control through the UP2B (Unit Pelaksana Penyaluran dan Pengatur Beban) system. UP2B operational data provide 30-minute temporal resolution measurements across five separate dispatch files (UP2B1 through UP2B5) covering seven provinces, representing approximately 60% of Indonesia's total electricity consumption [83].

UP2B operational data are organized by dispatch regions rather than administrative provinces, necessitating spatial disaggregation for energy system modeling compatibility. The five UP2B dispatch centers provide aggregated demand measurements that require methodological translation to the individual provincial framework used in calliope-indonesia energy system modeling.

The temporal aggregation methodology converts 30-minute measurements to hourly profiles through mean aggregation within each hour rather than simple pairwise averaging:

$$D_{\text{hourly}}(p,h) = \frac{1}{n_h} \sum_{i \in H_h} D_{\text{30min}}(p,i) \tag{3.29}$$

where $H_h$ represents the set of 30-minute timesteps within hour $h$, and $n_h$ is the number of valid measurements within that hour. This approach provides robust handling of irregular timesteps and missing data while preserving energy conservation.

UP2B regional demand measurements are spatially disaggregated to individual provinces using electricity sales proportions as allocation weights for multi-province dispatch regions:

$$D_{p,\text{disaggregated}}(t) = D_{\text{UP2B\_region}}(t) \times w_{p,\text{region}} \tag{3.30}$$

$$w_{p,\text{region}} = \frac{\text{Sales}_{p,2024}}{\sum_{q \in \text{region}} \text{Sales}_{q,2024}} \tag{3.31}$$

where $w_{p,\text{region}}$ represents the sales-based allocation weight for province $p$ within its respective dispatch region. Single-province UP2B regions (UP2B2, UP2B4, UP2B5) undergo direct mapping without disaggregation, while multi-province regions (UP2B1, UP2B3) employ proportional allocation based on PLN Statistics 2024 electricity sales data.

The processing pipeline includes automatic unit detection and conversion, handling mixed format UP2B data where values may be recorded in either MW or GW units. UP2B data are converted to Coordinated

Universal Time (UTC) for consistency with renewable energy resource data and undergo validation for completeness and temporal integrity.

### Two-Phase Growth Methodology

The bottom-up scenario employs a two-phase growth methodology that applies RUPTL 2025-2034 provincial-specific growth rates followed by extrapolated average rates for the extended projection period. This approach reflects the higher certainty of near-term utility planning compared to long-term projections.

Phase 1 applies year-specific growth rates from RUPTL 2025-2034 through compound annual growth:

$$M_{\text{Phase1}}(p) = \prod_{y=2025}^{2034} (1 + r_{p,y}/100) \tag{3.32}$$

where $M_{\text{Phase1}}(p)$ represents the cumulative growth multiplier for province $p$ over the RUPTL planning period, $r_{p,y}$ denotes the annual growth rate (in percent) for province $p$ in year $y$, and the product operator $\prod$ applies compound annual growth across all years from 2025 to 2034.

Phase 2 extends projections to 2050 using filtered average growth rates to mitigate the impact of outlier values exceeding 30% annually:

$$\bar{r}_p = \frac{1}{|\mathcal{R}_p|} \sum_{r \in \mathcal{R}_p} r \quad \text{where } \mathcal{R}_p = \{r_{p,y} : r_{p,y} \leq 30\%\} \tag{3.33}$$

$$M_{\text{Phase2}}(p) = (1 + \bar{r}_p/100)^{16} \tag{3.34}$$

where $\bar{r}_p$ represents the filtered average annual growth rate for province $p$, $\mathcal{R}_p$ denotes the set of growth rates for province $p$ that do not exceed the 30% outlier threshold, $|\mathcal{R}_p|$ represents the cardinality (number of elements) in the filtered set, and $M_{\text{Phase2}}(p)$ denotes the growth multiplier applied over the 16-year extension period (2035-2050).

The complete bottom-up demand profile results from applying the combined growth multiplier to 2024 base profiles:

$$D^{\text{BU}}_{p,2050}(t) = D^{\text{base}}_{p,2024}(t) \times M_{\text{Phase1}}(p) \times M_{\text{Phase2}}(p) \tag{3.35}$$

where $D^{\text{BU}}_{p,2050}(t)$ represents the bottom-up projected hourly demand for province $p$ at time $t$ in 2050, $D^{\text{base}}_{p,2024}(t)$ denotes the baseline hourly demand for province $p$ at time $t$ in 2024, and the growth multipliers preserve temporal patterns while scaling demand magnitude according to projected growth trajectories.

The detailed provincial growth rates employed in this methodology are presented in Appendix C.7.

### Non-JAMALI Proxy Scaling Methodology

The methodology addresses demand profile development for 27 Indonesian provinces outside the JAMALI system through proxy scaling using Jawa Barat as the reference province. This selection reflects Jawa Barat's mixed economic structure, intermediate development level, and representative load characteristics within the Indonesian context, with a load factor of 72% falling within the 65-80% range typical of mixed industrial-residential electricity systems.

Proxy scaling preserves temporal patterns while adjusting demand magnitude through provincial electricity sales proportions:

$$D_{p,\text{norm}}(t) = \frac{D_{\text{JawaBarat}}(t)}{\max(D_{\text{JawaBarat}})} \tag{3.36}$$

$$\text{SF}_p = \frac{\text{Sales}_{p,2024}}{\text{Sales}_{\text{JawaBarat},2024}} \times \frac{\max(D_{\text{JawaBarat}})}{\text{Sales}_{\text{JawaBarat},2024}} \tag{3.37}$$

$$D_{p,\text{proxy}}(t) = D_{p,\text{norm}}(t) \times \text{SF}_p \tag{3.38}$$

where $\text{SF}_p$ represents the scaling factor for province $p$ derived from electricity sales proportions, and $D_{p,\text{proxy}}(t)$ denotes the resulting proxy-derived provincial demand profile.

Proxy-based provincial profiles carry estimated uncertainty of ±25%, reflecting inherent limitations of applying single-province demand patterns across Indonesia's diverse regional contexts. The methodology acknowledges that the 27 non-JAMALI provinces span vast geographic, climatic, and economic variations that no single proxy province can adequately represent, introducing systematic bias toward Java demand patterns across the non-JAMALI region.

### 3.4.3. Top-Down Policy-Aligned Scenario Development

#### RUKN 2024 Target Distribution Framework

The top-down scenario distributes national electricity demand targets from RUKN 2024 to individual provinces through a two-stage disaggregation process. Regional targets are first established based on RUKN 2024 policy specifications, then distributed to provinces using electricity sales-based allocation weights to ensure alignment with national policy frameworks while maintaining provincial-level spatial resolution.

**Table 3.7:** RUKN 2024 Regional Electricity Demand Targets for 2050

| Region | Target (TWh) |
|---|---|
| JAMALI | 784.0 |
| Sumatra | 279.5 |
| Kalimantan | 143.6 |
| Sulawesi | 144.5 |
| Eastern Indonesia | 140.0 |
| **Total** | **1,491.6** |

The provincial distribution methodology calculates allocation weights within each region based on electricity sales proportions from PLN Statistics 2024. This approach assumes that electricity consumption patterns correlate with economic activity levels, measured through annual electricity transactions rather than installed capacity or population metrics:

$$w_{p,r}^{\text{regional}} = \frac{\text{Sales}_{p,2024}}{\sum_{p \in R_r} \text{Sales}_{p,2024}} \tag{3.39}$$

$$T_{p,2050} = T_{r,2050}^{\text{RUKN}} \times w_{p,r}^{\text{regional}} \tag{3.40}$$

where $T_{p,2050}$ represents the 2050 target annual demand for province $p$, $T_{r,2050}^{\text{RUKN}}$ denotes the regional target from RUKN 2024, and $w_{p,r}^{\text{regional}}$ represents the provincial allocation weight within region $r$.

#### Shape-Preserving Scaling Implementation

The top-down scenario applies uniform scaling factors to 2024 baseline profiles to achieve provincial targets while preserving temporal patterns. This approach maintains diurnal and seasonal demand characteristics derived from the same baseline profiles used in the bottom-up scenario, while adjusting magnitude to meet policy objectives:

$$\text{SF}_p^{\text{policy}} = \frac{T_{p,2050}}{A_{p,2024}} \tag{3.41}$$

$$D_{p,2050}^{\text{TD}}(t) = D_{p,2024}^{\text{base}}(t) \times \text{SF}_p^{\text{policy}} \tag{3.42}$$

where $A_{p,2024}$ represents the annual demand total for province $p$ in the 2024 baseline, and $\text{SF}_p^{\text{policy}}$ denotes the policy-aligned scaling factor.

#### Common Baseline Framework and Proxy Dependencies

Both scenarios employ identical 2024 baseline temporal patterns, ensuring that differences in 2050 projections reflect growth methodology rather than baseline assumptions. For JAMALI provinces, both scenarios use the same UP2B-derived profiles with spatial disaggregation based on electricity sales proportions. For non-JAMALI provinces, both scenarios utilize Jawa Barat as the proxy reference province, scaled according to provincial electricity sales data.

Jawa Barat proxy selection is based on its economic structure diversity with mixed economic base spanning manufacturing, services, agriculture, and other sectors, load factor characteristics of 72% within typical ranges for mixed industrial-residential systems, and intermediate development level with per capita electricity consumption representing a middle ground between rural and highly industrialized regions. The proxy selection acknowledges significant limitations given Indonesia's regional diversity, as the 27 non-JAMALI provinces span vast geographic, climatic, and economic variations that no single proxy province can adequately represent.

The methodology implements temporal pattern preservation for non-JAMALI provinces while adjusting demand magnitude:

$$D_{p,\text{norm}}(t) = \frac{D_{\text{JawaBarat}}(t)}{\max(D_{\text{JawaBarat}})} \tag{3.43}$$

$$D_{p,\text{baseline}}(t) = D_{p,\text{norm}}(t) \times \text{Sales}_{p,2024} \times \text{CF}_{\text{conversion}} \tag{3.44}$$

where $\text{CF}_{\text{conversion}}$ represents the conversion factor from electricity sales to peak demand based on Jawa Barat reference characteristics.

This common baseline approach enables direct assessment of how growth methodology affects energy system optimization outcomes, isolating the impact of technical projections versus policy alignment approaches while maintaining methodological consistency in baseline establishment.

### 3.4.4. Energy System Integration and Output Formatting

#### Calliope Framework Compatibility

Both scenarios generate demand profiles compatible with the calliope-indonesia energy system modeling framework. The output formatting converts demand values to negative MW values following Calliope's demand convention, with consistent 2050 timestamps and standardized provincial naming:

$$D_{p,\text{calliope}}(t) = -|D_{p,2050}(t)| \tag{3.45}$$

$$t_{\text{calliope}} \in \{\text{2050-01-01 00:00:00}, \ldots, \text{2050-12-31 23:00:00}\} \tag{3.46}$$

The methodology handles leap year standardization by averaging February 28 and 29 demand values in the 2024 baseline to generate appropriate February 28 values for the non-leap year 2050, ensuring consistent 8760-hour annual profiles across both scenarios.

#### Output File Generation

The processing pipeline generates two primary output files for energy system modeling:

- *Demand_Profiles_2050_PLN_RUPTL.csv* containing the bottom-up scenario

- *Demand_Profiles_2050_RUKN.csv* containing the top-down scenario

Each file maintains identical structure with 8760 rows representing hourly timesteps and 34 columns representing provincial demand profiles, enabling direct integration with calliope-indonesia optimization scenarios.

### 3.4.5. Validation Framework and Quality Assurance

#### Multi-Level Validation Approach

The methodology employs a comprehensive validation framework addressing both internal consistency between scenarios and external validation against established energy system modeling studies. Internal validation examines the relationship between bottom-up and top-down scenarios through correlation analysis, temporal pattern comparison, and regional distribution assessment. External validation compares the bottom-up scenario against the Langer et al. [1] calliope-indonesia baseline to establish methodological credibility and consistency with established Indonesian energy system modeling approaches.

#### Statistical Validation Metrics

The validation framework employs multiple statistical metrics to assess scenario quality and methodological consistency. Correlation analysis examines temporal pattern preservation between scenarios, with high correlation coefficients indicating successful shape preservation during scaling operations. Peak demand ratio analysis validates magnitude scaling consistency across provinces and regions. Load factor comparison ensures realistic operational characteristics are maintained throughout the projection methodology.

Provincial-level validation examines annual energy totals, peak demand characteristics, and temporal pattern statistics. Regional-level validation aggregates provincial results to assess consistency with RUKN 2024 targets and regional energy planning objectives. System-level validation compares total national demand projections with established energy system modeling studies and policy planning documents.

#### External Benchmarking and Credibility Assessment

The bottom-up scenario undergoes systematic comparison with the Langer et al. [1] calliope-indonesia baseline to establish methodological credibility. This comparison examines differences in provincial growth assumptions, regional demand distribution, and temporal characteristics. The analysis identifies systematic differences resulting from updated utility planning data (RUPTL 2025-2034 vs. RUPTL 2021-2030) and enhanced provincial-specific growth modeling compared to regional average approaches.

Validation metrics include annual energy comparison by province and region, temporal pattern correlation analysis, peak demand timing assessment, and load duration curve comparison. These metrics enable systematic assessment of methodological improvements while maintaining consistency with established energy system modeling frameworks for Indonesia.

## 3.5. Energy System Optimization Modeling

This section outlines the energy system modeling approach used to evaluate the integration of marine renewable energy (MRE) technologies in Indonesia's power sector by 2050. The modeling framework is based on the open-source *Calliope* platform and the national-scale 'calliope-indonesia' model developed by Langer [1].

### 3.5.1. Model Framework

This study employs energy system optimization modeling to evaluate MRE integration in Indonesia's 2050 power system. The analysis builds upon Langer's calliope-indonesia model [1], extending the framework to incorporate wave and tidal energy technologies alongside existing renewable resources.

Calliope v0.6.10 [55] serves as the optimization platform, formulating Indonesia's electricity system as a linear programming problem that minimizes total annualized costs while satisfying demand and operational constraints. The framework uses modular YAML/CSV architecture enabling flexible technology and scenario definitions, solved using the Gurobi optimizer with academic license.

The spatial representation consists of 34 provincial nodes aggregating demand, generation potential,

and storage deployment at sub-national level. Each province connects via transmission links representing either intra-island AC connections or inter-island HVDC cables, depending on grid scenario configuration. This structure captures Indonesia's archipelagic geography while maintaining computational tractability for national-scale analysis.

Langer's baseline model includes established renewable technologies (geothermal, hydropower, solar PV, biomass, wind), storage systems (batteries, pumped hydro), and conventional generation, each characterized by technical parameters (efficiency, lifetime) and economic parameters (CAPEX, OPEX). System optimization determines least-cost capacity expansion and hourly dispatch to meet electricity demand while minimizing total system costs.

This thesis integrates wave power (point absorbers) and tidal stream power (horizontal-axis turbines) as additional supply technologies. Spatial deployment assessments and hourly generation profiles from Sections 3.1-3.2 are incorporated using Calliope's `energy_per_cap` format, enabling direct comparison of scenarios with and without MRE contributions.

The model operates at 3-hourly temporal resolution (2920 timesteps) for the 2050 target year. This resolution follows Langer's validation demonstrating negligible impact on system-wide results while significantly reducing computational requirements [1]. Weather data anchors to 2018 conditions across all variable renewable technologies to isolate deployment strategy effects from inter-annual meteorological variations.

Optimization enforces strict energy balance constraints requiring full demand satisfaction at every node and timestep, with no unmet demand permitted. Variable renewables operate within resource availability bounds defined by normalized capacity factor profiles. Technology deployment respects maximum installable capacity limits per province. Storage systems operate under round-trip efficiency and state-of-charge constraints. Transmission flows respect link capacity limits, with curtailment of renewable generation implicitly allowed but not economically penalized. Complete mathematical formulation is provided in Appendix B.1

### 3.5.2. Model Enhancements

This study extends the 'calliope-indonesia' framework through specific modifications addressing MRE integration requirements, cost parameter updates, and scenario design for comprehensive system analysis.

#### Technology Integration Framework

All energy supply technologies in the calliope-indonesia model are defined using modular YAML files, consistent with the open-source Calliope framework structure [18, 55]. Each technology is characterized by its energy carrier, efficiency, cost parameters, spatial constraints, and operational logic. These definitions are separated from the core optimization model, allowing transparent modification and reproducibility across scenarios.

The MRE technologies, specifically wave energy and tidal stream power, are introduced via dedicated YAML files: `wave.yaml` and `tidal_stream.yaml`. These follow the same structural convention used in existing technologies from Langer [1], such as `offshore_wind.yaml` and `otec.yaml`. Both wave and tidal are defined as `supply` technologies with `electricity` as their output carrier. They rely on hourly time-varying profiles provided externally in the `energy_per_cap` format.

The `energy_per_cap` files used in this study are normalized timeseries generated from physical resource data and device power curves, as described in Sections 3.1.5 and 3.2.11. Each file contains 8760 rows (hourly values for 2050) and one column per Calliope location ID. These profiles are multiplied internally by the decision variable `energy_cap` to calculate hourly energy generation at each node.

To enforce realistic deployment limits, each marine technology is constrained by a province-level capacity ceiling. These constraints are implemented via the `energy_cap_max` parameter in the YAML definitions or via override configuration. For wave energy, the upper bound is derived from the available deployment area per province and a packing density, consistent with assumptions in Lavidas et al. [17]. For tidal stream, the cap reflects the total number of devices per eligible TPXO grid cell multiplied

by rated capacity, summed at the provincial level. These static caps ensure that MRE deployment reflects spatial and technical feasibility, rather than unconstrained optimization potential.

The main technical and economic parameters for all renewable technologies—including wave and tidal—are summarized in Table 3.8 and further detailed in the following subsection.

**Table 3.8:** Technical and cost assumptions for renewable technologies

| Technology | Lifetime [years] | CAPEX [US$2023/MW] | Fixed OPEX [US$2023/MW/year] | Variable OPEX [US$2023/MWh] | Efficiency [-] |
|---|---|---|---|---|---|
| *Generation Technologies* | | | | | |
| Geothermal | 30 | 3,960,000 | 99,000 | 0.24 | 0.17 |
| Large hydro | 50 | 1,960,000 | 38,000 | 0.66 | 0.80 |
| Small hydro | 50 | 2,233,000 | 50,200 | 0.5 | 0.80 |
| Onshore solar PV[a] | 25 | 969,000 | 15,000 | – | – |
| Floating solar PV[a] | 25 | 1,106,000 | 22,120[b] | – | – |
| Onshore wind | 30 | 950,000 | 30,000 | – | 0.85 |
| Offshore wind | 30 | 2,870,000 | 81,290 | 3.9 | 0.79 |
| OTEC | 30 | 6,485,000 | 194,550[b] | – | – |
| Wave energy[c] | 25 | 1,760,000 | 88,000[d] | – | – |
| Tidal stream[c] | 20 | 1,760,000 | 88,000[d] | 8 | – |
| *Storage Technologies* | | | | | |
| Battery (Li-ion) | 30 | 230,000 | 7,350 | 1.6 | 0.98 |
| Pumped hydro | 50 | 1,200,000 | 18,700 | 0.94 | 0.89 |
| *Transmission Technologies* | | | | | |
| AC transmission[e] | 40 | 735,000 | – | 1.3 | 0.98 |
| HVDC submarine[f] | 40 | 175,860[g] + 4,262/km[h] | – | 1.7% CAPEX | 0.999965 |

[a] [84]
[b] 3% of CAPEX
[c] Thesis contribution
[d] 5% of CAPEX
[e] West Kalimantan's investment plan; million US$130/230MW [85]
[f] [86] [87]
[g] HVDC converter station (VSC) [86]
[h] HVDC XLPE submarine cables [86]

### Technical Assumptions

The technical parameters used for all renewable energy technologies—such as energy efficiency and device lifetime—follow the reference values defined in Langer [1], and are kept constant across all scenarios. In this thesis, a 100% renewable energy system is modeled for the year 2050, without fossil fuel-based technologies, to reflect an ambitious but technically feasible decarbonization target. While Indonesia's official net-zero target is set for 2060, the decision to model a fully renewable system by 2050 aligns with the most progressive scenarios and enables direct integration of wave and tidal profiles without requiring adjustments to fossil baselines.

Unlike Langer's pathway-based approach, which includes simulations for 2030, 2040, and 2050, this study focuses exclusively on the target year (2050) configuration. This decision reflects the exploratory nature of marine renewable integration, and avoids the need to generate intermediate-year timeseries data for new technologies. The wave and tidal stream profiles used in this study are developed specifically for 2050 conditions and would not be valid for earlier decades without full resource and demand reprocessing, which is outside the scope of this work.

### Biomass Exclusion

To sharpen the focus on the chosen marine energy integration, biomass and nuclear technologies are excluded from the system. These technologies are either constrained by uncertain sustainability criteria (biomass) or long-term development uncertainty in the Indonesian context (nuclear).

Biomass is excluded from this study due to both resource limitations and technical challenges associated with its use in the Indonesian context. Although agricultural residues such as rice straw and

palm oil empty fruit bunches (EFB) are widely available, their deployment for power generation faces key limitations. First, biomass availability is subject to competing demands from cooking, industry, and transport sectors, which restricts its scalability as a dispatchable renewable source for electricity generation.

From a technical standpoint, untreated Indonesian biomass suffers from low calorific value and a high risk of slagging and fouling due to elevated chemical contents that accelerate corrosion, ash melting, and boiler degradation at high combustion temperatures, as demonstrated by operational studies on EFB and palm shells [88]. Even advanced conversion processes such as wet torrefaction require elevated processing temperatures and add pre-treatment costs to reduce fouling risk. While wet torrefaction can enhance biomass quality and lowering slagging indices—it does not fully eliminate ash-related risks or maintenance overheads [89].

Given these concerns, and the need to focus this thesis on MRE contribution, biomass is removed from the scenario design. Its exclusion does not impact the ability to meet 100% renewable system targets, as other firm renewables such as geothermal and hydropower remain available in the model.

### Cost Assumptions

The cost assumptions presented in Table 3.8 for Indonesia's energy system optimization are primarily derived from the Technology Data for the Indonesian Power Sector 2024 Catalogue [42]. This source provides technology cost projections specifically developed for Indonesian deployment conditions through multi-stakeholder consultation involving the Directorate General of Electricity (MEMR), PLN, and the National Energy Council (DEN). The catalogue incorporates both local Indonesian project data and international projections from IRENA, IEA, and NREL, with cost figures representing consensus estimates based on current available knowledge from industry stakeholders.

The selection of this primary cost reference addresses three critical requirements for energy system modeling accuracy. First, the cost data reflects Indonesian-specific deployment conditions, including local content requirements, labor costs, and market structures that differ substantially from international averages. Second, the multi-stakeholder validation process ensures cost estimates incorporate practical deployment experience from Indonesia's power sector. Third, the catalogue's 2030–2050 projection timeline aligns with Indonesia's long-term energy planning frameworks, including RUPTL and national renewable energy targets.

### Solar PV Cost Modifications

Solar photovoltaic cost assumptions deviate from the Indonesian Technology Catalogue to account for land-use deployment constraints and system integration realities in Indonesia's electricity demand centers. The catalogue projects ground-mounted solar PV costs declining to 0.48 US$/kW by 2050, representing costs achievable for individual projects under optimal conditions. However, system-wide deployment faces significant spatial constraints documented by Langer et al. [90], who mapped technically feasible PV sites in Indonesia after applying restriction layers for steep terrain, peatlands, proximity to settlements, and other technical, environmental, and social constraints.

Java island, Indonesia's economic center with 158.1 million people [91], shows minimal suitable sites for utility-scale ground-mounted PV due to these deployment restrictions, making floating solar the primary solar option for meeting regional electricity demand. These land-use limitations create deployment bottlenecks that increase marginal costs as preferred sites become saturated, effects not captured in the catalogue's project-level cost projections. Without accounting for these spatial constraints, energy system optimization would unrealistically favor solar PV based solely on cost competitiveness while ignoring both physical deployment feasibility and the escalating costs of utilizing less suitable sites.

This study applies cost projections from NREL's Floating Solar Market Report [84], with ground-mounted PV costs declining from 1,030 US$/kW in 2021 to 969 US$/kW by 2050, and floating PV costs declining from 1,290 US$/kW to 1,106 US$/kW over the same period. These projections incorporate technological learning curves while maintaining realistic cost levels that enable balanced technology competition in energy system optimization.

### Transmission Infrastructure Cost Adjustments

Transmission cost assumptions are modified from previous Indonesia energy system studies to reflect the economic and technical realities of archipelagic grid development. Langer [1] applied HVDC subma-

rine cable costs of 293 US$/MW/km, with sensitivity analysis extending to 1,261 US$/MW/km, values that underestimate the infrastructure investment requirements for Indonesia's fragmented grid system where only the JAMALI system (Java–Madura–Bali) currently operates as an interconnected network.

This study applies submarine cable costs of 4,262 US$/MW/km derived from Australian transmission system analysis [87] and European transmission planning studies [86]. The Australian study reports submarine HVDC cable costs of 4,000 US$/MW/km for inter-regional connections, while detailed analysis of the Australia–Singapore interconnector project [92] identifies key cost drivers including water depths up to 1,900 meters, seabed congestion from existing infrastructure, extensive cable protection requirements, and complex installation logistics in tropical marine environments. After currency conversion to US$ 2023 and applying 18% cost reduction through technological learning 3.3.1, the modified transmission costs reflect the technical complexity and economic scale required for inter-island transmission development in Indonesian waters.

These higher submarine cable costs fundamentally alter transmission optimization outcomes compared to Langer's analysis, where even maximum costs of 1,261 US$/MW/km only moderately reduced inter-island transmission capacity [1]. At 4,262 US$/MW/km, transmission economics favor distributed generation technologies, including marine renewable energy systems, over centralized generation with long-distance submarine transmission.

### Currency Standardization and Cost Projection Framework

All cost data are standardized to US$ 2023 baseline using a two-step conversion methodology. EUR-denominated costs are converted to nominal US$ using annual average exchange rates from the International Monetary Fund Exchange Rates database [93], then adjusted to real 2023 US$ using inflation factors calculated from the US Bureau of Labor Statistics Consumer Price Index [94]. This approach maintains temporal alignment with the Indonesian Technology Catalogue's native price year, preserving data integrity while enabling accurate economic comparison across technologies.

Cost projections to 2050 apply technology-specific learning curves and market maturity assumptions. For marine renewable energy technologies, detailed cost evolution modeling is presented in 3.3. All other technologies follow cost trajectories specified in the Indonesian Technology Catalogue, with modifications limited to solar PV and transmission infrastructure as described above.

**Table 3.9:** Currency conversion rates for cost standardization to US$2023

| Year | EUR to US$ (annual average) | US$ inflation factor to 2023 baseline |
|---|---|---|
| 2011 | 1.39 | 1.36 |
| 2016 | 1.11 | 1.26 |
| 2018 | 1.18 | 1.21 |
| 2023 | 1.08 | 1.00 |
| 2024 | 1.08 | 0.97 |
| 2025 | 1.10 | 0.94 |

The currency conversion factors presented in Table 3.9 enable standardization of all cost data to US$2023 baseline for consistent economic analysis across the energy system optimization modeling framework. The EUR to US$ exchange rates represent annual average values sourced from the International Monetary Fund Exchange Rates database [93], ensuring accurate conversion of European technology cost data to US dollar equivalents using official international financial statistics.

The US$ inflation adjustment factors are calculated using the US Bureau of Labor Statistics Consumer Price Index calculator [94], with 2023 serving as the reference year (factor = 1.00). Historical cost data from 2011-2022 requires upward adjustment to account for cumulative inflation, while projected costs for 2024-2025 incorporate expected deflation trends based on Federal Reserve economic projections. This standardization methodology ensures that all technology cost assumptions, operational expenditures, and investment projections maintain consistent purchasing power basis for accurate economic comparison within the 'calliope-indonesia' optimization framework.

The conversion process follows a two-step methodology: first, EUR-denominated costs are converted to nominal US$ using the appropriate annual exchange rate, then adjusted to real 2023 US$ using the inflation factor. This approach maintains temporal accuracy while enabling direct cost comparison across technologies from different geographical origins and publication years, supporting robust economic analysis for Indonesia's renewable energy transition scenarios.

### 3.5.3. Scenario Configurations

This section outlines the scenario-based modeling approach used to examine the integration of MRE technologies into Indonesia's power system by 2050. The scenarios are designed to isolate the effects of wave and tidal energy on system cost, storage, and grid development, while accounting for future uncertainties in demand and capital costs. Each scenario represents a unique combination of technology configuration, demand or cost assumptions, and transmission grid layout. The structure follows the 'calliope-indonesia' framework developed by Langer [1], and is extended here to include marine technologies and additional sensitivity parameters relevant to this study.

To evaluate the contribution of MRE technologies to Indonesia's decarbonized energy mix, the model is configured with five distinct technology scenarios. These configurations reflect incremental additions of wave and tidal generation to a solar-based baseline, allowing the isolated and combined effects of each MRE technology to be assessed. All other parameters—including demand, non-MRE technologies, and spatial deployment limits—are held constant unless otherwise stated in the sensitivity cases.

The 'Reference' scenario includes almost all renewable technologies used in Langer [1] except biomass and nuclear 3.5.2, including the MRE (wave and tidal energy) as the scope of this study. The Solar-only scenario isolates solar-based generation (onshore PV and floating PV), while the remaining three scenarios progressively introduce wave and/or tidal energy into the system. This structure allows the model to capture changes in cost-optimal technology deployment, storage utilization, and transmission expansion triggered specifically by the inclusion of marine technologies.

**Table 3.10:** MRE Integration Scenarios for Indonesia Energy System Analysis

| Scenario | Year | Properties/changes from reference scenario |
|---|---|---|
| Reference | 2050 | Demand growth: RUKN 2024 targets<br>100% renewable technologies<br>Costs: 2050 reference (unit price: US$(2023)) |
| Solar only | 2050 | Only solar-based generators (onshore + floating PV) |
| Solar + Wave | 2050 | Solar-based generators + wave energy technology |
| Solar + Tidal | 2050 | Solar-based generators + tidal stream technology |
| Solar + Wave + Tidal | 2050 | Solar-based generators + both MRE technologies |

#### Sensitivity Cases

In addition to the core technology configurations, three sensitivity cases are applied to capture the uncertainty associated with future electricity demand and marine renewable energy (MRE) costs. These variations are designed to test the robustness of MRE integration outcomes across plausible system conditions and to provide insight into their system-level value under different planning assumptions.

The first sensitivity case explores the effect of alternative demand projections. While the Reference scenario uses national-level demand targets from RUKN 2024, the alternative profile is based on a bottom-up provincial demand forecast developed from the RUPTL 2021–2030 pathway. This case evaluates how spatial differences in demand growth influence the deployment of MRE technologies and the broader generation mix.

The second and third sensitivity cases test the impact of capital and operational cost uncertainty for wave and tidal technologies. In the optimistic case, marine energy costs are reduced to their minimum projected values for 2050, based on learning curve assumptions described in Section 3.3. The pessimistic case assumes maximum cost estimates. Costs for all other technologies remain fixed at reference levels, consistent with the Langer [1] implementation.

**Table 3.11:** Properties of Sensitivity Cases for MRE Scenario Analysis

| Sensitivity Case | Definition |
|---|---|
| Reference | National demand profile (RUKN 2024), MRE costs at 2050 reference values |
| Alternative demand profile | Bottom-up provincial demand forecast (RUPTL PLN pathway) |
| MRE cost optimistic | Wave and tidal CAPEX/OPEX set to minimum 2050 values 3.6 |
| MRE cost pessimistic | Wave and tidal CAPEX/OPEX set to maximum 2050 values 3.6 |

### Grid Configuration

Grid topology is a critical dimension in evaluating the system-wide impact of marine renewable energy (MRE) integration. Indonesia's archipelagic geography presents both opportunities and constraints for inter-island transmission, and the future extent of network interconnection remains uncertain. To reflect this, each scenario is simulated under two contrasting grid configurations: Supergrid and Fragmented.

The **Supergrid** configuration assumes full inter-island connectivity through high-voltage direct current (HVDC) submarine transmission links. This layout enables energy exchange across all provinces, supporting system balancing and geographical diversification of renewables. All HVDC links are considered endogenous to the optimization and may be expanded up to a maximum line capacity constraint, which is further explored in sensitivity (see Table 3.12).

The **Fragmented** configuration represents a more conservative development path in which no new inter-island connections are allowed. Only intra-island AC lines and the existing Java–Madura–Bali (JAMALI) interconnection remain active. This setting isolates the effect of regional balancing limitations on the optimal deployment of MRE and other technologies.

These two grid scenarios allow comparative assessment of spatial flexibility in system operation and investment, directly addressing Research Questions RQ2 and RQ4 related to optimal MRE integration and transmission expansion strategies.

### Scenario Matrix and Additional Parameters

The full scenario set consists of 18 core configurations derived from the cross-combination of:

- Five technology configurations (Reference, Solar-only, Solar+Wave, Solar+Tidal, Solar+Wave+Tidal),
- Three sensitivity cases (Reference, Alternative demand, MRE cost variation),
- Two grid configurations (Supergrid and Fragmented).

Each model run is independently optimized to minimize total system cost under the respective assumptions. This structure allows systematic comparison of how MRE technologies perform under varying demand, cost, and grid connectivity conditions.

In addition to the core scenario set, a parameter sweep is conducted to assess the effect of transmission network expansion limits. Specifically, the maximum HVDC transmission capacity per inter-island link is varied between 5 GW, 25 GW, and 50 GW. This variation enables targeted evaluation of grid build-out requirements (RQ2) under different MRE integration levels.

**Table 3.12:** Parameters Studied for MRE Integration Sensitivity Analysis

| Parameter | Range of Analysed Variations |
|---|---|
| Grid configuration | Supergrid (with inter-island links) vs. Fragmented (limited connectivity) |
| MRE deployment assessment | 1. With vs. without MRE technologies<br>2. Contribution to solar-dominant mix: Solar → +Wave → +Tidal → +Both MRE |
| Maximum HVDC transmission capacity | 5 GW, 25 GW, 50 GW per link |

### 3.5.4. Model Outputs and Interpretation

The Calliope model outputs are exported in NetCDF4 format as multi-dimensional `xarray` datasets, containing hourly and annual values for each technology, carrier, location, and time step. These results are post-processed using the Python data analysis stack to extract key performance indicators (KPIs) relevant to the thesis objectives.

The following metrics are computed and compared across scenarios:

- **Installed capacity** by technology and province (`energy_cap`)
- **Annual electricity generation** by source (`carrier_prod`)
- **Storage utilization and capacity** (battery and pumped hydro) over time (`storage`, `storage_cap`)
- **Transmission flows** between provinces (`carrier_prod` and `carrier_con` on link technologies)
- **System cost breakdown** including investment, fixed O&M, and variable O&M costs (`cost`)

These outputs are aggregated to annual or scenario-level summaries to enable cross-scenario comparison. For example, installed capacity maps and technology composition plots are used to assess the spatial impact of marine renewable energy (MRE) integration. Transmission flow visualizations and capacity scaling are analyzed to evaluate the role of inter-island links under Supergrid and Fragmented scenarios (RQ2). Storage dispatch patterns and cumulative deployment are compared to assess the flexibility needs imposed by MRE (RQ1). Cost indicators, including total system cost and LCOE per technology, are extracted to inform techno-economic comparisons (RQ3).

All outputs are interpreted in the context of the four research questions outlined in Section 1.3.1 for technical understanding of the role and system-level implications of wave and tidal stream power in Indonesia's decarbonized electricity system by 2050.

# 4. Results

## 4.1. Supporting Inputs for Energy System Modeling

This section showcases the input datasets for the Calliope-Indonesia optimization runs, including wave energy, tidal energy, demand projection results. Extended tables, validation steps, and additional figures are provided in Appendix C.1–D.

### 4.1.1. Wave Energy Potential

The wave energy resource assessment for Indonesia was conducted using ERA5 reanalysis data for 2018, covering all validated deployment sites that passed bathymetric and shoreline distance filters. Compared to global hotspots such as the North Atlantic or Southern Ocean, Indonesian waters are characterized by *moderate* wave conditions. Significant wave height averages 1.30 m (±0.77 m), with the 90th percentile reaching 2.34 m. Peak wave periods range between 1.8–21.5 s (mean: 8.9 ± 3.8 s), reflecting the combined influence of long-period Indian Ocean swells and shorter wind-sea components from local conditions, consistent with literature findings [11].

From an installation perspective, site filtering yielded 202 validated deployment sites, with depths between 40–150 m and shoreline distances below 100 km. At a packing density of 20 MW/km², these sites could theoretically accommodate 21.16 million WaveStar devices across 634,867 km² ocean area, equivalent to 12.47 GW of aggregate capacity. This illustrates the vast theoretical potential, though actual system contribution is shaped by spatial and techno-economic constraints.

To estimate performance, wave conditions were converted into electrical output using the *WaveStar* power matrix. Matrix validation showed that 340 of 400 wave state combinations were valid, while 42.3% of timesteps fell outside the calibrated matrix range. The resulting device-level output spans 0–522 kW, with an average of 150.2 kW, equivalent to a 37.5% capacity factor under idealized conditions.

#### Provincial Distribution

Provincial assignment yields 27 provinces with identified wave energy potential. Kepulauan Riau dominates in absolute capacity (3.59 GW across 58 sites), followed by Jawa Timur (1.85 GW, 30 sites) and Papua (0.99 GW, 16 sites). However, capacity-weighted provincial ranking differs from geographic distribution, with Lampung achieving highest mean capacity factor (29.5%) despite smaller total capacity (62 MW) (Table 4.1).

**Table 4.1:** Top provincial wave energy performance (capacity-weighted).

| Province | Capacity Factor (%) | Capacity (MW) |
|---|---|---|
| Lampung | 29.5 | 61,621 |
| Bengkulu | 17.3 | 123,671 |
| Bali | 14.2 | 61,280 |
| Maluku | 11.1 | 738,827 |
| Jawa Barat | 10.7 | 492,547 |
| Banten | 10.17 | 61,562 |

This highlights an important strategic point: provinces with small aggregate capacity can still deliver outsized performance, making them attractive candidates for pilot projects.

#### Provincial Capacity Factors

The spatial distribution of modeled capacity factors is shown in Figure 4.1. Highest performance is concentrated along the southern coasts of Java and Sumatra, where direct exposure to Southern Indian Ocean swells creates energetic wave climates. However, as illustrated in Figure 4.2, these regions are constrained by steep bathymetric drop-offs that limit eligible deployment zones.

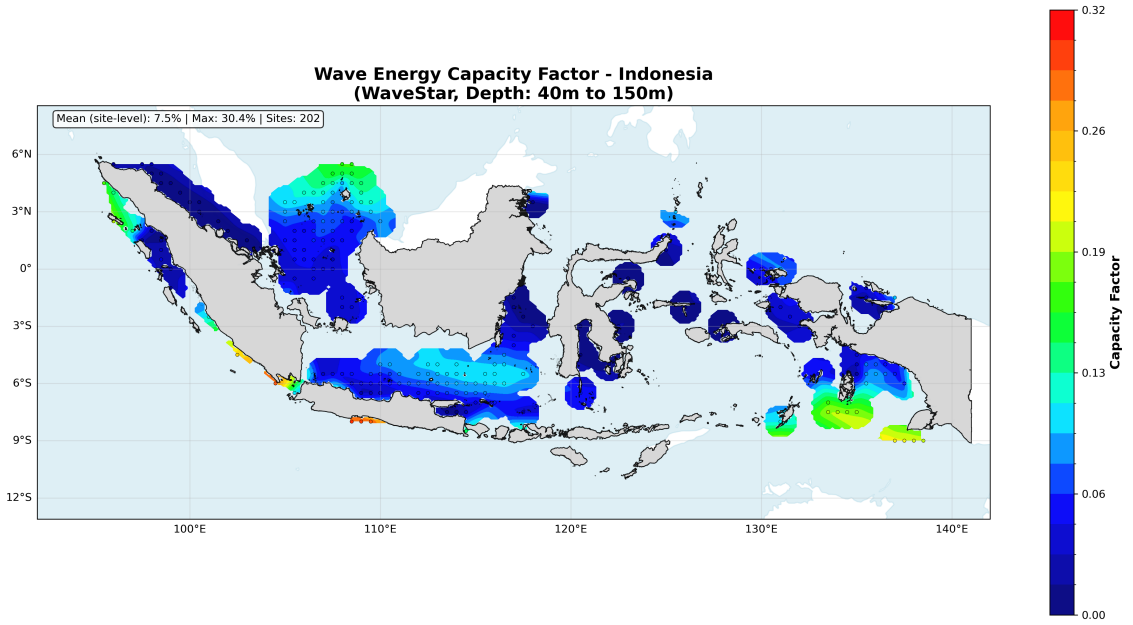


**Figure 4.1:** Modeled site-level capacity factors for WaveStar devices across Indonesia

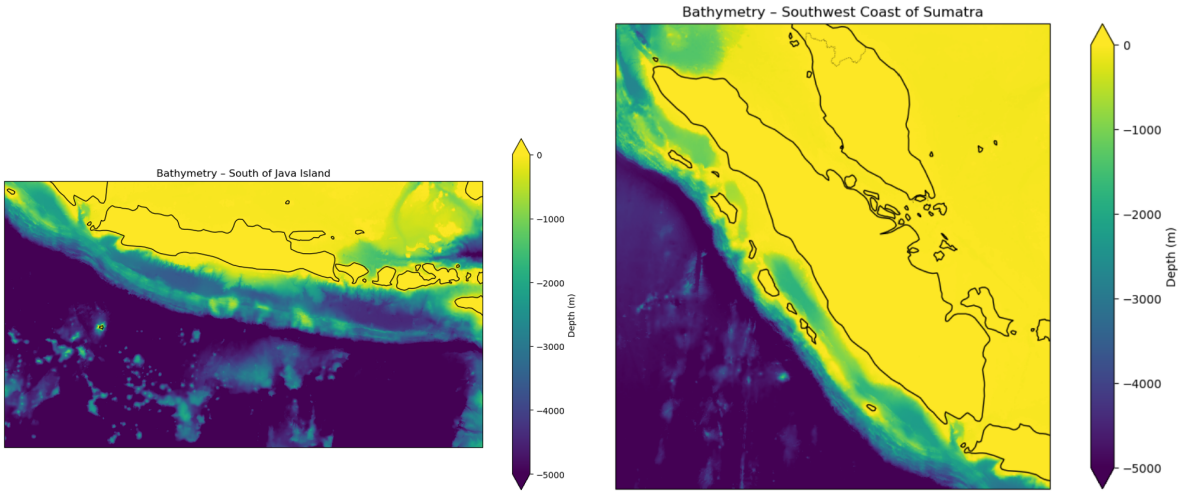


**(a)** Southern Java **(b)** Southern Sumatra

**Figure 4.2:** Bathymetric constraints: steep drop-offs limit eligible sites along the most energetic wave corridors

These constraints explain Indonesia's modest national average of 6.7% capacity factor (mean CF (site-level): 7.5%), despite the presence of high offshore wave power densities. Unlike regions where shallow continental shelves coincide with energetic waves, Indonesia's deepwater coastlines reduce practical opportunities for large-scale deployment.

Full provincial classifications and performance distributions are provided in Appendix C.1.

### Temporal Generation Patterns

Monthly capacity factor analysis reveals moderate seasonal variation, with a January peak of 10.4% and an April minimum of 3.8%, corresponding to the influence of the northwest monsoon (Figure 4.3). This pattern confirms year-round generation potential, while southern coastal sites experience additional reinforcement during the southeast monsoon (June–August), when Indian Ocean swells dominate Indonesian waters.

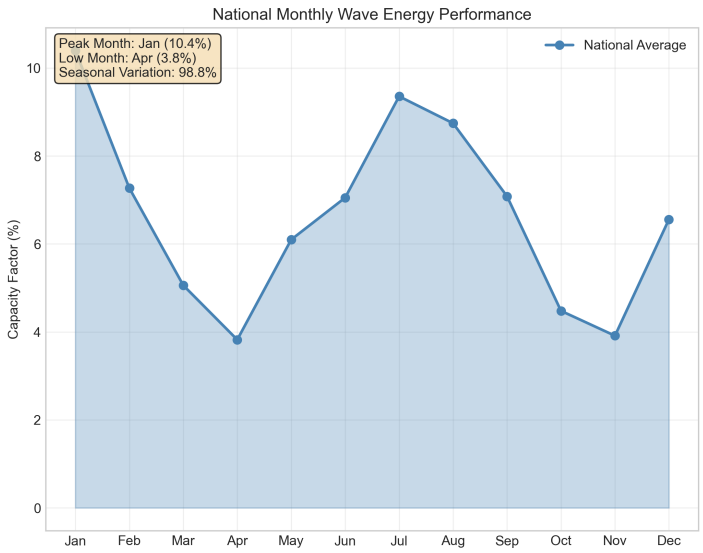


**Figure 4.3:** National monthly wave energy performance.

Seasonal stability contrasts with the more pronounced monsoon-driven variability of regional wind resources. In addition, site-level temporal diversity provides portfolio benefits: weekly analyses across random sites show low cross-correlation, with some locations delivering high performance (CF $>$ 0.6) while others simultaneously approach zero. This geographic diversity supports distributed deployment strategies to improve grid stability.

### 4.1.2. Tidal Energy Potential

The tidal stream energy resource assessment for Indonesia was conducted using the TPXO10-atlas-v2 [21] global tidal model. After applying sequential filters (depth 20–60 m, shoreline distance $\leq$20 km, exclusion of marine protected areas, and velocity threshold $\geq$1.0 m/s), the initial grid of 58.3 million points was reduced to 5,143 validated sites across 29 provinces. Table 4.2 summarizes the filtering process.

**Table 4.2:** Sequential site filtering for tidal stream deployment

| Filter Stage | Sites Remaining | Reduction (%) |
|---|---|---|
| Initial TPXO grid | 58,330,800 | - |
| Depth filter (20–60 m) | 30,102,983 | 48.4 |
| Distance filter ($\leq$20 km) | 121,371 | 99.6 |
| MPA exclusion | 112,357 | 7.4 |
| EEZ inclusion | 67,368 | 40.0 |
| Valid harmonics | 63,083 | 6.4 |
| Velocity threshold ($\geq$1.0 m/s) | 5,143 | 91.8 |

The velocity filter was the most restrictive, eliminating 91.8% of candidate sites. This indicates that high-velocity tidal environments are scarce in Indonesia, a finding consistent with global tidal assessments [45]. Nevertheless, the remaining 5,143 sites represent 11.7 TW of theoretical potential, far exceeding projected 2050 electricity demand. This highlights the abundance of the resource under idealized assumptions, even if practical deployment will be smaller.

Peak current velocities at validated sites range between 1.0–9.5 m/s, with a mean of 1.6 m/s. Table 4.3 shows that more than 40% of sites fall into the 1.5–2.5 m/s “moderate” category, well matched to the SeaGen-S cut-in (1.0 m/s) and rated velocity (2.5 m/s).

**Table 4.3:** Velocity classification of validated tidal sites

| Velocity Category | Range (m/s) | Sites | Percentage |
|---|---|---|---|
| Low velocity | 1.0–1.5 | 2,671 | 52.0 |
| Moderate velocity | 1.5–2.5 | 2,106 | 41.0 |
| High velocity | $\geq$2.5 | 366 | 7.0 |
| Total | - | 5,143 | 100.0 |

This distribution confirms that Indonesian tidal sites generally provide sustained moderate flows rather than extreme peaks. Such conditions are favorable for reliable operation, since excessively high velocities often force turbine cut-out. More detailed harmonic analysis and device-specific performance validations are included in Appendix C.2.

### Provincial Distribution

Table 4.4 presents the top 10 provinces by theoretical installed capacity. Kalimantan Barat leads with 1,680 GW, followed by Kepulauan Bangka Belitung (1,391 GW) and Riau (894 GW). The western Sumatra-Kalimantan region accounts for 54% of total theoretical capacity, reflecting the complex coastlines and shallow seas conducive to tidal energy development.

**Table 4.4:** Top 10 provinces by tidal energy capacity and performance

| Province | Sites | Capacity (GW) | CF |
|---|---|---|---|
| Kalimantan Barat | 737 | 1,680 | 0.304 |
| Kepulauan Bangka Belitung | 610 | 1,391 | 0.302 |
| Riau | 320 | 894 | 0.310 |
| Papua Barat | 395 | 716 | 0.304 |
| Kepulauan Riau | 379 | 666 | 0.293 |
| Kalimantan Tengah | 332 | 757 | 0.323 |
| Kalimantan Selatan | 419 | 955 | 0.297 |
| Maluku | 228 | 520 | 0.306 |
| Jawa Timur | 186 | 424 | 0.306 |
| Kalimantan Timur | 202 | 460 | 0.304 |

A comparative analysis of temporal generation patterns across several marine renewables, presented in Appendix C.3, highlights the unique stability of tidal energy relative to other ocean-based technologies.

### Provincial Capacity Factors

Provincial aggregation reveals distinct patterns in tidal energy potential across Indonesia's 29 provinces with validated resources. The distribution shows geographic clustering of high-capacity provinces in western Indonesia, while performance metrics vary independently of absolute capacity.

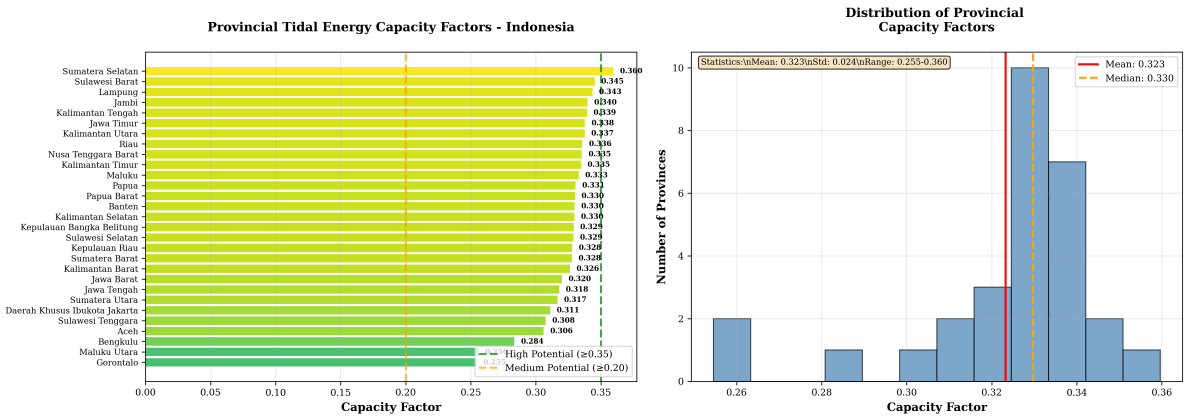


**Figure 4.4:** Provincial tidal energy capacity factor performance in Indonesia. **Left**: Capacity factor ranking for each of the 34 provinces, showing significant site-to-site variation. **Right**: Histogram of provincial capacity factor distribution, with mean CF of 32.3% and standard deviation of 2.4 percentage points. Thresholds are highlighted for high-potential provinces ($\geq$35%) and medium-potential provinces ($\geq$20%).

Figure 4.4 presents the capacity factor distribution across Indonesia's 29 provinces with tidal resources. The provincial capacity factors range from 0.255 (Sulawesi Tengah) to 0.360 (Sumatera Selatan), with a mean of 0.323 and standard deviation of 0.024. The narrow distribution indicates relatively consistent tidal resource quality across the archipelago, with most provinces clustering around the national average.

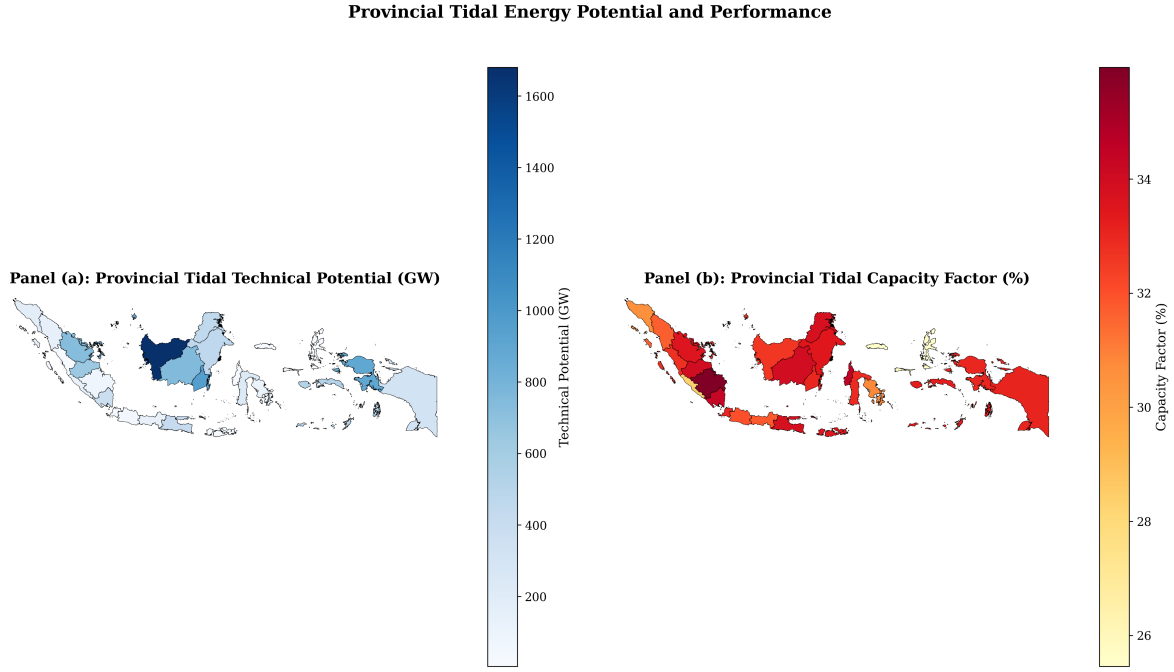


**Figure 4.5:** Provincial-level tidal stream power assessment in Indonesia. Panel (a) shows the technical potential (in GW) based on spatial deployment assumptions. Panel (b) illustrates the corresponding average capacity factor (%) derived from site-level simulations aggregated to each province.

Figure 4.5 illustrates the geographic distribution of capacity factors across Indonesia. The highest-performing provinces include Kalimantan Tengah (0.323), Jambi (0.322), and Sumatera Selatan (0.319), while the lowest performers are Sulawesi Tengah (0.255), Gorontalo (0.221), and Maluku Utara (0.231).

The provincial capacity factor range (0.255-0.360) demonstrates moderate variation in tidal resource quality. The narrow standard deviation (0.024) indicates relatively consistent tidal energy potential

across the Indonesian archipelago, contrasting with more variable solar and wind resources.

Notably absent from the analysis is Nusa Tenggara Timur (NTT) province, which contains Larantuka Strait—identified in literature as Indonesia's highest-velocity tidal site (3.4 m/s) [95, 47]. The provincial-scale methodology also cannot resolve narrow straits such as Lombok (2.9 m/s), Toyopakeh (3.2 m/s), and Pantar (2.91 m/s), which represent some of Indonesia's most promising tidal energy locations.

### Temporal Generation Patterns

Tidal generation exhibits highly predictable semi-diurnal cycles. At the monthly scale, variability remains low, with most provinces fluctuating within ±15% of their annual mean. Figure 4.6 illustrates representative cases.

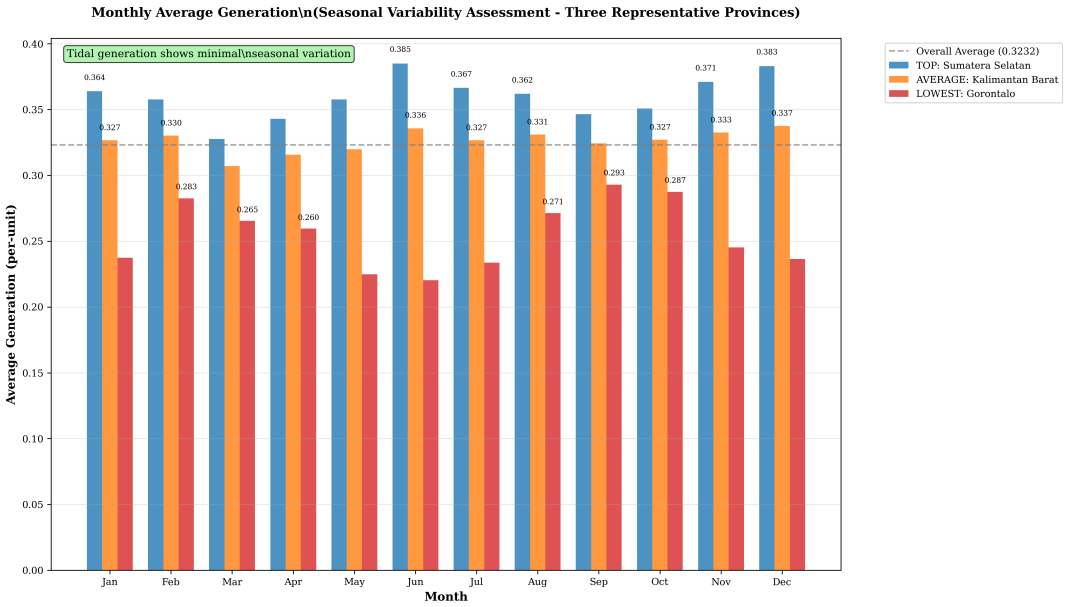


**Figure 4.6:** Monthly average tidal generation profile for three representative provinces (Sumatera Selatan, Kalimantan Barat, and Gorontalo) during the year 2050.

Monthly aggregation reveals minimal seasonal variation in tidal generation, with coefficient of variation ranging from 9.0% (Kalimantan Barat) to 24.8% (Gorontalo). Figure 4.6 shows that most provinces maintain generation within $\pm 15\%$ of their annual average throughout the year.

**Table 4.5:** Seasonal variability in tidal generation

| Province | Peak Month | Low Month | Variation (%) |
|---|---|---|---|
| Sumatera Selatan | June | March | 14.9 |
| Kalimantan Barat | December | March | 9.0 |
| Gorontalo | September | June | 24.8 |
| Average (29 provinces) | - | - | 16.2 |

The low seasonal variability (average 16.2%) contrasts favorably with solar photovoltaic systems in Indonesia, which typically experience 30-40% seasonal variation due to monsoon cloud cover patterns. This characteristic supports tidal energy's role as a predictable baseload renewable source.

Extended weekly cycles and seasonal variability tables are provided in Appendix C.2.

## 4.1.3. Demand Projection Results

Indonesian electricity demand projections for 2050 employ dual scenarios to capture uncertainty in regional development patterns and their implications for MRE integration. The bottom-up scenario applies RUPTL provincial growth rates, projecting 1,079 TWh total demand, while the top-down scenario

distributes RUKN 2024 national targets (1,492 TWh) across provinces using electricity sales proportions.

### Bottom-Up Demand Scenario Findings

The bottom-up scenario shows 2.90x growth (190.2% increase) over the 26-year period across JAMALI provinces, with total non-JAMALI demand reaching 69.5 TWh representing 28.9% of national electricity sales in 2024. Complete provincial scaling results and proxy methodology documentation are provided in Appendix C.4.1.

The highest growth multipliers occur in eastern provinces, with some Sulawesi regions achieving over 10x growth, while JAMALI provinces show more moderate 2-6x increases reflecting their mature baseline conditions. This creates total Indonesian electricity demand projection from 297.2 TWh in 2024 to 1,079 TWh in 2050, representing 263.1% growth.

Validation against Langer et al. [1] demonstrates strong methodological alignment with 5.5% difference in total demand (1,079 TWh vs 1,141 TWh) and cross-correlation coefficient of 0.883 at the provincial level, confirming approach reliability. Detailed validation analysis is presented in Appendix C.4.2.

### Top-Down Policy-Aligned Scenario Findings

The top-down scenario distributes RUKN 2024 national targets (1,492 TWh by 2050) using regional scaling factors ranging from 1.3x (Banten) to 21.1x (Eastern Indonesia). This creates distinct provincial development trajectories aligned with national policy objectives.

Eastern provinces receive the steepest scaling, with Papua increasing from 1.13 TWh to 23.75 TWh and Maluku from 0.53 TWh to 11.12 TWh. The 21.1x Eastern Indonesia multiplier creates 93 TWh additional demand compared to bottom-up projections (140 TWh vs 47 TWh), significantly improving resource-demand spatial correlation for tidal and wave technologies. Complete scaling factor documentation is provided in Appendix C.4.3.

### Scenario Comparison Analysis and MRE Integration Implications

System-level comparison reveals substantial differences between methodological approaches affecting MRE deployment potential. The top-down scenario projects 1,491.6 TWh total demand versus 1,079.6 TWh for bottom-up (+412.0 TWh, +38.2%), while maintaining high temporal correlation (0.965) indicating preserved demand shape patterns.

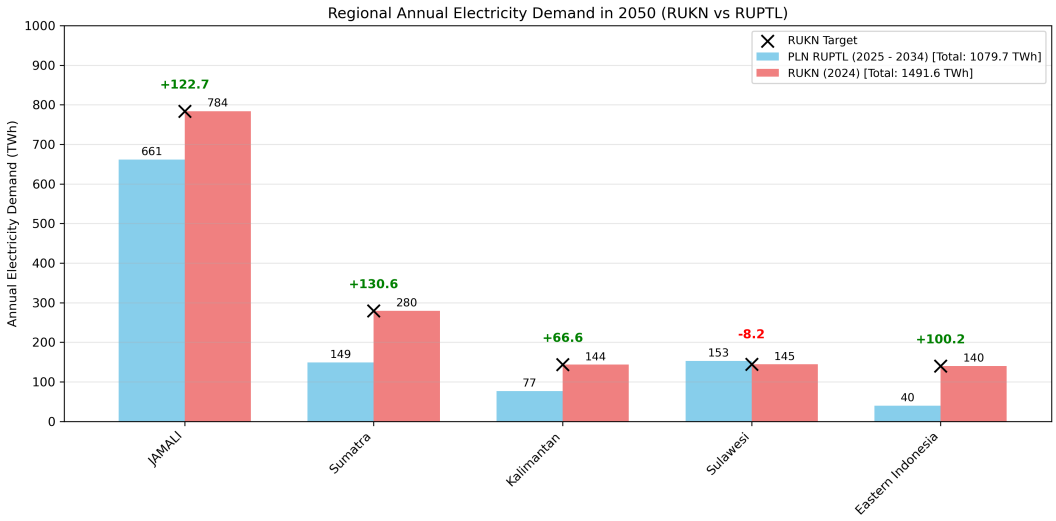


**Figure 4.7:** Regional Energy Comparison Between Bottom-Up and Top-Down Scenarios

Regional analysis demonstrates divergent development assumptions across Indonesian archipelago with critical implications for MRE integration. Eastern Indonesia exhibits the largest increase (+252.1%), transforming from 39.8 TWh to 140.0 TWh, while Sumatra and Kalimantan show substantial growth

(+87.7% and +86.6% respectively). JAMALI experiences moderate expansion (+18.6%), fundamentally altering marine renewable energy market potential.

**Table 4.6:** Regional Comparison Summary Between Demand Scenarios

| Region | Bottom-Up (TWh) | Top-Down (TWh) | Difference (TWh) | Change (%) |
|---|---|---|---|---|
| JAMALI | 661.3 | 784.0 | +122.7 | +18.6 |
| Sumatra | 148.9 | 279.5 | +130.6 | +87.7 |
| Kalimantan | 77.0 | 143.6 | +66.6 | +86.6 |
| Sulawesi | 152.7 | 144.5 | -8.2 | -5.4 |
| Eastern Indonesia | 39.8 | 140.0 | +100.2 | +252.1 |
| **Total** | **1079.6** | **1491.6** | **+412.0** | **+38.2** |

The demand scenario differences produce measurable impacts on MRE integration economics. Outer islands receive 708 TWh under policy-aligned projections compared to 418 TWh in utility-based scenarios (+69%), expanding potential markets for wave and tidal technologies across the archipelago. JAMALI's share decreases from 61.2% to 52.5% between scenarios, shifting the economic balance between centralized versus distributed MRE deployment.

Papua exemplifies this transformation: demand increases 21-fold from 1.13 TWh to 23.75 TWh under RUKN targets, converting a marginal electricity market into a substantial one where point absorber economics become viable. Maluku provinces show similar patterns (+411.0% growth), with demand expansion occurring in regions where tidal stream resources are most abundant based on bathymetry and current velocity data.

The regional redistribution affects grid integration strategies. Under fragmented grid scenarios, higher outer island demand supports local MRE deployment without requiring expensive submarine transmission links. Conversely, scenarios with strong JAMALI concentration favor centralized MRE development connected through supergrid infrastructure, where marine energy from resource-rich sites can serve major consumption centers.

Eastern Indonesia receives 93 TWh additional demand under policy targets compared to utility projections, creating new markets in provinces where wave energy potential exceeds 50 kW/m based on ERA5 reanalysis data. This demand-resource alignment improves the economic case for both nearshore wave systems and tidal installations in strait configurations between major islands.

### Model Implementation Framework

The dual-scenario framework captures uncertainty space through methodologically distinct approaches while maintaining temporal pattern preservation. Load factor analysis shows consistent diurnal and seasonal characteristics (load factor 0.801 for both scenarios), with coefficient of variation patterns indicating maintained demand volatility relationships.

The top-down scenario serves as the reference case for Calliope energy system modeling, representing policy-aligned development trajectories consistent with RUKN 2024 national targets. The bottom-up scenario provides alternative demand profile for sensitivity analysis, reflecting operational data-grounded projections based on RUPTL utility planning assumptions. Complete statistical validation, temporal correlation analysis, and provincial-level details are provided in Appendix C.4.

## 4.2. Impact on Energy Storage Requirements

**Research Question 1**

"What is the impact of marine renewable energy integration on energy storage requirements within Indonesia's power system?"

*MRE integration reduces storage requirements by 10.6 GW (-7.8%) in Supergrid systems but increases storage (+0.6 GW) in fragmented grids. Under cost-competitive conditions, storage reductions amplify to 15.4 GW in interconnected systems. Tidal energy provides superior storage displacement efficiency (0.94 GW saved per GW installed) compared to wave energy (0.09 GW/GW). Storage benefits depend entirely on transmission flexibility for spatial balancing.*

This section addresses *What is the impact of marine renewable energy integration on energy storage requirements within Indonesia's power system?* Analysis across technology scenarios reveals that MRE integration reduces system-wide storage needs, but benefits depend critically on grid configuration.

### 4.2.1. Full System Storage Impact

System-wide optimization results confirm MRE's grid-dependent storage benefits across all cost scenarios. Table 4.7 presents storage requirements under reference MRE cost assumptions, while Table 4.8 demonstrates sensitivity to MRE cost variations.

**Table 4.7:** Installed storage capacity (GW) under reference scenarios

| Technology | Fragmented | Fragmented – Without MRE | Fragmented – MRE Min Cost | Supergrid | Supergrid – Without MRE | Supergrid – MRE Min Cost |
|---|---|---|---|---|---|---|
| Battery | 195.33 | 181.38 | 171.88 | 96.31 | 107.77 | 77.13 |
| Pumped hydro | 58.09 | 71.40 | 53.64 | 28.74 | 27.89 | 43.09 |
| **Total storage capacity** | **253.42** | **252.78** | **225.52** | **125.05** | **135.66** | **120.22** |

Under reference MRE costs, Supergrid scenarios achieve 10.6 GW storage reduction (135.7→125.1 GW, -7.8%) while fragmented grids show negligible impact (+0.6 GW, +0.3% increase). This pattern reinforces that transmission flexibility determines whether MRE integration reduces or increases storage requirements.

Cost-competitive MRE deployment amplifies these storage benefits significantly. Table 4.8 shows that under minimum cost conditions, Supergrid storage requirements drop to 120.2 GW—a 15.4 GW reduction (-11.4%) compared to maximum cost scenarios. Fragmented systems achieve 27.0 GW storage reduction (-10.7%) under cost-competitive conditions, demonstrating that economic MRE deployment can overcome spatial constraints through local generation-demand matching.

**Table 4.8:** Installed storage capacity (GW) under cost sensitivity scenarios

| Technology | Fragmented – MRE Min Cost | Fragmented | Fragmented – MRE Max Cost | Supergrid – MRE Min Cost | Supergrid | Supergrid – MRE Max Cost |
|---|---|---|---|---|---|---|
| Battery | 171.88 | 195.33 | 181.16 | 77.13 | 96.31 | 107.64 |
| Pumped hydro | 53.64 | 58.09 | 71.40 | 43.09 | 28.74 | 27.87 |
| **Total storage capacity** | **225.52** | **253.42** | **252.56** | **120.22** | **125.05** | **135.51** |

The technology-specific storage trade-offs reveal contrasting patterns between grid configurations. In Supergrid systems, cost-competitive MRE reduces battery requirements (-19.2 GW) while increasing pumped hydro deployment (+15.2 GW), indicating a shift toward long-duration storage as MRE scales up. Fragmented grids show battery reductions (-23.5 GW) with minimal pumped hydro changes, reflecting localized storage optimization without inter-island balancing flexibility.

These full system results validate the controlled technology comparison findings while demonstrating that economic MRE deployment conditions fundamentally alter storage requirements across both grid configurations. The magnitude of storage reductions under cost-competitive scenarios suggests MRE's storage value increases non-linearly with deployment scale and cost competitiveness.

### 4.2.2. Grid Configuration Dependencies

Grid topology fundamentally determines whether MRE provides storage benefits or additional balancing challenges. Figure 4.8 demonstrates that storage benefits are only realized under interconnected grid conditions.

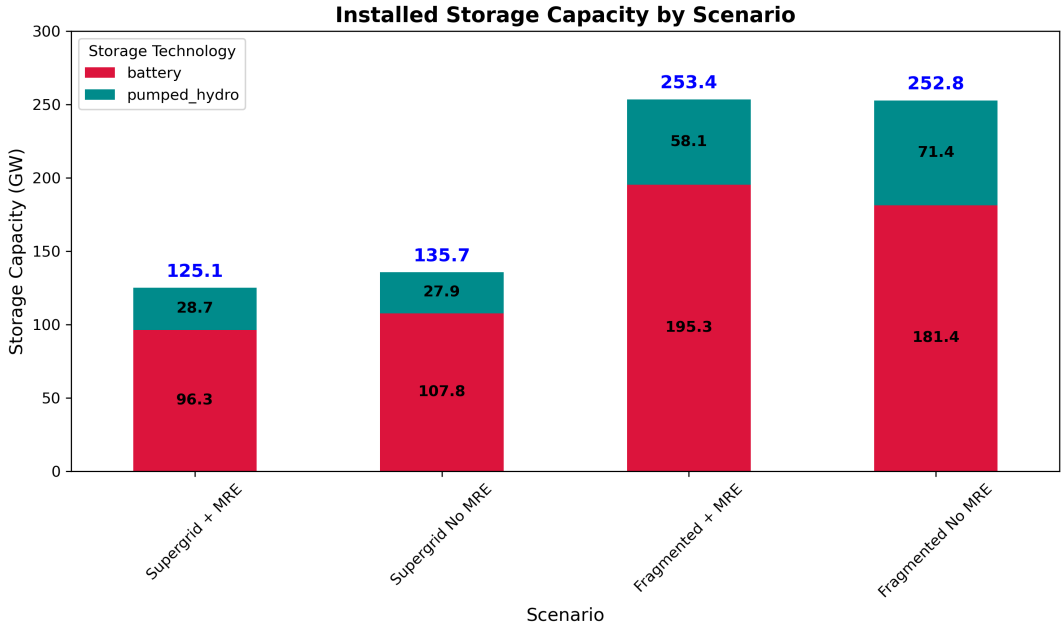


**Figure 4.8:** Installed storage capacity across four core scenarios in 2050, disaggregated by storage technology. Fragmented systems require nearly double the storage capacity of interconnected systems.

**Table 4.9:** Storage Requirements Across Grid Configurations (GW)

| Storage Type | Supergrid + MRE | Supergrid No MRE | Fragmented + MRE | Fragmented No MRE |
|---|---|---|---|---|
| Battery | 96.3 | 107.8 | 195.3 | 181.4 |
| Pumped Hydro | 28.7 | 27.9 | 58.1 | 71.4 |
| **Total** | **125.0** | **135.7** | **253.4** | **252.8** |
| MRE Impact | -10.7 GW | – | +0.6 GW | – |

Supergrid systems achieve 10.7 GW storage reduction through MRE integration, while fragmented grids show negligible impact (+0.6 GW increase). This demonstrates that MRE's storage benefits depend entirely on transmission flexibility for spatial balancing.

### 4.2.3. Technology-Specific Storage Efficiency

To isolate individual MRE technology impacts, we analyze controlled scenarios where solar capacity remains constant across four generation mixes: *Solar Only*, *Solar + Wave*, *Solar + Tidal*, and *Solar + Wave + Tidal*. This controlled analysis complements the full system optimization results presented earlier.

Under these solar-dominated scenarios, MRE integration reduces storage requirements by 44.9 GW (7.3%) through generation diversification. Combined wave-tidal deployment achieves the lowest total storage requirements (568.6 GW), demonstrating complementary rather than additive benefits.

**Table 4.10:** Storage Requirements by Technology Mix (GW)

| Storage Type | Solar Only | Solar+Wave | Solar+Tidal | Solar+MRE |
|---|---|---|---|---|
| Battery | 407.8 | 370.7 | 412.5 | 378.5 |
| Pumped Hydro | 205.7 | 238.5 | 172.5 | 190.1 |
| **Total** | **613.5** | **609.2** | **585.0** | **568.6** |

Combined wave-tidal deployment achieves the lowest total storage requirements (568.6 GW), demonstrating complementary rather than additive benefits. Wave energy provides greater battery displacement (37.1 GW reduction) while requiring additional pumped hydro capacity. Tidal energy achieves the lowest total storage needs among individual technologies (585.0 GW) through superior storage cycling alignment.

Storage displacement efficiency analysis reveals contrasting technology characteristics. These efficiency metrics derive from the controlled comparison scenarios above, using different capacity assumptions than the full system optimization presented in Section 4.2

**Table 4.11:** Storage Displacement Efficiency by MRE Technology

| Technology | Installed Capacity [GW] | Storage Reduction [GW] | Efficiency [GW/GW] |
|---|---|---|---|
| Wave | 49.5 | 60 | 0.09 |
| Tidal | 30.3 | 2 | 0.94 |
| Wave + Tidal | 76.7 | 61 | 0.59 |

Wave energy delivers substantial absolute storage reductions (60 GW) but operates at low efficiency (0.09 GW displaced per GW installed). Tidal energy demonstrates superior displacement efficiency (0.94 GW/GW) despite minimal absolute impact, reflecting predictable 12.4-hour cycles that align with storage cycling requirements.

Detailed storage dispatch patterns, utilization metrics, and operational mechanisms supporting these findings are provided in Appendix D.1.

## 4.3. Optimal Grid Expansion Strategy

**Research Question 2**

"What is the optimal grid expansion strategy to accommodate marine renewable energy in Indonesia's power system?"

*25 GW per HVDC link achieves minimum system cost (102.6 US$/MWh). MRE integration requires 95.9 GW additional transmission capacity system-wide under cost-competitive scenarios. Wave energy demands concentrated gateway infrastructure (Lampung-Banten +473% expansion) for resource evacuation, while tidal energy enables distributed grid balancing near demand centers, reducing overall transmission stress.*

This section addresses *What is the optimal grid expansion strategy to accommodate marine renewable energy in Indonesia's power system?* Analysis reveals that transmission capacity optimization determines MRE integration potential, with economic thresholds driving infrastructure priorities.

### 4.3.1. Optimal HVDC Capacity Requirements

The optimization of inter-island transmission capacity reveals distinct cost curves that demonstrate clear economic thresholds for HVDC investment. Figure 4.9 shows the sensitivity of levelized system cost to maximum HVDC transmission limits per link, comparing scenarios with and without MRE integration.

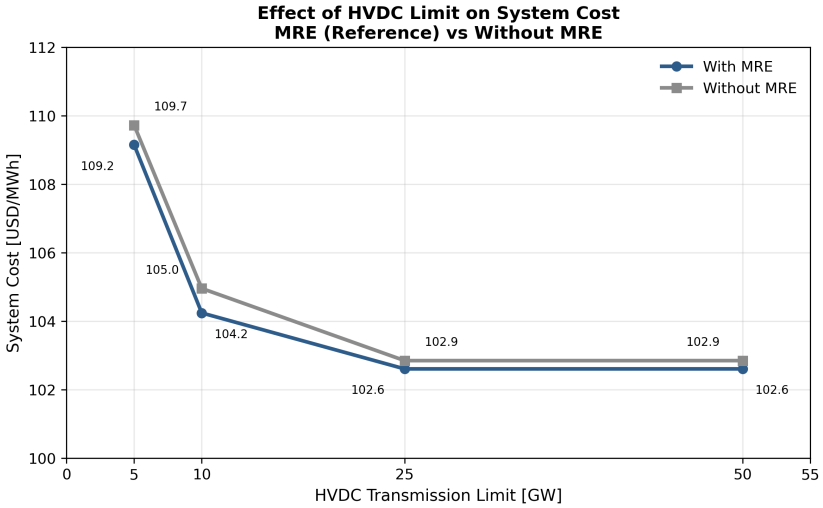


**Figure 4.9:** Effect of HVDC transmission limits on levelized system cost. Cost curve flattens beyond 25 GW per link, indicating diminishing returns from additional transmission investment.

The analysis identifies 25 GW per link as the optimal transmission capacity limit, achieving minimum system cost of 102.6 US$/MWh with MRE integration. Restrictive 5 GW limits impose 6.5 US$/MWh penalties, demonstrating significant economic benefits from adequate transmission capacity. Beyond 25 GW, the cost curve flattens, indicating diminishing returns from additional transmission investment.

MRE integration produces marginal but consistent transmission benefits across all capacity scenarios. The cost differential between MRE and non-MRE cases remains approximately 0.3 US$/MWh at optimal capacity levels, suggesting marine renewables provide modest system benefits through enhanced generation diversity.

At low transmission limits (5–10 GW), insufficient inter-island links force reliance on local generation and storage, raising system costs. When capacity reaches 25–50 GW, these bottlenecks are removed and overall costs converge across scenarios.

### 4.3.2. Infrastructure Requirements

MRE integration increases Indonesia's transmission requirements. Total HVDC capacity expands from 97.1 GW without MRE to 102.4 GW with reference MRE costs (+5.5%), reaching 137.6 GW under cost-competitive conditions (+41.8%). This non-linear scaling reflects economic optimization concentrating MRE deployment in high-resource areas rather than distributing generation near demand centers.

**Table 4.12:** Transmission Infrastructure Summary by MRE Integration Scenario

| Scenario | Inter-Island HVDC (GW) | Intra-Island AC (GW) | Total Investment (GW) |
|---|---|---|---|
| Without MRE | 97.1 | 128.3 | 225.4 |
| With MRE | 102.4 | 134.0 | 236.4 |
| With MRE (cost optimistic) | 137.6 | 184.8 | 322.4 |
| **Change vs. Without MRE** | | | |
| With MRE | +5.3 GW (+5.5%) | +5.7 GW (+4.4%) | +11.0 GW (+4.9%) |
| With MRE (cost optimistic) | +40.5 GW (+41.8%) | +56.5 GW (+44.0%) | +97.0 GW (+43.0%) |

Inter-island HVDC growth (+41.8%) matches intra-island AC expansion (+44.0%), totaling 97.0 GW additional capacity system-wide under cost-competitive MRE conditions. This balanced expansion indicates coordinated grid development requirements across all voltage levels.

### 4.3.3. Critical Transmission Corridors

Analysis of inter-island transmission capacity reveals strong correlation between MRE deployment patterns and corridor-specific infrastructure requirements. Figure 4.10 compares transmission patterns

across three scenarios: reference with MRE, no MRE, and cost-competitive MRE integration.

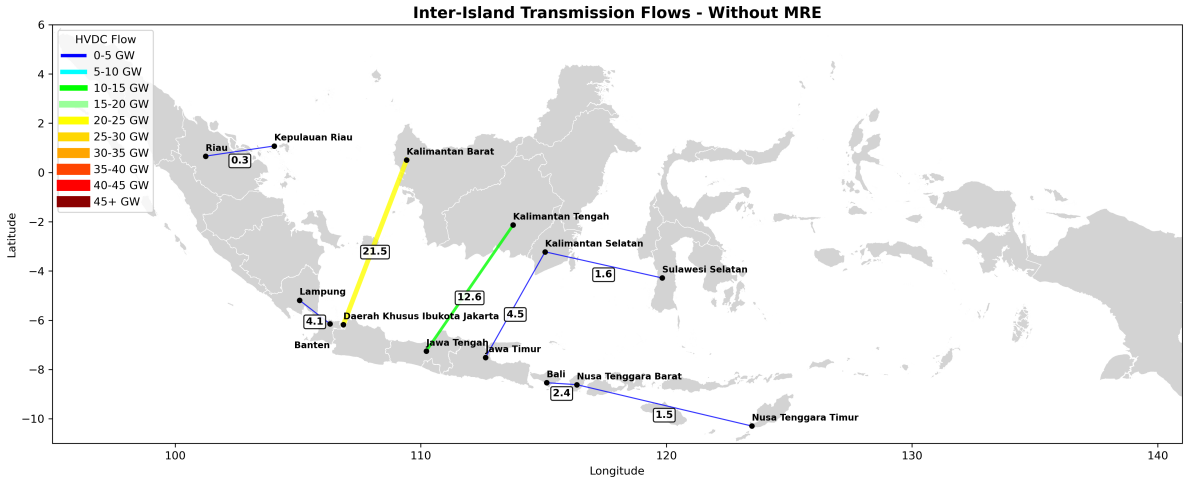


**(a)** Without MRE

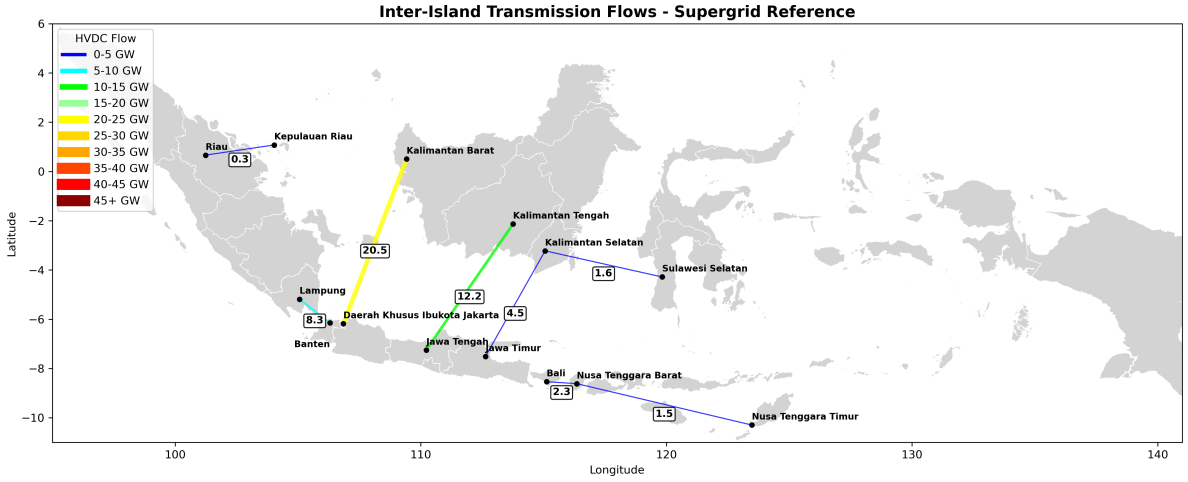


**(b)** Reference scenario with MRE

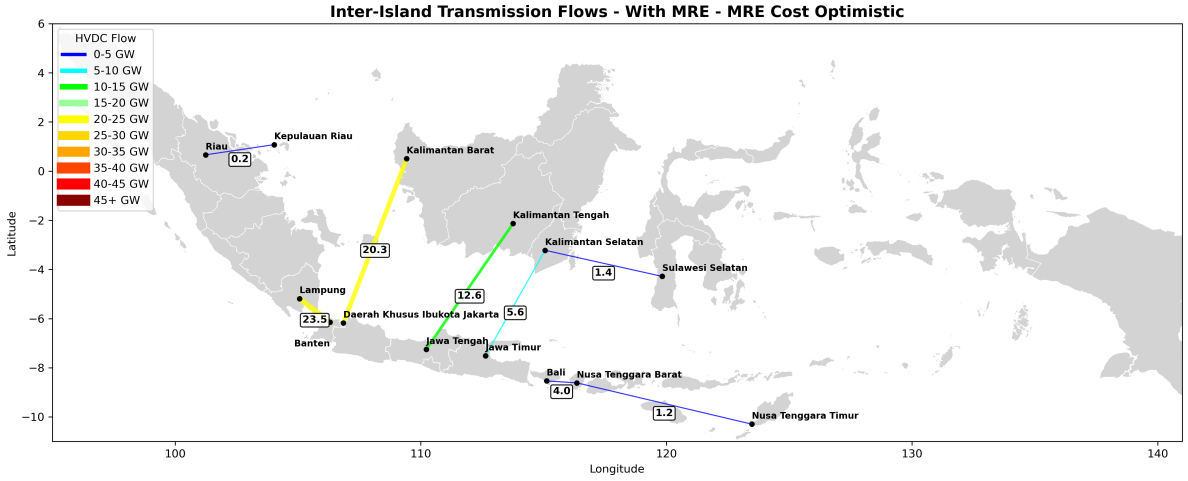


**(c)** Cost-competitive MRE scenario

**Figure 4.10:** Inter-island transmission flows under different MRE integration scenarios. Line thickness indicates flow magnitude.

Table 4.13 presents all eight HVDC corridors with capacity changes under cost-competitive MRE deploy-

ment, demonstrating asymmetric expansion requirements across Indonesia's inter-island transmission network.

**Table 4.13:** Inter-Island HVDC Transmission Corridor Capacity Changes (Without MRE vs MRE Optimistic Cost)

| HVDC Corridor | Capacity Change (GW) | Expansion Impact |
|---|---|---|
| Lampung – Banten | +19.4 | Major expansion (473%) |
| Kalimantan Barat – DKI Jakarta | -1.2 | Minor reduction |
| Jawa Timur – Kalimantan Selatan | +1.1 | Minor increase (24%) |
| Bali – Nusa Tenggara Barat | +1.6 | Moderate increase (67%) |
| Kalimantan Tengah – Jawa Tengah | -0.2 | Stable |
| Kalimantan Selatan – Sulawesi Selatan | -0.3 | Minor reduction |
| Kepulauan Riau – Riau | -0.8 | Minor reduction |
| Nusa Tenggara Timur – Nusa Tenggara Barat | -0.3 | Stable |

The spatial distribution of MRE deployment under cost-competitive scenarios reveals concentration patterns that drive transmission requirements. Wave energy deployment concentrates in Lampung province, expanding from 16.0 GW under reference conditions to 61.6 GW under cost-competitive scenarios, with secondary development in Bengkulu (18.3 GW). Tidal energy distributes across Java provinces with Jawa Barat (10.0 GW) and Jawa Timur (9.4 GW) leading deployment, supplemented by distributed installations in Riau (3.2 GW), DKI Jakarta (3.1 GW), and Sumatera provinces.

**Table 4.14:** Installed MRE Capacity by Province Under Cost-Competitive Scenarios

| Province | Wave Capacity (GW) | Tidal Capacity (GW) |
|---|---|---|
| Lampung | 61.6 | – |
| Bengkulu | 18.3 | – |
| Jawa Barat | – | 10.0 |
| Jawa Timur | – | 9.4 |
| Riau | – | 3.2 |
| DKI Jakarta | – | 3.1 |
| Sumatera Selatan | – | 1.7 |
| Sumatera Utara | – | 1.1 |
| Kepulauan Riau | – | 0.3 |

Notably, tidal capacity deployment in DKI Jakarta (3.1 GW) and Kepulauan Riau (0.3 GW) does not appear in the major transmission infrastructure changes, suggesting these installations provide highly localized grid benefits without requiring significant transmission upgrades. This pattern indicates that strategic tidal deployment in urban demand centers can enhance grid stability through local generation without imposing additional infrastructure costs.

The MRE-transmission correlation analysis demonstrates fundamentally different infrastructure requirements for wave versus tidal technologies. Table 4.15 quantifies the relationship between MRE deployment capacity and corresponding transmission infrastructure changes, revealing technology-specific expansion patterns.

**Table 4.15:** MRE Deployment and Transmission Infrastructure Correlation

| Province | Wave (GW) | Tidal (GW) | AC Change (GW) | AC (%) | HVDC Change (GW) | HVDC (%) |
|---|---|---|---|---|---|---|
| Lampung | 61.6 | – | +0.7 | +29% | +19.4 | +473% |
| Banten | – | – | +15.6 | +557% | +19.4 | +473% |
| Bengkulu | 18.3 | – | +3.1 | +91% | Regional | – |
| Jawa Barat | – | 10.0 | +16.9 | +222% | No direct | – |
| Jawa Timur | – | 9.4 | +2.6 | +74% | +1.1 | +24% |

### Wave Energy Gateway Infrastructure

Wave energy deployment creates concentrated evacuation requirements due to resource optimization in high-performance coastal locations. The Lampung-Banten corridor demonstrates this pattern most clearly, with 61.6 GW wave deployment in Lampung driving massive HVDC expansion from 4.1 GW to 23.5 GW—a 473% increase that transforms this corridor into Indonesia's dominant inter-island transmission pathway.

This concentration effect reflects wave energy's spatial characteristics: economic deployment prioritizes sites with highest capacity factors (Lampung 29.5%) rather than distributed coastal development. The resulting 45.6 GW capacity increase in Lampung creates substantial power evacuation needs that require dedicated transmission infrastructure to reach Java's industrial demand centers through the relatively short 30 km HVDC link.

Secondary wave corridors follow similar patterns. The Bali-Nusa Tenggara Barat connection requires capacity expansion from 2.4 GW to 4.0 GW to support Bali's wave resources, while Bengkulu's 18.3 GW wave deployment drives regional AC grid upgrades of 91%. Wave energy consistently creates point-to-point transmission requirements between optimal resource locations and distant demand centers.

### Tidal Energy Grid Balancing

Tidal energy deployment produces contrasting transmission impacts through distributed generation near major demand centers. Java's 22.5 GW total tidal capacity reduces dependency on remote conventional generation, fundamentally altering transmission flow patterns across multiple corridors.

The DKI Jakarta case demonstrates this load reduction effect most clearly. Local deployment of 3.1 GW tidal capacity enables reduced coal imports from Kalimantan Barat, with the corresponding HVDC corridor experiencing decreased flows of -1.4 TWh. Similarly, most traditional coal evacuation corridors show stable or declining transmission requirements as local marine resources provide alternative generation sources.

Jawa Timur represents the balancing requirements of tidal integration. The province's 9.4 GW tidal deployment requires modest HVDC expansion (+1.1 GW, +24%) to accommodate regional power balancing, while the bidirectional Jawa Timur-Kalimantan Selatan upgrade (+0.9 TWh) enables economic transport of cheaper MRE from Kalimantan Selatan when cost conditions permit.

The Nusa Tenggara corridors maintain minimal capacity changes despite regional tidal potential, with Nusa Tenggara Barat-Nusa Tenggara Timur flows remaining stable (-0.1 TWh). This stability reflects enhanced regional energy self-sufficiency through predictable tidal generation that matches local demand patterns more effectively than requiring inter-provincial power exchange.

### System-wide Transmission Implications

These findings reveal that MRE integration fundamentally rebalances Indonesia's power flow patterns from coal-centric imports toward coastal renewable generation. Wave energy requires massive point-to-point evacuation infrastructure due to concentrated optimal resources, while tidal energy enables distributed load reduction that decreases overall transmission stress.

The system optimization exploits this geographic advantage through strategic infrastructure investment: corridor capacity expansion concentrates in high-resource evacuation pathways (Lampung-Banten +473%) while traditional coal import corridors experience reduced utilization. Most corridors show minimal changes as the system rebalances toward local renewable generation rather than remote fossil fuel transport.

This technology-differentiated transmission strategy indicates that optimal MRE integration prioritizes resource quality over proximity to demand for wave energy, while tidal deployment enhances grid efficiency through predictable local generation. Indonesia's Supergrid development should accordingly prioritize concentrated wave evacuation infrastructure combined with distributed tidal deployment for grid load reduction.

## 4.4. Cost Competitiveness of Marine Renewables

**Research Question 3**

"What are the Levelized Cost of Electricity (LCOE) for marine renewable energy technologies in Indonesia, and how do they compare with other renewable energy sources?"

*Under optimal conditions (Supergrid + cost reductions), MRE technologies achieve competitive LCOE positioning: wave energy at 69.5 US$/MWh competes with small hydro (67.5 US$/MWh) and geothermal (61.7 US$/MWh), while tidal stream at 66.1 US$/MWh outperforms solar onshore (73.9 US$/MWh). However, MRE exhibits extreme cost sensitivity to grid configuration and technology costs. Tidal stream LCOE ranges from 1,232.6 US$/MWh under fragmented reference conditions to 66.1 US$/MWh under optimal scenarios—a 95% reduction reflecting deployment thresholds characteristic of early-stage technologies. Grid interconnection provides substantial economic benefits, enabling 4.1x higher MRE generation while reducing costs through enhanced resource access. Combined MRE generation reaches 261.4 TWh (17.3% system share) under optimal conditions, positioning these technologies as viable contributors to Indonesia's 2050 decarbonization strategy when supported by appropriate grid infrastructure and continued cost reductions.*

Levelized Cost of Electricity (LCOE) analysis across grid and cost scenarios reveals MRE economic positioning relative to established renewables. LCOE values are calculated from Calliope optimization results as annualized system costs divided by annual electricity generation, providing system-optimized technology competitiveness indicators for 2050 deployment in Indonesia's power system.

### 4.4.1. Technology LCOE Comparison

**Table 4.16:** Levelized Cost of Electricity Across Grid and Cost Scenarios (US$/MWh)

| Technology | Reference (Fragmented) | MRE Cost Optimistic (Fragmented) | Reference (Supergrid) | MRE Cost Optimistic (Supergrid) |
|---|---|---|---|---|
| Geothermal | 65.4 | 65.7 | 61.5 | 61.7 |
| Large Hydro | 57.6 | 57.6 | 57.6 | 57.6 |
| Offshore Wind | 3154 | 3141.4 | 2364.6 | 2933.9 |
| Onshore Wind | 38.9 | 38.2 | 37.3 | 37.1 |
| OTEC | 122.3 | 120.8 | 116.1 | 115.7 |
| Small Hydro | 73.7 | 77.5 | 69.0 | 67.5 |
| Solar (Floating) | 103.2 | 100.4 | 84.8 | 82.1 |
| Solar (Onshore) | 89.9 | 89.2 | 78.0 | 73.9 |
| **Tidal Stream**[1] | **1,232.6** | **178.5** | **125.3** | **66.1** |
| **Wave Energy** | **109.2** | **128.2** | **109.2** | **69.5** |

Under optimal conditions (Supergrid + MRE cost optimistic), both MRE technologies achieve competitive positioning within Indonesia's renewable energy hierarchy. Wave energy at 69.5 US$/MWh competes directly with small hydro (67.5 US$/MWh) and approaches geothermal competitiveness (61.7 US$/MWh), while tidal stream at 66.1 US$/MWh outperforms solar onshore (73.9 US$/MWh) and floating solar (82.1 US$/MWh). This represents a fundamental transformation from premium alternatives to cost-competitive renewable technologies.

Grid interconnection provides substantial economic benefits for MRE deployment. Supergrid configuration enables wave energy to maintain stable LCOE performance (109.2 US$/MWh across cost scenarios) while achieving dramatic competitiveness under cost reductions (69.5 US$/MWh). Tidal stream technology demonstrates the most pronounced grid dependency, with LCOE improving from 125.3 US$/MWh (Supergrid reference) to 66.1 US$/MWh (Supergrid optimistic)—a 47% reduction that reflects enhanced access to optimal marine resources through inter-island transmission infrastructure.

The extreme LCOE sensitivity observed for tidal stream technology, particularly the 1,232.6 US$/MWh

value under fragmented reference conditions, reflects critical deployment thresholds characteristic of early-stage technologies in constrained systems. As detailed in Section 4.4.3, these values represent economically rational deployment under transmission constraints rather than calculation anomalies, demonstrating how system-level optimization captures real-world deployment economics.

Both MRE technologies exhibit cost competitiveness trajectories that position them as viable contributors to Indonesia's 2050 decarbonization targets when supported by appropriate grid infrastructure and technology cost reductions. Under optimal conditions, MRE technologies achieve LCOE ranges comparable to established renewables, validating their potential role in Indonesia's energy transition beyond niche applications.

### 4.4.2. LCOE Sensitivity and Deployment Scale Analysis

**Table 4.17:** MRE Technology Economics: Deployment Scale vs. LCOE Performance

| Technology | Fragmented Reference | | | Fragmented Optimistic | | |
|---|---|---|---|---|---|---|
| | Total Cost (B US$) | Generation (TWh) | LCOE (US$/MWh) | Total Cost (B US$) | Generation (TWh) | LCOE (US$/MWh) |
| Wave Energy | 1.03 | 9.4 | 109.2 | 13.93 | 108.6 | 128.2 |
| Tidal Stream | 0.84 | 0.7 | 1,232.6[2] | 2.54 | 14.2 | 178.5 |

The fragmented grid scenario reveals contrasting deployment economics between MRE technologies. Wave energy demonstrates marginal site selection effects: despite cost reductions, LCOE increases from 109.2 to 128.2 US$/MWh as deployment expands 11.5-fold (9.4 → 108.6 TWh), indicating progression into lower-quality sites with reduced capacity factors.

Tidal stream technology exhibits opposite behavior, achieving 85% LCOE improvement (1,232.6 → 178.5 US$/MWh) through 20x deployment expansion (0.7 → 14.2 TWh). This reflects threshold economics where cost reductions unlock previously uneconomical high-quality tidal sites, enabling efficient large-scale deployment despite only 3x cost increase (0.84 → 2.54 billion US$).

These patterns demonstrate how deployment scale interacts with resource quality in system optimization: wave energy faces resource saturation at optimal sites, while tidal energy benefits from accessing superior resources under cost-competitive conditions.

### 4.4.3. Tidal Stream LCOE Sensitivity and Deployment Economics

Tidal stream technology demonstrates extreme cost sensitivity, with LCOE ranging from 1,232.6 US$/MWh (fragmented reference) to 178.5 US$/MWh (fragmented optimistic)—an 86% reduction that reflects critical deployment thresholds and system-level economic constraints. This dramatic variation occurs because Calliope's optimization determines economic viability based on system-wide cost minimization, where technologies deploy only when cost-competitive relative to alternatives, creating sharp transition points between minimal and substantial deployment.

**Table 4.18:** Provincial Energy Balance for Tidal Deployment Areas - Fragmented Reference Scenario

| Province | Tidal Capacity (GW) | Annual Demand (TWh) | Local Supply (TWh) | Supply Deficit (TWh) | Tidal Share (%) |
|---|---|---|---|---|---|
| Jakarta | 0.180 | 156.7 | 0.009 | -156.7 | 100.0 |
| Jawa_Barat | 0.607 | 195.3 | 98.0 | -97.3 | 0.03 |
| Banten | 1.116 | 47.7 | 64.1 | 16.4 | 0.09 |
| Sumatera_Utara | 0.086 | 76.0 | 59.9 | -16.2 | 0.36 |
| Kepulauan_Riau | 0.560 | 6.2 | 9.9 | 3.7 | 1.04 |

**Table 4.19:** Tidal Stream Deployment Economics Across Cost Scenarios - Fragmented Grid

| Scenario | Total Capacity (GW) | Generation (TWh) | System Costs (B US$) | LCOE (US$/MWh) | Capacity Factor (%) |
|---|---|---|---|---|---|
| Reference | 2.83 | 0.68 | 0.84 | 1,232.6 | 2.7 |
| Optimistic | 14.78 | 14.21 | 2.54 | 178.5 | 11.0 |

The extreme LCOE values under reference conditions reflect deployment constraints imposed by transmission limitations and high technology costs. Jakarta exemplifies this pattern, with a massive 156.7 TWh supply deficit requiring imports through limited transmission capacity (21.3 GW maximum). Under these constraints, even expensive tidal generation (1,232.6 US$/MWh) becomes economically rational compared to unmet demand, as the optimization prioritizes system feasibility over individual technology economics.

The 86% LCOE reduction between scenarios results from two concurrent effects: technology cost reductions enabling broader deployment, and site optimization as lower costs make previously uneconomical high-quality tidal resources accessible. Under optimistic cost conditions, tidal deployment shifts from deficit-driven locations (Jakarta, Jawa_Barat) to provinces with superior tidal resources, increasing average capacity factors from 2.7% to 11.0% while expanding deployment 5.2-fold.

This deployment pattern validates the economic logic of system-level optimization: under reference costs, tidal serves as expensive backup generation in transmission-constrained areas, while under optimistic costs, it transitions to mainstream renewable energy competing on resource quality rather than grid constraints. The extreme LCOE sensitivity thus reveals critical cost thresholds where early-stage technologies transform from economically marginal to viable contributors in decarbonization scenarios.

**Table 4.20:** Transmission Constraints vs Import Requirements for High-Deficit Provinces

| Province | Import Need (TWh/year) | Max Transmission Capacity (GW) | Required Utilization (%) | Constraint Level |
|---|---|---|---|---|
| Jakarta | 156.7 | 21.3 | 84 | High |
| Jawa_Barat | 97.3 | 35.5 | 31 | Medium |
| Sumatera_Utara | 16.2 | 8.7 | 21 | Low |

Note: Required utilization assumes continuous import at average rate (Import Need ÷ 8760 hours ÷ Transmission Capacity).

Jakarta's transmission constraint analysis confirms the economic rationale for expensive local generation. With 84% minimum transmission utilization required for deficit coverage, peak demand periods likely exceed available import capacity, necessitating local generation regardless of cost. This system-level constraint explains why Calliope deploys tidal at 1,232.6 US$/MWh: the alternative—unmet demand—violates the model's feasibility requirements.

The contrasting deployment pattern under cost-optimistic conditions further validates this interpretation. When technology costs decrease sufficiently, deployment shifts from constraint-driven (Jakarta, Jawa_Barat) to resource-optimized locations (Riau, Jawa_Timur in optimistic scenarios), demonstrating that extreme LCOE values reflect real economic constraints rather than calculation artifacts. This analysis establishes that tidal stream LCOE sensitivity reveals fundamental deployment thresholds characteristic of early-stage technologies transitioning toward commercial viability in constrained energy systems.

### 4.4.4. Grid Configuration Impact on MRE Economics

**Table 4.21:** LCOE Performance and Generation Scale Across Grid Scenarios

| Scenario | Wave LCOE (US$/MWh) | Tidal LCOE (US$/MWh) | Total MRE Generation (TWh) | System Share (%) |
|---|---|---|---|---|
| Fragmented Reference | 109.2 | 1,232.6 | 10.1 | 0.8 |
| Fragmented Optimistic | 128.2 | 178.5 | 122.8 | 8.0 |
| Supergrid Reference | 109.2 | 125.3 | 41.4 | 3.1 |
| Supergrid Optimistic | 69.5 | 66.1 | 261.4 | 17.3 |

Grid interconnection delivers substantial economic benefits for MRE deployment through enhanced resource access and transmission efficiency. Under reference cost conditions, Supergrid infrastructure enables 4.1x higher MRE generation (10.1 → 41.4 TWh) while reducing tidal stream LCOE by 90% (1,232.6 → 125.3 US$/MWh), demonstrating how transmission connectivity addresses fundamental deployment constraints in archipelagic systems.

The economic transformation becomes pronounced under optimistic cost scenarios, where Supergrid configuration enables both technologies to achieve competitive LCOE positioning: wave energy at 69.5 US$/MWh and tidal stream at 66.1 US$/MWh. This represents LCOE improvements of 36% for wave energy (128.2 → 69.5 US$/MWh) and 63% for tidal stream (178.5 → 66.1 US$/MWh) compared to fragmented optimistic conditions, indicating that grid infrastructure benefits compound with technology cost reductions.

Tidal stream technology exhibits the highest grid dependency, with Supergrid infrastructure delivering 95% LCOE reduction from fragmented reference conditions (1,232.6 → 66.1 US$/MWh under optimal scenarios). This extreme sensitivity reflects access to high-velocity tidal channels in eastern Indonesian straits, where resource quality substantially exceeds western coastal sites available under fragmented grid constraints. The corresponding generation increase from 0.7 TWh to 79.2 TWh (113x expansion) validates the critical role of transmission infrastructure in unlocking geographically concentrated tidal resources.

Combined MRE generation under optimal conditions (261.4 TWh, 17.3% system share) demonstrates significant scaling potential when grid and cost barriers are simultaneously addressed. This transition from marginal (0.8%) to substantial system contribution positions MRE technologies as viable components of Indonesia's 2050 decarbonization strategy, contingent on coordinated transmission infrastructure development and technology cost reduction trajectories.

## 4.5. Optimal MRE Integration Configuration

**Research Question 4**

"What is the optimal configuration for integrating marine renewable energy into Indonesia's power system under different grid configurations (Supergrid vs. fragmented grid) to support the net-zero strategy?"

*Marine renewable energy achieves optimal integration through Supergrid configuration with wave-tidal complementarity under cost-competitive conditions. This configuration enables 2.1x higher MRE deployment (261.4 vs 122.8 TWh) while delivering the lowest system cost (97.7 US$/MWh) through spatial resource optimization and transmission flexibility.*

### 4.5.1. System Performance Comparison

The optimal MRE configuration emerges from comparing system performance across grid topologies and cost scenarios. Figure 4.11 demonstrates the transformative impact of grid connectivity on MRE deployment, with supporting detailed data in Appendix D.3.


**Figure 4.11:** System performance comparison across optimal MRE integration scenarios. Top to bottom: installed generation capacity, storage capacity, electricity generation, and levelized system cost. Supergrid configuration with cost-competitive MRE achieves lowest system cost (97.7 US$/MWh) while enabling highest MRE deployment scale.

**Table 4.22:** Optimal MRE integration comparison across grid configurations

| Scenario | Wave Gen. (TWh) | Tidal Gen. (TWh) | Total MRE Share (%) | Storage Req. (GW) | System Cost (US$/MWh) |
|---|---|---|---|---|---|
| *Fragmented Grid* | | | | | |
| Reference | 9.4 | 0.7 | 0.8% | 253.4 | 123.9 |
| MRE Min Cost | 108.6 | 14.2 | 8.0% | 225.5 | 122.4 |
| *Supergrid* | | | | | |
| Reference | 41.4 | 0.002 | 3.1% | 125.1 | 102.6 |
| MRE Min Cost | 182.2 | 79.2 | 17.3% | 120.2 | 97.7 |

Three critical findings define optimal MRE integration:

### Finding 1: Grid Connectivity Enables Transformative MRE Deployment

Supergrid configuration proves critical for optimal MRE deployment, as shown in the capacity and generation panels of Figure 4.11. Under cost-competitive conditions, Supergrid achieves 2.1x higher MRE generation (261.4 vs 122.8 TWh) and 17.3% system contribution versus 8.0% in fragmented scenarios.

This performance differential stems from transmission flexibility that unlocks remote, high-quality marine

resources. The generation panel clearly shows tidal energy achieving 79.2 TWh in Supergrid versus minimal deployment in fragmented grids, demonstrating how inter-island connectivity enables access to specialized tidal straits that would otherwise remain isolated from demand centers.

#### Finding 2: Wave-Tidal Complementarity Provides Optimal Technology Mix

The optimal technology configuration combines wave energy for scale with tidal energy for baseload characteristics. Figure 4.11 shows wave energy contributing 182.2 TWh while tidal provides 79.2 TWh in the optimal Supergrid scenario, leveraging wave energy's broader deployment potential and tidal energy's higher capacity factors (32.3% vs 6.7%).

This complementarity proves most effective in Supergrid configuration, where wave energy provides consistent semi-baseload generation filling overnight demand valleys when solar is unavailable, while tidal energy delivers predictable 12.4-hour cycles that enhance grid stability. The temporal diversity reduces storage cycling requirements and provides more reliable renewable supply than either technology alone.

Technology-specific performance patterns reveal strategic deployment advantages: wave energy demonstrates resilience across scenarios, maintaining economic deployment even under baseline cost conditions, while tidal energy shows extreme cost sensitivity but delivers superior storage displacement efficiency when cost-competitive. Detailed capacity breakdowns across cost scenarios are available in Appendix D.3.

#### Finding 3: Cost Competitiveness Gates System-Scale Impact

MRE cost trajectory determines system integration scale. Reference costs limit MRE to 3.1% system share even in optimal Supergrid configuration, while optimistic cost reductions enable 17.3% system contribution. The system cost panel in Figure 4.11 shows Supergrid with cost-competitive MRE achieving the lowest overall system cost (97.7 US$/MWh).

### 4.5.2. System Integration Benefits

Cost-competitive MRE integration delivers system-wide optimization benefits beyond direct generation contribution. The integrated system analysis examines how MRE affects overall system costs under both grid configurations.

**Table 4.23:** System costs in Fragmented Grid configuration (US$/MWh)

| Scenario | System Cost |
|---|---|
| Baseline 2050 | 123.9 |
| Without MRE | 123.8 |
| MRE Max Cost | 123.8 |
| MRE Min Cost | 122.4 |

**Table 4.24:** System costs in Supergrid configuration (US$/MWh)

| Scenario | System Cost |
|---|---|
| Baseline 2050 | 102.6 |
| Without MRE | 102.9 |
| MRE Max Cost | 102.9 |
| MRE Min Cost | 97.7 |

#### Supergrid Superiority: Comparative Analysis

The integrated analysis confirms Supergrid superiority across all performance metrics. Supergrid with cost-competitive MRE achieves the lowest system cost (97.7 US$/MWh) while delivering 24.7 US$/MWh advantage over the equivalent fragmented grid scenario—demonstrating the transformative value of inter-island connectivity.

Three quantitative measures establish Supergrid's superior MRE integration performance:

1. **Cost reduction effectiveness:** Supergrid delivers 3.3x better cost reduction (4.9 US$/MWh vs 1.4 US$/MWh) compared to fragmented grids, demonstrating enhanced economic optimization through transmission flexibility and spatial resource access.
2. **Deployment scale achievement:** Supergrid enables 261.4 TWh MRE generation (17.3% system share) versus 122.8 TWh (8.0%) in fragmented configuration, confirming 2.1x higher deployment potential through optimal resource utilization.
3. **Storage system optimization:** Supergrid achieves superior storage efficiency with 17.3 GW total reduction versus 10.8 GW in fragmented grids. The optimization includes 31.9 GW battery capacity reduction and 14.6 GW pumped hydro increase, indicating MRE-enabled storage technology rebalancing that improves overall system flexibility.

These performance advantages stem from Supergrid's ability to access high-quality remote marine resources while optimizing system-wide generation diversity. Inter-island connectivity enables tidal energy deployment at optimal sites (achieving 79.2 TWh generation) that remain inaccessible in fragmented systems, while wave energy scales efficiently across diverse coastal locations.

### 4.5.3. Strategic Implications

The optimal MRE configuration—Supergrid with wave-tidal complementarity under cost-competitive conditions—aligns with Indonesia's policy framework while revealing critical implementation requirements.

Inter-island transmission infrastructure must precede or parallel MRE deployment to capture optimal resource sites. Without adequate grid connectivity, high-quality MRE resources remain stranded assets unable to contribute meaningfully to national decarbonization targets. This finding validates the RUKN 2024 Supergrid development pathway but emphasizes the temporal sequencing of infrastructure investment.

Wave energy provides consistent deployment potential across scenarios, offering a reliable foundation for MRE development programs. Tidal energy delivers high-value niche applications when cost-competitive, with superior capacity factors but limited suitable sites. The complementary characteristics suggest differentiated development strategies rather than uniform technology promotion.

Cost trajectory emerges as the primary determinant of MRE's system role. Current analysis reveals a threshold effect: reference costs limit MRE to premium alternative status (3.1% system share), while optimistic cost reductions enable mainstream renewable contributor potential (17.3% system share). This cost sensitivity indicates that continued technology development and learning curve effects prove essential for realizing MRE's contribution to Indonesia's 2050 decarbonization strategy.

The Supergrid configuration achieves superior performance across all metrics—deployment scale, system cost, and storage optimization—confirming this pathway as optimal for MRE integration under Indonesia's archipelagic geography and renewable energy transition objectives.

# 5. Discussion & Limitations

## 5.1. Discussion

### 5.1.1. Storage Requirements

The central observation is that transmission flexibility governs whether marine renewables substitute or amplify storage. In the interconnected case, spatial smoothing through inter-island transfers reduces the need for short-duration balancing and allows pumped storage to take a steadier, energy-oriented role; in fragmented systems the same injections are seen locally as additional variability that the operator covers with batteries. This transmission gating effect explains why the sign and magnitude of the storage change differ so sharply across grid topologies while technology assumptions remain the same, and it is consistent with the broader evidence on the dominant role of pumped hydro in grid-scale energy shifting [96] and the emerging potential of marine-integrated concepts with comparable round-trip efficiencies [97].

Technology-specific effects are visible once scale is considered. Tidal stream shows higher storage displacement per unit installed—0.94 GW of storage saved per GW tidal capacity—reflecting predictable semidiurnal cycles that align with storage cycling and reduce the amplitude of net-load swings; this echoes early insights that tidal predictability can deliver firm capacity with modest storage when coupled correctly [98]. Wave energy offers a broader temporal spread and contributes to absolute reductions at large scale, but with a lower marginal displacement intensity of 0.09 GW per GW installed; the literature on wave integration increasingly emphasises hybridisation and system co-operation beyond device hydrodynamics, which is consistent with the idea that wave primarily eases battery cycling rather than acting as a strict predictability resource [99, 17].

Two boundary conditions follow. First, these displacement metrics are estimated as marginal slopes across paired scenarios (change in total storage divided by change in installed marine capacity) and should be read as context-dependent properties of the 2050 system rather than technology constants. Second, controlled "technology-mix" experiments are useful for intuition but should not be mixed numerically with system-optimal totals unless their assumptions match; the auxiliary tables that explored solar-dominated mixes are therefore moved to the appendix and flagged for recalculation so that storage totals and displacement efficiencies remain consistent with the canonical Results scenarios.

In short, storage benefits from marine renewables are real but conditional. They materialise when inter-island transfers are available and when marine capacity is allowed to scale at the best coasts, at which point batteries give way to energy-shifting resources and the system carries less fast cycling overall. Without those links, the same technologies become local balancing problems rather than substitutes for storage.

### 5.1.2. Transmission Capacity Requirements

This section interprets the transmission outcomes with an emphasis on mechanism and planning implications, rather than repeating the Results tables. References are to Figure 4.9, Table 4.12, and the corridor ranking in Table 4.13.

The cost–capacity response points to a clear economic threshold for inter-island transfers. The system cost curve flattens once maximum HVDC transfer per link reaches roughly 25 GW, with materially higher costs at tighter caps; in our runs, 5 GW limits add about 6.5 US$/MWh and 10 GW limits about 1.6 US$/MWh, while additional headroom beyond 25 GW yields diminishing returns. These are system-level signals rather than design rules: they indicate the order of magnitude at which inter-island constraints cease to dominate the dispatch, not that every corridor should be sized to that level. In practice, uniform caps are rarely optimal. Strategic phasing that prioritises a small number of high-value links, while holding others at lower limits, preserves most of the cost benefit with less capital exposure. This interpretation is consistent with the Supergrid framing used in the literature, where a limited number of strong backbones carry bulk transfers across islands [1].

MRE integration increases total transfer needs but in a concentrated way. Under cost-competitive

marine deployment, inter-island HVDC rises from 97.1 to 137.6 GW and intra-island AC from 128.3 to 184.8 GW (Table 4.12). The non-linear scaling reflects the optimiser's preference to cluster wave and, to a lesser extent, tidal capacity at the best coasts and move power over a few strengthened paths, rather than forcing even build-out near load. Read this together with the cost–capacity threshold: the economic case is strongest when added HVDC removes the main bottlenecks that isolate high-quality coastal sites, not when capacity is sprinkled everywhere.

#### Critical Transmission Corridors

Corridor-level changes mirror technology geography. Three priorities emerge from the corridor analysis at cost-competitive marine costs:

a) Lampung–Banten (HVDC): This Java–Sumatra gateway expands by about 473% (Table 4.13), becoming the principal path for evacuating wave-rich southern Sumatra and adjacent coasts into Java's load centres. The scale-up is a direct consequence of high-capacity-factor wave sites that are not co-located with demand.

b) Bengkulu (AC): Regional AC reinforcements of the order of +90% support wave collection and injection on Sumatra's west coast, connecting coastal generation to the HVDC landing points and inland demand nodes.

c) West Java (AC): Intra-Java AC increases by roughly +220%, reflecting the need to move imported power across Java's dense load pocket and to integrate distributed tidal additions near the demand.

These corridors illustrate two distinct patterns. Wave-dominated zones call for point-to-point evacuation from concentrated coastal clusters toward Java, typically via strengthened HVDC backbones and supporting AC spurs. By contrast, tidal additions close to load centres reduce flows on some traditional import paths and require only modest transfer increases where regional balancing remains valuable. The net effect is an asymmetric build: a few large HVDC gateways grow a lot, while many other paths remain stable or decline.

#### System-wide transmission implications

Connectivity is an enabler rather than a burden for marine integration. With the Supergrid in place, marine output reaches 261.4 TWh in 2050 (about 17.3% of total generation), compared with 122.8 TWh in the fragmented case; the difference is not primarily about the technologies themselves but about the ability to move their output from resource coasts to load. The model's behaviour is internally consistent: once the main inter-island constraints are relieved, batteries are less heavily used for fast cycling, pumped storage plays a steadier energy-shifting role, and marine capacity becomes a substitute for—not an additional driver of—storage.

Sequencing matters for investment. If grid expansion lags marine development, projects are pushed into suboptimal sites or curtailed behind constraints, eroding competitiveness. A staged plan that brings forward the high-value gateways (for example Lampung–Banten) and the necessary onshore AC reinforcements, while deferring low-value corridors, captures most of the cost reduction seen at high HVDC caps without committing to uniform overbuild. This strategy also fits institutional reality: fewer, larger packages reduce interface risk and make permitting and delivery more tractable.

#### Technology-specific transmission patterns

The transmission signals differ by technology in ways that help planning. Wave deployments concentrate at a limited set of high-energy coasts; they tend to require strong evacuation to Java and benefit most from reinforced HVDC backbones and coastal AC collectors. Tidal tends to add nearer to load on Java and selected straits; it often lowers net imports on some corridors and needs only targeted increases where regional balancing remains economic. Taken together, the two form a complementary picture: wave leans on a small number of gateways, while tidal tidies local balances and reduces stress on legacy import paths. Planning that recognises this split—large, early HVDC for wave evacuation; selective AC and modest HVDC for tidal—delivers better cost–benefit than uniform expansion.

### 5.1.3. Cost Competitiveness

The cost figures reported in the Results should be read as system-embedded outcomes rather than catalogue device costs. They are computed ex post from annualised total system expenditure divided by

annual generation after the optimisation has co-determined the portfolio, transmission use, curtailment, and dispatch. This construction is appropriate for a whole-system assessment because it internalises interactions among technologies; however, it implies that LCOEs are most meaningfully compared within a given scenario and modelling set-up, and they should not be lifted as universal benchmarks independent of network access, co-deployment, and operating conditions [1, 17].

Within this framing, two patterns emerge. Wave shows relatively smooth behaviour across scenarios: it deploys at reference costs and moves into a clearly competitive band when costs fall and transmission is available. By contrast, tidal exhibits threshold economics. Under fragmented and reference-cost conditions the optimiser selects only small volumes in constrained locations, resulting in very high attributed LCOE. Once costs decline and inter-island transfer opens access to high-quality straits, tidal crosses a viability threshold: deployment rises sharply and the attributed LCOE drops into the main pack. This is not a numerical artefact; it reflects lumpy site quality, the role of transmission in making those sites accessible, and the optimiser's willingness to carry small, expensive volumes to maintain system feasibility before switching to larger, cheaper volumes when the system can exploit better resources.

Transmission therefore operates as a first-order cost lever. The Supergrid unlocks higher capacity factors at coastal marine sites and reduces balancing penalties through spatial smoothing; both mechanisms pull the system-embedded LCOE down. In fragmented configurations the logic reverses: even with lower technology costs, marine output tends to compete behind local constraints against storage and peaking options, and small volumes can carry high attributed cost. The implication for planning is that aggregate "more transmission" is not sufficient; which corridors are reinforced, and in what sequence, determines whether wave and tidal can express their intrinsic quality at the system boundary [1].

Positioning against comparators in the favourable package (interconnection and cost reductions) shows marine technologies sitting alongside established renewables in our model environment, with wave and tidal in the same band as small hydro and geothermal and below onshore solar. Outliers in other technologies should be interpreted cautiously: extremely high values typically signal near-zero deployment combined with fixed costs or unfavourable curtailment patterns in that specific configuration, not a general verdict on the technology. The broader reading is that marine resources can reside in the competitive band when scale and access are present; when either is missing, the model signals this by attributing high cost to the small amounts it still needs.

For policy and investment, three points follow. First, cost reductions and grid access are complements: pushing one without the other leaves value unrealised. Second, early volumes should be targeted where the system-embedded cost falls fastest with scale—wave at the best coasts behind reinforced gateways, and tidal in straits that are actually reachable within the evolving network. Third, financing conditions matter materially: the results are sensitive to cost of capital and local supply-chain premia. Instruments such as time-limited contracts for difference for clustered wave projects and small tidal pilots near demand centres can accelerate the move into the competitive band relative to undirected support spread thinly across many locations [1, 17].

Two caveats are important for interpretation. Ancillary services and diversity benefits are not priced as explicit adders; they appear indirectly through lower total system costs when portfolios are co-optimised. And the analysis uses a single representative year on the demand and non-tidal renewables side; multi-year sampling and explicit reserve and stability constraints would provide a more complete cost picture. These refinements are unlikely to overturn the qualitative hierarchy observed here—threshold behaviour for tidal, smoother decline for wave, and the central role of transmission—but they would narrow uncertainty and sharpen the policy signals.

## 5.2. Strategy for Indonesia's Energy Transition

The results indicate that marine renewables scale only when transmission access and technology costs move in step, and the strategy for Indonesia should therefore be framed as a coordinated programme that couples inter-island reinforcement with targeted wave and tidal siting and finance instruments that accelerate learning without overbuilding the grid. In the fragmented configuration, even resilient technologies remain confined to niche volumes because their output is trapped behind local constraints

and competes unfavourably with storage and peakers; under the Supergrid, by contrast, marine output reaches 261.4 TWh in 2050 (17.3% of generation) and resides in the competitive cost band. The planning implication is that transmission must be treated as a first-order cost lever rather than a passive backdrop: the system cost curve flattens once per-link headroom is sufficient, but the benefit is captured most efficiently by concentrating capacity on a few high-value corridors rather than applying uniform limits everywhere [1].

In practical terms this means staging a small number of HVDC gateways that unlock the best marine coasts while delivering the supporting onshore AC reinforcements that move power across Java's dense load pocket. The Lampung–Banten link should be brought forward as the principal evacuation path for the southern Sumatra wave resource, with regional AC strengthening in Bengkulu and West Java to connect coastal clusters to landing points. Uniform 25 GW caps are not design rules; they are system signals that the binding constraint has been relaxed, and a sequenced build focused on the highest-leverage links will capture most of the cost reduction with less capital at risk. Grid works need to be packaged with coastal collectors and credible landfall solutions, and marine spatial planning should explicitly integrate shipping lanes and landfall constraints to avoid late re-routing and stranded interconnection. Taken together, these measures convert transmission from a bottleneck into the enabling infrastructure that allows marine resources to express their intrinsic quality at the system boundary [1].

Technology targeting follows from this geography. Wave should be clustered at the best capacity-factor coasts behind reinforced gateways, with coastal AC networks designed to avoid local bottlenecks and with early curtailment used deliberately where it lowers delivered cost relative to oversizing storage or advancing second-order links. Tidal should be deployed first where the network can actually reach it—near load on Java and selected Nusa Tenggara nodes—using modest reinforcements where regional balancing remains valuable; its predictable cycles then reduce local imports and tidy short-term balances rather than demanding long-haul transfer. Storage planning should be co-optimised with this buildout: batteries retained for diurnal cycling and local contingencies, pumped storage expanded where inter-island transfers shift energy across provinces, and the combination used to reduce fast cycling once spatial smoothing is available.

Moreover, finance and governance complete the strategy. Because the system-embedded costs are sensitive to cost of capital and supply-chain, time-limited contracts for difference for wave clusters at reinforced gateways, together with small, standardized tidal pilots near demand centres, can pull attributed costs into the competitive band faster than undirected support scattered across many locations. Programme design should be modular so that capacity can scale as evidence accumulates, and data should be public: province-level marine profiles, assumptions used in planning, and multi-year measurements at priority sites improve bankability and shorten siting cycles. Sequencing procurement is important, hence the HVDC gateways, coastal collectors, and onshore AC reinforcements arrive together avoids stranded generation. With these enablers: targeted interconnection, disciplined siting, and finance aligned to learning, marine renewables operate as system resources rather than scattered additions, supporting the 2050 target at competitive system-embedded prices; without them, deployment remains local and expensive, contributing marginally rather than at the scale the transition requires.

## 5.3. Thesis Limitations

This section sets out the principal scope limits and modelling choices that could influence the magnitude or direction of the reported outcomes. The purpose is to support interpretation, not to discount the findings. Where helpful, each item explains what was done, why it matters, and the likely direction of bias.

1. Data and resource assessment

    a) Wave resource resolution (ERA5, 0.5° × 0.5°): Wave conditions are derived from ERA5 at a coarse spatial resolution. Such grids smooth nearshore gradients and bathymetric effects that are important for WEC performance and survivability. Even with depth and distance-to-shore filters, coarse fields can miss local shadowing and coastal refraction or diffraction. In complex coastlines, this may overstate deployable capacity and understate variability close to shore.

    b) Tidal resource resolution (TPXO10-atlas-v2, 1/30°, approximately 3.7 km): Tidal currents are

computed from barotropic harmonics on the TPXO grid and then aggregated to provinces for the power-system runs. Narrow straits such as Larantuka (about 650 m width), Lombok, and Toyopakeh are below grid scale and are averaged with surrounding cells. Two offsetting biases can appear: sub-grid accelerations and head losses around constrictions are not captured, which can understate peak velocities and hotspot capacity; at the same time, multi-row array wake interactions are not represented, which can overstate large-array yields. The analysis is regional and planning-oriented and differs from site-specific feasibility studies in purpose and expected precision.

c) Single-year (2018) representativeness: Hourly wave and power-system time series use 2018 as a proxy year for 2050. Interannual climate variability is not sampled, and long-term change is not represented. Tidal predictions are harmonic and therefore not tied to a specific meteorological year, but the system model still sees one representative year of demand and non-tidal renewables. Results should be read as central estimates rather than a climate-robust envelope.

2. Technology and performance modelling

a) Device representation and operations: Wave uses a single power matrix (WaveStar v1, 600 kW) applied across eligible cells without site-specific retuning; survivability in extreme sea states is not modelled explicitly. Tidal uses a validated SeaGen-S 2 MW curve, but bi-directional array optimization, turbulence effects, yaw or tilt strategies, and detailed availability losses are outside scope. Literature reports material downstream reductions for tidal arrays (order tens of percent), which are not simulated explicitly here.

b) Spatial deployment rules and exclusions: Deployment densities and spacing follow simple rules. Exclusion layers for ports, shipping lanes, fisheries, and cable landfalls are partial: a shipping-lanes dataset is not used, and cable landfall constraints would require additional data. As a result, technical potential may be optimistic in congested nearshore waters or rugged landfall zones.

3. Power-system modelling scope

a) Network representation: Inter-island transfers are represented by HVDC and AC link capacities with per-link caps of 50 GW, consistent with the Supergrid representation. There is no AC power flow, no voltage or reactive constraints, and no N–1 security assessment. Losses are handled at aggregate levels. This can understate congestion on dense corridors and overstate deliverability from remote coasts if multiple large injections coincide.

b) Operations and flexibility: The model does not include unit commitment, minimum up or down times, reserve or inertia constraints, or frequency stability limits. Storage is energy-only with fixed round-trip efficiency and no degradation. Curtailment is allowed, but ancillary-services valuation is not explicit. Short-term balancing needs in fragmented grids may therefore be understated.

4. Costs and finance

a) Learning curves and Indonesian context: Marine cost paths use literature-based learning with global deployment proxies, and non-marine cost parameters largely come from catalogues. Indonesian-specific WACC, supply chains, local-content rules, and marine O&M adders remain uncertain. Depending on policy and industry scale-up, future costs may deviate in either direction.

b) Transmission cost scaling: HVDC and AC costings are treated at corridor level. Route engineering, seabed conditions and burial depth, landfall civil works, and permitting delays are not explicitly modelled. Long subsea links on difficult routes might therefore be more expensive than represented.

5. Demand projections

a) Top-down versus bottom-up frameworks: The RUKN-aligned trajectory achieves national targets using scaled shapes, whereas the bottom-up RUPTL path uses provincial growth rates available for 2025–2034 and extrapolates to 2050. The bottom-up aggregation tends to fall below the RUKN 2050 total because post-2034 data are missing and the extrapolation is conservative. In

this study the RUPTL-based demand is interpreted as a spatial-allocation sensitivity that is credible for where demand grows, but it is not definitive for the national 2050 sum without updated post-2034 inputs.

b) Load shapes and sectoral change: Provincial hourly shapes inherit JAMALI or proxy patterns. Explicit electrification of transport, heat, and hydrogen is not modelled, so timing and coincidence effects are simplified. This can shift storage sizing and some transmission conclusions at the margin.

6. External validity and implementation risk: Supergrid delivery is a multi-decadal effort with procurement, permitting, and coordination risks that sit outside the optimization. Marine coexistence and social-licence issues in fisheries, navigation, defence, and tourism are only partially represented. Global scale-up of wave and tidal supply chains is uncertain and not under Indonesia’s direct control.

# 6. Conclusion & Recommendations

## 6.1. Conclusion

This thesis quantified how wave and tidal power fit into Indonesia's fully decarbonised 2050 power system under two grid topologies: an inter-island Supergrid and a fragmented grid. Using the Calliope–Indonesia framework, we evaluated storage impacts, grid expansion, cost competitiveness, and the optimal configuration for integrating marine renewables. The conclusions below refer to the Results tables where relevant.

### 6.1.1. RQ1. Impact on energy storage requirements

Marine renewables change storage needs in opposite directions depending on transmission flexibility. With inter-island transfers, total storage falls from 135.7 GW (Supergrid–Without MRE) to 125.1 GW (Supergrid), a net reduction of 10.6 GW (−7.8%) (Table D.5). Batteries do most of the work (−11.5 GW), while pumped hydro rises slightly (+0.9 GW), indicating that spatial balancing replaces short-duration balancing at the margin. Under cost-competitive MRE, the reduction deepens to 15.4 GW (120.2 vs 135.7 GW), driven by a larger battery drop (−30.6 GW) partially offset by more pumped hydro (+15.2 GW).

In the fragmented grid at reference costs, MRE increases total storage by 0.6 GW (253.4 vs 252.8 GW): batteries rise (+14.0 GW) and pumped hydro falls (−13.3 GW). Without transmission headroom, MRE adds variability that must be firmed locally.

Tidal stream shows the highest storage displacement per unit installed: 0.94 GW storage saved per GW of tidal, versus 0.09 GW per GW of wave. Tidal's predictability makes it an efficient substitute for short-duration storage when it can reach scale; wave contributes, but with smaller displacement intensity. Transmission flexibility is the precondition for realising the storage benefit.

### 6.1.2. RQ2. Optimal grid expansion strategy

MRE integration tilts the optimal grid plan toward a few high-leverage corridors and a stronger inter-island backbone. Three priorities emerge from the model runs:

- Lampung–Banten (HVDC): the key Java–Sumatra gateway, with a +473% expansion relative to the no-MRE case.
- Bengkulu (AC): intra-Sumatra reinforcements of around +91%, supporting coastal MRE export paths.
- West Java (AC): intra-Java capacity rises by +222% to move imported power to load centres.

At system level (Table 4.12), inter-island HVDC grows from 97.1 GW (Without MRE) to 102.4 GW (With MRE, +5.5%), and to 137.6 GW under cost-optimistic MRE (+41.8%). Intra-island AC rises from 128.3 to 134.0 and 184.8 GW (+4.4% and +44.0%). The scaling is non-linear: once MRE becomes cheap enough, the optimiser concentrates deployment at top resource coasts and ships power via a few strengthened links rather than building everywhere.[1]

### 6.1.3. RQ3. Cost competitiveness of wave and tidal

Under the favourable package (Supergrid plus optimistic costs), marine technologies land in the main pack of renewables: wave at 69.5 US$/MWh and tidal at 66.1 US$/MWh. These values sit alongside small hydro at 67.5 and geothermal at 61.7 US$/MWh, and beat onshore solar at 73.9 US$/MWh (all rounded to one decimal).

The spread is wide when grid topology and costs turn against marine. Tidal's worst case reaches 1,232.6 US$/MWh (fragmented plus reference costs), reflecting deployment thresholds typical of early-stage technologies. Interconnection both lowers delivered costs and enables scale by unlocking better sites.

[1] Per-link transfer capacities are capped at 50 GW in line with the Supergrid representation used in prior work; conclusions on direction and concentration are insensitive to the cap.

### 6.1.4. RQ4. Optimal MRE configuration for net-zero

The best-performing integration is Supergrid with cost-competitive wave and tidal, combining complementarity and spatial smoothing. In this setting, marine renewables produce 261.4 TWh in 2050, or 17.3% of total system generation (1,514.2 TWh). The system's average cost is 97.7 US$/MWh. Relative to the fragmented reference, MRE output is 2.1× higher (261.4 vs 122.8 TWh). Transmission flexibility raises feasible scale, trims storage needs, and pulls delivered costs down.

### 6.1.5. Synthesis

Across RQ1–RQ4, one chain explains the results. Inter-island transmission enables spatial balancing, which reduces battery needs and raises feasible marine scale. At scale, tidal's predictability and wave–tidal complementarity show up as lower system costs and a meaningful generation share. Without the Supergrid, most of these gains evaporate or flip sign. To make marine renewables work for Indonesia by 2050, build the links that let them breathe and let storage do the job it is best at.

## 6.2. Future Research Directions

Further work could improve physical realism, Indonesian context, and decision relevance.

1. High-resolution marine resource modelling: Use nested SWAN/ROMS (waves) and unstructured tidal models that resolve narrow straits; derive site-specific power matrices with blockage and wake corrections.
2. Device heterogeneity and technology pathways: Represent multiple wave converter types (point absorbers, attenuators, OWSC, OWC, overtopping) and tidal devices (axial/cross-flow, ducted, tidal kites); build a small library of representative devices with Indonesian CAPEX/OPEX/WACC and learning rates.
3. Multi-year variability and extremes: Construct multi-year wave hindcasts and include tidal nodal modulation; propagate variability and downtime into adequacy and storage cycling rather than relying on a single profile year.
4. Spatial constraints and coexistence: Add explicit layers for AIS shipping lanes, port approaches, fisheries, MPAs, and defence zones; include landfall feasibility and cable routing cost surfaces (bathymetry, substrate, burial depth).
5. Provincial demand and sector coupling. Develop province-specific hourly profiles and extend RUPTL growth beyond 2034 with documented extrapolation; add electrification of transport, heat, desalination, and hydrogen with managed demand.
6. Indonesian cost validation and financing. Produce bottom-up cost stacks for marine arrays and transmission; quantify WACC and local-content effects, and HVDC cap-and-floor within the system model.
7. Transmission routing and staging. Shift from corridor totals to route-level engineering (converter siting, burial/protection, landfall civil works) and optimise staged packages that co-deliver HVDC gateways, coastal collectors, and onshore AC.
8. MRE pathways, not single-year targets: Move from a static 2050 point estimate to staged 2030–2050 pathways with interim capacity and generation milestones, sequenced corridor build-out, learning-rate checkpoints, and decision gates; quantify uncertainty bands and trigger rules so procurement and siting adapt as evidence and costs evolve.

# References


[1] Jannis Langer et al. “The role of inter-island transmission in full decarbonisation scenarios for Indonesia’s power sector”. In: *Environmental Research: Energy* 1.2 (2024), p. 025006. DOI: 10.1088/2753-3751/ad53cb.

[2] Institute for Essential Services Reform (IESR). *Indonesia Energy Transition Outlook 2025: Navigating Indonesia’s Energy Transition at the Crossroads: A Pivotal Moment for Redefining the Future*. Jakarta: Institute for Essential Services Reform (IESR), 2024. URL: https://iesr.or.id/en/pustaka/indonesia-energy-transition-outlook-ieto-2025/.

[3] Kementerian Energi dan Sumber Daya Mineral Republik Indonesia. *Rencana Umum Energi Nasional (RUEN)*. 2017. URL: https://www.esdm.go.id/assets/media/content/content-rencana-umum-energi-nasional-ruen.pdf.

[4] DPR RI Pusat Analisis Keparlemenan. *Isu Sepekan, Vol. III / PUSLIT - Februari 2025*. 2025. URL: https://berkas.dpr.go.id/pusaka/files/isu_sepekan/Isu%20Sepekan---III-PUSLIT-Februari-2025-206.pdf.

[5] Robert Cribb and Michele Ford. *Indonesia as an Archipelago: Managing Islands, Managing the Seas*. Ed. by Robert Cribb and Michele Ford. Singapore: ISEAS Publishing (Institute of Southeast Asian Studies), 2009, pp. 1–27.

[6] M. Faure, M. G. Faure, and J. Hu. *Prevention and Compensation of Marine Pollution Damage: Recent Developments in Europe, China and the US*. Comparative Environmental Law & Policy Series. Kluwer Law International, 2006, p. 99. ISBN: 9789041123381. URL: https://books.google.nl/books?id=E5NafsG5RiEC.

[7] *Marine Renewable Energy*. European Commission. 2025. URL: https://oceans-and-fisheries.ec.europa.eu/ocean/blue-economy/marine-renewable-energy_en.

[8] Francisco Taveira-Pinto, Paulo Rosa-Santos, and Tiago Fazeres-Ferradosa. “Marine renewable energy”. In: *Renewable Energy* 150 (2020), pp. 1160–1164. ISSN: 0960-1481. DOI: https://doi.org/10.1016/j.renene.2019.10.014.

[9] Ristiyanto Adiputra et al. *Ocean-Renewable Energy in Indonesia: A Brief on the Current State and Development Potential*. Dec. 2023. ISBN: 978-623-8372-25-6. DOI: 10.55981/brin.900.c782.

[10] Secretariate General of the National Energy Council. *Indonesia Energy Outlook 2023*. Jakarta, Indonesia: Bureau of Energy Policy and Assembly Facilitation, Secretariate General of the National Energy Council, 2023. URL: https://www.den.go.id/publikasi/Outlook-Energi-Indonesia#.

[11] Agustinus Ribal et al. “A high-resolution wave energy resource assessment of Indonesia”. In: *Renewable Energy* 160 (2020), pp. 1349–1363. ISSN: 0960-1481. DOI: https://doi.org/10.1016/j.renene.2020.06.017.

[12] A.M. Rizal and N.S. Ningsih. “Ocean wave energy potential along the west coast of the Sumatra island, Indonesia”. In: *Journal of Ocean Engineering and Marine Energy* 6 (2020), pp. 137–154. DOI: 10.1007/s40722-020-00164-w. URL: https://doi.org/10.1007/s40722-020-00164-w.

[13] Ahmad Firdaus. “OMAE2023-108028 TIDAL ENERGY IN INDONESIA: OPPORTUNITIES AND CHALLENGES”. In: July 2023.

[14] Ministry of Energy and Indonesia Mineral Resources. *Rencana Umum Ketenagalistrikan Nasional (RUKN) 2024*. 2024. URL: https://gatrik.esdm.go.id/assets/uploads/download_index/files/2f251-rukn-2024.pdf.

[15] Institute for Essential Services Reform (IESR). *National Energy General Plan (RUEN): Existing Plan, Current Policies Implication, and Energy Transition Scenario*. 2020. URL: https://www.iesr.or.id.

[16] Stefan Pfenninger, Adam Hawkes, and James Keirstead. “Energy systems modeling for twenty-first century energy challenges”. In: *Renewable and Sustainable Energy Reviews* 33 (2014), pp. 74–86. ISSN: 1364-0321. DOI: https://doi.org/10.1016/j.rser.2014.02.003.

[17] George Lavidas, Felix Elizundia, and Kornelis Blok. “Integration of wave energy into Energy Systems: an insight to the system dynamics and ways forward”. In: Sept. 2023. DOI: 10.36688/ewtec-2023-paper-157.

[18] Stefan Pfenninger and Bryn Pickering. “Calliope: a multi-scale energy systems modelling framework”. In: *Journal of Open Source Software* 3.29 (2018), p. 825. DOI: 10.21105/joss.00825. URL: https://doi.org/10.21105/joss.00825.

[19] European Centre for Medium-Range Weather Forecasts (ECMWF). *ECMWF Reanalysis v5 (ERA5)*. 2025. URL: https://www.ecmwf.int/en/forecasts/dataset/ecmwf-reanalysis-v5.

[20] GEBCO Compilation Group. *GEBCO Gridded Bathymetry Data*. 2024. URL: https://www.gebco.net/data_and_products/gridded_bathymetry_data/.

[21] Gary D. Egbert and Svetlana Y. Erofeeva. “Efficient Inverse Modeling of Barotropic Ocean Tides”. In: *Journal of Atmospheric and Oceanic Technology* 19.2 (2002), pp. 183–204. DOI: 10.1175/1520-0426(2002)019<0183:EIMOBO>2.0.CO;2. URL: https://journals.ametsoc.org/view/journals/atot/19/2/1520-0426_2002_019_0183_eimobo_2_0_co_2.xml.

[22] T. C. Sutterley et al. *pyTMD: Python-based tidal prediction software*. https://github.com/tsutterley/pyTMD. Accessed 2025-07-15. 2017. DOI: 10.5281/zenodo.5555395.

[23] SIMEC Atlantis Energy. *SeaGen: World’s First Commercial Scale Tidal Stream Generator*. Brochure. 2016. URL: https://simecatlantis.com/wp-content/uploads/2016/08/SeaGen-Brochure.pdf.

[24] Central Intelligence Agency. *The World Factbook - Indonesia*. 2025. URL: https://www.cia.gov/the-world-factbook/countries/indonesia/.

[25] Wikipedia contributors. *Provinces of Indonesia — Wikipedia, The Free Encyclopedia*. 2025. URL: https://en.wikipedia.org/wiki/Provinces_of_Indonesia.

[26] World Bank. *Population, total*. 2023. URL: https://data.worldbank.org/indicator/SP.POP.TOTL?end=2023&most_recent_value_desc=true&start=2023&view=map (visited on 12/24/2023).

[27] International Energy Agency. *Indonesia: Efficiency and Demand*. 2025. URL: https://www.iea.org/countries/indonesia/efficiency-demand.

[28] Ministry of Energy and Mineral Resources, Republic of Indonesia. *Rencana Umum Energi Nasional (RUEN)*. Accessed: March 2024. 2024. URL: https://www.esdm.go.id/assets/media/content/content-rencana-umum-energi-nasional-ruen.pdf.

[29] International Energy Agency (IEA). *Indonesia - Emissions*. 2025. URL: https://www.iea.org/countries/indonesia/emissions.

[30] PT PLN (Persero). *Rencana Usaha Penyediaan Tenaga Listrik (RUPTL) 2021-2030*. 2021. URL: https://web.pln.co.id/statics/uploads/2021/10/ruptl-2021-2030.pdf.

[31] European Commission, Directorate-General for Maritime Affairs, and Fisheries. *Market study on ocean energy – Final report*. Publications Office, 2018. DOI: doi/10.2771/89934.

[32] W.H. Frederick and R.L. Worden. *Indonesia: A Country Study*. Area handbook series v. 550. Federal Research Division, Library of Congress, 1993, p. xxxii. ISBN: 9780844407906. URL: https://books.google.nl/books?id=6dgmXWMgWcwC.

[33] M. deCastro et al. “Evaluating the economic viability of near-future wave energy development along the Galician coast using LCoE analysis for multiple wave energy devices”. In: *Journal of Cleaner Production* 463 (2024), p. 142740. ISSN: 0959-6526. DOI: https://doi.org/10.1016/j.jclepro.2024.142740.

[34] International Energy Agency (IEA). *Projected Costs of Generating Electricity 2020*. Licence: CC BY 4.0. Paris: IEA, 2020. URL: https://www.iea.org/reports/projected-costs-of-generating-electricity-2020.

[35] International Energy Agency (IEA). *World Energy Outlook 2024*. Paris: IEA, 2024. URL: https://www.iea.org/reports/world-energy-outlook-2024.

[36] George Lavidas and Kornelis Blok. "Shifting wave energy perceptions: The case for wave energy converter (WEC) feasibility at milder resources". In: *Renewable Energy* 170 (2021), pp. 1143–1155. ISSN: 0960-1481. DOI: https://doi.org/10.1016/j.renene.2021.02.041.

[37] International Renewable Energy Agency (IRENA). *Wave Energy: Technology Brief*. 2014. URL: https://www.irena.org/publications/2014/Jun/Wave-energy.

[38] Arthur Pecher and Jens Peter Kofoed, eds. *Handbook of Ocean Wave Energy*. Cham: Springer International Publishing, 2017. ISBN: 978-3-319-39889-1. DOI: 10.1007/978-3-319-39889-1. URL: https://link.springer.com/book/10.1007/978-3-319-39889-1.

[39] António F. de O. Falcão. "Wave energy utilization: A review of the technologies". In: *Renewable and Sustainable Energy Reviews* 14.3 (2010), pp. 899–918. ISSN: 1364-0321. DOI: https://doi.org/10.1016/j.rser.2009.11.003.

[40] Magagna D. "Ocean Energy - Technology Development Report 2020". In: KJ-BK-21-007-EN-N (online),KJ-BK-21-007-EN-C (print) (2020). ISSN: 1831-9424 (online),1018-5593 (print),2600-0466 (online) 2600-0458 (print). DOI: 10.2760/81693(online),10.2760/102596(print).

[41] Nicolas Guillou, George Lavidas, and Georges Chapalain. "Wave energy resource assessment for exploitation-A review". In: *Journal of Marine Science and Engineering* 8.9 (2020). Cited by: 90; All Open Access, Gold Open Access, Green Open Access. DOI: 10.3390/JMSE8090705. URL: https://www.scopus.com/inward/record.uri?eid=2-s2.0-85092257318&doi=10.3390%2fJMSE8090705&partnerID=40&md5=f6f43d162cb90e6a94445326d92e9276.

[42] *Technology Data for the Indonesian Power Sector 2024*. Direktorat Jenderal Ketenagalistrikan, Kementerian Energi dan Sumber Daya Mineral, 2024. URL: https://gatrik.esdm.go.id/assets/uploads/download_index/files/c4d42-technology-data-for-the-indonesian-power-sector-2024-annoteret-af-kb-.pdf.

[43] Aries Kurniawan et al. "Optimizing Energy Output for Oscillating Water Column (OWC) Wave Energy Converter System at Pantai Baron, Gunung Kidul, DI Yogyakarta". In: *Applied Engineering and Technology* 3 (Aug. 2024), pp. 125–132. DOI: 10.31763/aet.v3i2.1773.

[44] Simon P. Neill et al. "A review of tidal energy—Resource, feedbacks, and environmental interactions". In: *Journal of Renewable and Sustainable Energy* 13.6 (2021), p. 062702. ISSN: 1941-7012. DOI: 10.1063/5.0069452. eprint: https://pubs.aip.org/aip/jrse/article-pdf/doi/10.1063/5.0069452/15719353/062702_1_online.pdf. URL: https://doi.org/10.1063/5.0069452.

[45] Matt Lewis et al. "Power variability of tidal-stream energy and implications for electricity supply". In: *Energy* 183 (2019), pp. 1061–1074. ISSN: 0360-5442. DOI: https://doi.org/10.1016/j.energy.2019.06.181.

[46] Kadir Orhan et al. "Investigation of the Energy Potential from Tidal Stream Currents in Indonesia". In: Nov. 2016. DOI: 10.9753/icce.v35.management.10.

[47] Kadir Orhan and Roberto Mayerle. "Assessment of the tidal stream power potential and impacts of tidal current turbines in the Strait of Larantuka, Indonesia". In: *Energy Procedia* 125 (2017). European Geosciences Union General Assembly 2017, EGU Division Energy, Resources & Environment (ERE), pp. 230–239. ISSN: 1876-6102. DOI: https://doi.org/10.1016/j.egypro.2017.08.199.

[48] Gavin Smart and Miriam Noonan. *Tidal Stream and Wave Energy Cost Reduction and Industrial Benefit*. 2018. URL: https://www.marineenergywales.co.uk/wp-content/uploads/2018/05/ORE-Catapult-Tidal-Stream-and-Wave-Energy-Cost-Reduction-and-Ind-Benefit-FINAL-v03.02.pdf.

[49] Lara Dixon et al. "The Philippines' Energy Transition: Assessing Emerging Technology Options Using OSeMOSYS (Open-Source Energy Modelling System)". In: *Climate* 13.1 (2025). ISSN: 2225-1154. DOI: 10.3390/cli13010014.

[50] Hans-Kristian Ringkjøb, Peter M. Haugan, and Ida Marie Solbrekke. “A review of modelling tools for energy and electricity systems with large shares of variable renewables”. In: *Renewable and Sustainable Energy Reviews* 96 (2018), pp. 440–459. ISSN: 1364-0321. DOI: https://doi.org/10.1016/j.rser.2018.08.002.

[51] Markus Groissböck. “Are open source energy system optimization tools mature enough for serious use?” In: *Renewable and Sustainable Energy Reviews* 102 (2019), pp. 234–248. ISSN: 1364-0321. DOI: https://doi.org/10.1016/j.rser.2018.11.020.

[52] Lorenzo Laveneziana, Matteo Prussi, and David Chiaramonti. “Critical review of energy planning models for the sustainable development at company level”. In: *Energy Strategy Reviews* 49 (2023), p. 101136. ISSN: 2211-467X. DOI: https://doi.org/10.1016/j.esr.2023.101136.

[53] Energy Exemplar. *PLEXOS - Market Simulation Software*. 2025. URL: https://www.energyexemplar.com/plexos.

[54] Miguel Chang et al. “Trends in tools and approaches for modelling the energy transition”. In: *Applied Energy* 290 (2021), p. 116731. ISSN: 0306-2619. DOI: https://doi.org/10.1016/j.apenergy.2021.116731.

[55] Stefan Pfenninger and Bryn Pickering. *Calliope: A multi-scale energy systems modelling framework*. 2024. URL: https://calliope.readthedocs.io/en/stable/index.html.

[56] Andreas Jessen. “Bachelor Thesis”. Energietechnik M-5. MA thesis. Hamburg, Germany: Technische Universität Hamburg, 2023. DOI: 10.15480/882.5078. URL: http://hdl.handle.net/11420/15213.

[57] Stefan Pfenninger and James Keirstead. “Renewables, nuclear, or fossil fuels? Scenarios for Great Britain’s power system considering costs, emissions and energy security”. In: *Applied Energy* 152 (2015), pp. 83–93. ISSN: 0306-2619. DOI: https://doi.org/10.1016/j.apenergy.2015.04.102.

[58] Paula Díaz Redondo and Oscar van Vliet. “Modelling the Energy Future of Switzerland after the Phase Out of Nuclear Power Plants”. In: *Energy Procedia* 76 (2015). European Geosciences Union General Assembly 2015 - Division Energy, Resources and Environment, EGU 2015, pp. 49–58. ISSN: 1876-6102. DOI: https://doi.org/10.1016/j.egypro.2015.07.843.

[59] Francesco Lombardi et al. “Policy Decision Support for Renewables Deployment through Spatially Explicit Practically Optimal Alternatives”. In: *Joule* 4.10 (2020), pp. 2185–2207. ISSN: 2542-4351. DOI: https://doi.org/10.1016/j.joule.2020.08.002.

[60] Priyanka Laha and Basab Chakraborty. “Cost optimal combinations of storage technologies for maximizing renewable integration in Indian power system by 2040: Multi-region approach”. In: *Renewable Energy* 179 (2021), pp. 233–247. ISSN: 0960-1481. DOI: https://doi.org/10.1016/j.renene.2021.07.027.

[61] Nicolò Stevanato et al. “Advancing the representation of reservoir hydropower in energy systems modelling: The case of Zambesi River Basin”. In: *PLOS ONE* 16.12 (Dec. 2021), pp. 1–25. DOI: 10.1371/journal.pone.0259876. URL: https://doi.org/10.1371/journal.pone.0259876.

[62] U Schilt et al. “Modelling of multi-energy systems of residential buildings with Calliope and validation of results”. In: *Journal of Physics: Conference Series* 2600.3 (2023), p. 032005. DOI: 10.1088/1742-6596/2600/3/032005.

[63] Bryn Pickering and Ruchi Choudhary. “Quantifying resilience in energy systems with out-of-sample testing”. In: *Applied Energy* 285 (2021), p. 116465. ISSN: 0306-2619. DOI: https://doi.org/10.1016/j.apenergy.2021.116465.

[64] Simon Morgenthaler, Wilhelm Kuckshinrichs, and Dirk Witthaut. “Optimal system layout and locations for fully renewable high temperature co-electrolysis”. In: *Applied Energy* 260 (2020), p. 114218. ISSN: 0306-2619. DOI: https://doi.org/10.1016/j.apenergy.2019.114218.

[65] Tim Tröndle et al. “Trade-Offs between Geographic Scale, Cost, and Infrastructure Requirements for Fully Renewable Electricity in Europe”. In: *Joule* 4.9 (2020), pp. 1929–1948. ISSN: 2542-4351. DOI: https://doi.org/10.1016/j.joule.2020.07.018.

[66] Luigi Bottecchia et al. “The Potential of Simulating Energy Systems: The Multi Energy Systems Simulator Model”. In: *Energies* 14.18 (2021). ISSN: 1996-1073. DOI: 10.3390/en14185724. URL: https://www.mdpi.com/1996-1073/14/18/5724.

[67] LLC Gurobi Optimization. *Gurobi Optimizer Reference Manual*. 2024. URL: https://www.gurobi.com/.

[68] Moses Jeremiah Barasa Kabeyi and Oludolapo Akanni Olanrewaju. “The levelized cost of energy and modifications for use in electricity generation planning”. In: *Energy Reports* 9 (2023), pp. 495–534. DOI: https://doi.org/10.1016/j.egyr.2023.06.036.

[69] Wei Shen et al. “A comprehensive review of variable renewable energy levelized cost of electricity”. In: *Renewable and Sustainable Energy Reviews* 133 (2020), p. 110301. DOI: https://doi.org/10.1016/j.rser.2020.110301.

[70] International Renewable Energy Agency (IRENA). *Fostering a Blue Economy: Offshore Renewable Energy*. Abu Dhabi: International Renewable Energy Agency, 2020. URL: https://www.irena.org/publications/2020/Nov/Fostering-a-blue-economy-Offshore-renewable-energy.

[71] Cristobal Rodriguez-Delgado, Rafael J. Bergillos, and Gregorio Iglesias. “Dual wave farms and coastline dynamics: The role of inter-device spacing”. In: *Science of The Total Environment* 646 (2019), pp. 1241–1252. ISSN: 0048-9697. DOI: https://doi.org/10.1016/j.scitotenv.2018.07.110. URL: https://www.sciencedirect.com/science/article/pii/S0048969718325932.

[72] George Lavidas. “Selection index for Wave Energy Deployments (SIWED): A near-deterministic index for wave energy converters”. In: *Energy* 196 (2020), p. 117131. ISSN: 0360-5442. DOI: https://doi.org/10.1016/j.energy.2020.117131.

[73] GADM. *GADM Database of Global Administrative Areas (Level 0 and Level 1)*. Accessed 2025-07-15. 2023. URL: https://gadm.org/download_country.html.

[74] UNEP-WCMC and IUCN. *Protected Planet: The World Database on Protected Areas (WDPA) and World Database on Other Effective Area-based Conservation Measures (WD-OECM) [Online]*. Cambridge, UK: UNEP-WCMC and IUCN. Accessed May 2025. May 2025. URL: https://doi.org/10.34892/6fwd-af11.

[75] Flanders Marine Institute (VLIZ). *Marine Regions: Standardized Geographical Names and Boundaries*. Accessed: 2025-07-05. 2024. URL: https://www.marineregions.org/downloads.php.

[76] E. Segura et al. “Techno-economic challenges of tidal energy conversion systems: Current status and trends”. In: *Renewable and Sustainable Energy Reviews* 77 (2017), pp. 536–550. ISSN: 1364-0321. DOI: https://doi.org/10.1016/j.rser.2017.04.054. URL: https://www.sciencedirect.com/science/article/pii/S1364032117305567.

[77] Jannis Langer, Jaco Quist, and Kornelis Blok. “Upscaling scenarios for ocean thermal energy conversion with technological learning in Indonesia and their global relevance”. In: *Renewable and Sustainable Energy Reviews* 158 (2022), p. 112086. ISSN: 1364-0321. DOI: https://doi.org/10.1016/j.rser.2022.112086. URL: https://www.sciencedirect.com/science/article/pii/S1364032122000168.

[78] M Junginger, A Faaij, and W.C Turkenburg. “Global experience curves for wind farms”. In: *Energy Policy* 33.2 (2005), pp. 133–150. ISSN: 0301-4215. DOI: https://doi.org/10.1016/S0301-4215(03)00205-2. URL: https://www.sciencedirect.com/science/article/pii/S0301421503002052.

[79] Arnulf Grübler. *Technology and Global Change*. Cambridge University Press, 1998.

[80] Mirko Previsic and Julia Chozas. *International Levelised Cost of Energy for Ocean Energy Technologies*. May 2015. DOI: 10.13140/RG.2.2.34304.38407.

[81] Rasul Satymov et al. “Techno-economic assessment of global and regional wave energy resource potentials and profiles in hourly resolution”. In: *Applied Energy* 364 (2024), p. 123119. ISSN: 0306-2619. DOI: https://doi.org/10.1016/j.apenergy.2024.123119. URL: https://www.sciencedirect.com/science/article/pii/S0306261924005026.

[82] Mohammad Hossein Jahangir, Fatemeh Salmanpour, and Erfan Sadeghitabar. “Feasibility assessment of using Wavestar energy converter in a grid-connected hybrid renewable energy system (a case study)”. In: *Energy Conversion and Management: X* 24 (2024), p. 100784. ISSN: 2590-1745. DOI: https://doi.org/10.1016/j.ecmx.2024.100784. URL: https://www.sciencedirect.com/science/article/pii/S2590174524002629.

[83] Perusahaan Listrik Negara. *Statistical Report - PT PLN (Persero)*. https://web.pln.co.id/en/stakeholders/statistical-report. Accessed: 2025-07-18. 2024. URL: https://web.pln.co.id/en/stakeholders/statistical-report.

[84] Vignesh Ramasamy and Robert Margolis. *Floating Photovoltaic System Cost Benchmark: Q1 2021 Installations on Artificial Water Bodies*. American English. Other. 2021. DOI: 10.2172/1828287.

[85] Asian Development Bank (ADB) and PT PLN (Persero). *ADB–PLN Electrical Grid Strengthening Program: Final Report*. Tech. rep. Asian Development Bank, 2021. URL: https://iea.blob.core.windows.net/assets/a4ca843e-5566-4a36-bdd3-186901beaaa9/ADB-PLNElectricalGridStrengtheningProgram-23Feb2021final.pdf.

[86] e-Highway2050 Project Consortium. *Deliverables D3.1 – Technology Assessment from 2030 to 2050*. Tech. rep. European Commission, FP7 e-Highway2050 Project, 2015. URL: https://docs.entsoe.eu/baltic-conf/bites/www.e-highway2050.eu/fileadmin/documents/Results/D3_1_Technology_assessment_from_2030_to_2050.pdf.

[87] Andrew Blakers, Bin Lu, and Matthew Stocks. “100% renewable electricity in Australia”. In: *Energy* 133 (2017), pp. 471–482. ISSN: 0360-5442. DOI: 10.1016/j.energy.2017.05.168. URL: https://www.sciencedirect.com/science/article/pii/S0360544217309568.

[88] Fairuz Milkiy Kuswa et al. “Investigation of the combustion and ash deposition characteristics of oil palm waste biomasses”. In: *Biomass Conversion and Biorefinery* 14.19 (2024), pp. 24375–24395. ISSN: 2190-6823. DOI: 10.1007/s13399-023-04418-z. URL: https://doi.org/10.1007/s13399-023-04418-z.

[89] Muhammad Efendi, Toto Hardianto, and Pandji Prawisudha. “Wet torrefaction of Indonesian agricultural waste biomass: product evaluation and analysis of slagging-fouling potential”. In: *Clean Energy* 9 (May 2025). DOI: 10.1093/ce/zkaf009.

[90] Jannis Langer et al. “Geospatial analysis of Indonesia’s bankable utility-scale solar PV potential using elements of project finance”. In: *Energy* 283 (2023), p. 128555. ISSN: 0360-5442. DOI: https://doi.org/10.1016/j.energy.2023.128555.

[91] Badan Pusat Statistik. *Statistik Indonesia 2025*. Statistical Yearbook of Indonesia 2025. 2025. URL: https://www.bps.go.id/id/publication/2025/02/28/8cfe1a589ad3693396d3db9f/statistik-indonesia-2025.html (visited on 01/16/2025).

[92] Jeremy Gordonnat and James Hunt. “Subsea cable key challenges of an intercontinental power link: case study of Australia–Singapore interconnector”. In: *Energy Transitions* 4.2 (2020), pp. 169–188. ISSN: 2520-114X. DOI: 10.1007/s41825-020-00032-z. URL: https://doi.org/10.1007/s41825-020-00032-z.

[93] International Monetary Fund. *Exchange Rates, Selected Indicators*. IMF Data Explorer: Exchange rates dataset, annual average EUR/USD rates. 2023. URL: https://data.imf.org/en/Data-Explorer?datasetUrn=IMF.STA:ER(4.0.1) (visited on 01/16/2025).

[94] U.S. Bureau of Labor Statistics. *CPI Inflation Calculator*. Consumer Price Index inflation adjustment tool. 2023. URL: https://data.bls.gov/cgi-bin/cpicalc.pl?cost1=1.00&year1=202501&year2=202301 (visited on 01/16/2025).

[95] Ahmad Mukhlis et al. “Opportunities for Tidal Stream Energy in Indonesian Waters”. In: Aug. 2017.

[96] Muhammed Y. Worku. “Recent Advances in Energy Storage Systems for Renewable Source Grid Integration: A Comprehensive Review”. In: *Sustainability* 14.10 (2022). ISSN: 2071-1050. DOI: 10.3390/su14105985. URL: https://www.mdpi.com/2071-1050/14/10/5985.

[97] R.M. Nienhuis et al. “Investigating the efficiency of a novel offshore pumped hydro energy storage system: Experimental study on a scale prototype”. In: *Journal of Energy Storage* 74 (2023), p. 109374. ISSN: 2352-152X. DOI: https://doi.org/10.1016/j.est.2023.109374. URL: https://www.sciencedirect.com/science/article/pii/S2352152X2302772X.

[98] I.G Bryden and D.M Macfarlane. “The utilisation of short term energy storage with tidal current generation systems”. In: *Energy* 25.9 (2000), pp. 893–907. ISSN: 0360-5442. DOI: https://doi.org/10.1016/S0360-5442(00)00020-7. URL: https://www.sciencedirect.com/science/article/pii/S0360544200000207.

[99] Danial Khojasteh et al. “A large-scale review of wave and tidal energy research over the last 20 years”. In: *Ocean Engineering* 282 (2023), p. 114995. ISSN: 0029-8018. DOI: https://doi.org/10.1016/j.oceaneng.2023.114995. URL: https://www.sciencedirect.com/science/article/pii/S0029801823013793.

[100] Richard D. Ray, Gary D. Egbert, and Svetlana Y. Erofeeva. “A Brief Overview of Tides in the Indonesian Seas”. In: *Oceanography* 18.4 (Dec. 2005), pp. 74–79. DOI: 10.5670/oceanog.2005.07. URL: https://doi.org/10.5670/oceanog.2005.07.

# Appendices Overview

This thesis includes four appendices which provide supporting material and additional results that complement the main text:

- **Appendix A: Key Literature Synthesis** — presents a synthesis of the most relevant studies reviewed in Chapter 2, highlighting their relevance to this work.
- **Appendix B: Additional Methodological Information** — contains second-layer methodological detail that supports Chapter 3, including the full mathematical formulation of the optimization problem and detailed technology assumptions.
- **Appendix C: Supporting Results for Resource Modeling** — provides extended results that complement Section 4.1, including detailed wave and tidal energy site classifications, demand projection validations, and additional temporal statistics.
- **Appendix D: Results for Energy System Optimization** — contains extended outputs that support Sections 4.2–4.5, including detailed storage dispatch, transmission expansion maps, cost competitiveness sensitivity analyses, and full system configuration results.

# A. Key Literature Synthesis

Table A.1 synthesizes key literature of this thesis work reviewed in Chapter 2. This appendix serves as an extended reference to 2.1.2.

**Table A.1:** Key Literature and Their Insights

| Author | Year | Title | Key Insights |
|---|---|---|---|
| Institute for Essential Services Reform (IESR) | 2020 | National Energy General Plan (RUEN): Existing Plan, Current Policies Implication, and Energy Transition Scenario | Analyzes Indonesia's energy transition, highlighting MRE's potential but lacking integration pathways, addressed in this study. |
| Ministry of Energy and Mineral Resources (ESDM) | 2024 | Rencana Umum Ketenagalistrikan Nasional (RUKN) 2024 | Outlines Indonesia's power sector plan, emphasizing MRE integration and grid modernization for decarbonization. |
| PT PLN (Persero) | 2021 | Rencana Usaha Penyediaan Tenaga Listrik (RUPTL) 2021-2030 | Details PLN's renewable energy and grid stability strategies, lacking specific MRE targets, a gap this thesis addresses. |
| Ristiyanto Adiputra (BRIN) | 2023 | Ocean-Renewable Energy in Indonesia: A Brief on the Current State and Development Potential | Examines Indonesia's MRE sector progress and challenges, informing this study's system-wide modeling approach. |
| Langer et al. | 2024 | The role of inter-island transmission in full decarbonisation scenarios for Indonesia's power sector | Develops Calliope-Indonesia model, excluding MRE, a gap filled by integrating wave and tidal energy in this study. |
| Pfenninger et al. | 2014 | Energy systems modeling for twenty-first century energy challenges | Outlines ESOM principles like Calliope, supporting this study's modeling tool choice. |
| Ribal et al. | 2020 | A high-resolution wave energy resource assessment of Indonesia | Maps Indonesia's wave energy potential (>30 kW/m), providing site data, but lacks energy system integration, addressed here. |
| Lavidas et al. | 2023 | Integration of wave energy into Energy Systems: an insight to the system dynamics and ways forward | Demonstrates wave energy grid benefits and cost reductions, guiding Calliope-Indonesia adaptation. |
| Orhan et al. | 2016 | Investigation of the Energy Potential from Tidal Stream Currents in Indonesia | Assesses tidal potential (>3 m/s), offering site data, extended by this study's grid integration. |
| Dixon et al. | 2025 | The Philippines' Energy Transition: Assessing Emerging Technology Options Using OSeMOSYS | Integrates tidal energy for island grids, paralleling this study's Calliope-Indonesia adaptation. |
| Lewis et al. | 2019 | Power variability of tidal-stream energy and implications for electricity supply | Highlights tidal energy's predictability, informing this study's grid stability analysis. |
| Ueckerdt et al. | 2013 | System LCOE: What are the costs of variable renewables? | Introduces System LCOE for VRE integration costs, applied to MRE in this study. |

*...continued on the next page*

| Author | Year | Title | Key Insights |
|---|---|---|---|
| Coe et al. | 2022 | Minimizing Cost in a 100% Renewable Electricity Grid: A Case Study of Wave Energy in California | Uses LACE to assess wave energy value, enhancing this study's techno-economic analysis. |
| Ringkjøb et al. | 2018 | A review of modelling tools for energy and electricity systems with large shares of variable renewables | Validates Calliope's adaptability for MRE, reinforcing this study's approach. |
| Shen et al. | 2020 | A comprehensive review of variable renewable energy levelized cost of electricity | Critiques LCOE, advocating VALCOE, aligning with this study's MRE assessment. |
| International Energy Agency (IEA) | 2024 | Global Energy and Climate Model | Introduces VALCOE for system-wide value, key to evaluating MRE viability in this study. |
| Van Den Akker | 2021 | Techno-economic analysis and grid reliability contribution of seven wave energy converters at WaveHub | Proposes probabilistic VALCOE, enhancing this study's risk-based MRE analysis. |
| Dragoon | 2006 | Z-method for power system resource adequacy applications | Provides Z-method for MRE capacity credit, supporting this study's grid reliability modeling. |

Table A.2 summarizes comparison of energy system models available that relevant to the thesis context, as mentioned in 2.7.1.

**Table A.2:** Comparison of Energy System Models for MRE Integration

| Model | Open-Source & Python-Based? | Spatial Resolution | Temporal Resolution | Scalability | Strengths & Limitations |
|---|---|---|---|---|---|
| Calliope | Yes (Apache 2.0) & Yes (Pyomo backend) | Fully user-defined (multi-node), can model from urban districts to continents | Fully user-defined (commonly hourly; supports full time series or clustered days) | Yes, applied from local city-level to national/-continental studies | **Strengths:** User-friendly YAML setup; supports investment and dispatch modes; actively developed. **Limitations:** New tool (2015); solver dependency; large models face long solve times. |
| PyPSA | Yes (via GitHub) & Yes (Python) | Multi-node network (from local grids to continental scale) | High-resolution time series (hourly default; sub-hourly possible) | Yes, used for national and pan-European grid models | **Strengths:** Robust power system modeling; handles network constraints; proven for large-scale studies. **Limitations:** Limited multi-year planning; electricity-sector focus requires extensions. |
| Oemof (solph) | Yes (MIT License) & Yes (Python) | Flexible, user-defined buses/nodes (supports regional grids or single-site) | Flexible, from seconds to years (user-defined temporal granularity) | Yes, applicable from micro-grids to country scale | **Strengths:** Modular multi-sector modeling; highly flexible spatial/temporal detail. **Limitations:** Steep learning curve; requires extensive coding; no GUI. |

*...continued on the next page*

Table A.2 – *Comparison of Energy System Models for MRE Integration (continued)*

| **Model** | **Open-Source & Python-Based?** | **Spatial Resolution** | **Temporal Resolution** | **Scalability** | **Strengths & Limitations** |
|---|---|---|---|---|---|
| OSeMOSYS | Yes (GNU GPL) & No (model formulated in GNU MathProg; interfaces in Excel, etc.) | Multi-region possible, but typically coarser regional aggregation (community to continental scales) | User-defined time slices (intra-annual resolution), but usually low temporal granularity (e.g. 12–36 representative time-slices/year) | Partial, designed for national/regional long-term scenarios (10–100+ year horizons), not detailed local studies | **Strengths:** Simple, transparent; ideal for long-term capacity expansion. **Limitations:** Coarse time detail misrepresents variability; not Python-native; lacks operational detail. |
| EnergyPLAN | No (free but closed-source) & No (standalone GUI in C++) | Single-region (aggregated system model – no intra-model grid nodes) | High temporal resolution (hourly simulation over a year) but no multi-year optimization | Limited – suited to national/regional scenario analysis; not designed for detailed local grids or multi-region interaction | **Strengths:** Easy GUI; detailed hourly operational simulation. **Limitations:** Closed-source; no capacity optimization; single-area focus limits spatial analysis. |
| Switch (PySwitch) | Yes (open-source, Apache 2.0) & Yes (Python implementation) | Multi-region (originally designed for islands and regional grids) | High temporal resolution (hourly chronological dispatch; multi-year investment stages) | Yes, used for utility-scale grids (e.g. Hawaii) and can be adapted to broader regions | **Strengths:** Strong capacity expansion; optimized for high-RE grids. **Limitations:** Scenario-specific setup; limited documentation; power-sector focus. |

Note: IDS = Investment Decision Support; ODS = Operational Decision Support; LP = Linear Programming; MIP = Mixed Integer Programming

# B. Additional Methodological Information

## B.1. Mathematical Formulation of Energy System Optimization

This appendix provides the detailed mathematical formulation of the energy system optimization implemented using Calliope v0.6.10 [55]. The model solves a linear programming problem using the Gurobi solver to minimize total annual system cost, subject to constraints on generation, storage, and transmission.

### B.1.1. Objective Function

The optimization seeks to minimize the total annualized cost of the system:

$$\min z = \sum_{\text{loc,tech,cost}} (\text{cost}_{\text{loc,tech,cost}} \times \text{weight}_{\text{cost}}) \tag{B.1}$$

This includes annualized capital costs, fixed and variable operation costs, and transmission investment, aggregated over all technologies and locations.

### B.1.2. Storage System Constraints

Storage operation is modeled through state-of-charge (SOC) dynamics with losses and efficiency limits:

$$\boldsymbol{storage}(t) = \boldsymbol{storage}(t-1) \cdot (1-loss) - \boldsymbol{carrier_{con}} \cdot \eta - \frac{\boldsymbol{carrier_{prod}}}{\eta} \tag{B.2}$$

$$\boldsymbol{storage}(t) \leq \boldsymbol{storage_{cap}} \tag{B.3}$$

$$|\boldsymbol{carrier_{con/prod}}| \leq \boldsymbol{energy_{cap}} \cdot timestep\_resolution \tag{B.4}$$

### B.1.3. Transmission Constraints and Grid Topologies

The model enforces directional power balance across inter-node transmission:

$$-\boldsymbol{carrier_{con}}(from \rightarrow to, t) \cdot \eta = \boldsymbol{carrier_{prod}}(to \rightarrow from, t) \tag{B.5}$$

Grid topology is defined through two scenarios:

**Fragmented Grid:**

$$\boldsymbol{carrier_{prod/con}}(i, j, t) = 0 \quad \forall \text{ inter-island pairs} \tag{B.6}$$

**Supergrid:**

$$|\boldsymbol{carrier_{prod/con}}(i, j, t)| \leq \boldsymbol{energy_{cap}}(i, j) \tag{B.7}$$

### B.1.4. Constraint Categories Summary

**Table B.1:** Key constraint categories in the calliope-indonesia model

| Constraint Category | Description |
|---|---|
| Energy balance | Electricity demand must be met at every node and timestep with no allowance for unmet demand. |
| Resource availability | Variable renewable generators (solar, wind, wave, tidal, OTEC) are bound by hourly `energy_per_cap` profiles. |
| Technology deployment limits | Maximum installable capacity (`energy_cap_max`) defined per node. For wave and tidal, limits derived from Sections 3.1-3.2. |
| Storage operation | Battery and pumped hydro storage operate with defined round-trip efficiency, charging/discharging limits, and state-of-charge constraints. |
| Transmission limits | Each inter-node transmission link has maximum power transfer limit, adjustable in sensitivity scenarios (5-50 GW HVDC). |

# C. Supporting Results for Resource Modeling

This appendix contains the second-layer results related to Section 4.1. It includes extended figures and tables not shown in the main text, such as detailed wave provincial classifications, statistical distributions, and extended tidal validation results.

## C.1. Wave Energy Modeling

### C.1.1. Provincial Performance Validation

Provincial capacity factor analysis across 27 provinces reveals significant spatial variability in wave energy potential. Figure C.1 demonstrates clear performance hierarchy, with Lampung achieving 29.5% capacity factor as the national benchmark, followed by Bengkulu (17.3

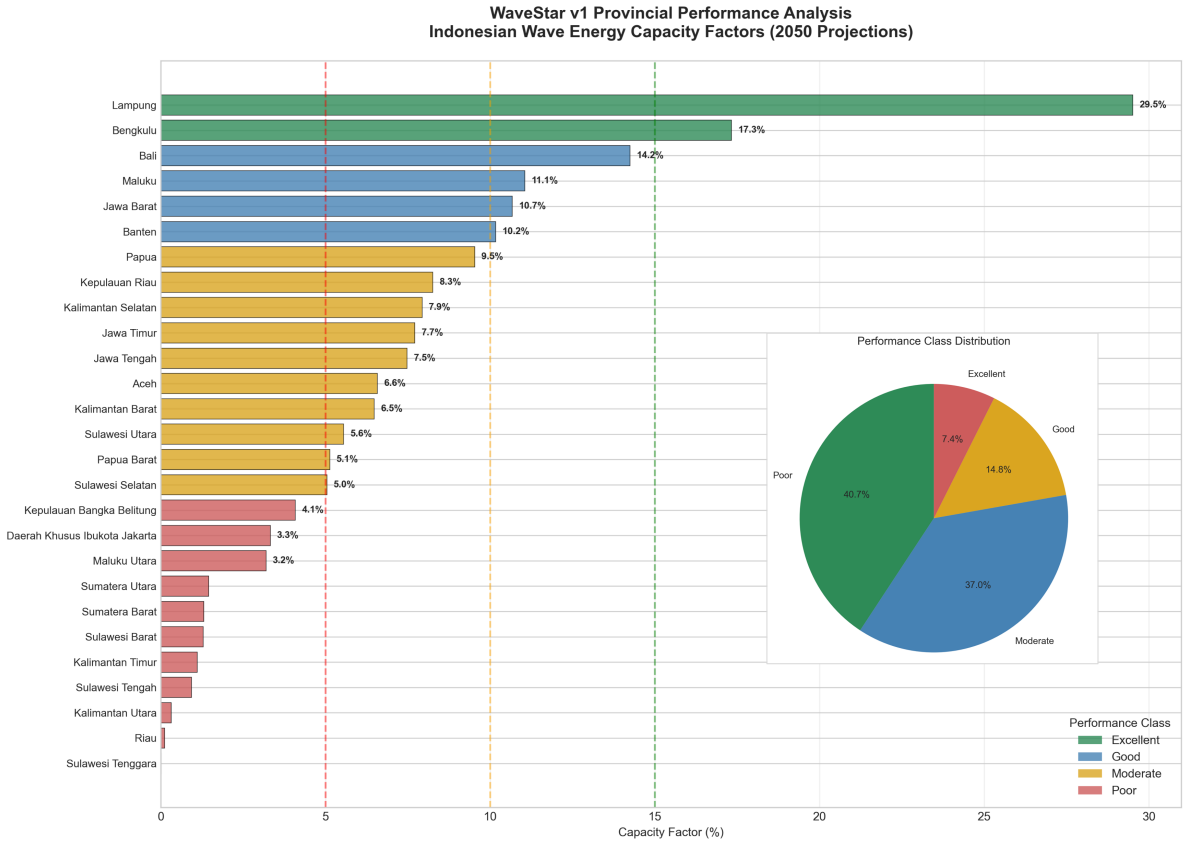


**Figure C.1:** WaveStar v1 Provincial Performance Analysis - Indonesian Wave Energy Capacity Factors (2050 Projections)

Performance classification yields 6/27 provinces (22.2%) exceeding 10% capacity factor threshold for viable deployment, with 2/27 provinces (7.4%) achieving excellent performance above 15%. Overall, 16/27 provinces (59.3%) demonstrate >5% capacity factor, indicating basic wave energy viability across majority of Indonesian coastal regions.

Statistical distribution analysis confirms 6.7% national average with significant provincial spread. Performance classification shows 40.7% of provinces in poor category (<5% CF), 37.0% moderate (5-10% CF), 14.8% good (10-15% CF), and 7.4% excellent (>15% CF), validating selective deployment strategies focused on high-resource provinces for economic viability.

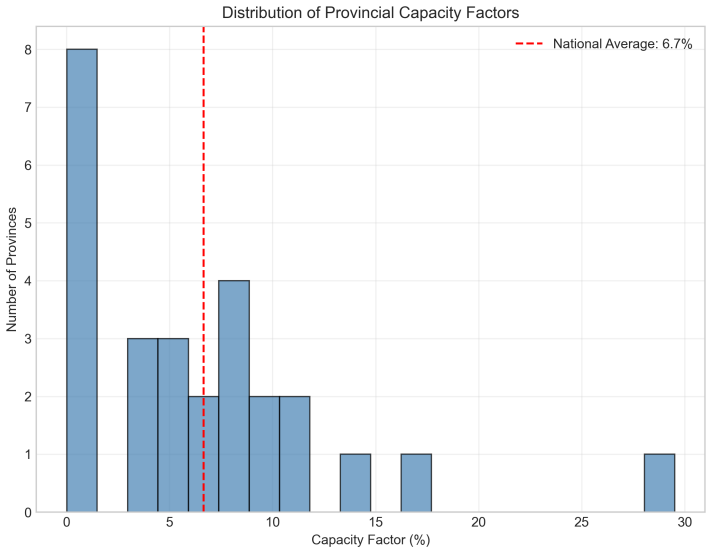


**Figure C.2:** WaveStar v1 Performance Distribution Analysis

### C.1.2. Calliope Integration Outputs

Normalized power profiles generate province-specific timeseries for Calliope energy system optimization. Final outputs include:

1. Technology type: `supply`
2. Carrier: `electricity`
3. `WEC_Profiles_2050_WaveStar.csv`: 8,760-hour normalized power production profile *(timeseries data)*
4. Provincial `energy_cap_max` constraints: 12.47 GW total across 27 provinces *(input per node in* locations.yaml*)*. Refer to Table C.1 for the complete input
5. Mean system capacity factor: 6.7% (province-aggregated)
6. Lifetime: 25 years
7. Costs: Refer to Table 3.8, 3.6

These parameters provide realistic wave energy integration constraints for Indonesian archipelago energy system scenarios through 2050.

**Table C.1:** Maximum Installable Capacity of Wave Energy Converter (WEC) (`energy_cap_max`) per Province for Calliope Input

| Province | energy_cap_max (MW) |
|---|---|
| Aceh | 679,573.11 |
| Bali | 61,280.13 |
| Banten | 61,562.42 |
| Bengkulu | 123,671.45 |
| Daerah_Khusus_Ibukota_Jakarta | 61,675.46 |
| Jawa_Barat | 492,546.79 |
| Jawa_Tengah | 924,303.09 |
| Jawa_Timur | 1,847,991.49 |
| Kalimantan_Barat | 123,841.22 |
| Kalimantan_Selatan | 370,500.48 |
| Kalimantan_Timur | 123,862.45 |
| Kalimantan_Utara | 61,845.14 |
| Kepulauan_Bangka_Belitung | 123,845.93 |
| Kepulauan_Riau | 3,588,653.33 |
| Lampung | 61,621.28 |
| Maluku | 738,827.48 |
| Maluku_Utara | 123,883.68 |
| Papua | 986,136.86 |
| Papua_Barat | 309,621.93 |
| Riau | 247,545.65 |
| Sulawesi_Barat | 123,777.54 |
| Sulawesi_Selatan | 370,038.94 |
| Sulawesi_Tengah | 123,834.15 |
| Sulawesi_Tenggara | 61,724.93 |
| Sulawesi_Utara | 123,827.07 |
| Sumatera_Barat | 123,911.99 |
| Sumatera_Utara | 433,213.22 |

## C.2. Tidal Stream Energy Modeling

This appendix provides the detailed tidal stream modeling results that complement Section 4.1.2.

### C.2.1. Tidal Resource Characterization

Tidal velocity characterization utilized TPXO10-atlas-v2 harmonic constants to generate time series predictions for 2050. The analysis extracted 15 harmonic constituents (M2, S2, N2, K2, K1, O1, P1, Q1, M4, MS4, MN4, 2N2, MF, MM, S1) and applied a 15-day spring-neap analysis period for velocity statistics.

Peak velocities range from 1.00 to 9.49 m/s across validated sites, with a mean of 1.60 m/s. Table 4.3 presents the velocity distribution classification based on tidal energy development potential.

The 1.0 m/s velocity threshold corresponds to the SeaGen-S cut-in velocity, ensuring power generation capability at all validated sites. The maximum velocity of 9.49 m/s, while high for sustained tidal currents, remains within physically plausible ranges for Indonesian straits, consistent with literature reports of 3-4 m/s in high-energy locations such as Larantuka Strait [47].

#### SeaGen-S Power Curve Implementation

The SeaGen-S 2MW power curve was implemented based on technical specifications [23], with key parameters:

- Cut-in velocity: 1.0 m/s (100 kW initial power)
- Rated velocity: 2.5 m/s (2,000 kW rated power)
- Cut-out velocity: 4.0 m/s (safety shutdown)
- Operating range: Power increases as $P = P_{\text{cut\_in}} + (P_{\text{rated}} - P_{\text{cut\_in}}) \cdot v_{\text{norm}}^{2.5}$

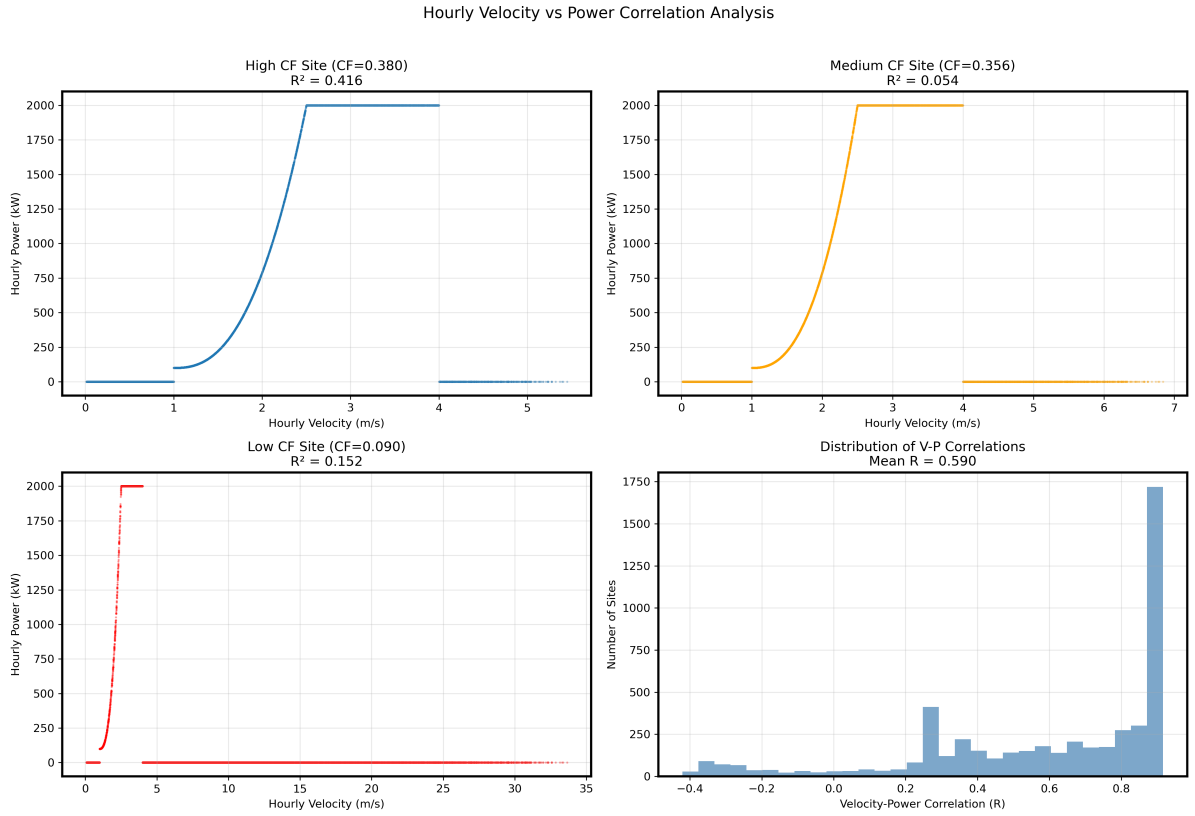


**Figure C.3:** Hourly tidal velocity versus power correlation across selected sites. Top panels show scatter plots for high (CF=0.380), medium (CF=0.356), and low (CF=0.090) capacity factor sites, including respective $R^2$ values. Bottom right panel summarizes the correlation distribution across all sites (Mean $R = 0.590$).

Figure C.3 validates the power curve implementation through hourly velocity-power correlations across representative sites. The analysis reveals mean correlation of R = 0.590 across all sites, confirming accurate SeaGen-S curve implementation. High-capacity-factor sites (CF = 0.380) demonstrate strong velocity-power correlation ($R^2$ = 0.416) with clear power curve characteristics, while medium-performance sites (CF = 0.356) show weaker correlation ($R^2$ = 0.054), indicating more variable velocity patterns.

Low-capacity-factor sites (CF = 0.090) exhibit poor correlation ($R^2$ = 0.152) despite extreme velocities exceeding 30 m/s. This poor performance results from frequent cut-out above 4.0 m/s, where turbines generate zero power during high-velocity periods. The correlation distribution shows most sites cluster around R = 0.8-0.9, demonstrating consistent power curve behavior across the velocity range. Sites with velocities consistently between 1.0-4.0 m/s achieve optimal performance, while extreme velocity sites suffer from cut-out penalties that reduce overall capacity factors.

### Harmonic Analysis Validation

The Indonesian archipelago features some of the world's most complex tidal systems, characterized by complicated coastal geometries, narrow straits, rugged bathymetry, and large tidal energy inputs from both Indian and Pacific Oceans [100]. The TPXO harmonic extraction successfully captured this complexity through 15 harmonic constituents (M2, S2, N2, K2, K1, O1, P1, Q1, M4, MS4, MN4, 2N2, MF, MM, S1), consistent with Ray et al.'s recommendations for Indonesian waters.

The extracted constituents reflect established regional patterns, with M2 semidiurnal tides dominated by Indian Ocean forcing and K1 diurnal tides primarily driven by Pacific Ocean energy [100]. The geographic distribution shows mixed diurnal tides west of 118E longitude (Java Sea region) transitioning to predominantly semidiurnal tides in the eastern archipelago, validating the spatial representativeness of the TPXO10-atlas-v2 dataset for Indonesian tidal energy assessment.

The 15-constituent model captures both primary astronomical forcing (M2, K1, O1) and shallow-water nonlinear effects (M4, MS4) critical for accurate tidal stream predictions in Indonesia's complex coastal waters. This approach builds upon the TPXO foundation established by Ray et al. while utilizing the enhanced resolution and accuracy of the TPXO10-atlas-v2 global model for regional tidal energy resource characterization.

## C.2.2. Capacity Factor Analysis

Capacity factor analysis reveals the relationship between tidal velocity characteristics and energy conversion efficiency. Site-level capacity factors range from 0.090 to 0.380, while provincial aggregation yields a narrower range of 0.255 to 0.360 due to spatial averaging effects.

### Velocity-Capacity Factor Correlations

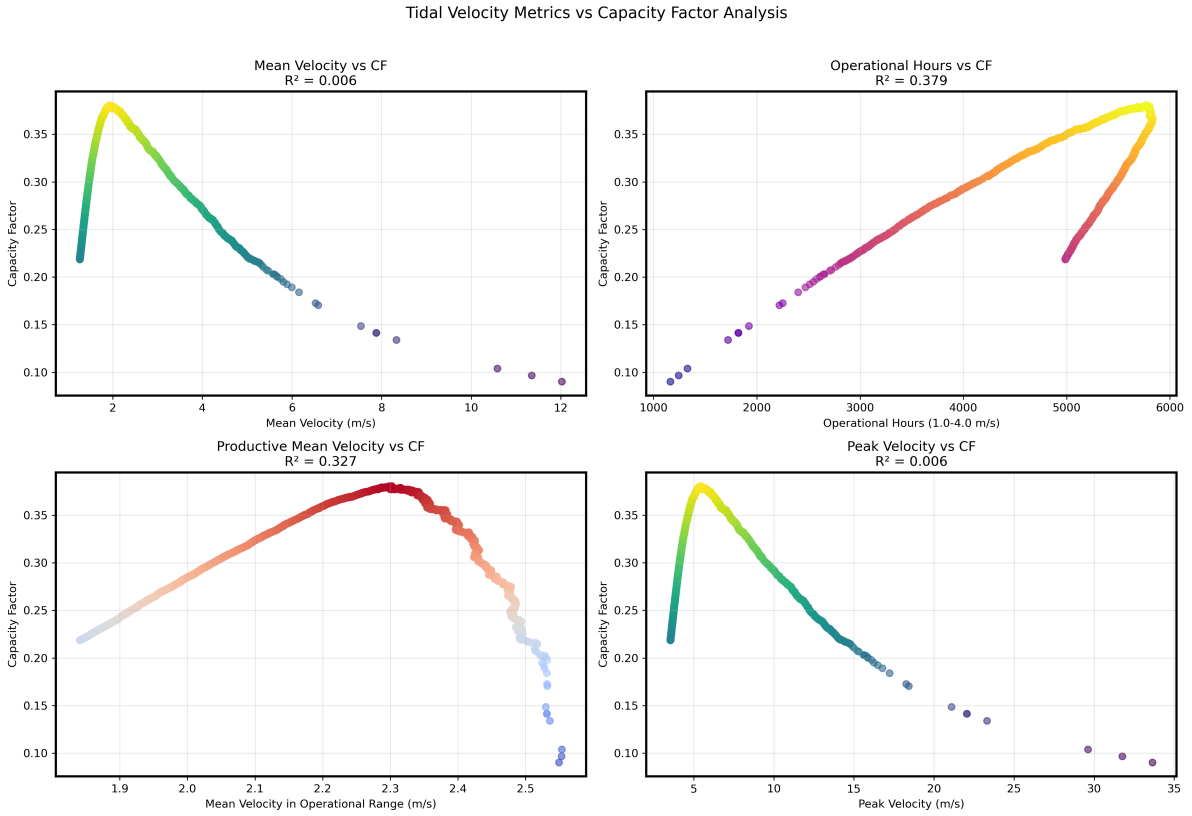


**Figure C.4:** Relationship between tidal velocity metrics and capacity factor (CF) across all valid sites. The top-left panel shows that mean velocity has weak correlation with CF ($R^2 = 0.006$). The strongest predictor is operational hours within the 1.0–4.0 m/s range (top-right, $R^2 = 0.379$), followed by productive mean velocity (bottom-left, $R^2 = 0.327$). Peak velocity also shows weak correlation with CF (bottom-right, $R^2 = 0.006$).

Figure C.4 demonstrates that operational hours (velocity between 1.0-4.0 m/s) provide the strongest correlation with capacity factor ($R^2$ = 0.379), followed by productive mean velocity ($R^2$ = 0.327). Peak velocity and mean velocity both show weak correlation ($R^2$ = 0.006), indicating that sustained moderate velocities matter significantly more than extreme peaks for energy generation. This finding validates that capacity factor depends on velocity distribution over time rather than peak performance, as sites with extreme velocities may experience frequent cut-out above 4.0 m/s, resulting in zero power generation during high-velocity periods. The optimal productive mean velocity occurs around 2.2-2.3 m/s, corresponding to the upper portion of the SeaGen power curve's operating range. Sites with 4,000-5,000 operational hours annually (46-57% of the year) achieve the highest capacity factors (0.35-0.38), while sites with fewer than 2,000 operational hours struggle to exceed 0.25 capacity factor regardless of peak velocities.

## C.2.3. Temporal Generation Patterns

Temporal analysis of tidal generation patterns demonstrates the predictable nature of tidal energy compared to variable renewable sources. The analysis covers weekly cycles to validate semi-diurnal patterns and monthly aggregation to assess seasonal variability implications for energy storage requirements.

### Weekly Generation Cycles

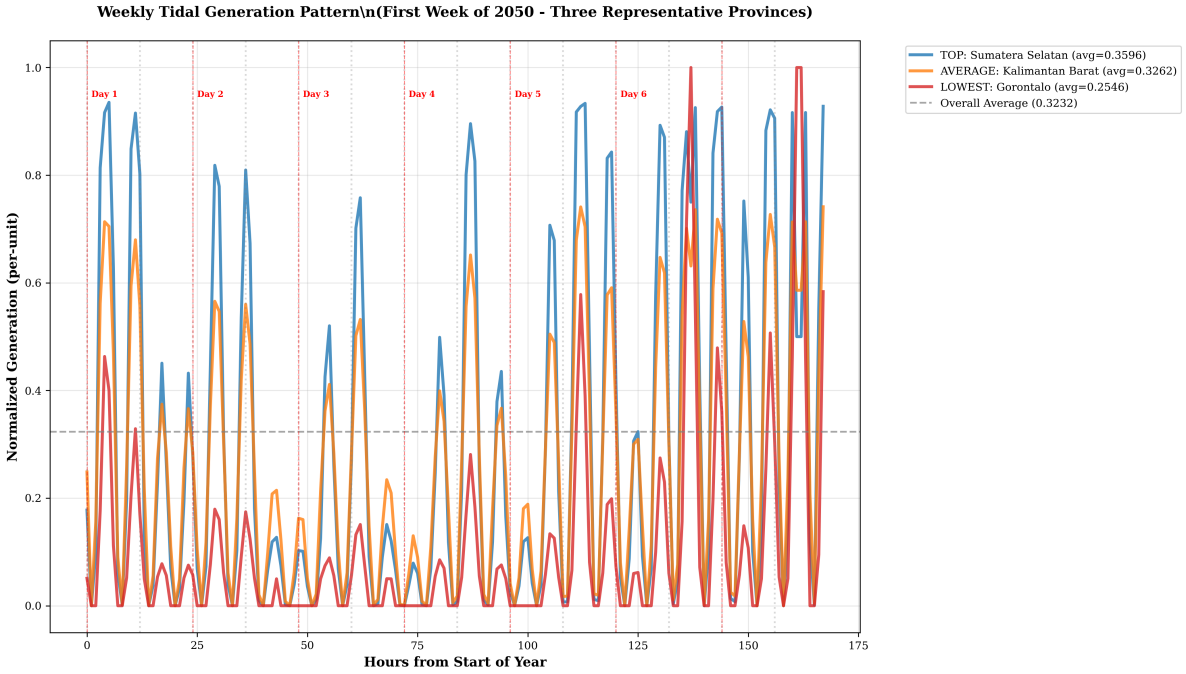


**Figure C.5:** Weekly tidal generation pattern for three representative provinces during the first week of 2050. Sumatera Selatan (top CF), Kalimantan Barat (near-average CF), and Gorontalo (lowest CF) are shown. The figure highlights the diurnal and semidiurnal tidal cycles as well as inter-site variation in normalized output. The horizontal dashed line indicates the overall mean capacity factor (0.3232).

Figure C.5 displays normalized generation patterns for three representative provinces during the first week of 2050. Clear semi-diurnal cycles are evident across all provinces, with approximately 12.4-hour intervals between peak generation periods, consistent with M2 tidal constituent dominance.

Sumatera Selatan (highest CF: 0.360) shows consistent high-amplitude cycles with 19 zero-generation hours out of 168 weekly hours (11%). Kalimantan Barat (average CF: 0.326) demonstrates moderate generation variability with 8 zero hours (5%). Gorontalo (lowest CF: 0.255) exhibits more intermittent generation with 79 zero hours (47%), indicating insufficient velocity for consistent power production.

### Grid Integration Implications

The predictable semi-diurnal cycles and minimal seasonal variation (average 16.2%) contrast favorably with weather-dependent renewables. Unlike solar and wind resources, tidal generation patterns follow astronomical forcing and can be forecasted using harmonic analysis. The 12.4-hour generation cycles provide consistent output during both day and night periods, though the phase relationship between tidal cycles and demand patterns varies by geographic location. The low seasonal variability supports tidal energy's potential role as a predictable renewable baseload source in Indonesia's energy system.

## C.2.4. Performance Validation

Validation of the tidal energy assessment methodology compares results against published literature and identifies limitations inherent in the TPXO-based approach. The comparison reveals both consistencies and discrepancies that inform the interpretation of results.

### Literature Comparison

The calculated capacity factor range (0.255-0.360 provincial, 0.090-0.380 site-level) aligns with the expected range of 0.05-0.35 reported by Orhan et al. [46] for Indonesian waters. The peak velocities (1.00-9.49 m/s) encompass literature values, with the maximum of 9.49 m/s approaching but not exceeding the 3-4 m/s sustained velocities reported for Larantuka Strait.

However, significant discrepancies exist in capacity estimates. This study's power density of 167 MW/km$^2$ substantially exceeds the 67-100 MW/km$^2$ implied by Orhan et al.'s assessment of Larantuka Strait (200-300 MW total capacity over 3 km$^2$). The difference reflects this study's theoretical deployment assumptions without wake interaction modeling or site-specific constraints.

### Uncertainty Assessment

The results represent technical potential under specified spatial constraints (3D $\times$ 10D turbine spacing) rather than economically viable or practically deployable capacity. Key uncertainties include TPXO model accuracy in shallow coastal waters ($\pm 20 - 30\%$), power curve implementation variations across turbine designs, site-specific environmental and engineering constraints, and economic viability thresholds for different velocity ranges. Despite these limitations, the methodology provides consistent framework for comparing tidal energy potential across Indonesian provinces and identifying priority regions for detailed assessment.

**Table C.2:** Maximum Installable Capacity (`energy_cap_max`) per Province for Tidal Stream Power (Calliope Input)

| Province | energy_cap_max (MW) |
|---|---|
| Aceh | 182,400 |
| Banten | 50,160 |
| Bengkulu | 123,120 |
| Daerah_Khusus_Ibukota_Jakarta | 70,680 |
| Gorontalo | 4,560 |
| Jambi | 642,960 |
| Jawa_Barat | 61,560 |
| Jawa_Tengah | 132,240 |
| Jawa_Timur | 424,080 |
| Kalimantan_Barat | 1,680,360 |
| Kalimantan_Selatan | 955,320 |
| Kalimantan_Tengah | 756,960 |
| Kalimantan_Timur | 460,560 |
| Kalimantan_Utara | 456,000 |
| Kepulauan_Bangka_Belitung | 1,390,800 |
| Kepulauan_Riau | 864,120 |
| Lampung | 376,200 |
| Maluku | 519,840 |
| Maluku_Utara | 4,560 |
| Nusa_Tenggara_Barat | 18,240 |
| Papua | 323,760 |
| Papua_Barat | 900,600 |
| Riau | 729,600 |
| Sulawesi_Barat | 25,080 |
| Sulawesi_Selatan | 228,000 |
| Sulawesi_Tenggara | 102,600 |
| Sumatera_Barat | 13,680 |
| Sumatera_Selatan | 82,080 |
| Sumatera_Utara | 145,920 |

## C.3. MRE Timeseries Input

Wave and tidal stream energy exhibit contrasting characteristics in terms of resource stability and availability across Indonesia's provinces. Table C.3 summarizes the key performance indicators of the modeled marine renewable energy profiles in 2050, based on hourly power generation inputs.

**Table C.3:** Summary of modeled marine renewable energy (MRE) profiles in 2050

| Indicator | Wave Energy | Tidal Energy |
|---|---|---|
| Mean capacity factor (CF) | 0.067 | 0.323 |
| Variability (coefficient of variation) | 0.476 | 0.897 |
| Available provinces | 27 | 29 |

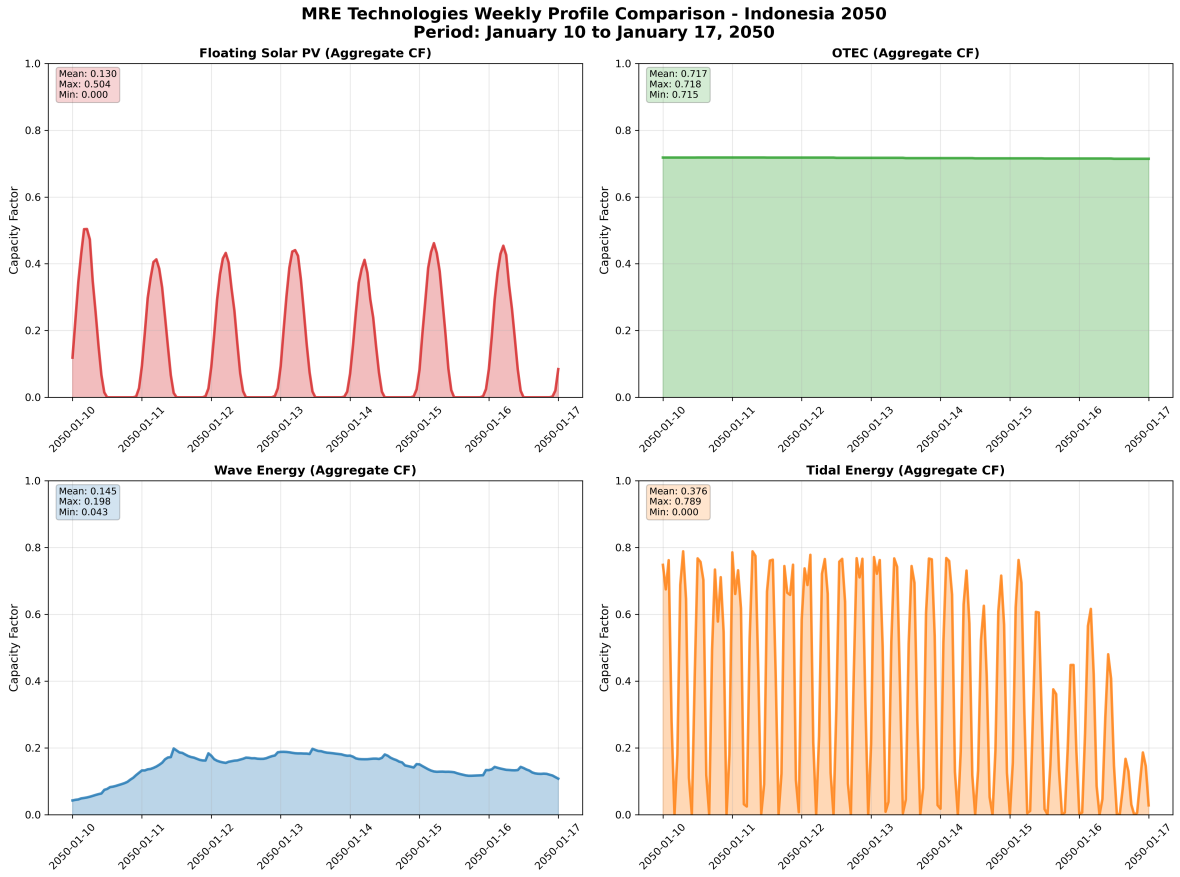


**Figure C.6:** Weekly generation profiles of marine and ocean renewable technologies in Indonesia for January 2050. Comparison includes floating solar PV, OTEC, wave energy, and tidal energy showing distinct temporal characteristics and variability patterns.

Figure C.6 reveals distinct temporal generation patterns that influence grid integration strategies and transmission requirements. OTEC demonstrates exceptional stability with near-constant output (CF: 0.717, variation <0.3%), providing reliable baseload capacity that minimizes transmission planning complexity. This stability contrasts sharply with the highly variable nature of other marine technologies.

Wave energy exhibits moderate temporal variability with gradual multi-day fluctuations around a mean capacity factor of 0.145. The smooth profile transitions suggest wave energy can provide semi-baseload generation with predictable seasonal patterns, requiring less short-term grid balancing compared to solar technologies. However, the significantly lower capacity factor compared to tidal energy (0.067 vs 0.323) indicates substantial capacity oversizing requirements to achieve equivalent energy output.

Tidal energy displays highly regular semi-diurnal cycles with predictable 12.4-hour periodicity, enabling precise grid integration planning despite high variability (coefficient of variation: 0.897). The zero-generation periods (371 hours annually) require coordinated dispatch strategies or storage systems to maintain continuous supply. Unlike wave energy's gradual variations, tidal energy's sharp peak-to-zero oscillations demand more sophisticated transmission and storage coordination.

Floating solar PV provides the reference point for intermittent renewable integration, with strong diurnal cycling that complements tidal generation timing. The combination of solar daytime peaks and tidal semi-diurnal cycles creates potential for improved system load balancing, though both technologies require substantial backup capacity during simultaneous low-generation periods.

These temporal characteristics directly influence transmission planning priorities. OTEC's stability justifies dedicated transmission corridors for baseload evacuation, while tidal energy's predictable variability supports regional balancing strategies. Wave energy's moderate variability positions it between baseload and peak generation applications, requiring flexible transmission infrastructure to accommodate multi-day generation variations.

## C.4. Demand Projection Details

This appendix provides complete technical documentation for the dual demand projection framework, including detailed methodological validation, provincial-level results, and statistical analyses supporting the main text findings in Section 4.1.3.

### C.4.1. Bottom-Up Demand Scenario (RUPTL) - Complete Results

The detailed provincial scaling results, proxy load profiles, and validation figures are presented here.

**Table C.4:** JAMALI Provincial Demand Projection Results (2024 → 2050)

| Province | Peak 2024 (GW) | Annual 2024 (GWh) | Phase 1 Mult. | Phase 2 Mult. | Total Mult. | Annual 2050 (GWh) | Peak 2050 (GW) |
|---|---|---|---|---|---|---|---|
| Jawa Barat | 6.93 | 48,398.4 | 1.495 | 1.902 | 2.844 | 137,632.0 | 19.72 |
| Jawa Tengah | 4.86 | 32,493.9 | 1.740 | 2.428 | 4.223 | 137,229.8 | 20.53 |
| Jawa Timur | 6.86 | 47,899.4 | 1.428 | 1.761 | 2.515 | 120,445.3 | 17.24 |
| Jakarta | 7.23 | 50,347.1 | 1.373 | 1.655 | 2.272 | 114,394.6 | 16.43 |
| Banten | 5.38 | 37,427.8 | 1.361 | 1.630 | 2.218 | 83,016.8 | 11.92 |
| Bali | 1.18 | 7,765.5 | 1.965 | 2.952 | 5.801 | 45,051.1 | 6.86 |
| Yogyakarta | 0.62 | 4,160.3 | 2.002 | 3.042 | 6.089 | 25,332.7 | 3.79 |
| **JAMALI Total** | **33.07** | **228,492.5** | **1.492** | **1.905** | **2.902** | **663,102.2** | **96.50** |

JAMALI projections show 2.90x growth (190.2% increase) over the 26-year period, with Yogyakarta exhibiting the highest growth multiplier (6.09x) and Jakarta the lowest (2.27x). The system maintains load factor consistency while scaling from 33.1 GW to 96.5 GW peak demand, reflecting provincial-specific growth trajectories from RUPTL 2025-2034 planning data.

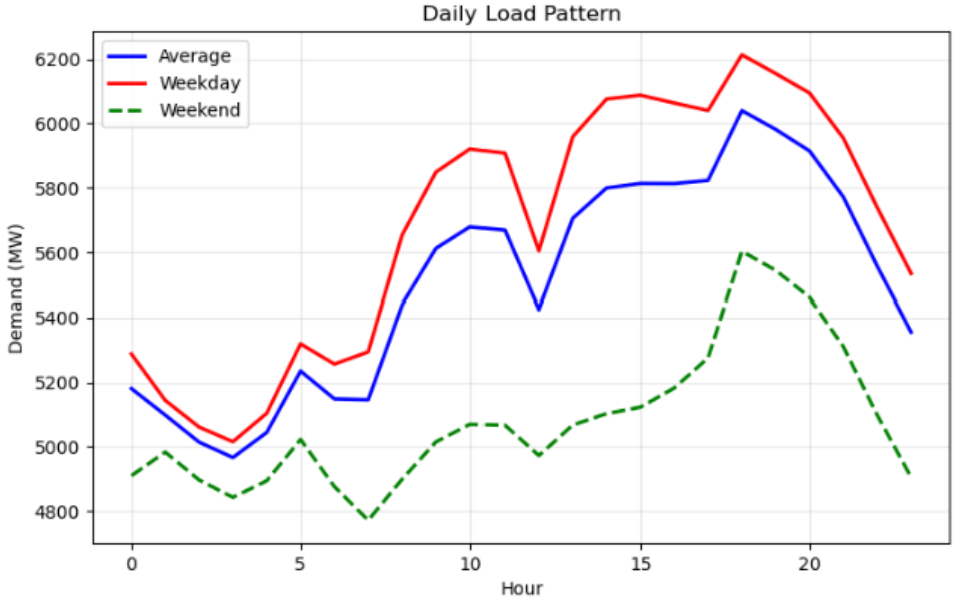


**Figure C.7:** Jawa Barat Daily Load Pattern for Non-JAMALI Proxy Scaling

Jawa Barat serves as the proxy reference province for 27 non-JAMALI provinces based on its representative load characteristics. The daily load pattern demonstrates typical mixed industrial-residential demand with morning and evening peaks (5,849 MW and 6,214 MW respectively) and a night base load of 5,081 MW, yielding a moderate peak-to-base ratio of 1.22. The load factor of 79.5% and low daily variability (CV = 0.061) indicate stable demand patterns suitable for proxy scaling. The weekday-to-weekend ratio of 1.12 reflects balanced economic activity, making Jawa Barat representative of Indonesia's intermediate development provinces.

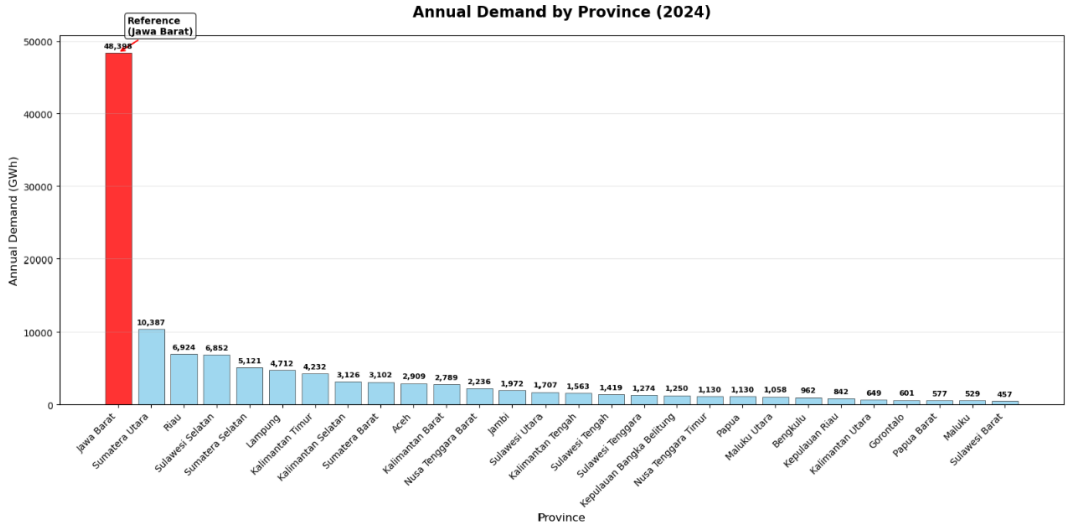


**Figure C.8:** Annual Demand by Province (2024) - Proxy Scaling Results

The proxy scaling methodology scales Jawa Barat temporal patterns to 27 non-JAMALI provinces using PLN Statistics 2024 electricity sales proportions, refer to Table C.8. Sumatera Utara leads with the largest scaling factor (0.2146), while Sulawesi Barat represents the smallest (0.0094). Total non-JAMALI demand reaches 69.5 TWh, representing 28.9% of national electricity sales in 2024.

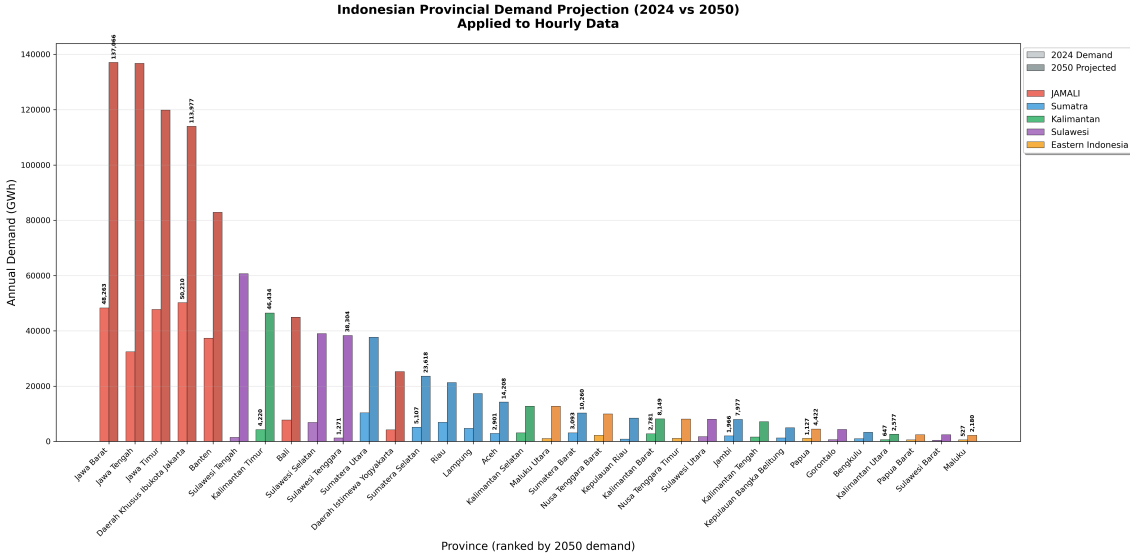


**Figure C.9:** Indonesian Provincial Demand Projection (2024 vs 2050) - Bottom-Up Scenario

The bottom-up scenario projects total Indonesian electricity demand from 297.2 TWh in 2024 to 1,079 TWh in 2050, representing 263.1% growth over the 26-year period. JAMALI maintains its position as the dominant consumption region, though its relative share decreases from 76.7% to 61.2% as outer island provinces experience higher growth rates. Jawa Barat leads absolute demand at 137.6 TWh by 2050, followed by Jawa Tengah (137.2 TWh) and Jawa Timur (120.4 TWh). The highest growth multipliers occur in eastern provinces, with some Sulawesi regions achieving over 10x growth, while JAMALI provinces show more moderate 2-6x increases reflecting their mature baseline conditions.

### C.4.2. Bottom-Up Validation Analysis

The bottom-up demand projections require validation against established methodologies to assess their suitability for MRE integration analysis. Validation is performed through comparison with Langer et al. [1], which represents the current state-of-practice for Indonesian energy system modeling and provides the baseline calliope-indonesia framework upon which this study builds.

Langer et al. [1] developed provincial demand profiles through Malaysian reference scaling with Indonesian provincial electricity sales proportions, applying constant regional growth rates from PLN's 2021-2030 business plan. The present bottom-up

approach integrates UP2B operational dispatch data for JAMALI provinces while maintaining Jawa Barat proxy scaling for non-JAMALI regions, creating a hybrid methodology with higher Indonesian data content.

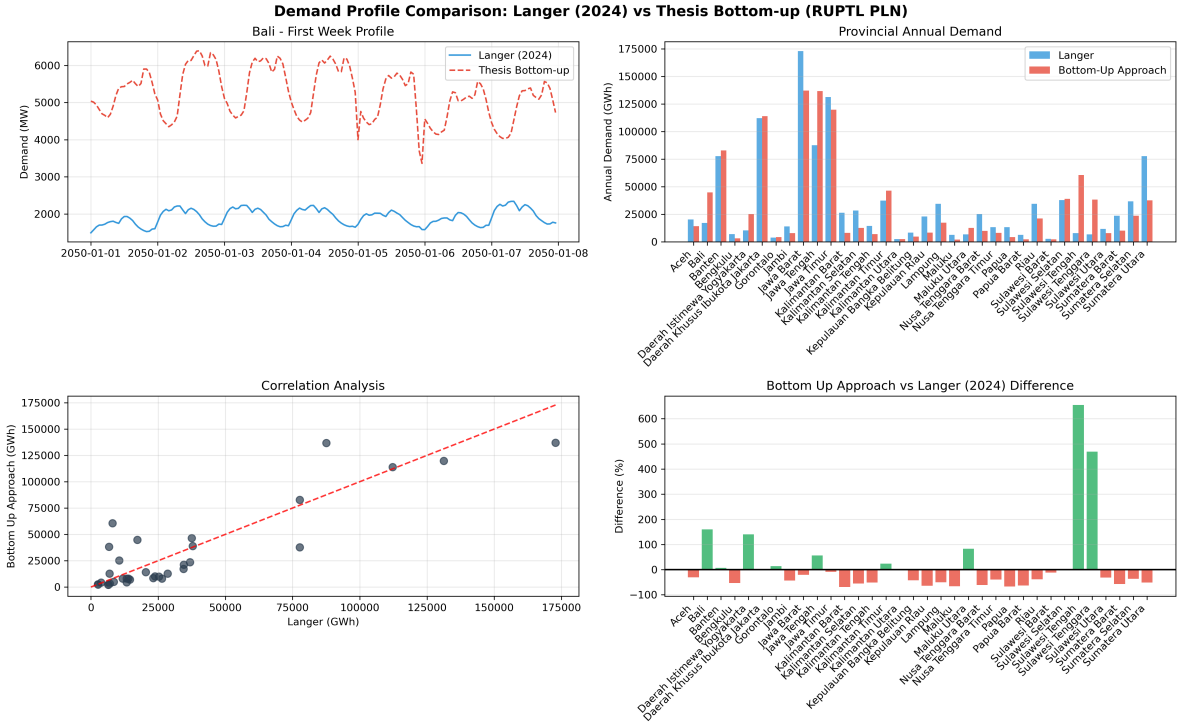


**Figure C.10:** Demand Profile Comparison: Langer (2024) vs Thesis Bottom-up (RUPTL PLN)

National demand comparison reveals strong methodological alignment. The bottom-up approach projects 1,079 TWh total demand by 2050 compared to Langer's 1,141 TWh, representing a 5.5% difference that falls within established uncertainty bounds for long-term projections ($\pm 15 - 25\%$). Cross-correlation analysis yields a coefficient of 0.883 at the provincial level, demonstrating strong statistical relationship despite distinct data sources. Load factor preservation at 0.801 for both scenarios confirms consistent temporal demand distribution patterns.

Regional demand redistribution reflects different assumptions about provincial development trajectories. The bottom-up approach shows largest increases in Sulawesi Tengah (+654.4%), Jawa Tengah (+56.2%), and Sulawesi Tenggara (+469.2%), while projecting decreases in Sumatera Utara (-51.5%) and Jawa Barat (-20.7%). These variations emphasize infrastructure expansion in Sulawesi and industrial development in Central Java, while projecting conservative growth in established Sumatran centers.

The bottom-up approach produces significant shifts in regional demand concentration, with JAMALI share increasing from 53.4% (Langer) to 61.2% (+7.9 percentage points), while Sumatra share decreases from 24.6% to 13.8% (-10.8 percentage points). This redistribution toward JAMALI concentration fundamentally alters MRE integration dynamics, favoring centralized deployment strategies and submarine transmission investment. Reduced outer island demand (418 TWh vs 532 TWh, -21.4%) limits distributed MRE market potential despite abundant marine resources in eastern Indonesia.

Figure C.10 demonstrates the methodological comparison across multiple dimensions. The first week temporal profile shows distinct diurnal patterns, with the bottom-up approach exhibiting higher variability (4,000-6,000 MW range) compared to Langer's smoother profile (1,800-2,500 MW range) for Bali province. Provincial annual demand comparison reveals systematic differences across all 34 provinces, with the correlation scatter plot showing strong linear relationship ($R^2$ = 0.883) but notable deviations for high-demand provinces like Jakarta and Jawa Barat. The percentage difference analysis highlights regional clustering effects, where JAMALI provinces show moderate variations ($\pm 50\%$) while outer island provinces exhibit extreme variations ($\pm 600\%$ for Sulawesi provinces), indicating fundamentally different development assumptions between methodologies.

Temporal validation reveals methodological divergence with sample week correlation of 0.024 and peak demand timing difference of 4,187 hours ( 6 months offset). The load duration curves show similar shapes but different seasonal peak positioning, affecting capacity factor calculations for variable renewables. This temporal divergence impacts renewable energy integration modeling, particularly for technologies with seasonal resource variations like wave energy. Higher JAMALI concentration strengthens centralized MRE deployment under Supergrid scenarios while reducing distributed development attractiveness under fragmented grid conditions.

The validated bottom-up projections represent the inclusion in the dual-scenario framework, with strong national correlation (0.883), total demand difference within uncertainty bounds (-5.5%), and methodologically distinct baseline using Indonesian op-

erational data. The approach enables assessment of MRE integration across alternative development pathways, complementing the top-down RUKN scenario to bracket demand uncertainty space for energy system optimization.

### C.4.3. Top-Down Demand Projection Scenario

The top-down scenario distributes RUKN 2024 national targets (1,492 TWh by 2050) across 34 provinces using electricity sales proportions as economic activity proxies. Regional scaling factors range from 1.3x (Banten) to 21.1x (Eastern Indonesia), creating distinct provincial development trajectories aligned with national policy objectives.

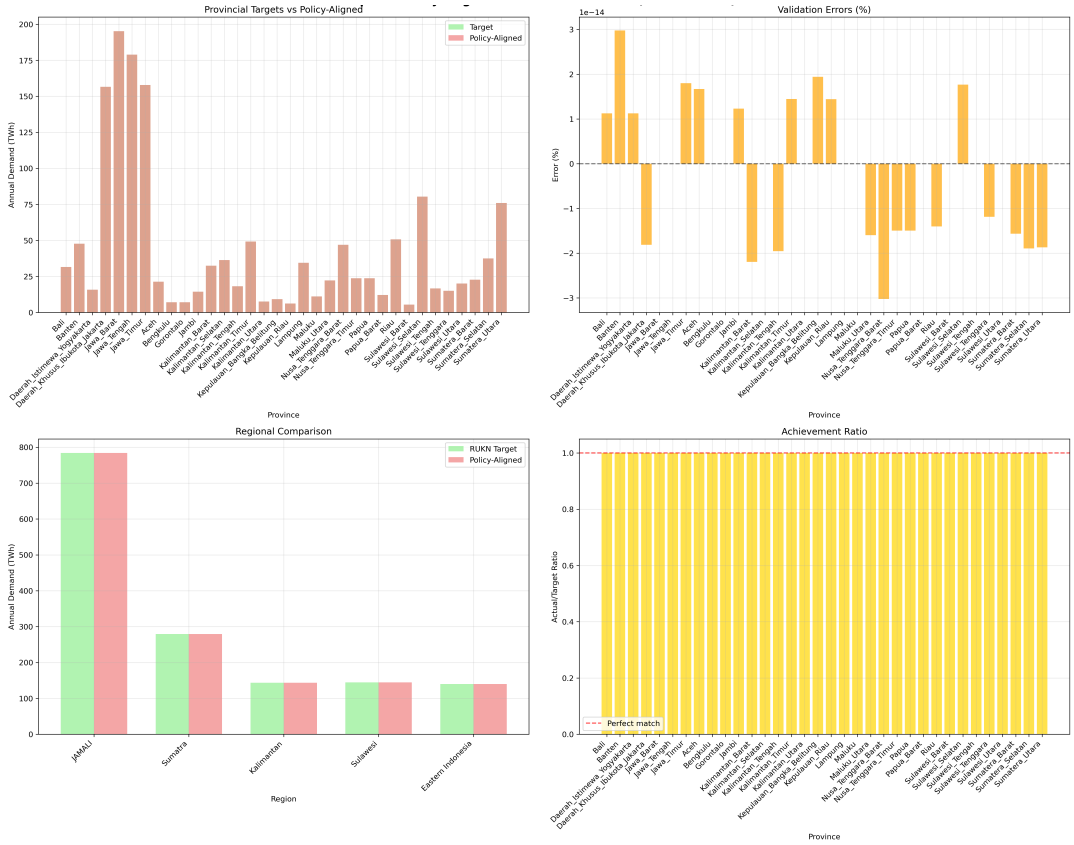


**Figure C.11:** Top Down / Policy-Aligned Scenario Validation (34 Provinces)

Figure C.11 confirms target implementation accuracy with validation errors <0.1% and achievement ratios of exactly 1.0 across all provinces.

**Table C.5:** Regional Distribution and Scaling Factors for Top-Down Scenario

| Region | 2050 Demand (TWh) | Share (%) | Scaling Factor | Development Pattern |
|---|---|---|---|---|
| JAMALI | 784.0 | 52.5 | 1.3–5.5x | Moderate growth, mature markets |
| Sumatra | 279.5 | 18.7 | 7.3x | Uniform regional scaling |
| Kalimantan | 143.6 | 9.6 | 11.7x | High industrial expansion |
| Sulawesi | 144.5 | 9.7 | 11.8x | Infrastructure development |
| Eastern Indonesia | 140.0 | 9.4 | 21.1x | Aggressive development targets |
| **Total** | **1,491.6** | **100.0** | **-** | **-** |

Outer islands receive 708 TWh versus 418 TWh in RUPTL scenarios (+69%), fundamentally altering MRE market potential. Eastern provinces receive the steepest scaling, with Papua increasing from 1.13 TWh to 23.75 TWh and Maluku from 0.53 TWh to 11.12 TWh.

The 21.1x Eastern Indonesia multiplier creates 93 TWh additional demand compared to bottom-up projections (140 TWh vs 47 TWh), improving resource-demand spatial correlation for tidal and wave technologies. Papua's 21x scaling transforms its position from marginal demand (1.13 TWh baseline) to significant MRE market (23.75 TWh target), supporting distributed deployment economics for point absorbers in high-resource coastal zones.

The RUKN framework produces 38.3% higher total demand (1,492 TWh vs 1,079 TWh) with outer island share increasing from

38.8% to 47.5%. Eastern provinces receive 93 TWh additional demand compared to RUPTL projections, improving resource-demand spatial correlation for marine technologies across Indonesian archipelago waters.

### C.4.4. Comprehensive Temporal and Statistical Analysis

System-level comparison reveals substantial differences between methodological approaches. The top-down scenario projects 1,491.6 TWh total demand versus 1,079.6 TWh for bottom-up (+412.0 TWh, +38.2%), while maintaining high temporal correlation (0.965) indicating preserved demand shape patterns. Average peak ratio of 2.053 reflects consistent scaling across temporal profiles.

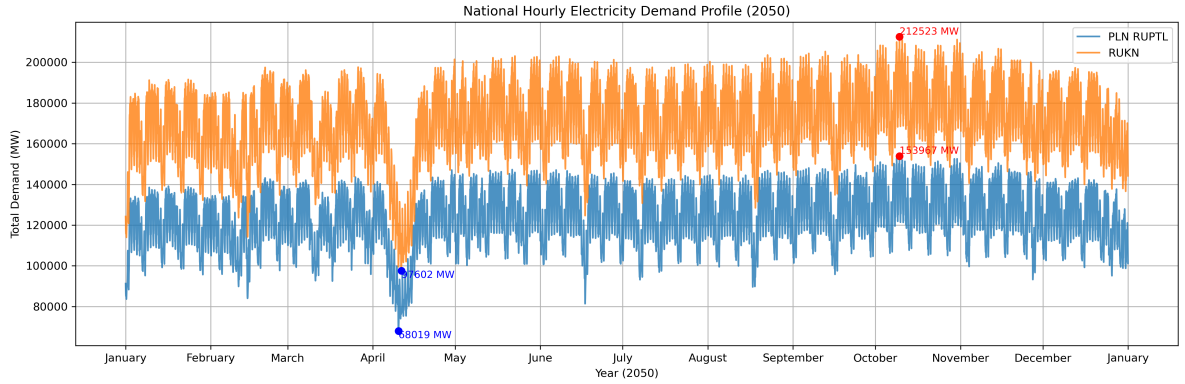


**Figure C.12:** National Hourly Electricity Demand Profile (2050)

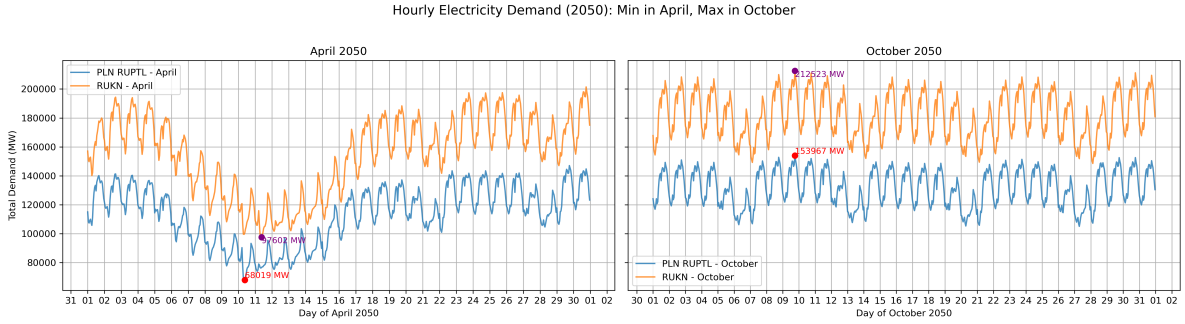


**Figure C.13:** Hourly Electricity Demand (2050): Min in April, Max in October

Temporal analysis shows distinct seasonal patterns with peak demand occurring in October (top-down: 212,523 MW, bottom-up: 153,967 MW) and minimum in April (top-down: 97,602 MW, bottom-up: 68,019 MW). The 38.2% scaling maintains diurnal cycles while amplifying seasonal variations, creating higher peak-to-minimum ratios in the policy-aligned scenario.

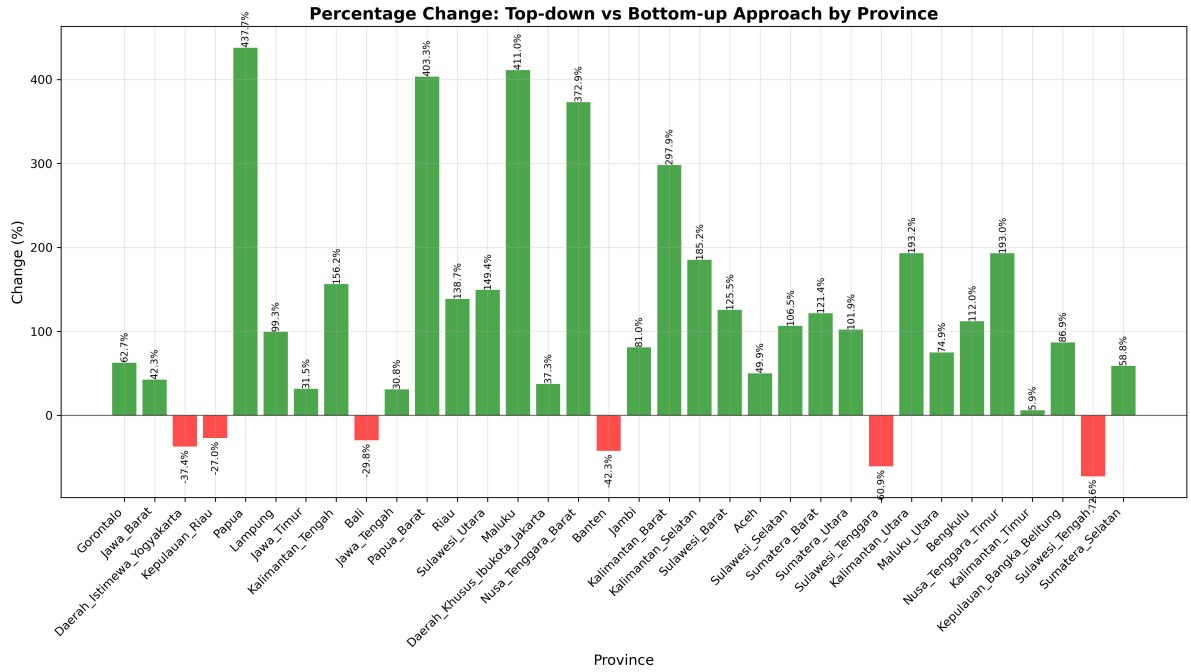


**Figure C.14:** Provincial Percentage Change Between Demand Scenarios

Provincial extremes highlight methodological divergence impacts. Papua leads increases (+437.7%) from 4.3 TWh to 23.8 TWh, followed by Maluku (+411.0%) and Papua Barat (+403.3%). Conversely, Sulawesi Tengah shows the largest decrease (-72.6%) from 60.8 TWh to 16.7 TWh, with Sulawesi Tenggara (-60.9%) and Banten (-42.3%) also declining substantially.

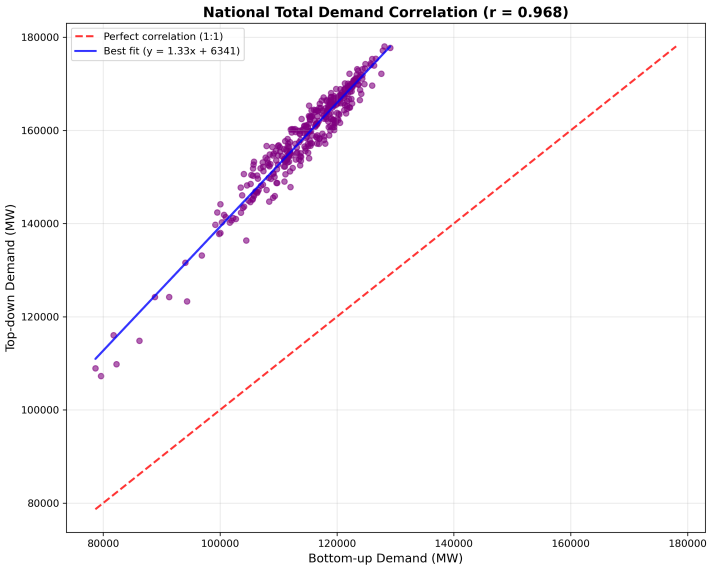


**Figure C.15:** National Demand Correlation Between Scenarios

Statistical validation confirms temporal pattern preservation across scenarios. Load factor analysis shows consistent diurnal and seasonal characteristics, while coefficient of variation patterns indicate maintained demand volatility relationships. Kolmogorov-Smirnov test results validate distributional similarity between scenarios.

The dual-scenario framework captures uncertainty space through methodologically distinct approaches. The top-down scenario serves as the reference case for Calliope energy system modeling, representing policy-aligned development trajectories consistent with RUKN 2024 national targets. The bottom-up scenario provides the alternative demand profile, reflecting operational data-grounded projections based on RUPTL utility planning assumptions.

**Table C.6:** Calliope Model Input Configuration

| **Scenario** | **Input File** | **Methodology** |
|---|---|---|
| Reference | Demand_Profiles_2050_RUKN.csv | Top-down policy targets |
| Alternative | Demand_Profiles_2050_PLN_RUPTL.csv | Bottom-up operational data |
| **Uncertainty Range** | **+38.2% total demand** | **Regional redistribution** |

**Table C.7:** Provincial Electricity Sales Projection (%) based on RUPTL PLN (2025-2034) report

| **Province Name** | **2025** | **2026** | **2027** | **2028** | **2029** | **2030** | **2031** | **2032** | **2033** | **2034** |
|---|---|---|---|---|---|---|---|---|---|---|
| Aceh | 3.7 | 3.1 | 3.7 | 4.1 | 4.2 | 8.5 | 3.6 | 3.5 | 26.7 | 2.7 |
| Sumatera Utara | 7.34 | 3.18 | 4.19 | 4.39 | 5.35 | 5.32 | 5.3 | 5.29 | 5.28 | 5.28 |
| Sumatera Barat | 4.05 | 4.04 | 3.91 | 4.08 | 5.02 | 5.09 | 5.13 | 5.23 | 5.3 | 5.36 |
| Riau | 1.21 | 1.92 | 4.54 | 4.82 | 3.85 | 3.83 | 3.78 | 3.96 | 7.04 | 9.31 |
| Kepulauan Riau | 2.8 | 3.9 | 5 | 5.1 | 5.1 | 5.5 | 324 | 1.4 | 1.4 | 1.5 |
| Jambi | 5.82 | 5.37 | 54.88 | 3.47 | 3.45 | 3.45 | 3.44 | 3.45 | 3.45 | 3.46 |
| Bengkulu | 3.26 | 4.53 | 5.12 | 5.18 | 5.17 | 5.19 | 5.17 | 5.15 | 5.13 | 5.09 |
| Sumatera Selatan | 7.15 | 6.17 | 5.08 | 5.1 | 6.25 | 7.62 | 4.99 | 4.96 | 8.61 | 4.77 |
| Kepulauan Bangka Belitung | 6.22 | 6.13 | 5.93 | 5.69 | 5.48 | 5.28 | 5.09 | 4.91 | 4.75 | 4.59 |
| Lampung | 5.67 | 5.68 | 5.63 | 5.54 | 5.44 | 5.38 | 4.63 | 4.54 | 4.49 | 4.44 |
| Banten | 3.3 | 2.3 | 3.3 | 3.2 | 3.1 | 3.1 | 3.2 | 3.2 | 3.2 | 3.4 |
| DKI Jakarta | 2.85 | 2.96 | 4.02 | 3.84 | 5.48 | 2.37 | 2.69 | 2.6 | 2.73 | 2.68 |
| Jawa Barat | 4.5 | 6.4 | 5 | 4.6 | 3 | 5 | 3 | 3.6 | 3.1 | 2.9 |
| Jawa Tengah | 8.8 | 4.9 | 4.8 | 5.6 | 5.3 | 5.9 | 7.2 | 4.7 | 4.9 | 4.9 |
| DI Yogyakarta | 5 | 7.8 | 7.3 | 7.4 | 7.4 | 7.4 | 7.4 | 7.4 | 7.4 | 7.4 |
| Jawa Timur | 4.3 | 4.9 | 4.8 | 3.8 | 4.2 | 2.2 | 2.9 | 2.8 | 3.4 | 3 |
| Bali | 7.8 | 7.7 | 6.3 | 6.6 | 7 | 7 | 6.8 | 6.9 | 6.9 | 6.9 |
| NTB | 7.5 | 6.6 | 6.3 | 6.1 | 5.9 | 5.7 | 5.5 | 5.3 | 5.2 | 5.1 |
| NTT | 9.7 | 9.7 | 6.5 | 8.9 | 8.1 | 7.5 | 7.3 | 7.2 | 7.1 | 6.9 |
| Kalimantan Barat | 3.5 | 5 | 5.4 | 4.3 | 4.2 | 4.1 | 4 | 4 | 4 | 3.72 |
| Kalimantan Tengah | 9.22 | 6.66 | 5.8 | 5.62 | 5.47 | 5.47 | 5.49 | 5.5 | 5.56 | 5.25 |
| Kalimantan Selatan | 8.37 | 7.39 | 6.35 | 5.43 | 4.87 | 4.77 | 4.7 | 4.67 | 4.63 | 4.49 |
| Kalimantan Timur | 20.72 | 12.26 | 17.39 | 2.01 | 12.69 | 6.38 | 3.96 | 15.35 | 4.15 | 2.44 |
| Kalimantan Utara | 5.53 | 5.46 | 5.42 | 5.39 | 5.36 | 5.34 | 5.42 | 5.47 | 5.55 | 5.63 |
| Sulawesi Utara | 5.6 | 5.5 | 15.2 | 6.3 | 6 | 5.9 | 4.3 | 4.3 | 4.3 | 4.3 |
| Gorontalo | 7.8 | 8.4 | 17.1 | 35 | 4.8 | 9.1 | 4.4 | 3.4 | 3.4 | 4.4 |
| Sulawesi Tengah | 12.5 | 5.3 | 16.4 | 16.1 | 20.2 | 32.1 | 29.9 | 21.1 | 10.8 | 3 |
| Sulawesi Selatan | 7.9 | 4.7 | 6.9 | 5.3 | 6 | 9.4 | 10 | 8.7 | 6.3 | 4.1 |
| Sulawesi Tenggara | 46.3 | 41.3 | 33.4 | 10.1 | 6.9 | 17.5 | 18.4 | 14.2 | 7.7 | 2.2 |
| Sulawesi Barat | 7.1 | 6.9 | 6.8 | 6.6 | 6.4 | 6.4 | 6.4 | 6.3 | 6.4 | 6.4 |
| Maluku | 5.8 | 5.9 | 5.8 | 5.8 | 5.6 | 5.6 | 5.5 | 5.4 | 5.4 | 5.3 |
| Maluku Utara | 6.5 | 4 | 5 | 11.7 | 8.2 | 12.1 | 4.1 | 8.3 | 61.2 | 32.6 |
| Papua | 6.6 | 6.2 | 5.9 | 5.6 | 5.3 | 5.2 | 5 | 4.9 | 4.7 | 4.6 |
| Papua Barat | 6.13 | 6.01 | 5.81 | 5.7 | 5.58 | 5.55 | 5.52 | 5.49 | 5.47 | 5.45 |

Note: Growth rates are expressed as percentages. Data represents annual growth projections for Indonesian provinces from 2025 to 2034.
Source: PLN Statistics 2024 [83]

**Table C.8:** Non-JAMALI Provincial Scaling Results (2024 Baseline)

| Province | Sales (%) | Scaling Factor | Peak Load (MW) | Annual Demand (GWh) |
|---|---|---|---|---|
| *Reference Province* | | | | |
| Jawa Barat | 20.13 | 1.0000 | 6,934 | 48,398.4 |
| *Sumatra (10 provinces)* | | | | |
| Sumatera Utara | 4.32 | 0.2146 | 1,488 | 10,386.6 |
| Riau | 2.88 | 0.1431 | 992 | 6,924.4 |
| Sumatera Selatan | 2.13 | 0.1058 | 734 | 5,121.1 |
| Lampung | 1.96 | 0.0974 | 675 | 4,712.4 |
| Sumatera Barat | 1.29 | 0.0641 | 444 | 3,101.5 |
| Aceh | 1.21 | 0.0601 | 417 | 2,909.2 |
| Jambi | 0.82 | 0.0407 | 282 | 1,971.5 |
| Kepulauan Bangka Belitung | 0.52 | 0.0258 | 179 | 1,250.2 |
| Bengkulu | 0.40 | 0.0199 | 138 | 961.7 |
| Kepulauan Riau | 0.35 | 0.0174 | 121 | 841.5 |
| *Kalimantan (5 provinces)* | | | | |
| Kalimantan Timur | 1.76 | 0.0874 | 606 | 4,231.6 |
| Kalimantan Selatan | 1.30 | 0.0646 | 448 | 3,125.6 |
| Kalimantan Barat | 1.16 | 0.0576 | 400 | 2,789.0 |
| Kalimantan Tengah | 0.65 | 0.0323 | 224 | 1,562.8 |
| Kalimantan Utara | 0.27 | 0.0134 | 93 | 649.2 |
| *Sulawesi (6 provinces)* | | | | |
| Sulawesi Selatan | 2.85 | 0.1416 | 982 | 6,852.2 |
| Sulawesi Utara | 0.71 | 0.0353 | 245 | 1,707.0 |
| Sulawesi Tengah | 0.59 | 0.0293 | 203 | 1,418.5 |
| Sulawesi Tenggara | 0.53 | 0.0263 | 183 | 1,274.3 |
| Gorontalo | 0.25 | 0.0124 | 86 | 601.1 |
| Sulawesi Barat | 0.19 | 0.0094 | 65 | 456.8 |
| *Eastern Indonesia (6 provinces)* | | | | |
| Nusa Tenggara Barat | 0.93 | 0.0462 | 320 | 2,236.0 |
| Papua | 0.47 | 0.0233 | 162 | 1,130.0 |
| Nusa Tenggara Timur | 0.47 | 0.0233 | 162 | 1,130.0 |
| Maluku Utara | 0.44 | 0.0219 | 152 | 1,057.9 |
| Papua Barat | 0.24 | 0.0119 | 83 | 577.0 |
| Maluku | 0.22 | 0.0109 | 76 | 528.9 |
| **Total (27 provinces)** | **28.91** | **N/A** | **9,958** | **69,508.2** |

The following figures provide detailed statistical and temporal analysis supporting the demand scenario comparison presented in Section C.4.4, convering insights into provincial energy distributions, temporal patterns, and load characteristics across bottom-up and top-down projection methodologies.

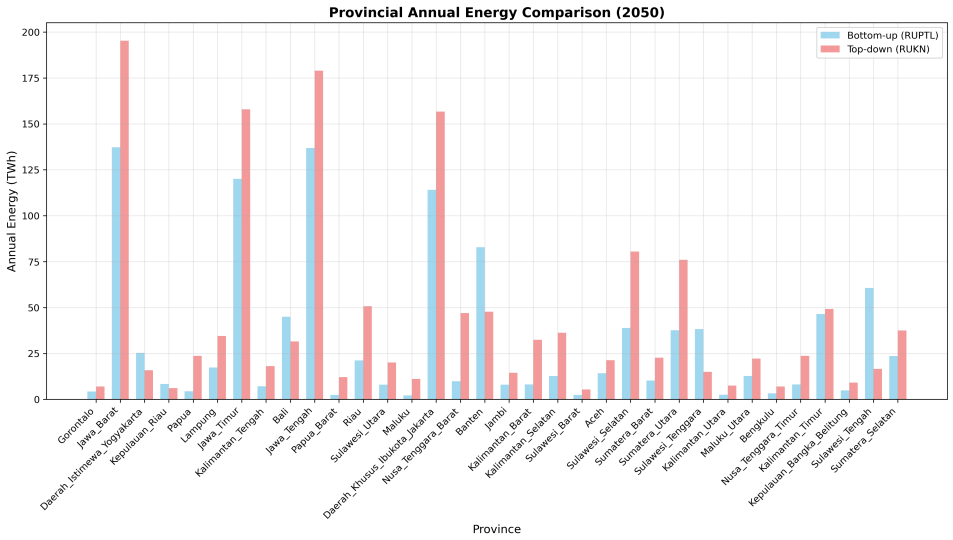


**Figure C.16:** Provincial Annual Energy Comparison: Bottom-Up vs Top-Down Scenarios (2050)

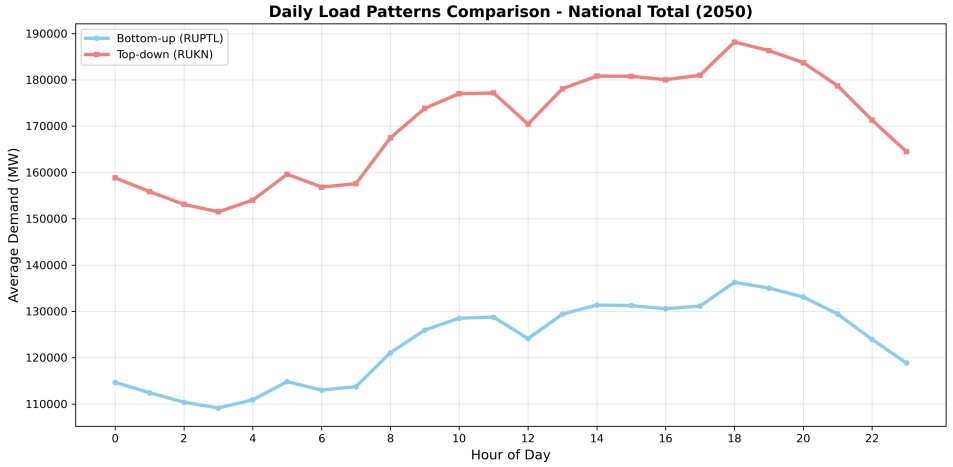


**Figure C.17:** National Daily Load Patterns Comparison Between Scenarios

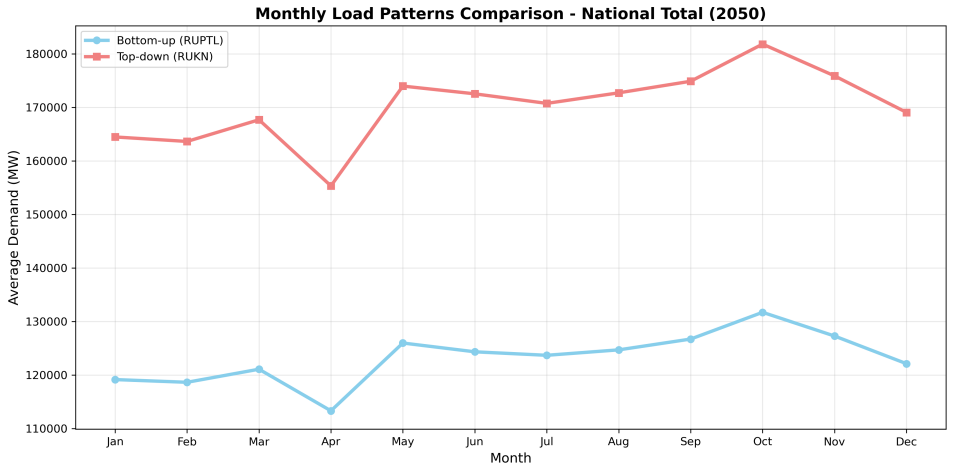


**Figure C.18:** National Monthly Load Patterns Comparison Between Scenarios

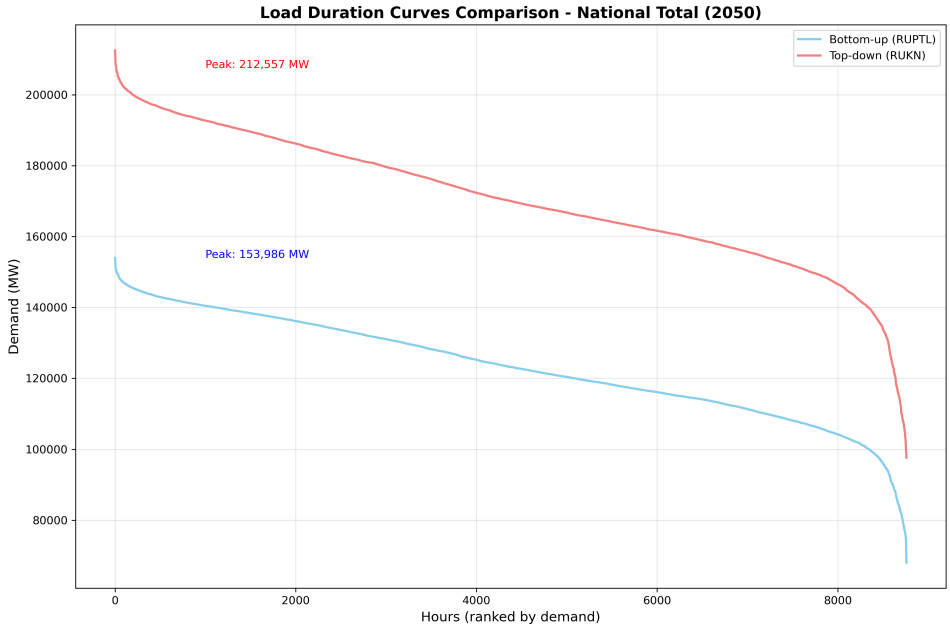


**Figure C.19:** National Load Duration Curves Comparison Between Scenarios

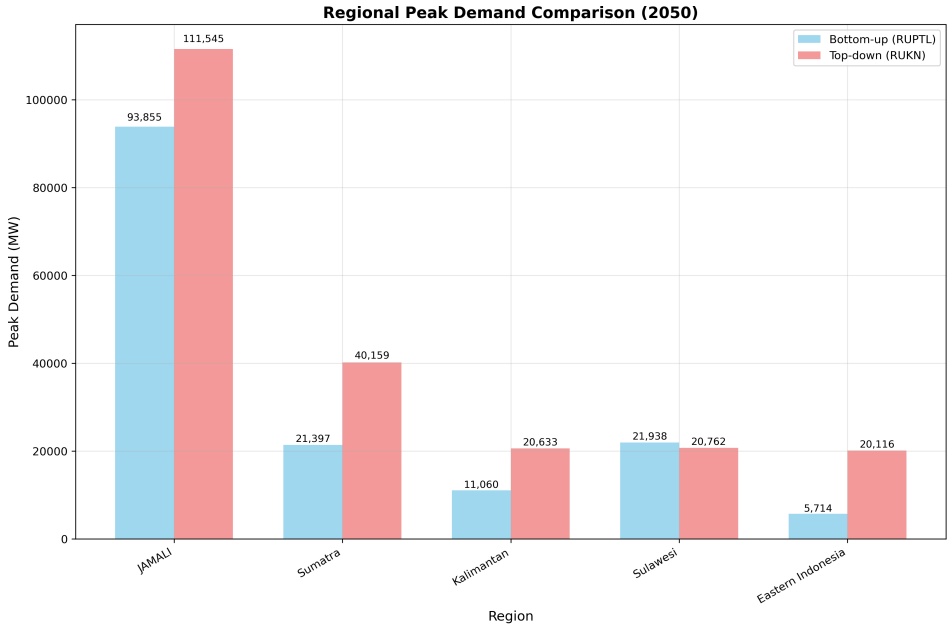


**Figure C.20:** Regional Peak Demand Comparison Between Scenarios

Tables C.9 and C.10 provide detailed statistical and quantitative analysis supporting the dual demand scenario framework. The bottom-up scenario uses PLN operational data with RUPTL 2025-2034 growth rates, while the top-down scenario spatially distributes RUKN 2024 national targets. The 412.0 TWh total difference (38.2% higher under top-down) demonstrates substantial methodological impact with pronounced regional variations including Papua's 437.7% increase and Sulawesi Tengah's 72.6% decrease.

**Table C.9:** Statistical Comparison Analysis Between Demand Scenarios

| Province | Correlation | Peak Ratio | Load Factor Bottom-Up | Load Factor Top-Down |
|---|---|---|---|---|
| Aceh | 1.000 | 1.50 | 0.794 | 0.794 |
| Bali | 0.954 | 0.70 | 0.747 | 0.747 |
| Banten | 0.777 | 0.58 | 0.793 | 0.793 |
| Bengkulu | 1.000 | 2.12 | 0.795 | 0.795 |
| Daerah Istimewa Yogyakarta | 0.836 | 0.63 | 0.762 | 0.761 |
| Daerah Khusus Ibukota Jakarta | 0.777 | 1.37 | 0.793 | 0.793 |
| Gorontalo | 1.000 | 1.63 | 0.795 | 0.795 |
| Jambi | 1.000 | 1.81 | 0.794 | 0.794 |
| Jawa Barat | 0.744 | 1.42 | 0.795 | 0.795 |
| Jawa Tengah | 0.836 | 1.31 | 0.761 | 0.761 |
| Jawa Timur | 0.775 | 1.31 | 0.795 | 0.795 |
| Kalimantan Barat | 1.000 | 3.98 | 0.795 | 0.795 |
| Kalimantan Selatan | 1.000 | 2.85 | 0.794 | 0.794 |
| Kalimantan Tengah | 1.000 | 2.56 | 0.794 | 0.794 |
| Kalimantan Timur | 1.000 | 1.06 | 0.795 | 0.794 |
| Kalimantan Utara | 1.000 | 2.93 | 0.794 | 0.795 |
| Kepulauan Bangka Belitung | 1.000 | 1.87 | 0.794 | 0.795 |
| Kepulauan Riau | 1.000 | 0.73 | 0.794 | 0.794 |
| Lampung | 1.000 | 1.99 | 0.794 | 0.794 |
| Maluku | 1.000 | 5.10 | 0.794 | 0.794 |
| Maluku Utara | 1.000 | 1.75 | 0.794 | 0.795 |
| Nusa Tenggara Barat | 1.000 | 4.73 | 0.795 | 0.794 |
| Nusa Tenggara Timur | 1.000 | 2.93 | 0.794 | 0.794 |
| Papua | 1.000 | 5.38 | 0.794 | 0.794 |
| Papua Barat | 1.000 | 5.04 | 0.795 | 0.794 |
| Riau | 1.000 | 2.39 | 0.794 | 0.794 |
| Sulawesi Barat | 1.000 | 2.25 | 0.794 | 0.795 |
| Sulawesi Selatan | 1.000 | 2.07 | 0.794 | 0.794 |
| Sulawesi Tengah | 1.000 | 0.27 | 0.795 | 0.794 |
| Sulawesi Tenggara | 1.000 | 0.39 | 0.794 | 0.794 |
| Sulawesi Utara | 1.000 | 2.49 | 0.794 | 0.795 |
| Sumatera Barat | 1.000 | 2.21 | 0.794 | 0.794 |
| Sumatera Selatan | 1.000 | 1.59 | 0.794 | 0.794 |
| Sumatera Utara | 1.000 | 2.02 | 0.795 | 0.794 |
| **Average** | **0.962** | **2.146** | **-** | **-** |

**Table C.10:** Provincial Demand Scenarios Comparison Report (2050)

| Province | Bottom-Up (TWh) | Top-Down (TWh) | Difference (TWh) | Change (%) |
|---|---|---|---|---|
| Aceh | 14.2 | 21.3 | +7.1 | +49.9 |
| Bali | 44.9 | 31.5 | -13.4 | -29.8 |
| Banten | 82.8 | 47.7 | -35.1 | -42.3 |
| Bengkulu | 3.3 | 7.0 | +3.7 | +112.0 |
| Daerah Istimewa Yogyakarta | 25.3 | 15.8 | -9.4 | -37.4 |
| Daerah Khusus Ibukota Jakarta | 114.1 | 156.7 | +42.6 | +37.3 |
| Gorontalo | 4.3 | 7.1 | +2.7 | +62.7 |
| Jambi | 8.0 | 14.4 | +6.5 | +81.0 |
| Jawa Barat | 137.2 | 195.3 | +58.1 | +42.3 |
| Jawa Tengah | 136.8 | 179.0 | +42.1 | +30.8 |
| Jawa Timur | 120.1 | 157.9 | +37.8 | +31.5 |
| Kalimantan Barat | 8.1 | 32.4 | +24.3 | +297.9 |
| Kalimantan Selatan | 12.7 | 36.3 | +23.6 | +185.2 |
| Kalimantan Tengah | 7.1 | 18.2 | +11.1 | +156.2 |
| Kalimantan Timur | 46.4 | 49.2 | +2.7 | +5.9 |
| Kalimantan Utara | 2.6 | 7.5 | +5.0 | +193.2 |
| Kepulauan Bangka Belitung | 4.9 | 9.2 | +4.3 | +86.9 |
| Kepulauan Riau | 8.4 | 6.2 | -2.3 | -27.0 |
| Lampung | 17.3 | 34.5 | +17.2 | +99.3 |
| Maluku | 2.2 | 11.1 | +8.9 | +411.0 |
| Maluku Utara | 12.7 | 22.2 | +9.5 | +74.9 |
| Nusa Tenggara Barat | 9.9 | 47.0 | +37.1 | +372.9 |
| Nusa Tenggara Timur | 8.1 | 23.8 | +15.6 | +193.0 |
| Papua | 4.4 | 23.8 | +19.3 | +437.7 |
| Papua Barat | 2.4 | 12.1 | +9.7 | +403.3 |
| Riau | 21.2 | 50.7 | +29.5 | +138.7 |
| Sulawesi Barat | 2.4 | 5.4 | +3.0 | +125.5 |
| Sulawesi Selatan | 38.9 | 80.4 | +41.5 | +106.5 |
| Sulawesi Tengah | 60.7 | 16.7 | -44.0 | -72.6 |
| Sulawesi Tenggara | 38.3 | 15.0 | -23.3 | -60.9 |
| Sulawesi Utara | 8.0 | 20.0 | +12.0 | +149.4 |
| Sumatera Barat | 10.3 | 22.7 | +12.4 | +121.4 |
| Sumatera Selatan | 23.6 | 37.5 | +13.9 | +58.8 |
| Sumatera Utara | 37.7 | 76.0 | +38.4 | +101.9 |
| **Total** | **1079.6** | **1491.6** | **+412.0** | **+38.2** |

# D. Results for Energy System Optimization

This appendix contains detailed outputs from the energy system optimization that complement Sections 4.2–4.5 (Chapter 4.2–4.5). It provides additional figures, sensitivity runs, and model diagnostics.

## D.1. Storage Analysis

This appendix provides detailed storage dispatch patterns, utilization metrics, and operational mechanisms supporting the findings presented in Section 4.2.

### D.1.1. Storage Utilization Patterns by Technology Mix

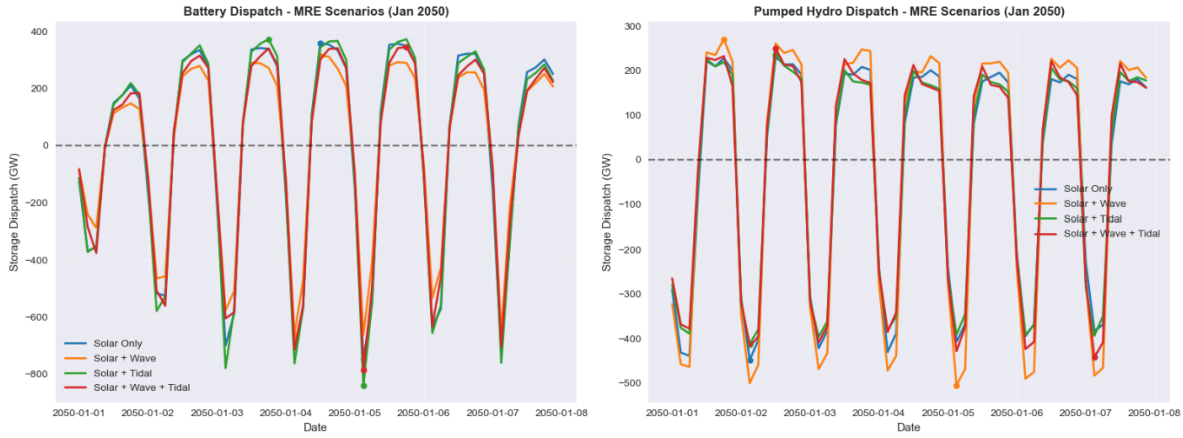


**Figure D.1:** Normalized storage dispatch pattern under different MRE integration scenarios, battery and pumped hydro shown separately.

**Table D.1:** Storage utilization metrics under different MRE integration scenarios (Supergrid, 2050)

| Scenario | Storage Type | Max Discharge [GW] | Max Charge [GW] | Avg Discharge [GW] | Avg Charge [GW] | Discharge Hours [h] |
|---|---|---|---|---|---|---|
| Solar Only | Battery | 497.9 | 1016.2 | 281.5 | 449.6 | 1767 |
| | Pumped Hydro | 361.0 | 461.7 | 181.5 | 324.1 | 1705 |
| Solar + Wave | Battery | 466.9 | 907.0 | 229.8 | 386.6 | 1803 |
| | Pumped Hydro | 400.8 | 546.9 | 204.3 | 394.1 | 1761 |
| Solar + Tidal | Battery | 539.1 | 1062.5 | 287.0 | 478.0 | 1796 |
| | Pumped Hydro | 346.1 | 443.6 | 173.2 | 303.0 | 1691 |
| Solar + Wave + Tidal | Battery | 508.6 | 994.2 | 255.4 | 434.6 | 1811 |
| | Pumped Hydro | 357.4 | 496.8 | 179.1 | 334.9 | 1740 |

Wave energy provides the greatest benefit for battery system stress reduction. Adding wave energy reduces maximum battery discharge from 497.9 GW to 466.9 GW and maximum charge from 1016.2 GW to 907.0 GW. Average discharge power drops from 281.5 GW to 229.8 GW, while average charge decreases from 449.6 GW to 386.6 GW. This reduction reflects wave energy's semi-continuous generation profile, which fills nighttime demand valleys and reduces the amplitude of diurnal storage cycling.

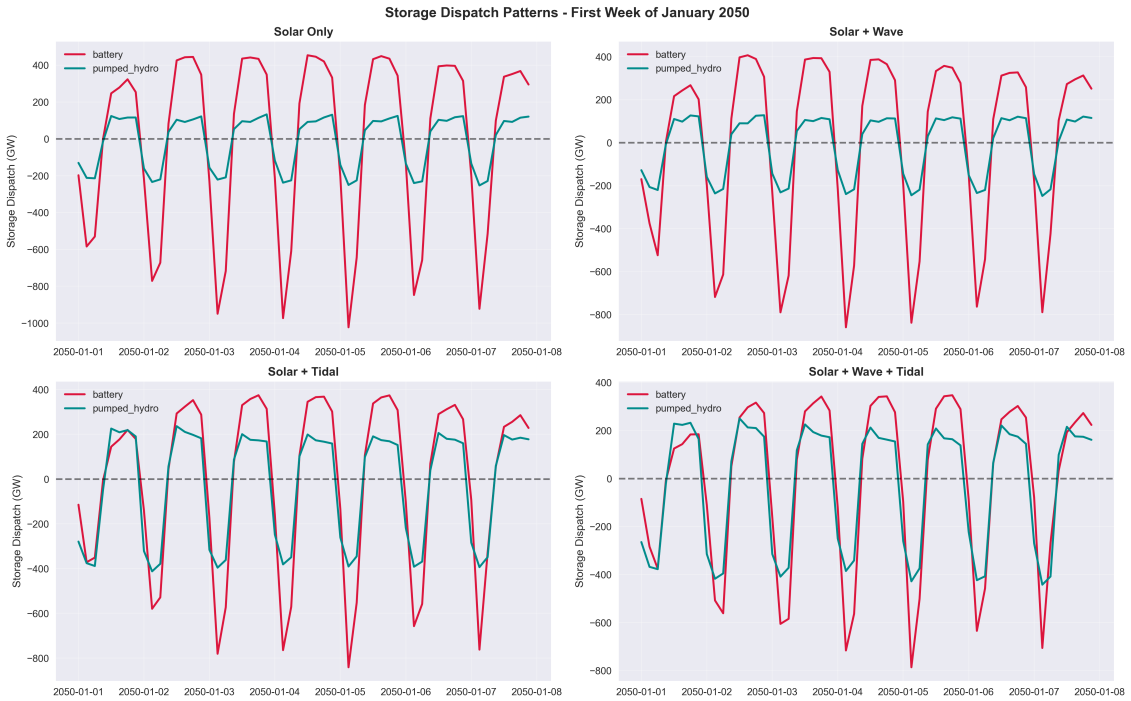


**Figure D.2:** Maximum storage discharge and charge capacity by scenario. Wave energy significantly reduces battery stress while tidal energy shifts balancing responsibility between storage technologies.

Conversely, tidal energy increases battery system demands. The Solar + Tidal scenario shows the highest maximum battery discharge (539.1 GW) and elevated average charge requirements (478.0 GW). Despite tidal energy's predictability, its 12.4-hour cycles do not align optimally with solar generation gaps, creating additional short-term balancing needs.

The storage technology trade-off becomes evident in pumped hydro patterns. Wave energy increases pumped hydro usage, with maximum discharge rising from 361.0 GW to 400.8 GW and maximum charge from 461.7 GW to 546.9 GW. This indicates wave energy shifts balancing responsibility from short-duration batteries to long-duration pumped hydro. Tidal energy produces the opposite effect, reducing pumped hydro maximum discharge to 346.1 GW while stressing batteries more heavily.

The combined Solar + Wave + Tidal scenario yields intermediate results for both storage technologies, confirming that wave and tidal energy provide complementary rather than additive benefits. Maximum battery discharge (508.6 GW) and charge (994.2 GW) fall between the individual MRE scenarios, while pumped hydro shows moderate increases in both discharge (357.4 GW) and charge (496.8 GW) requirements.

### D.1.2. Residual Load Analysis

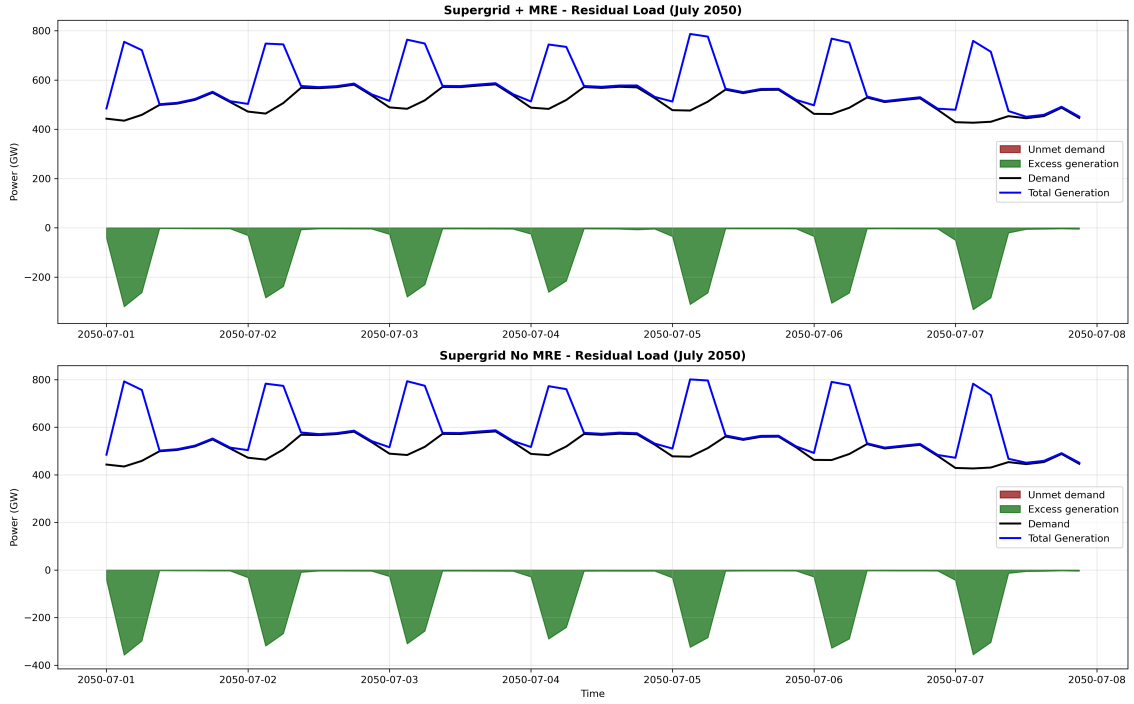


**Figure D.3:** Residual load behavior over a representative week in July 2050 for the Supergrid configuration. MRE integration reduces excess generation magnitude and smooths residual demand variations.

MRE integration reduces maximum excess generation from 397 GW to 366 GW and average excess generation from 82.1 GW to 75.2 GW, indicating that MRE fills demand valleys more effectively than solar alone. This smoothing effect explains why wave energy reduces battery stress: by providing more consistent generation throughout the day, MRE systems reduce sharp ramping requirements that drive peak storage discharge rates.

### D.1.3. Dispatch Statistics and Grid Topology Effects

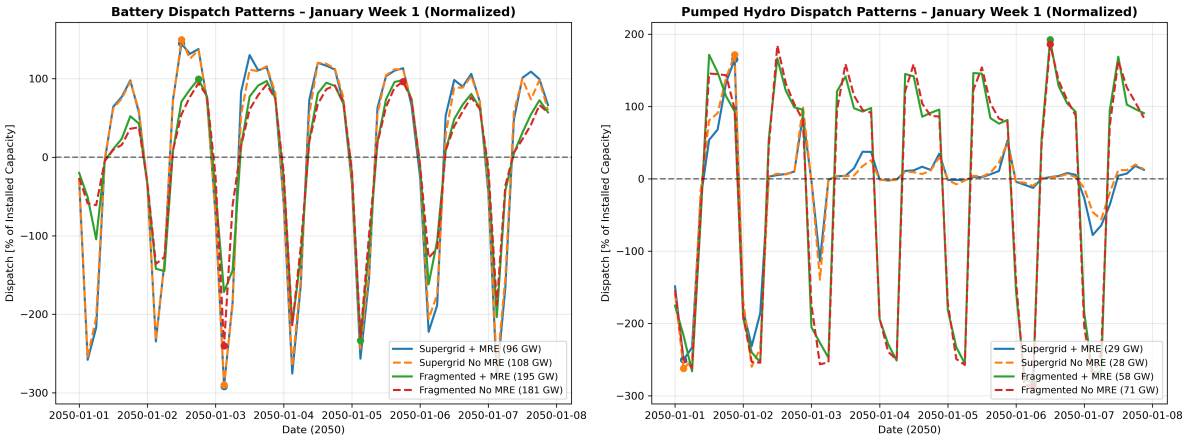


**Figure D.4:** Normalized storage dispatch patterns during January Week 1, 2050. Battery operates in rapid diurnal cycles while pumped hydro exhibits longer-duration phases.

**Table D.2:** Normalized dispatch statistics for battery and pumped hydro during January Week 1, 2050

| Scenario | Storage Type | Max [%] | Min [%] | Std [%] |
|---|---|---|---|---|
| Supergrid + MRE | Battery | 188.6 | -299.5 | 154.7 |
| | Pumped Hydro | 291.6 | -272.2 | 70.8 |
| Supergrid No MRE | Battery | 181.7 | -299.1 | 152.4 |
| | Pumped Hydro | 292.0 | -279.1 | 78.7 |
| Fragmented + MRE | Battery | 144.4 | -289.5 | 108.6 |
| | Pumped Hydro | 279.0 | -284.7 | 166.1 |
| Fragmented No MRE | Battery | 152.2 | -288.0 | 102.2 |
| | Pumped Hydro | 265.3 | -289.2 | 169.0 |

Grid topology fundamentally alters how MRE affects storage operations. In Supergrid systems, MRE reduces pumped hydro variability significantly (standard deviation drops from 78.7% to 70.8%) while having minimal impact on battery cycling. This indicates inter-island transmission allows MRE generation spatial redistribution, reducing long-duration storage stress without affecting short-term balancing needs.

Fragmented grids show opposite patterns. MRE slightly increases battery dispatch variability (102.2% to 108.6% standard deviation) while marginally reducing pumped hydro variability (169.0% to 166.1%). Higher baseline pumped hydro variability in fragmented systems (166–169% vs 71–79% in Supergrid) demonstrates the fundamental constraint: without transmission flexibility, islands rely heavily on local storage to balance supply-demand mismatches.

## D.2. Grid Expansion Analysis

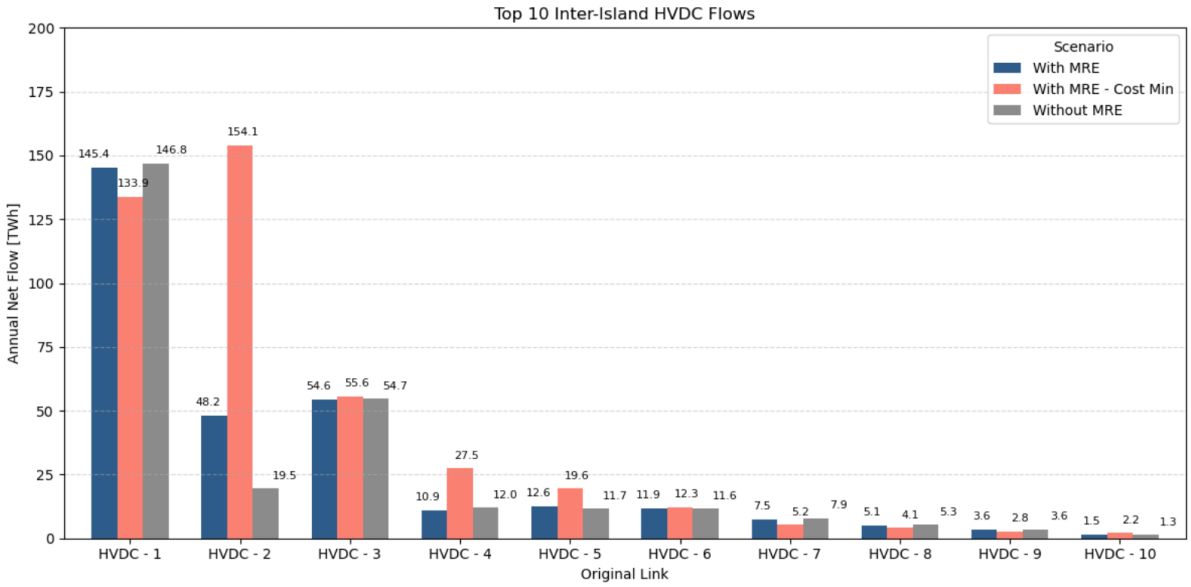


**Figure D.5:** Top 10 inter-island HVDC transmission flows across MRE integration scenarios.

## D.3. Optimal MRE Configuration


**Figure D.6:** Core scenario results comparing installed generation, storage, electricity generation, and system cost between Fragmented and Supergrid configurations, with and without MRE integration.

**Table D.3:** Installed generation capacity (in GW) under different scenarios

| Technology | Fragmented | Fragmented – Without MRE | Fragmented – MRE Min Cost | Supergrid | Supergrid – Without MRE | Supergrid – MRE Min Cost |
|---|---|---|---|---|---|---|
| Geothermal | 23.57 | 23.57 | 23.57 | 23.69 | 23.69 | 23.69 |
| Large hydro | 52.83 | 52.83 | 52.80 | 66.98 | 66.98 | 66.98 |
| Offshore wind | 0.03 | 0.03 | 0.03 | 0.03 | 0.03 | 0.03 |
| Onshore wind | 6.10 | 6.10 | 6.22 | 12.57 | 12.50 | 11.69 |
| OTEC | 60.14 | 64.89 | 52.73 | 58.63 | 58.83 | 42.60 |
| Small hydro | 11.04 | 9.34 | 10.90 | 48.38 | 48.75 | 44.49 |
| Solar floating | 453.68 | 452.05 | 387.86 | 149.18 | 167.29 | 82.64 |
| Solar onshore | 130.11 | 124.39 | 123.28 | 120.69 | 131.21 | 106.36 |
| Tidal stream | 2.83 | – | 14.78 | 0.000724 | – | 28.69 |
| Wave | 3.66 | – | 87.81 | 16.04 | – | 79.88 |
| **Total system capacity** | **744.00** | **733.20** | **760.00** | **496.20** | **509.30** | **477.10** |

**Table D.4:** Electricity generation (TWh/year) under different scenarios

| Technology | Fragmented | Fragmented – Without MRE | Fragmented – MRE Min Cost | Supergrid | Supergrid – Without MRE | Supergrid – MRE Min Cost |
|---|---|---|---|---|---|---|
| Geothermal | 187.75 | 186.44 | 186.99 | 200.68 | 200.76 | 200.01 |
| Large hydro | 218.70 | 218.69 | 218.56 | 277.42 | 277.41 | 277.42 |
| Offshore wind | 0.0041 | 0.0049 | 0.0041 | 0.0055 | 0.0060 | 0.0044 |
| Onshore wind | 20.50 | 20.45 | 21.29 | 44.05 | 43.82 | 41.16 |
| OTEC | 348.37 | 379.31 | 309.20 | 357.96 | 359.09 | 260.83 |
| Small hydro | 41.54 | 34.58 | 38.99 | 194.66 | 195.30 | 182.91 |
| Solar floating | 551.95 | 556.81 | 485.07 | 220.88 | 247.03 | 126.27 |
| Solar onshore | 165.18 | 153.90 | 157.65 | 176.62 | 191.01 | 164.23 |
| Tidal stream | 0.68 | – | 14.21 | 0.00182 | – | 79.15 |
| Wave | 9.45 | – | 108.61 | 41.40 | – | 182.22 |
| **Total generation** | **1,544.27** | **1,550.59** | **1,540.56** | **1,513.35** | **1,514.41** | **1,514.60** |

**Table D.5:** Installed storage capacity (GW) under different scenarios

| Technology | Fragmented | Fragmented – Without MRE | Fragmented – MRE Min Cost | Supergrid | Supergrid – Without MRE | Supergrid – MRE Min Cost |
|---|---|---|---|---|---|---|
| Battery | 195.33 | 181.38 | 171.88 | 96.31 | 107.77 | 77.13 |
| Pumped hydro | 58.09 | 71.40 | 53.64 | 28.74 | 27.89 | 43.09 |
| **Total storage capacity** | **253.42** | **252.78** | **225.52** | **125.05** | **135.66** | **120.22** |

## D.3.1. Cost Sensitivity Summary

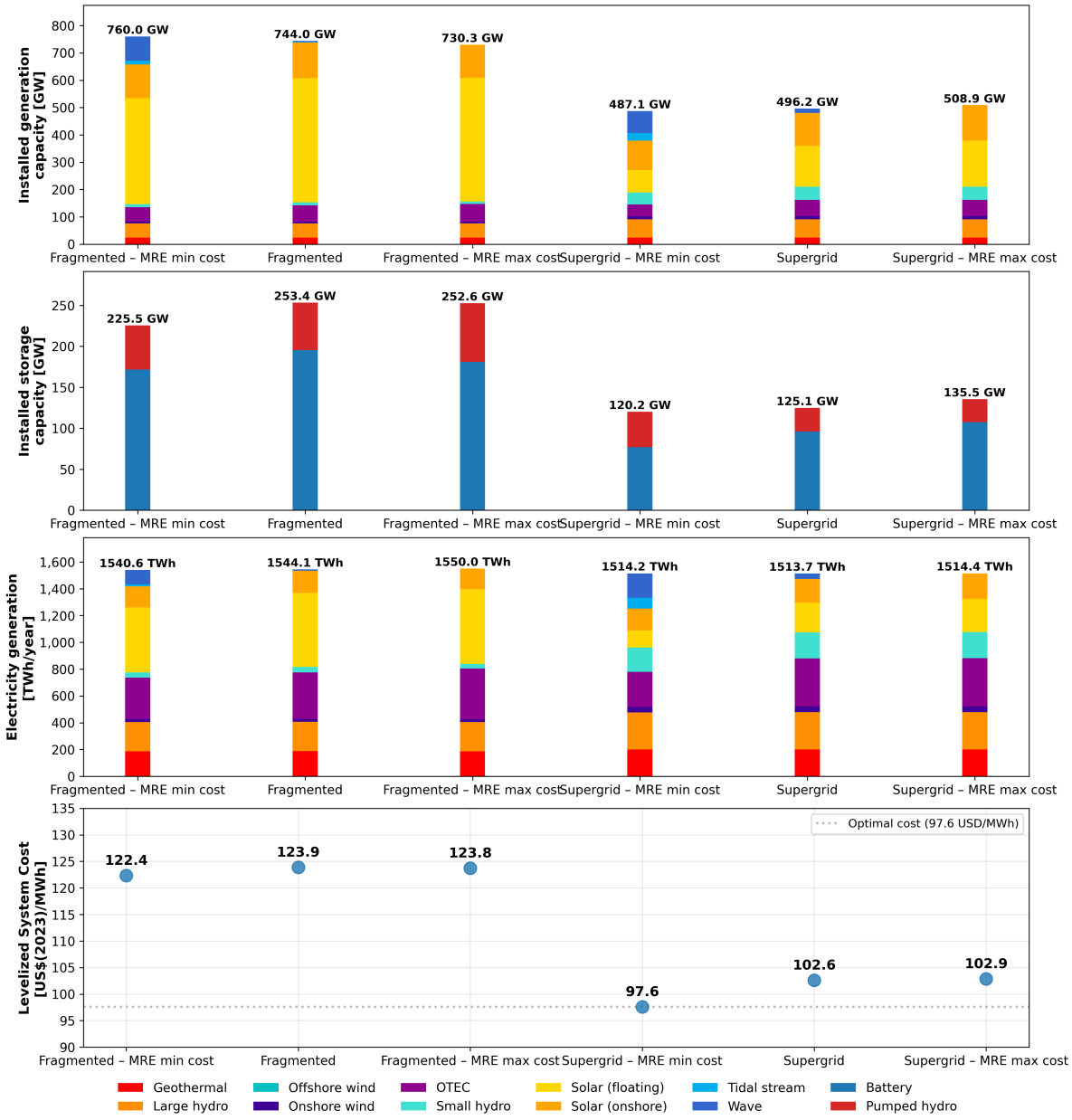


**Figure D.7:** Cost sensitivity scenarios for MRE integration under Fragmented and Supergrid grids, showing changes in installed generation, storage, electricity generation, and system cost.

**Table D.6:** Installed generation capacity (GW) under cost sensitivity scenarios

| Technology | Fragmented – MRE Min Cost | Fragmented - Baseline | Fragmented – MRE Max Cost | Supergrid – MRE Min Cost | Supergrid - Baseline | Supergrid – MRE Max Cost |
|---|---|---|---|---|---|---|
| Geothermal | 23.57 | 23.57 | 23.57 | 23.69 | 23.69 | 23.69 |
| Large hydro | 52.80 | 52.83 | 52.83 | 66.98 | 66.98 | 66.98 |
| Offshore wind | 0.03 | 0.03 | 0.03 | 0.03 | 0.03 | 0.03 |
| Onshore wind | 6.22 | 6.10 | 6.10 | 11.69 | 12.57 | 12.36 |
| OTEC | 52.73 | 60.14 | 64.89 | 42.60 | 58.63 | 59.03 |
| Small hydro | 10.90 | 11.04 | 9.34 | 44.49 | 48.38 | 48.69 |
| Solar floating | 387.86 | 453.68 | 452.06 | 82.64 | 149.18 | 167.78 |
| Solar onshore | 123.28 | 130.11 | 120.96 | 106.36 | 120.69 | 130.36 |
| Tidal stream | 14.78 | 2.83 | 0.53 | 28.69 | 0.000724 | 0.000078 |
| Wave | 87.81 | 3.66 | 0.000002 | 79.88 | 16.04 | 0.000038 |
| **Total system capacity** | **760.8** | **764.1** | **724.6** | **486.8** | **526.3** | **538.9** |

**Table D.7:** Electricity generation (TWh/year) under cost sensitivity scenarios

| Technology | Fragmented – MRE Min Cost | Fragmented | Fragmented – MRE Max Cost | Supergrid – MRE Min Cost | Supergrid | Supergrid – MRE Max Cost |
|---|---|---|---|---|---|---|
| Geothermal | 186.99 | 187.75 | 186.40 | 200.01 | 200.68 | 200.74 |
| Large hydro | 218.56 | 218.70 | 218.70 | 277.42 | 277.42 | 277.42 |
| Offshore wind | 0.0041 | 0.0041 | 0.0040 | 0.0044 | 0.0055 | 0.0057 |
| Onshore wind | 21.29 | 20.50 | 20.46 | 41.16 | 44.05 | 43.33 |
| OTEC | 309.20 | 348.37 | 378.20 | 260.83 | 357.96 | 360.27 |
| Small hydro | 38.99 | 41.54 | 34.57 | 182.91 | 194.66 | 195.09 |
| Solar floating | 485.07 | 551.95 | 558.87 | 126.27 | 220.88 | 247.81 |
| Solar onshore | 157.65 | 165.18 | 152.73 | 164.23 | 176.62 | 189.74 |
| Tidal stream | 14.21 | 0.68 | 0.11 | 79.15 | 0.00182 | 0.000165 |
| Wave | 108.61 | 9.45 | 0.0000002 | 182.22 | 41.40 | 0.000014 |
| **Total generation** | **1,540.2** | **1,544.2** | **1,550.1** | **1,514.2** | **1,513.9** | **1,514.4** |

**Table D.8:** Installed storage capacity (GW) under cost sensitivity scenarios

| Technology | Fragmented – MRE Min Cost | Fragmented | Fragmented – MRE Max Cost | Supergrid – MRE Min Cost | Supergrid | Supergrid – MRE Max Cost |
|---|---|---|---|---|---|---|
| Battery | 171.88 | 195.33 | 181.16 | 77.13 | 96.31 | 107.64 |
| Pumped hydro | 53.64 | 58.09 | 71.40 | 43.09 | 28.74 | 27.87 |
| **Total storage capacity** | **225.52** | **253.42** | **252.56** | **120.22** | **125.05** | **135.51** |

### D.3.2. Sensitivity Analysis: Fragmented Grid Scenarios

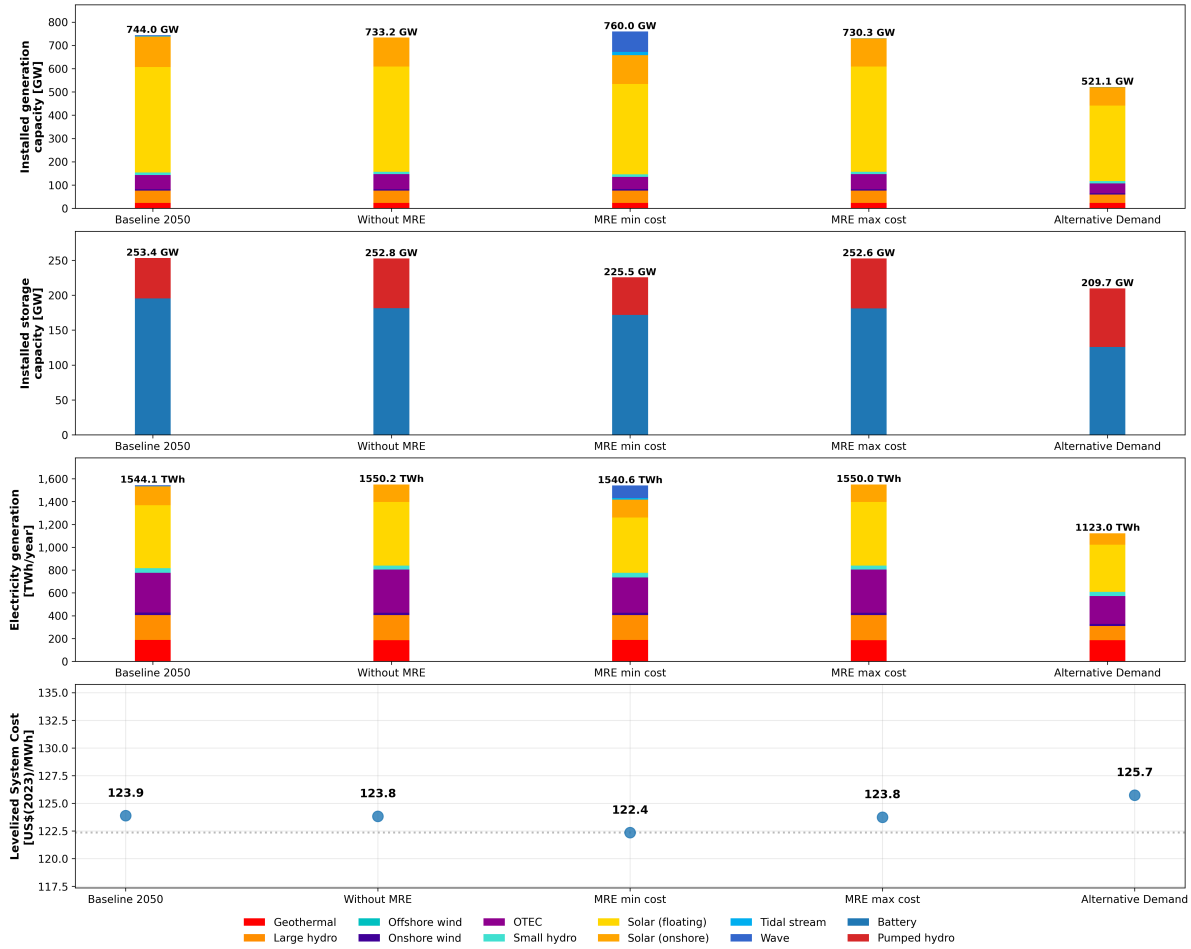


**Figure D.8:** Fragmented scenarios comparing installed generation, storage, electricity generation, and system cost across Baseline 2050, Without MRE, MRE min cost, MRE max cost, and Alternative Demand cases.

**Table D.9:** Fragmented Scenarios: Installed generation capacity (GW) under different scenarios

| Technology | Baseline 2050 | Without MRE | MRE Min Cost | MRE Max Cost | Alternative Demand |
|---|---|---|---|---|---|
| Geothermal | 23.57 | 23.57 | 23.57 | 23.57 | 22.86 |
| Large hydro | 52.83 | 52.83 | 52.80 | 52.83 | 36.45 |
| Offshore wind | 0.03 | 0.03 | 0.03 | 0.03 | 0.00 |
| Onshore wind | 6.10 | 6.10 | 6.22 | 6.10 | 5.30 |
| OTEC | 60.14 | 64.89 | 52.73 | 64.89 | 41.99 |
| Small hydro | 11.04 | 9.34 | 10.90 | 9.34 | 10.69 |
| Solar floating | 453.68 | 452.05 | 387.86 | 452.06 | 323.90 |
| Solar onshore | 130.11 | 124.39 | 123.28 | 120.96 | 79.14 |
| Tidal stream | 2.83 | – | 14.78 | 0.53 | 0.80 |
| Wave | 3.66 | – | 87.81 | 0.00 | 0.00 |
| **Total system capacity** | **744.00** | **733.20** | **760.00** | **730.30** | **521.10** |

**Table D.10:** Fragmented Scenarios: Electricity generation (TWh/year) under different scenarios

| Technology | Baseline 2050 | Without MRE | MRE Min Cost | MRE Max Cost | Alternative Demand |
|---|---|---|---|---|---|
| Geothermal | 187.75 | 186.44 | 186.99 | 186.40 | 185.64 |
| Large hydro | 218.70 | 218.69 | 218.56 | 218.70 | 124.18 |
| Offshore wind | 0.00 | 0.00 | 0.00 | 0.00 | 0.00 |
| Onshore wind | 20.50 | 20.45 | 21.29 | 20.46 | 17.97 |
| OTEC | 348.37 | 379.31 | 309.20 | 378.20 | 244.27 |
| Small hydro | 41.54 | 34.58 | 38.99 | 34.57 | 37.93 |
| Solar floating | 551.95 | 556.81 | 485.07 | 558.87 | 412.25 |
| Solar onshore | 165.18 | 153.90 | 157.65 | 152.73 | 100.63 |
| Tidal stream | 0.68 | – | 14.21 | 0.11 | 0.15 |
| Wave | 9.45 | – | 108.61 | 0.00 | 0.00 |
| **Total generation** | **1544.10** | **1550.20** | **1540.60** | **1550.00** | **1123.00** |

## D.3.3. Sensitivity Analysis: Supergrid Scenarios

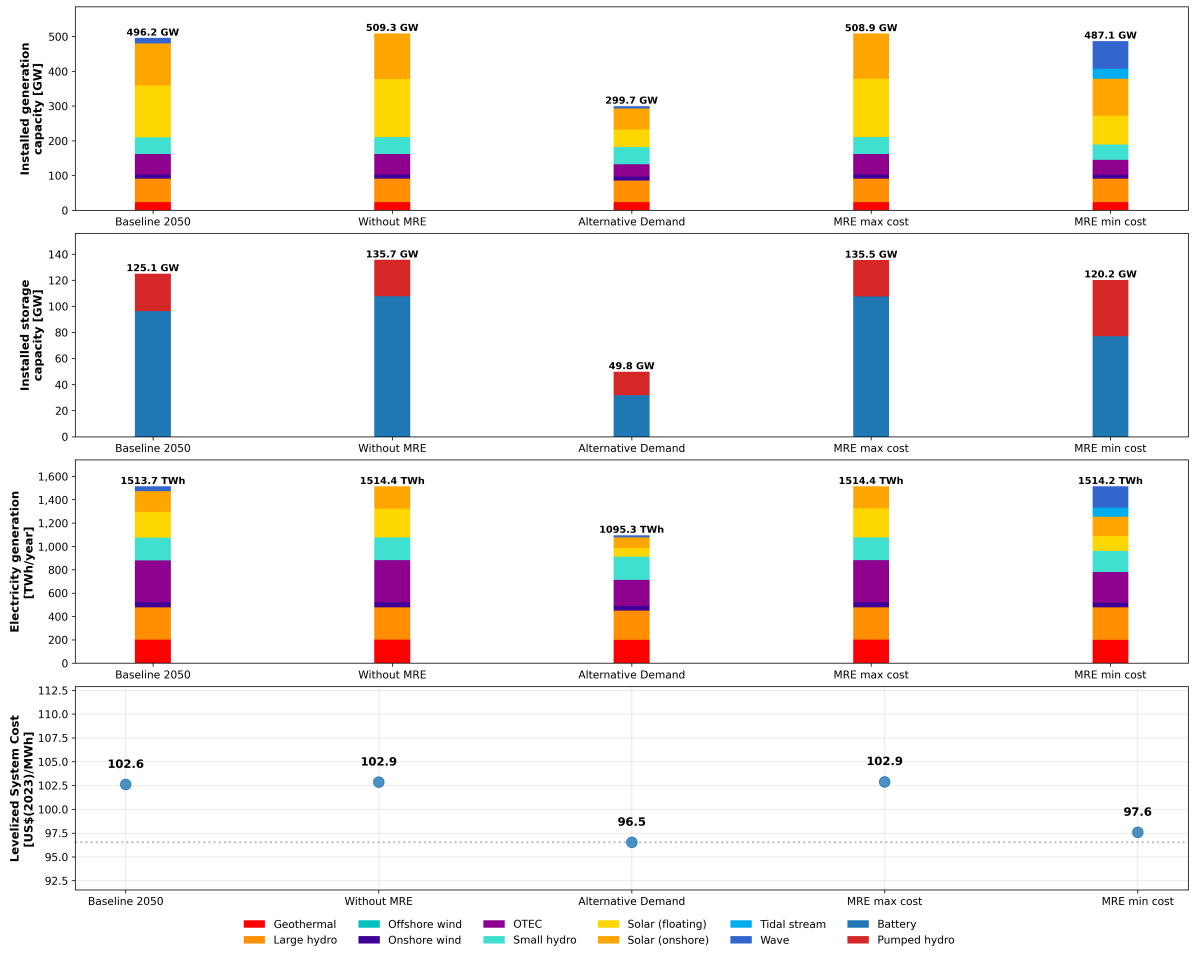


**Figure D.9:** Supergrid sensitivity scenarios comparing installed generation, storage, electricity generation, and system cost across Baseline 2050, Without MRE, Alternative Demand, MRE max cost, and MRE min cost cases.

**Table D.11:** Supergrid Scenarios: Installed generation capacity (GW) under different scenarios

| Technology | Baseline 2050 | Without MRE | Alternative Demand | MRE Max Cost | MRE Min Cost |
|---|---|---|---|---|---|
| Geothermal | 23.69 | 23.69 | 23.27 | 23.69 | 23.69 |
| Large hydro | 66.98 | 66.98 | 62.16 | 66.98 | 66.98 |
| Offshore wind | 0.03 | 0.03 | 0.00 | 0.03 | 0.03 |
| Onshore wind | 12.57 | 12.50 | 11.33 | 12.36 | 11.69 |
| OTEC | 58.63 | 58.83 | 35.79 | 59.03 | 42.60 |
| Small hydro | 48.38 | 48.75 | 49.11 | 48.69 | 44.49 |
| Solar floating | 149.18 | 167.29 | 50.93 | 167.78 | 82.64 |
| Solar onshore | 120.69 | 131.21 | 60.10 | 130.36 | 106.36 |
| Tidal stream | 0.00 | – | 0.00 | 0.00 | 28.69 |
| Wave | 16.04 | – | 7.05 | 0.00 | 79.88 |
| **Total system capacity** | **496.20** | **509.30** | **299.70** | **508.90** | **487.10** |

**Table D.12:** Supergrid Scenarios: Electricity generation (TWh/year) under different scenarios

| Technology | Baseline 2050 | Without MRE | Alternative Demand | MRE Max Cost | MRE Min Cost |
|---|---|---|---|---|---|
| Geothermal | 200.68 | 200.76 | 200.30 | 200.74 | 200.01 |
| Large hydro | 277.42 | 277.41 | 250.01 | 277.42 | 277.42 |
| Offshore wind | 0.01 | 0.01 | 0.00 | 0.01 | 0.00 |
| Onshore wind | 44.05 | 43.82 | 40.22 | 43.33 | 41.16 |
| OTEC | 357.96 | 359.09 | 222.27 | 360.27 | 260.83 |
| Small hydro | 194.66 | 195.30 | 197.89 | 195.09 | 182.91 |
| Solar floating | 220.88 | 247.03 | 74.90 | 247.81 | 126.27 |
| Solar onshore | 176.62 | 191.01 | 91.50 | 189.74 | 164.23 |
| Tidal stream | 0.00 | – | 0.00 | 0.00 | 79.15 |
| Wave | 41.40 | – | 18.22 | 0.00 | 182.22 |
| **Total generation** | **1513.70** | **1514.40** | **1095.30** | **1514.40** | **1514.20** |